Dissecting the Hippo signalling pathway in HPV-driven cervical cancer

Molly Rose Patterson

Submitted in accordance with the requirements for the degree of

Doctor of Philosophy

Astbury Centre for Structural Molecular Biology

School of Molecular and Cellular Biology

The University of Leeds

September, 2022

The candidate confirms that the work submitted is her own, except where work which has formed part of jointly authored publications has been included. The contribution of the candidate and the other authors to this work has been explicitly indicated below. The candidate confirms that appropriate credit has been given within the thesis where reference has been made to the work of others.

Data from chapter 3 was used in “Morgan EL*, Patterson MR*, Ryder EL, Lee SY, Wasson CW, et al. (2020) MicroRNA-18a targeting of the STK4/MST1 tumour suppressor is necessary for transformation in HPV positive cervical cancer. PLOS Pathogens 16(6): e1008624. https://doi.org/10.1371/journal.ppat.1008624”. Unless explicitly stated all work in this thesis is credited to the candidate.

Work by Dr Ethan Morgan: Figure 3.1 B, Figure 3.2 C, Figure 3.4 A

Work by Emma Ryder: Figure 3.2 C

Acknowledgements

Firstly, I would like to thank my supervisor Professor Andrew Macdonald, who has provided continuous help and support throughout my PhD, despite already knowing how terrible I was through my MBiol. Giving me the freedom to pursue my research along with his invaluable guidance has allowed me to grow as a researcher. I would also like to thank my second supervisor Professor Ade Whitehouse who has always made time to give me advice. I would also like to thank my unofficial supervisor Dr Ethan Morgan who somehow didn't strangle me within a day but instead essential taught me how to be a researcher. Without your continuous patience I wouldn't be where I am today. I would also like to express my gratitude Dr Chris Randall for being a voice of sanity and has shaped me as a mentor.

I am grateful to members of the Macdonald group both past and present for putting up with me over the years. In particular I would like to say a massive thank you to Dr Gemma Swincoe, Dr Michelle Antoni, Dr David Kealy, James Scarth, Corinna Brockhaus and Joe Cogan (my on-call bioinformatician), all of whom provided many entertaining times and I wish you all the best in the future. It has been a particular pleasure to go through the whole PhD process with both James and Corinna, somehow we all survived it together!

I have also been lucky to be surrounded with many talent researchers both on level 8 and level 9 but I would like to give a special thanks to Ellie Harrington (along with the rest of the rabble which makes up the Whitehouse group) and Connor Hayward (I think our coffees got me through the dark times of post-covid!).

I feel Katie Harper needs thanking more than most for putting up with me for so many years. Thank you for being my rather worrying moral backbone and for sharing a single brain cell with me.

Finally, I would also like to thank my parents, my brother and my grandad for encouragement and constant support over the years and I love you all.

Abstract

Human papillomaviruses (HPVs) are a major cause of malignancy worldwide. HPV hijacks host signalling pathways to promote proliferation and cell survival, ultimately contributing to carcinogenesis. The Hippo pathway has been identified as a key signalling pathway in HPV+ cancers, with the downstream effector of this pathway YAP known to play a critical pro-oncogenic role. Recent work in the Macdonald group has confirmed literature and highlighted how the dysregulation of signalling pathways is important in cervical cancer tumourigenesis and found in particular that the Hippo signalling pathway is pivotal in transformation. Preliminary data found STK4, the key kinase of the Hippo signalling pathway to be lost in cervical cancer but the mechanism of how this occurred remained elusive.

Analysis of the expression level of critical components of the Hippo pathway in a panel of cervical cancer cell lines revealed that, in contrast to YAP, which was upregulated in all HPV+ cell lines on a protein level, TAZ expression was only significantly increased in HPV18+ cell lines. Significantly, we found that TAZ upregulation occurred at the transcript level. Further, *TAZ* mRNA was significantly upregulated in HPV18+, but not HPV16+, cervical disease clinical samples, increasing with disease severity. Subsequent investigation found *TAZ* mRNA was increased due to increased TAZ promoter activity via a HPV18 E7/EGFR/ERK(1/2)/SP1 signalling axis. Crucially, the overexpression of YAP was not able to rescue the proliferation defect in the TAZ knockdown cells, suggesting that YAP and TAZ have distinct targets, essential for growth in HPV cancer cell lines. RNA-seq confirmed this, revealing that TAZ and YAP have distinct target profiles, including a number of genes that have not previously been linked with cervical cancer. Thus, in HPV18+ cancers, both YAP and TAZ play non-redundant roles in regulating transformation. We chose three potential genes for further study, *TOGARAM2*, *SSTR5* and *IFIT2*, which we confirmed as novel TAZ-dependent genes. We further showed TOGARAM2 is a potential novel oncogene while SSTR5 and IFIT2

are tumour suppressive in HPV18+ cervical cancer. In summary, this study identifies TAZ as a crucial oncogene in HPV18+ cervical cancer and unveils a novel transcriptional control network distinct to that of YAP.

Table of contents

List of figures

List of tables

Abbreviations

°C Degrees Celsius

AGO Argonaute

AKT a serine/threonine protein kinase

AREG ampiregulin

ATM Ataxia-telangiectasia mutated

ATR Ataxia-telangectasia and Rad3 related

ATP Adenosine triphosphate

Bak Bcl-2 homologous antagonist killer

Bax Bcl-2-associated X protein

BCA Bicinchoninic acid

Bcl B-cell lymphoma

BH Bcl-2 Homology

BID BH3 interacting-domain death agonist

BLAST Basic local alignment search tool

BM Basement membrane

Bp Base pair

BPV1 Bovine papillomavirus 1

BS Binding site

BSA Bovine serum albumin

Ca Calcium

CAD caspase-activated DNase

CARM1 coactivator associated arginine methyltransferase 1

CC Cervical cancer

CC coiled coil

CDK2 Cyclin dependent kinase 2

ceRNA competing endogenous RNA

Chk2 checkpoint kinase 2

CHX Cyclohexamide

CIN Cervical intraepithelial neoplasia

circRNA circularRNA

CPSF3 cleavage and polyadenylation specificity factor subunit 3

CR conserved region

cSCC Cutaneous squamous cell carcinoma

CSL CBF-1/Su(H)/LAG1

CTCF connective tissue growth factor

C-terminus Carboxyl-terminus

CyPs cylophilins

CYR61 cysteine-rich angiogenic inducer 61

Da Daltons

DAPI 4′,6-diamidino-2-phenylindole

DBC1 Deleted in Breast Cancer 1

DDR DNA damage repair

DENV Dengue virus

DGCR8 DiGeorge Syndrome Critical Region 8

DKK3 Dickkopf-related protein 3

DMEM Dulbecco’s modified Eagle’s medium

DMSO Dimethyl sulfoxide

DNA Deoxyribonucleic acid

DNMT1 DNA methyltransferases

dNTP Deoxyribonucleotide triphosphate

ds Double stranded

Drosha

DTT Dithiothreitol

Dvl Dishevelled

E Early

E2F E2 Transcription Factor

E6-AP E6-associated protein

EBV Epstein-Barr Virus

EDTA Ethylenediamine tetraacetic acid

EGF Epidermal growth factor

EGFR Epidermal growth factor receptor

EGR2 early growth response 2

eIF elongation initiation factor

EMT Epithelial-to-mesenchymal

ER Endoplasmic reticulum

ERα Estrogen receptor α

ERK Extracellular-signal-regulated kinase

EV Epidermodysplasia verruciformis

FADD Fas-associated protein with death domain

FBS Fetal bovine serum

FER1L4 Fer-1-like protein 4

FPN ferroportin

FOXO Forkhead box O

FRE FOXO recognition elements

G2 Growth 2

G2/M Growth2/ Mitosis

GCPR G protein-coupled receptor

GCK germinal centre kinase

GFP Green fluorescent protein

GSK3β

GTP guanosine triphosphate

H Histone

H_2O Water

HA hemagglutinin

HAT histone acetyltransferases

HBP1 HMG box-containing protein 1

HCV hepatitis C virus

HDAC histone deacetylases

HEPES-BSS HEPES-buffered saline solution

HIF1A Hypoxia Inducible Factor 1 Subunit Alpha

HIV Human immunodeficiency virus

hnRNP Heterogeneous nuclear ribonucleoproteins

HMT histone methyltransferases

HNSCC Head and neck squamous cell carcinoma

HPV Human papillomavirus

HR-HPV High risk-HPV

HSIL High-grade squamous intraepithelial lesion

HSPG heparin sulfate proteoglycans

hTERT human telomerase reverse transcriptase

IFIT Interferon-induced protein with tetratricopeptide repeats family

IFN Interferon

ISG Interferon stimulated genes

IRAK4 interleukin-1 receptor-associated kinase 4

IRF Interferon regulatory factor

ISY1 ISY1 splicing factor homolog

ITCH itchy E3 ubiquitin protein ligas

JNK c-Jun N-terminal kinase

Kb Kilobase

kDa Kilodaltons

KGFR Keratinocyte growth factor receptor

KIBRA kidney and brain expressed protein

KLK8 Kallikrein-8

KSHV Kaposi's sarcoma-associated herpesvirus

L Late

LATS Large tumor suppressor kinase

LB Luria-Bertani

LCR Long coding region

LLPS Liquid liquid phase seperation

LMP1 latent membrane protein 1

lncRNA long non-coding RNA

LR-HPV Low risk-HPV

LRIG1 leucine-rich repeats and immunoglobulin-like domains 1

LSIL Low-grade squamous intraepithelial lesion

NMR Nuclear magnetic resonance

N terminal amino terminal

M Molar

MAP Mitogen activated protein

MAPK Mitogen activated kinase

MAPKK Mitogen activated kinase kinase

MAP3K Mitogen activated kinase kinase kinase

MDM2 Mouse double minute 2 homologue protein

MEKK MAP kinase kinase kinase

Mg Milligram

MHC Major histocompatibility complex

min Minutes

miRNA MicroRNA

mM Millimolar

MMPs Matrix metalloproteinases

MOB1 MOB kinase activator 1

mRNA Messenger RNA

NaCl Sodium Chloride

NES Nuclear export signal

ncRNA non-coding RNA

ng Nanogram

NF Neurofibromin

NFκB nuclear factor kappa B

NHK Normal human keratinocytes

NICD Notch intracellular domain

NKT natural killer T

NLS Nuclear localisation signal

nM Nanomolar

NONO Non-POU domain-containing octamer-binding protein

NS Non-structural protein

NSCLC Non-small cell lung cancer

N-terminus Amino-terminus

NuRD Nucleosome Remodeling and Deacetylase

OPSCC Oropharyngeal squamous cell carcinoma

ORF Open reading frame

Ori Origin of replication

p Phosphorylated

PAK p21-activated kinase

PBS Phosphate buffered saline

PD-L1 Programmed death-ligand 1

PDZ Post synaptic density protein, drosophila disc large tumour suppressor,

PE Early promoter

PFA Paraformaldehyde

PH Pleckstrin homology

PI Propidium iodide

PIAS3 protein inhibitor of activated STAT3

PI3K Phosphatidylinositol 3-kinase

PIP2 phosphatidylinositol-4,5-bisphosphate

PIP3 phosphatidylinositol-3,4,5-trisphosphate

pmol Picomoles

PRMT1 protein arginine methyltransferase 1

PTEN Phosphatase and Tensin Homolog deleted on Chromosome 10

PTPN14 protein tyrosine phosphatase non-receptor type 14

PV Papillomaviruses

RASSF Ras association domain family

Rb Retinoblastoma

RECK Reversion-inducing Cysteine-rich protein with Kazal motifs

RISC RNA-Induced Silencing Complex

RNA Ribonucleic acid

RNA-seq RNA-sequencing

R.T. Room temperature

RUNX3 RUNX Family Transcription Factor 3

S Synthesis

S6K1 S6 kinase beta-1

SARAH Sav/RASSF/Hpo

SAV Salvador homolog 1

SCF Skp-Cullin-F box

SDS Sodium dodecyl sulfate

SDS PAGE Sodium dodecyl sulfate polyacrylamide gel electrophoresis

SET7 SET domain containing lysine methyltransferase

SH3 Src homology 3

shNTC Short hairpin non targeting control

shRNA Short hairpin RNA

siRNA Small interfering RNA

SND1 Staphylococcal nuclease and Tudor domain containing 1

SP1 specificity protein 1

ss Single stranded

SSTR Somatostatin receptor type

STAT3 Signal Transducer And Activator Of Transcription 3

STK serine/threonine kinase

TAE Tris-acetate-EDTA

TAO1 thousand and one amino acid kinase 1

TAZ transcriptional co-activator with PDZ-binding motif

TBS-T Tris Buffered Saline

TCA Trichloroacetic acid

TEAD TEA domain family member

TGF-β transforming growth factor β

TIMP3 TIMP Metallopeptidase Inhibitor 3

TLR Toll-like receptors

TOG Tumour overexpressed gene

TOGARAM TOG array regulator of axonemal microtubules protein

TRAIL tumour necrosis factor-related apoptosis inducing ligand

ULK1 Unc-51 Like Autophagy Activating Kinase 1

URR Upstream regulatory region

UTR Untranslated region

UV Ultraviolet

VLP Virus-like particle

w/v Weight/volume

WT Wild type

WWTR1 WW Domain Containing Transcription Regulator 1

YAP yes-associated protein

Chapter 1- Introduction

1.1 Papillomaviridae

The *Papillomaviridae* (PV) are DNA viruses that infect the basal keratinocytes of the epithelium in humans and many animals including marsupials, canines, reptiles, fish and birds (1). The family is predicted to have emerged 450 million years ago and members typically cause chronic infections with some arguing they are members of the commensal flora and therefore, opportunistic pathogens (2, 3). PVs are classified into 53 genera with 5 that exclusively infect humans and are considered host restrictive. The 5 genera of Human PVs (HPVs) are; alpha, beta, gamma, mu and nu, (Figure 1.1). Each genus is split into species, with HPV types sharing similar 71–89% similarity in late 1 (L1) nucleotide sequences and similar characteristics grouped as a species. To be classified as a novel HPV type, there must be less than 90% similarity in the L1 nucleotide sequence with existing HPV types. HPVs with 90-98% similarity of L1 nucleotide sequence are classified as subspecies and a greater than 98% similarities are classified as variants (4). Collectively, there are over 300 types of HPV with the majority classified in the gamma genera. The advent of deep sequencing technologies has significantly increased the number of HPV types discovered. For example, a single study by Pastrana *et al*, revealed 85 novel types (5).

Alpha HPV types mostly infect the mucosal epithelium, with a small number which infect the cutaneous epithelium including HPV 2, 3, 7, 10, 27, 28, and 57 leading to the development of planar warts. Alpha HPV types are split into high risk (HR) and low risk (LR) according to the diseases associated with infection. HR-HPV infection can lead to intraepithelial neoplasia and cancer while LR-HPV infection can result in the development of benign lesions. HR-HPVs fall into alpha HPV species 7 and 9 and include types; 16, 18, 31, 33, 35, 39, 45, 51, 52, 56, 58, 59, 68, 73 and 82. HPV16 and HPV18 are the most prevalent, together, causing over 70% of cervical cancer cases alone along

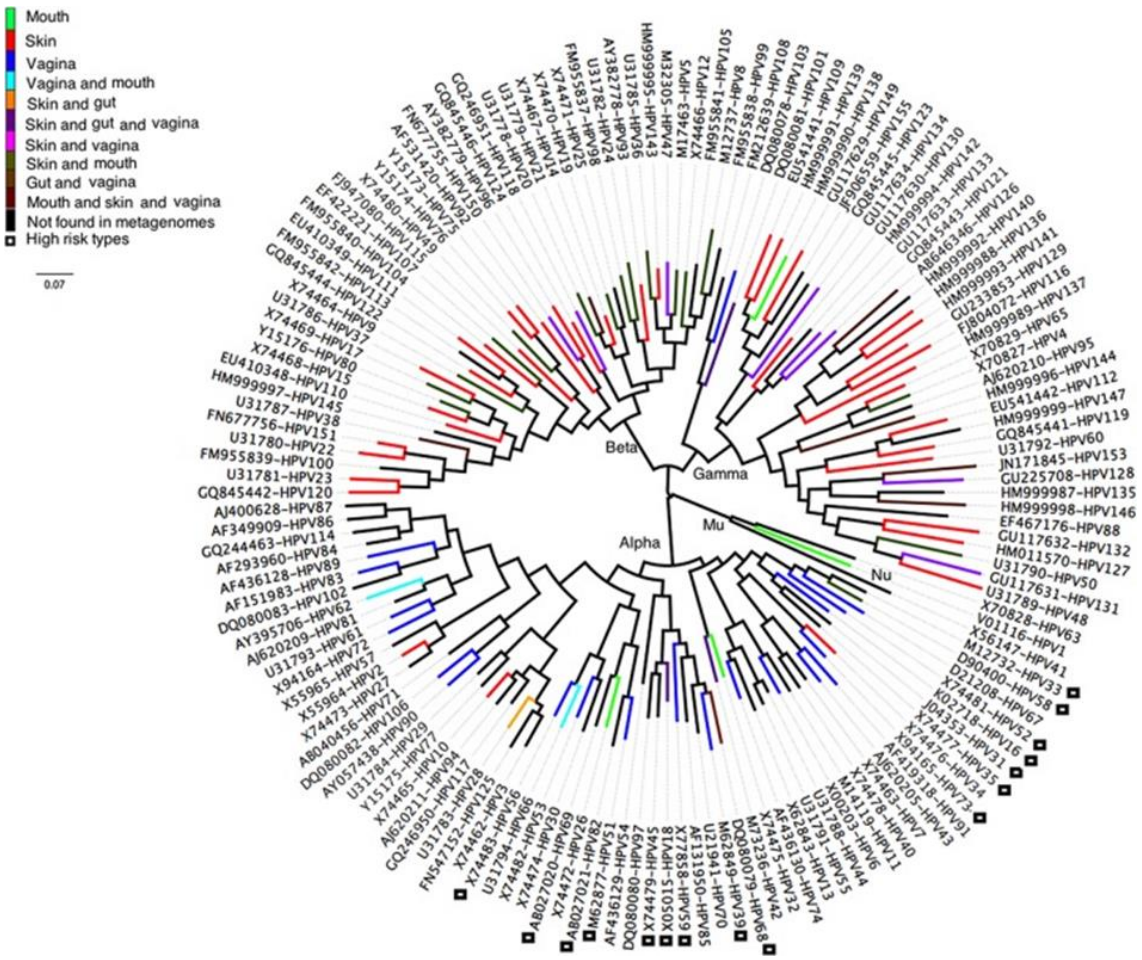

Figure 1.1 Phylogeny and Classification of Human Papillomavirus. The five HPV genera are Alpha, Beta, Gamma, Mu and Nu. HPV types are classified according the sequence of their L1 capsid proteins. High risk HPV types (highlighted in the key) are confirmed to be carcinogenic (6).

with the majority of HPV+ Head and neck squamous cell carcinomas (HNSCC). LR-HPVs include 6 and 11 and infection results in condyloma acuminata (benign genital warts). Other alpha-HPV types such as 32 and 13 are linked to Heck's disease or Focal epithelial hyperplasia, a benign infection of the oral mucosa. It is evident that despite high similarities in the L1 nucleotide sequence, different HPV types can have different tropisms. For example, despite the high level of similarity between 6 and 11, the former is more common in anogenital warts whereas the latter is more common in laryngeal papillomas (4, 7, 8).

1.2 Virus structure and genome

Each PV particle consists of a 60 nm icosahedral capsid containing a circular episomal chromatinised DNA genome. The virus capsid is made up of 72 capsomeres, each containing 5 L1 proteins. The carboxyl-terminal (C terminal) tail of the L1 protein is key for interactions between capsomeres (9). Virus particles also contain up to 72 molecules of late 2 (L2) protein which are not exposed until L1 binding during virus entry (10).

The circular genome of members of the PV family is approximately 8 kb in length (11) and ranges from 6,953 bp (*Chelonia mydas* papillomavirus) to 8,607 bp (*Cotton rabbit* papillomavirus 1) (12). PV genomes can be split into 3 functional sections; early (E) and late (L) which includes 10 open region frames (ORFs) (generally 9 genes, 7 genes in the early region and 2 in the late region, which are expressed on polycistronic transcripts) and a long non-coding region (LCR). The three regions are separated by an early and late polyadenylation site. The LCR contains the origin of DNA replication and the transcriptional control sequences important for the regulation of the early and late promoters as well as RNA polymerase II transcription (13). Recent sequencing of the several HR-HPV genomes discovered virally encoded microRNAs (miRNAs) that are hypothesised to aid infection (14).

The genome organisation of HPV16 is the most intensively studied. The HPV16 genome contains 2 major promoters. P97 is responsible for expression of the early genes and lies upstream of the E6 ORF while P670 which is responsible for late gene expression (L1 and L2), lies in the E7 ORF (15, 16). P97 is equivalent to P105 in HPV18 (17). Although there are multiple minor promoters, their functions are less characterised (18). In HR-HPV types, E6 and E7 are encoded on the same mRNA transcript and therefore, both E6 and E7 are under the control of the same promoter with splicing allowing for expression of each ORF. However, in LR-HPVs such as HPV6 and 11, two

major promoters P90 and P270 replace P97, allowing for expression of E6 and E7 independently (19).

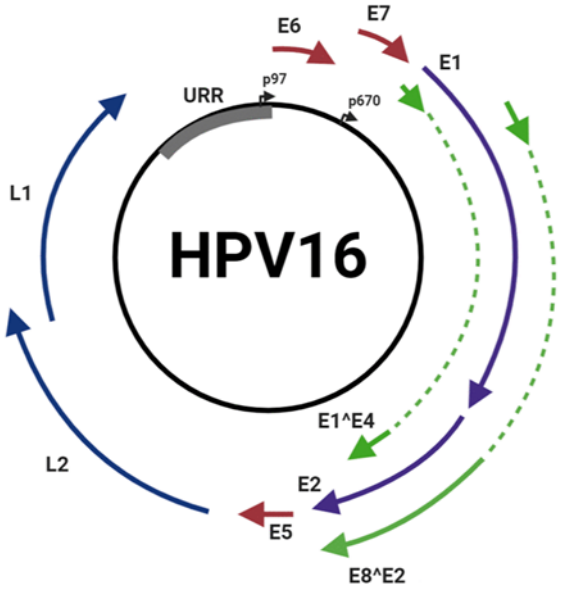

Figure 1.2 HPV genome. Organisation of the HPV16 genome showing early proteins E1, E2, E4, E5, E6 and E7 as well as late proteins L1 and L2. E6 and E7 are under the control of the p97 promoter. All other genes are under the control of the p670 promoter. (11)

Regulation of transcription is tied to the differentiation of the epithelium and is crucial to avoid the premature production of virus particles in the lower suprabasal layers of the epithelium, potentially triggering an immune response. Furthermore, it restricts the transcription of early and late genes to when they are required in the HPV lifecycle (20).

1.3 Virus infection

1.3.1 Cell binding

HPV infects the squamous epithelium through microabrasions to access undifferentiated basal epithelial cells (as seen in Figure 1.3). These are the only proliferative cells in the epithelium and are necessary for HPV replication. In the upper levels however, the daughter cells have terminally differentiated and exited the cycle, thus cannot support HPV genome replication (21).

Although the exact mechanism of HPV entry is argued, cell binding most likely occurs by L1, the major capsid protein, interacting with heparin sulfate proteoglycans (HSPG). HSPG are glycoproteins containing one or more heparan sulfate chains and are predominantly found on the cell plasma membrane or in the extracellular matrix (22). Early studies showed heparinase inhibited virus infection by preventing the binding of virus-like particles (VLPs) or pseudovirus (PsV) to the cell plasma membrane through HSPGs (23). Binding to HSPGs cause conformational changes in L1 that reveal the L2 minor capsid protein allowing cleavage of its amino terminus by host enzyme furin, a necessary step for later trafficking of viral DNA. Multiple other proteases are suggested to be important for exposure of L2 such as Kallikrein-8 (KLK8) which cleaves L1 (24).

Other receptors are thought to be utilised by HPV including α6 integrin, a member of the integrin family of transmembrane cell adhesion receptors. Although knockdown of α6 integrin leads to a decrease in HPV16 PsV uptake, other studies have shown that it is not necessary for all HPV types such as HPV33 (22, 24). Additionally, through the use of β4 knockout mice, it has been shown that β4 integrin also aids HPV16 PsV infection by playing a necessary role in the cleavage and cell membrane localisation of α6 integrin (25). The α6β4-complex is only one example of tetraspanins that have been suggested to be important for HPV infection, with CD151 and CD63 being another example, having observed to be internalised with HPV16 PsV upon infection (26, 27).

1.3.2 Cell entry

After cell binding, the virus is endocytosed into the cell, via various mechanism depending on virus and cell type (28). Knockdown of specific endocytosis components have shown that HPV internalisation is clathrin, caveolin, lipid raft and dynamin-independent and could be dependent on tetraspanins such as CD151 (29). Live cell imaging suggests that CD151 directs the virus to the cell membrane entry site, but any further mechanism has yet to be elucidated (27).

After internalisation HPV localises at the early endosome for up to 4 hours post-infection before trafficking to late endosomes/lysosomal compartments (30). At this point the majority of L1 is retained to the lytic compartment for degradation following capsid disassembly, while L2 remains bound to the genome forming the pseudogenome (31). The mechanism for capsid disassembly is currently unclear but host cell factors such as cyclophilins (CyPs) contribute towards successful capsid disassembly. HPV PsVs containing a CyPs-binding defective L2 show increased L1 co-localisation with the pseudogenome, implicating failure of capsid disassembly, leading to inhibition of infection. This also highlights that the separation of L1 from the pseudogenome is a necessary step in virus infection (32).

1.3.3 Subcellular trafficking

The separation of L1 and the pseudogenome is necessary for the localisation of the pseudogenome to the *trans* Golgi network, the next step in virus infection before trafficking to the ER and the nucleus. HPV does not encode its own polymerase therefore the genome must reach the nucleus in order to be transcribed and replicate. This is mediated by the L2 protein and host cell factors, as the pseudogenome in L1 only VLPs is not trafficked. L2 and the viral genome are transported in vesicles formed from the Golgi during G2/M transition where the vesicles are trafficked along microtubules. The containment of viral DNA in these vesicles prevents cGAS/STING activation. In these vesicles, the transmembrane L2 facilities the retrograde trafficking by recruiting cytosolic sorting factors. Upon mitosis and subsequent nuclear envelop breakdown, the pseudogenome is tethered to chromatin by L2 binding with it chromatin-binding domain, ensuring viral DNA is included on daughter cell nuclei after mitotic exit into G1 (33).

1.4 Virus lifecycle

1.4.1 Keratinocyte differentiation

The HPV lifecycle is dependent on epithelial differentiation. The structure of the epithelium is complex, the only proliferative cells are found in a single basal layer

attached to the basement membrane. After dividing, the new daughter cell undergoes several stages of differentiation, leading to formation of different zones in the epithelium; suprabasal (spinous), granular, and stratum corneum. This is a dynamic process ending with the continuous sloughing off of cells at the top of the epithelium. Between each stage of differentiation there are major changes in morphology. Upon differentiation into the suprabasal layer, there is an increase in cell-to-cell crosslinking which increases as the cell fully differentiates. After a keratinocyte is fully differentiated it is functionally dead, lacking organelles such as a nucleus which are needed for HPV replication (34).

1.4.2 Productive Virus lifecycle

In contrast to most viruses, HPV produces new virions in a differentiated daughter cell not the original infected basal cell. As HPV genomes are established as extrachromosomal elements and as HPV does not encode its own polymerase, the HPV lifecycle is tied to the cycle of the cell. This leads to a reliance on host cell machinery (35, 36). After infection of the basal cell, the genome is amplified to around 50-100 copies per cell, mediated by the virally encoded proteins E2 and E1. E1 is the primary replication protein, acting as a helicase to unwind viral DNA to initiate replication and E2 enhances its functions by loading E1 onto the replication origin. E2 also plays a vital role in tethering the viral episomes to the host chromosome, ensuring viral genome maintenance in mitosis (37, 38). After this point in the basal cell the number of genomes is maintained and virus protein expression is minimal, aiding in avoidance of the immune response. The suppression of viral gene expression is mediated by E2 which represses the P97 promoter through interactions of its DNA binding domain, preventing transcription factors accessing the promoter (39). As the infected basal cell divides, the genome is carried with the new daughter cell higher into the epithelium. The production of new virions requires vegetative viral DNA replication, which occurs once per cell cycle. However, as this must occur in differentiated cells which have exited the cell cycle and are no longer

capable of supporting DNA replication, viral proteins E6 and E7 activate host cellular

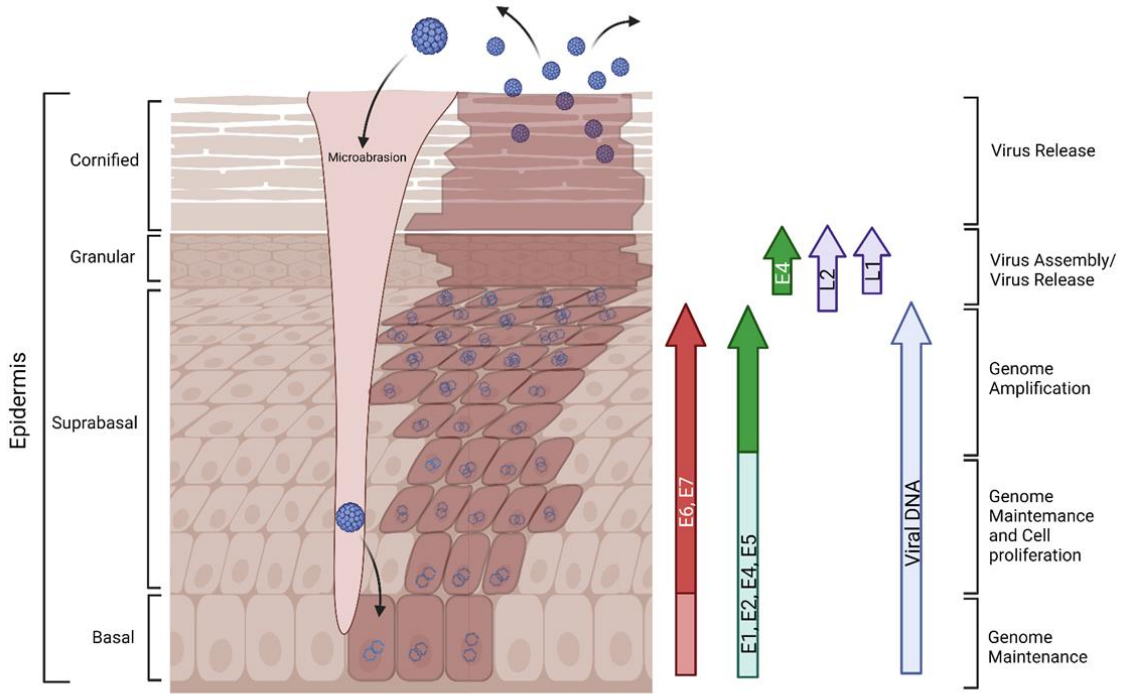

Figure 1.3 Productive HPV infection. Schematic of epithelium architecture and HPV lifecycle with viral gene expression. The stages of the virus lifecycle are outlined and are tied to the epithelium differentiation. HPV infects basal cells through microwounds and abrasions. Infected cells are shown in dark pink (created in biorender) (11).

DNA synthesis machinery (11, 40). The HPV-encoded oncogenes manipulate cells in many ways and much of the current research into HPV focuses on these interactions. E7 activates the cell cycle to allow for DNA replication through targeting retinoblastoma (Rb) for proteasomal mediated degradation as well as other transcription factors (41). This allows for the release of E2F from a repressive complex resulting in its constitutive activation and transcription of E2F target genes such as cyclins A and E, promoting S-phase entry. Furthermore, E7 also potentiates cyclin-dependent kinase 2 (CDK2) a crucial kinase for S-phase entry, by suppressing CDK inhibitors p21 and p27 (11). E6 targets p53 for proteasome mediated degradation, inhibiting proapoptotic responses to DNA damage caused by the abnormal extended S phase entry (42).

Towards the end of the virus lifecycle the accumulation of L1, L2 and E1^E4 leads to genome packaging and the assembly of virions in the nucleus (11). Virions are then released from the epithelial surface upon terminal differentiation of infected keratinocytes with loss of nuclear integrity and the shedding of keratinocytes from the epithelium (43).

1.4.3 Non-productive virus infection

Non-productive infections are characterised by the production of viral proteins but no infectious virions. It is generally associated with a dysregulated E6 and E7 expression, leading to increases in their activities. Frequently, E6 and E7 overexpression occurs due to the loss of E2 upon integration of the viral genome. This leads to host genomic instability associated with HR-HPV lesions including amplifications, deletions and translocation. Non-productive virus infection is a leading factor for cancer development in HR-HPV infections and is associated with cancerous lesions at a variety of sites (44).

1.5 Transmission

HPV is one of the most common sexually transmitted diseases globally with this thought to be the primary method of transmission for most HPV infections. Another form of horizontal transmission (between individuals of the same generation) is through skin abrasions, the most common method of transfer for ‘butchers’ warts’ (due to HPV 7 infection). HPV can also be vertically transferred (from mother to child) by passage through an infected birth canal. This can lead to juvenile recurrent respiratory papillomatosis which can be a potential danger to new born babies (45). Most infections clear within 6-12 months, however, persistent infection that fails to clear can result in the formation of high grade squamous intraepithelial lesions (HSIL) (46).

1.6 Epidemiology of HPV malignancies

Approximately 80% of women will become infected with HPV in their lifetime. Although it varies from country to country, in low-grade neoplasia (LSIL) and asymptomatic cervical infections, the most common HPV types responsible are HPV16,

HPV18, HPV31 and HPV58 (46). HPV detection increases with cervical disease severity, with HPV detected in 50-70% of cervical intraepithelial neoplasia (CIN)1/ LSIL lesions and between 90-100% in CIN3 infections (most severe before carcinoma) (see Figure 1.4). CIN grades are determined by the proportion of dysplastic cells (cells infected with HPV commonly exhibit koilocytosis, a perinuclear "halo" alongside irregular nuclei) in a sample. CIN 1 refers to less than a third of the epithelium is irregular, whereas CIN 2 is between a third to two thirds of the epithelium is irregular and CIN3 is more than two thirds. The transition from CIN3 to cancer is characterised by the invasion of the basement membrane (47). It is important to note that CIN1 is representative of an HPV infection and often regresses without treatment due to the immune response, not necessarily representing disease progression (48).

The first types of HPV associated with cancer were discovered in immunocompromised patients with the genetic disorder, epidermodysplasia verruciformis (EV). It was observed that these patients were unable to clear infections of beta HPV types 5 and 8, leading to the malignant transformation of warts and development of non-melanoma skin cancer (49). However, it is typically HR-HPVs which are associated with cancer, particularly HPV16 and HPV18 which together are responsible for approximately 70% of HPV-driven cancers. HPV is associated with cancers at a variety of sites such as anal, vaginal and penile cancers. Around 50% of penile cancers, 40-50% of vulvar cancers, 91% of vaginal cancers and up to 94% of anal cancers are HPV-driven (50). Additionally, HPV is predominantly associated with both cervical cancer and certain subsets of Head and Neck squamous cell carcinoma (HNSCC).

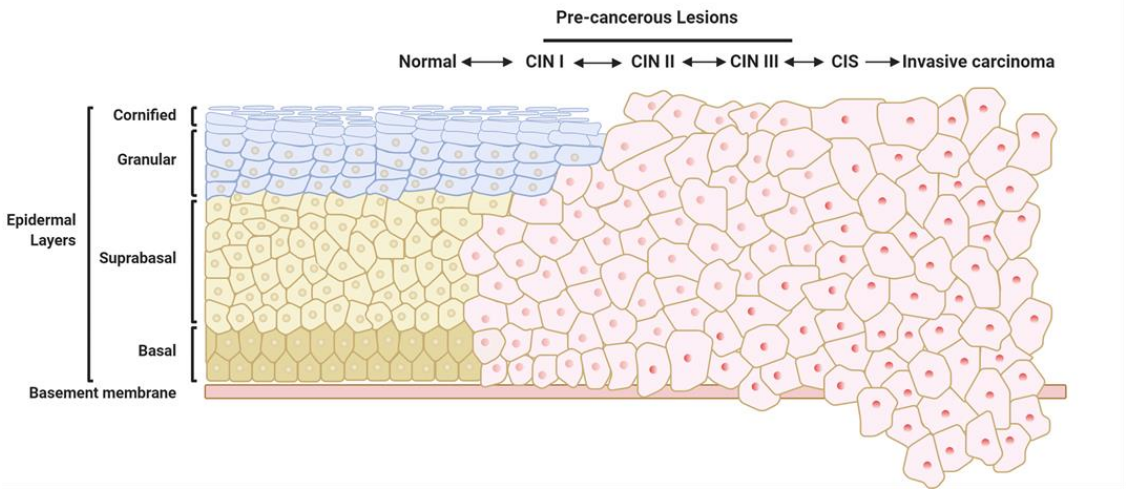

Figure 1.4 CIN grades. Schematic of changes to the epithelium from normal cells, progressing through CIN grades to cervical cancer (11).

1.6.1 Cervical carcinoma

Cervical cancer is the 4th most frequent cancer in women. In 2012 there was estimated to be 528,000 cases and 266,000 deaths globally with the majority of deaths occurring in low-income countries (51). HR-HPVs are responsible for nearly all cases. Characterised at the site which they occur, either squamous cell carcinoma (SCC) or adenocarcinoma (glandular epithelium of the endocervical canal) (52). Analysis of patient samples has shown that HPV16 is more prevalent in SCC and HPV18 is predominantly associated with adenocarcinoma (53). SCC accounts for roughly 70% of cervical cancer cases while adenocarcinoma accounts for roughly 20%. Interestingly, SCC rates are decreasing, in Europe, whilst adenocarcinoma rates are increasing, perhaps as cervical screening methods are less effective for this cancerous subset. While treatment does not differ between the two cervical cancer subsets, prognosis does with adenocarcinoma associated with poorer survival and a higher likelihood of metastasis. Furthermore, adenocarcinomas cases have a poorer response to chemotherapy and radiotherapy compared to SCC. The difference between the two cancer subsets that results in these phenotypes is not well understood (54). Additionally,

mortality and incidence rate for cervical cancer differs between developed and developing countries (Figure 1.5).

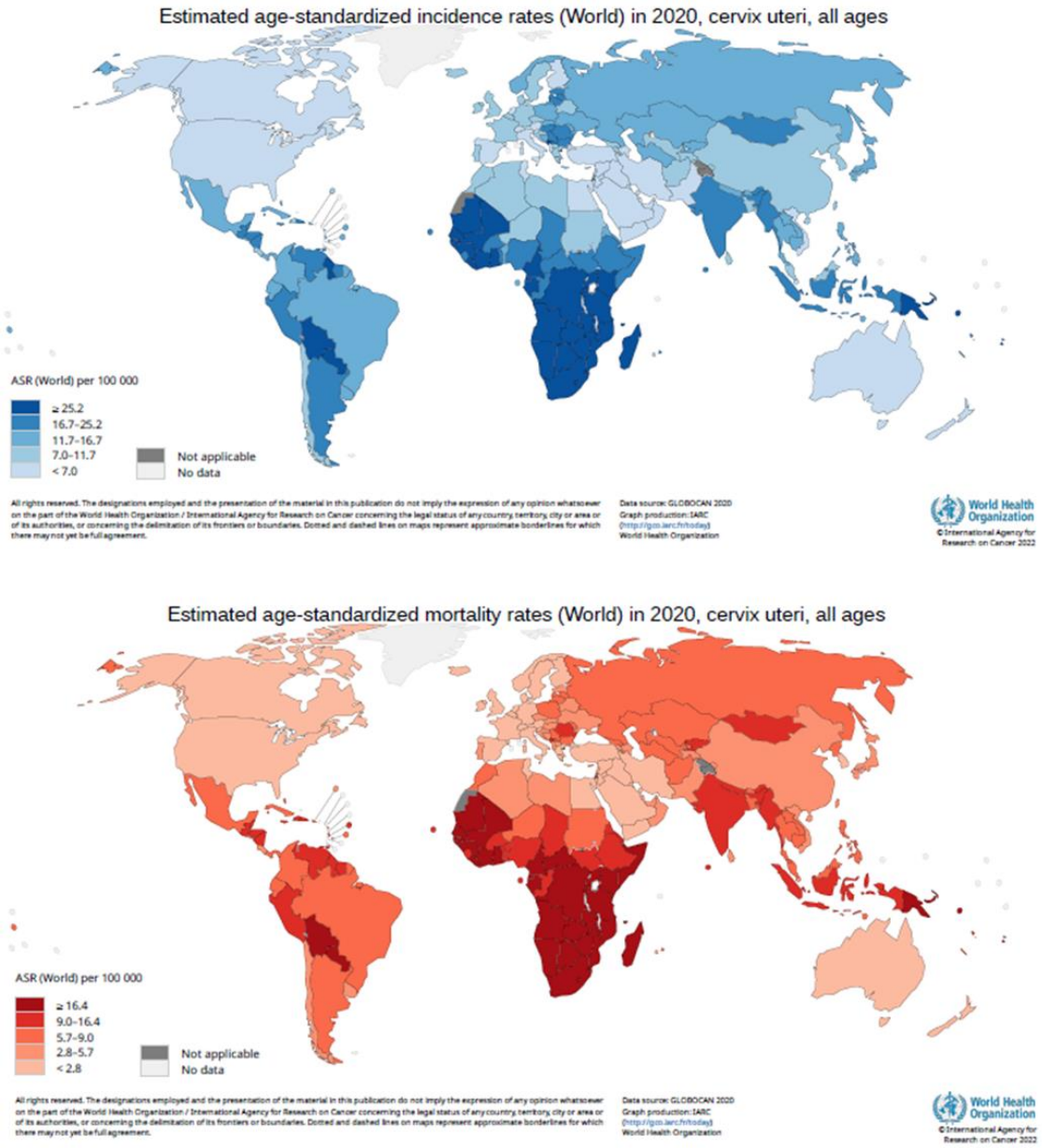

Figure 1.5 Age standardised rate of incidents (blue) and mortality (red) worldwide (51).

1.6.2 HNSCC

HNSCC are the 6th most common cancer globally and up to 70% of subsets such as oropharyngeal carcinoma, occurring in tonsils of the tongue are associated with HPV. HPV is considered the characterising feature of non-keratinized SCC, with neither tobacco nor alcohol playing a major role. Additionally, pharyngeal and oral cancers have

been associated with HPV but to a lesser extent (55, 56). Although HPV-negative tobacco related HNSCC cases have decreased by 50% between 1988 and 2004 HPV-positive cases have risen by 225% (57). Similarly to cervical cancer, integration of the HPV genome is a major step in the development of HPV-driven oropharyngeal carcinomas. These cancers are distinct and have a better prognosis compared to HPV-negative oropharyngeal carcinomas.

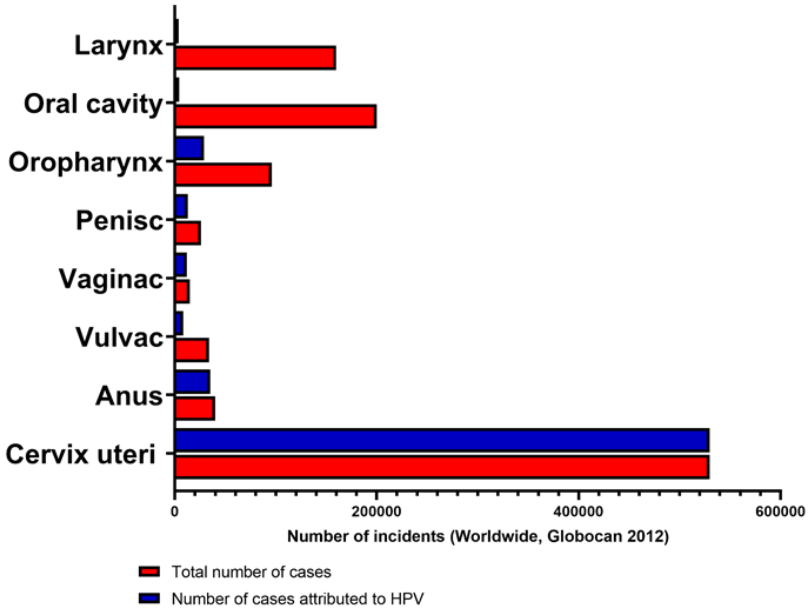

Figure 1.6 HPV-associated cancers. Graph of HPV-associated cancers worldwide in 2012. Includes both total number of cases and number of cases attributed to HPV (roughly 630,000 in total) (52).

1.7 Prevention and treatment of HPV-associated malignancies

1.7.1 Prevention and treatment strategies

Currently there is a 2-pronged approach in the prevention of cervical cancer, vaccinations and cervical screenings. The approach is defined in the 90:70:90 motto (90% vaccinated, 70% screened, 90% offered effective cervical cancer treatment). However, as over 80% of the cervical cancer burden is in developing countries, this approached is unable to be implemented, largely because of an absence of effective

cervical screening and a low vaccine uptake rate. For example, only 1% of vaccinated girls worldwide reside in developing countries (58).

1.7.2 Cervical screenings

The introduction of cervical screenings has been a relative success in developed countries with the proper infrastructure to ensure effective follow-up treatment where necessary. In the UK the NHS screening programme screens 3 million women for cervical cancer and is approximated to prevent 4500 cervical cancer associated deaths each year (59). Pap cytology and liquid-based cytology are two standard methods of screening with that latter more a more modern development. Usually, these screenings focus on the detection of CIN and if positive, detection of HPV components such as the genome or E6/E7 mRNA (60). Although a success in developed countries, cervical screening is yet to be effectively implemented in developing countries mostly due to limited funding, poor coverage, lack of screening quality and limited follow up treatment (61).

1.7.3 Vaccination

Currently there are several available prophylactic vaccines including; the 2006 tetravalent vaccine against HPV 6, 11, 16 and 18 (Gardasil), the 2007 bivalent vaccine against HPV 16 and HPV18 (Cervarix) and the 2016 nonvalent vaccine against HPV 6, 11, 16, 18, 31, 33, 45, 52, 58 (Gardasil 9). The latest vaccine Gardasil 9 not only protects against the causative agents for approximately 90% of cervical cancers but also HPV 6, 11 a major cause of genital warts. All three vaccines are based upon L1 only VLPs, which caused a strong immune response without infection. Originally given on a schedule of 3 doses to girls between the ages of 9-13 years old, it is currently recommended to be given on a two-dose schedule to anyone under the age of 15. The three-dose schedule is still recommended for 15- 45 years old and immunocompromised patients. The inclusion of males under the age of 15 to be given the vaccine is most likely a response to the increase in HNSCC being observed globally, especially in developed countries.

The use of conventional enzyme-linked immunosorbent assays measured vaccine-induced antibody responses to be at almost 100% in vaccinated individuals against L1 in a type restricted manner. Additionally, studies 10 years post vaccination showed that individuals retain high seropositivity in all age groups, showing that the vaccines are very effective. Although less information is available, it is thought that the vaccines prevent infection of HPV at other sites well, with one study estimating at 84% decrease in anal infections (50).

1.7.4 Treatments

Although the prophylactic vaccines are highly effective, only 8% of developing countries have vaccination programmes and a drawback of these vaccines is that they are not therapeutic and do not induce cell immunity. Currently there are no specific therapeutic treatments for HPVs. Therefore, it can be assumed that in developing countries at least, cervical cancer and other HPV related malignancies will remain a problem for decades to come (62).

Currently the three recommended strategies against cervical cancer are the three broad treatments for any cancer; surgery, radiotherapy and hormone chemotherapy. Although the current surgical method Wertheim-Meigs is less drastic then other historical procedures, it is only recommended for the early stages of cervical cancer due to metastasis to the regional lymph nodes commonly occurring with no distinctive clinical presentation (63).

1.8 HPV-encoded oncoproteins

1.8.3 E5 oncoprotein

E5 is the smallest and least characterised oncoprotein encoded by HPV. It is a highly hydrophobic transmembrane protein and in the case of HPV 16 is 83 amino acids long (10 kDa). E5 has been found to be localised to the Golgi, ER and nuclear membranes (64). Although originally thought to be lost upon virus integration, high levels

of E5 have been detected in a sub-set of cervical cancers and HNSCC (65). Although considered minor in comparisons to E6 and E7, it is the major transforming protein in Bovine Papillomavirus (BPV1). Although BPV1 E5 displays strong transforming abilities, HPV E5 only display weak activity *in vitro (66)*. Nevertheless, E5 is classified as an oncoprotein as both in human keratinocytes and mouse fibroblasts it can induce anchorage-independent growth and tumours but is not needed for either E6 or E7 cell transformation (67). As E5 is expressed at high levels in the early stages of transformation, it has been suggested as a possible target to halt the progression of premalignant lesion to cervical cancer (68). E5 is hypothesised to enhance the activities of E6 and E7, cooperating to stimulate proliferation in mouse primary cells. Additionally, transgenic mice expressing HPV 16 E5 developed spontaneous skin tumours and epidermal dysplasia while also showing enhanced DNA synthesis and aberrant differentiation (69). Although it has been shown that E5 activity is not required in undifferentiated primary keratinocytes, E5 is thought to play a key role in the productive virus lifecycle in differentiated cells through regulating the host cell cycle and viral genome amplification (70).

1.8.3.1 E5 as a viroporin

E5 is a viroporin (viral pore-forming membrane protein) (68). Viroporins contain one or more hydrophobic transmembrane regions which are alpha helical in structure. Upon insertion into membrane, viroporins oligomerise to form a hydrophilic pore (71). Expression of viroporins allow viruses to induce membrane permeability, which is often crucial for virus entry, production of infectious virions and/or release. Viroporins have also been documented to mediate host cellular processes such as vesicle trafficking and apoptosis which can be crucial for virus lifecycles (72). E5 has been documented to form a hexameric complex, which is essential for E5-mediated activation of host cell signalling pathways such as extracellular signal-regulated kinase1/2 mitogen-activated protein kinase (ERK 1/2-MAPK), key regulators and proliferation (68).

1.8.3.2 E5 functions

Research has shown that E5 binds to many host proteins, including modulators of host signalling pathways. This includes dysregulation of epithelial growth factor receptor (EGFR) signalling. EGFR signalling plays key roles in keratinocyte differentiation. Not only does increased EGFR signalling lead to increased proliferation, but it also suppresses keratinocyte differentiation (73, 74). Furthermore, loss of EGFR signalling induces G2/M arrest (75). E5-induced epithelial dysplasia in transgenic mouse models is mediated by EGFR signalling as the phenotype is lost with the expression of a dominant negative form of EGFR (69). The mechanism for E5 modulation of EGFR signalling is still debated. Although it was originally thought that E5 suppressed the degradation of EGFR through binding to the 16K subunit of the vacuolar H+ ATPase preventing the acidification of endosomes, other studies have argued that the binding does not occur in high enough levels to mediate this process (76). One study suggested as little as 5% of available 16K is bound to E5 in a 1:1 ratio, too low to prevent assembly of the H+ V-ATPase complex. The same study suggests the suppression of EGFR degradation is due to E5-induced dysregulation of trafficking. The perturbation of endocytic trafficking by E5 is noted to be both pH independent and transport independent but the exact mechanism has yet to be elucidated (77).

It has also been suggested that E5-mediated regulation of EGFR occurs on a protein level as no changes in the mRNA expression have been observed (78). One possible mechanism is through disruption of the CBL-EGFR interaction by E5. CBL is an ubiquitin ligase which ubiquitinates EGFR, targeting it for degradation. It is hypothesised that E5 can physically block this interaction, leading to increased EGFR (79).

There is evidence that E5 also suppresses keratinocyte growth factor receptor/fibroblast growth factor receptor 2b (KGFR/FGFR2b) signalling. In contrast to most growth factors receptors, KGFR signalling has tumour suppressive functions, playing a crucial role in the regulation of epithelial differentiation (80). In mice lacking

KGFR/FGFR2b, there was an increase in the development of papillomas and mice were more sensitive to chemical carcinogenesis (81). qPCR analysis showed a transcriptional downregulation of KGFR expression in E5 expressing keratinocytes, suggesting an E5 mediated downregulation of KGFR signalling (80).

In addition, to modulating proliferation, E5 inhibits apoptosis. Dysregulation of DNA synthesis and the other activities of E6 and E7 should induce apoptosis in normal keratinocytes. E5 has been shown to suppress both FAS and tumour necrosis factor-related apoptosis inducing ligand (TRAIL)- mediated apoptosis and ultraviolet radiation-induced apoptosis in keratinocytes. E5-mediated suppression of apoptosis occurs through the targeting of Bcl-2-associated X protein (Bax) for ubiquitin-mediated degradation, but the exact mechanism has yet to be elucidated (82). Additionally, E5 is suggested to suppress apoptosis through increasing signalling through both the phosphatidylinositol 3-kinase-Akt (PI3K/ Akt) and ERK1/2-MAPK signalling pathways (83).

A crucial step towards cervical cancer is the failure of the immune system to clear the virus infection and E5 aids this. E5 does this in numerous ways: dysregulation of Major Histocompatibility complex I and II (MHC 1 and II), suppressing interferon- κ (*IFNK)* transcription and NK activities (84-87). For instance, E5 disrupts antigen presentation through dysregulating MHC antigen processing by blocking trafficking between the ER, Golgi and cell membrane of MHC components by binding to the MHC heavy chain (85). Additionally, E5 leads to retention of CD1d, a glycoprotein key for antigen presentation to CD1d-restricted invariant NKT cells (84, 88). E5 also suppresses the production of keratinocyte specific IFK-κ through suppressing *IFNK* transcription in an EGFR-dependent manner (87). Together these activities allow for E5 to promote evasion of the immune response in the virus lifecycle.

1.8.2 E6 oncoprotein

HR-HPV E6 was first suspected to be an oncoprotein in the 1980s as it was found to be retained and highly expressed in cervical tumours (89). E6 was found to transform both human mammary epithelial and rat primary cells, demonstrating oncogenic activity (90, 91). Although LR-HPV E6 share some activities with the HR-HPV E6, they are unable to induce transformation in primary cells, hence their classification as low risk. It is notable that keratinocytes transformed with E6 are only able to form tumours in mice after extended passage, resembling HPV-driven cancer progression (92). Despite the oncogenic activity of E6, malignant progression occurs through the cooperation of E6 and E7 (93). Although many of the functions of E6 have been characterised, it is clear that additional functions remain to be better elucidated and some remain undiscovered.

1.8.2.1 HR-HPV E6 structure

Although the full-length structure of E6 has recently been resolved by nuclear magnetic resonance (NMR), much of our previous understanding of the specific domains in E6 has been deduced through analysis of the protein sequence. HR-HPV E6s are approximately 150 amino acids long and contain two zinc finger domains (formed of 3 β-sheets and 2 short helices are separated by a short α-helix), which are essential for E6 activities, formed by a pair of CXXC sequences (94, 95). Furthermore, the C-terminus contains a PDZ-binding motif (PBM) consisting of a XTXV/L sequence (95). Together, these domains allow E6 to target a multitude of host cellular factors and disrupt host processes and signalling pathways despite a lack of intrinsic enzymatic activity.

1.8.2.2 HR-HPV E6 functions

E6 is capable of binding to multiple host cell proteins to perturb several key host cell functions (Figure 1.7). The best studied function of E6 is the degradation of the p53 tumour suppressor protein. p53 is a sequence

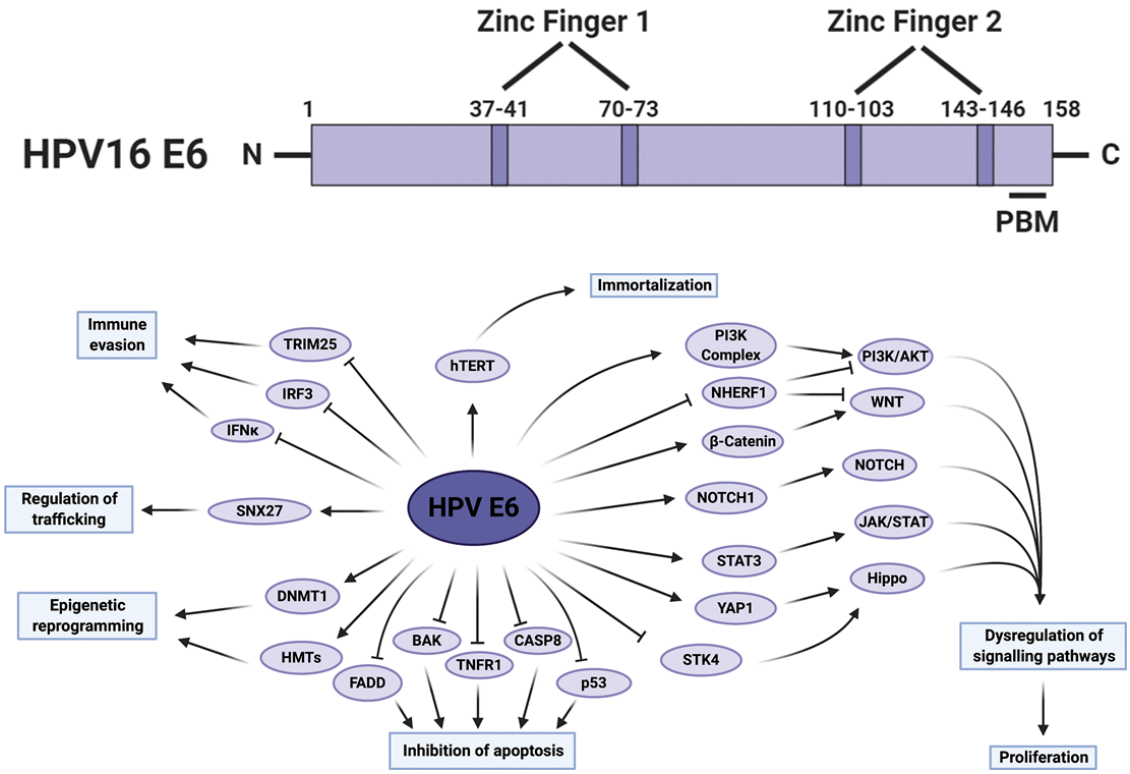

Figure 1.7 HR-HPV E6. A) HPV16 E6 oncoprotein structure. Numbers refer to amino acid positions. B) Summary of E6 activities that contribute towards transformation and carcinogenesis (11).

specific, DNA binding protein that serves as an effector of DNA damage. It is mutated or inactivated in over 50% of cancers in humans and regulates the cell cycle, cellular senescence and apoptosis through transcriptional regulation (96). It is under exquisite control by a number of mechanisms, including by protein-protein interactions with the E3 ubiquitin ligase Mouse double minute 2 homolog (MDM2). Under normal cellular conditions, MDM2 binds to the transcription activation domain of p53, preventing its transcriptional activity and targeting p53 for proteasomal degradation. Loss of the MDM2-p53 interaction subsequently allows for p53 activation (97, 98).

The stabilisation and activation of p53 can be induced by multiple stimuli, including cellular stress, acute DNA breaks or errors in DNA replication. For example, when double stranded DNA breaks occur, the ATM kinase is activated, which subsequently phosphorylates checkpoint kinase 2 (Chk2) resulting in Chk2-mediated

phosphorylation of p53 at serine 20. This phosphorylation is in the site where MDM2 binds to p53, thus preventing the interaction, leading to p53 stabilisation and activation. Additionally, ATM phosphorylates MDM2 at serine 395, leading to increased ATM binding to p53 mRNA, promoting transcription, upregulating p53 activity (99). Single stranded DNA breaks activate the Ataxia-telangectasia and Rad3 related (ATR) kinase which phosphorylates p53 at serine 15 and also decreases MDM2 binding to p53 (100). E6 binds with the conserved LXXLL motif of E6-associated protein (E6-AP) forming a stable complex which can bind p53, targeting it for proteasomal-mediated degradation, inhibiting p53-mediated apoptosis (42).

In addition to targeting p53, E6 targets other proteins involved in apoptosis such as Bak to suppress intrinsic apoptosis pathways. Under normal physiological conditions, anti-apoptotic Bcl-2 proteins antagonise the activity of the pro-apoptotic effector molecule proteins such as Bak. When activated, Bak undergoes conformational changes to expose its Bcl-2 Homology (BH) domains, followed by homo-dimerisation which allows binding to pro-survival proteins, leading to their inhibition (101). This activity causes morphological changes in the inner mitochondrial membrane resulting in the opening of mitochondrial permeability transition pores and the subsequent loss of mitochondrial membrane potential (102). This allows for the release of pro-apoptotic proteins which are normally sequestered in the mitochondrial intermembrane space, inducing apoptosis through DNA fragmentation of chromatin condensation (103). Similarly to p53, E6 complexes with E6-AP to target Bak for ubiquitin-mediated degradation (104). Furthermore, E6 also dysregulates the extrinsic apoptosis pathway through interactions with Fas-associated protein with death domain (FADD) and caspase 8 (11).

E6 can promote oncogenesis through chromosome instability due to the activation of human telomerase reverse transcriptase (hTERT) in the telomerase complex. Increased telomerase activity allows for indefinite proliferation due to the lengthening of telomeres. Normally, the shortening of telomeres signals the end of a

cells' life and activates a DNA damage response, leading to the cell entering senescence, however the overexpression of E6 and subsequent activation of telomerase enables cells to circumvent senescence (11, 105).

Another method by which E6 transforms cell is through altering gene expression profiles of cells, a common event in cancer (106). One method by which E6 regulates gene expression is via DNA methylation. Hypermethylation of CpG sites in the promoter regions of tumour suppressive genes has long been linked with suppression of gene expression and the promotion of oncogenesis (107). Conversely, the hypomethylation of CpG sites of oncogenes leads to increased gene expression (108). DNA methylation is regulated by DNA methyltransferases (DNMTs), widely observed to be dysregulated in cancer and strongly linked to oncogenesis (109). E6 indirectly increases DNMT1 expression due to the degradation of p53, leading to the release of specificity protein 1 (SP1)which upregulates *DNMT1* expression (110). A study in 2012 found that over 5000 and 2000 genes respectively showed increased methylation, while over 3000 and 4000 respectively had decreased methylation in HPV16 and HPV18 associated cervical cancer (111). This significant shift in host gene methylation profiles indicates that DNA methylation plays an important role in HPV-induced carcinogenesis. E6 also dysregulates global gene expression through alteration of histone alteration machinery. Histones are key for the correct packaging of DNA and therefore, are crucial for the regulation of gene expression. Histones 2A (H2A), 2B (H2B), 3 (H3) and 4 (H4) are essential chromatin subunits. Each nucleosome unit consists of two H2A-H2B dimers and two H3-H4 dimers forming a histone octamer that 147 DNA base pairs can wrap around. The C-terminal structure of H2A, H2B, H3 and H4 is essential for histone interactions while the N-terminal is much less structured and is it thought that modification of the N-terminal allows for changes in accessibility of the genome for example by histone deacetylases (HDACs) and histone acetyltransferases (HATs). HDAC and HATs modify the acetylation status of histone to regulate gene expression.

Acetylation of histones weakens the DNA-histone interaction, favouring gene expression, whereas deacetylation favouring the compact form of chromatin, reducing gene expression. The expression of HDACs and HATs is often found dysregulated in cancer (112).

Another histone modification of importance to epigenetics is histone methylation. In contrast to acetylation/deacetylation, methylation leads to the formation of a binding site for chromatin-associated proteins containing specific methyl histone-binding domains. The lysine residues of histones can be mono, di or tri methylated whereas arginine is either mono or di methylated. The associated effects of certain methylation events on H3 and H4, in particular, have been extensively researched. The consequence of methylation differs between specific residues leading to either transcriptionally active or transcriptionally repressed chromatin conformations (113).

E6 has been documented to dysregulate histone modifications, leading to changes in global gene expression. One mechanism of dysregulation is through interactions with the histone acetyltransferases p300 and CBP, inhibiting their activity. HPV16 E6 inhibits the activation of p53 and NFκB in a p300/CBP dependent manner (114). Additionally, E6 interacts and inhibits histone methyltransferases (HMTs) such as coactivator associated arginine methyltransferase 1 (CARM1), protein arginine methyltransferase 1 (PRMT1) and SET domain containing lysine methyltransferase (SET7), inhibiting their enzymatic activity. Although these proteins are mostly known to be recruited to p53-target genes promoters, it is thought they have wider cellular functions that contribute to global mRNA expression which are not yet elucidated (115). The inhibition of HATS and HMTs highlights the ability of E6 to induce genome-wide changes to mRNA expression through aberrant changes in chromatin structure through manipulation of histone modifications.

1.8.2.3 Dysregulation of host signalling pathways by E6

Another critical function of E6 is dysregulation of host cellular signalling pathways. Signalling pathways are essential mechanisms utilised by a cell to communicate with other cells and respond to the environment. The binding of ligands to specific receptors triggers a cascade, subsequently affecting transcription of host genes, regulating host processes. Therefore, many signalling pathways are dysregulated in cancer. Amongst others, E6 manipulates host cell signalling pathways such as the Wnt/β-catenin, Notch, STAT3 and PI3K/Akt pathway to promote cell survival, transformation and proliferation (11). For instance, E6 in complex with E6-AP stabilises β-catenin, the main effector of the Wnt signalling pathway leading to its aberrant nuclear accumulation. This was recently discovered to occur via the targeting of NHERF1, a suggested tumour suppressor, by the E6/E6-AP complex (116). This nuclear accumulation leads to the formation of a complex with β-catenin binding factors and the recruitment of histone modification proteins leading the transcription of genes promoting proliferation and survival (117).

E6 also is known to dysregulate a single signalling pathway such as the PI3K pathway by several mechanisms. E6 can directly interact with and activate the PI3K complex, activating the pathway, inactivate PTEN, a pathway repressor and block TSC Complex Subunit 1/2 (TSC1/2) mediated repression of mTOR. Given the essential role that PI3K pathway plays in the regulation of proliferation, it is unsurprising that HR-HPV E6 dysregulates this pathway at multiple points (118-120). The aberrant activation of the pathway by E6 allows for the dysregulation of proliferation and the suppression of apoptosis amongst other cellular processes.

Collectively, the dysregulation of these pathways drives survival, proliferation and transformation of cancer cells.

1.8.2.4 E6 and PDZ proteins

HR-HPV E6 oncoproteins C-terminal PDZ binding motif is used to interact with PDZ domain containing proteins. Although E6 interacts with just a fraction of PDZ proteins (19 out of 200), these interactions are vital for its activity. Often the interaction of E6 with these proteins results in their degradation or mislocalisation, hence in the case of Scribble Planar Cell Polarity Protein (SCRIB) leads to disruption of cell polarity, commonly seen in malignant cells. This domain is also key for the activation of proteins such as JNK, resulting in activation of the pathway and increase proliferation and Epithelial-mesenchymal transition (EMT) (11).

1.8.2.5 LR-HPV E6 interactions

LR-HPV E6 proteins share significant sequence homology to HR-HPV E6 but they do not usually possess transformative abilities and generally have not been investigated to the same extent as HR-HPV E6 proteins (121). Although LR-HPV E6s can target some of the same host cellular factors, it is well evidenced that they do not share all the same targets as HR-HPV E6s. For example, whilst LR-HPV E6 proteins can bind and inhibit p53 they do not tend to degrade the protein. Generally, LR-HPV E6s bind to p53 with a low affinity and do not interact with E6-AP (122). In contrast, overexpression of LR-HPV E6s leads to the accumulation of β-catenin in a NHERF1-dependent mechanism (116). Furthermore, overexpression of LR-HPV E6s also leads to the degradation of Bak, similar to HR-HPV E6s (123). Together, these interactions suggest LR-HPV E6s are still capable of promoting proliferation and disrupting apoptosis, necessary functions for the productive virus lifecycle, but not to the same extent as HR-HPV E6s.

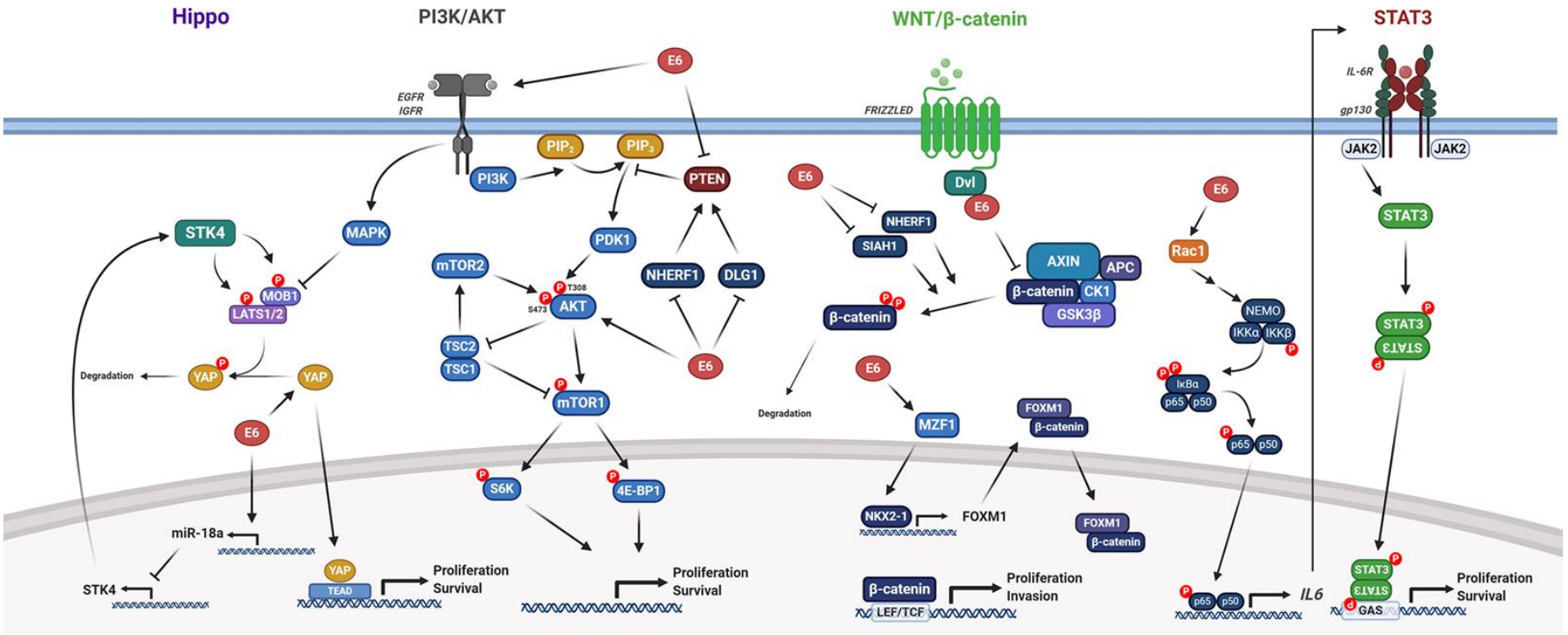

Figure 1.8 HR-HPV E6 modulation of host signalling pathways. Schematically summary of the mechanism of how HR-HPV E6 dysregulates host cell signalling pathways (11).

1.8.3 E7 oncoprotein

E7 was the first HPV oncogene to be characterised, shortly before E6, in the late 1980s (124). Although it is well documented that E6 and E7 cooperate to promote oncogenesis, studies have shown that expression of E7 alone in transgenic mice was sufficient to induce cervical dysplasia and invasive cervical cancer (125). E7 predominantly localises to the nucleus but can shuttle to and from the cytoplasm (11).

1.8.3.1 E7 structure

HR-HPV E7 consists of approximately 100 amino acids and shares homology with proteins from other DNA tumour viruses. E7 contains 3 conserved regions (CR), CR1, CR2 and CR3, of which CR1 and CR2 are conserved with adenovirus and SV40 including a highly conserved LXCXE motif, essential for E7s binding to Rb (126). CR3 of E7 is a zinc finger binding domain, consisting of two CXXC motifs that interact with a $Zinc^{2+}$ ion separated by 29-30 amino acids. Mutational analysis showed this region is critical for multiple E7 functions (127).

E7 can be post-translationally modified by phosphorylation and ubiquitination which regulate its function. The phosphorylation of E7 by casein kinase II (CKII) at residues 32 and 34 enhances the interactions between E7 and cellular targets, although not all of these interactions have been characterised. Loss of the phosphorylation sites through mutation leads to a decrease in cell growth (128). Another characterised phosphorylation event is the phosphorylation of E7 by protein kinase C at residue 7, which has been linked to E7 stability and transformative activity (129). Furthermore, it is documented that UbcH7, an E2 ubiquitin-conjugating enzyme and SCF (Skp-Cullin-F box) ubiquitin ligase ubiquitinates the amino terminal of E7 leading to ubiquitin-dependent degradation (130). Although E7 from several different low and high-risk HPV types have been reported to be ubiquitinated, the residues are often not conserved and therefore the importance of the ubiquitination has not yet been elucidate, but mutational analysis shows the modification may have roles in protein stability (131).

1.8.3.2 HR-HPV E7 functions

Like E6, E7 perturbs many host cell process through binding to multiple host cell proteins. Perhaps the best characterised interaction of E7 is the degradation of Rb. The gene encoding Rb, *RB1* was identified in 1987 (132). Much of what we know today of the functions of Rb was elucidated from studies of DNA tumour viruses, including its role as a cell cycle regulator (133). Now it is understood that Rb has roles in cellular processes such as apoptosis, cell-cycle checkpoints, replication and differentiation (134, 135).

The first Rb interaction characterised was with E2F. Rb binds to the transactivation domain of E2F using a highly conserved region of the Rb pocket domain, inhibiting E2F activity (136). There is also an additional interaction between the Rb carboxy-terminal domain (RBC) and the marked box of E2F, hypothesised to be important for the regulation of E2F1-specific activities (137). Early research showed that the interaction between Rb-E2F leads to the inhibition of E2F-target gene expression. These genes would usually promote DNA synthesis and cell cycle progression (138). However, cyclin dependent kinases (CDKs) can phosphorylate pRb, preventing pRb-dependent repression of E2F. This is because phosphorylation disrupts the E2F binding site within the pocket domain. Mutational analysis showed that the inactivation of Rb is not dependent upon one phosphorylation event, but several such as by CDK2, 4 and 6 in complex with cyclins D or E. The activation of E2F leads to cell cycle progression into S-phase (139). Rb possesses other non-canonical tumour suppressive activities such as regulation of heterochromatin and E-cadherin, but these are less characterised. Rb activity is frequently lost in cancer, either due to loss of Rb expression or hyperphosphorylation of Rb. Osteosarcoma tumours with loss of Rb are more aggressive and have higher rates of metastasis (140).

HR-HPV E7 bind to Rb with high affinity and is key for its transforming activity. E7 binding to Rb leads to subsequent degradation and allows for uncontrolled activation

of E2F. This allows for cells to enter the S-phase unscheduled, despite a lack of signals, allowing for DNA replication, key for the virus lifecycle (141). Although this would usually induced p53- dependent apoptosis, in HPV infection and HPV-driven cancers, this is negated with E6 activity, evidencing the cooperation between E6 and E7.

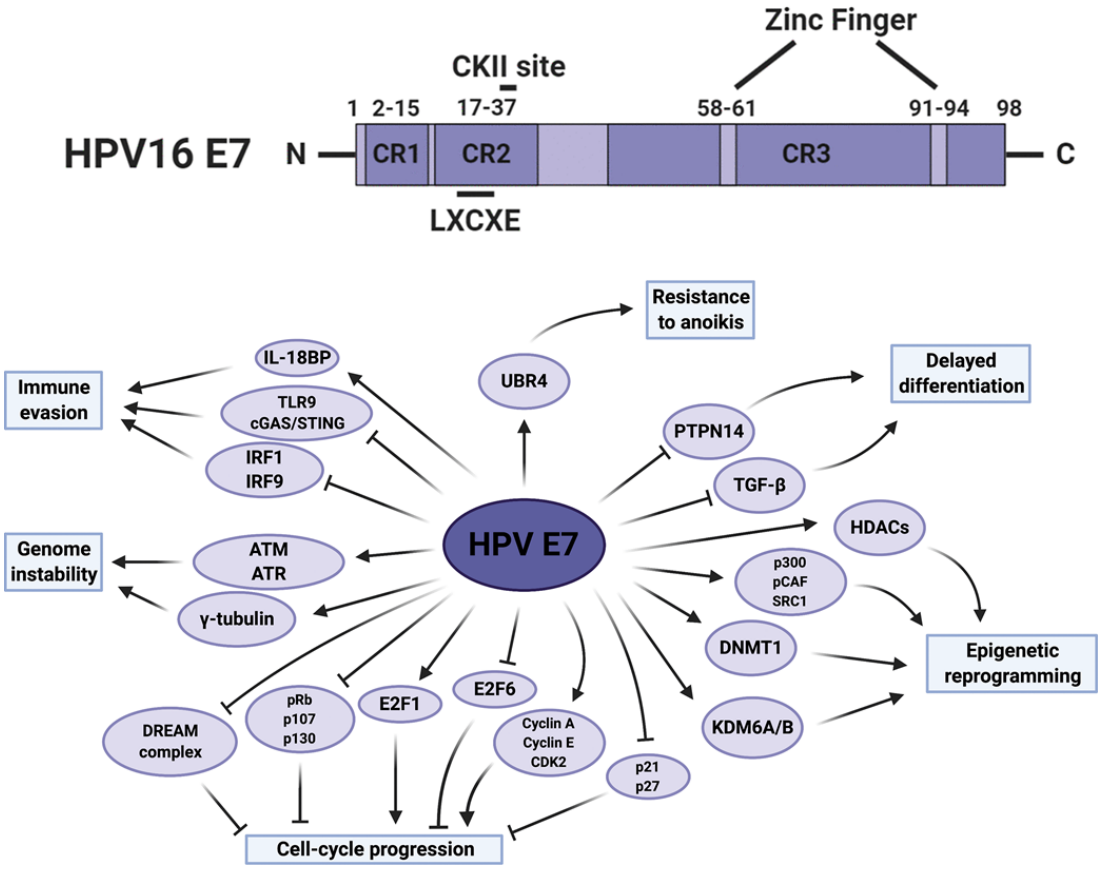

Figure 1.9 HR-HPV E7. A) HPV16 E7 oncoprotein structure. Numbers refer to amino acid positions. B) Summary of E7 activities that contribute towards transformation and carcinogenesis (11).

Another host cell target of E7 is γ-tubulin, one of the five currently identified tubulin isoforms forming the tubulin family of guanosine triphosphateases (GTPases). Predominantly localised to the cytoplasm, γ-tubulin forms dynamic structures such as γ-tubules and γ-strings creating a meshwork that varies depending on the cell cycle. Evidence suggests that γ-tubulin is a critical regulator of G1-S phase cell cycle transition as well as cytokinesis and mitotic progression. It has also been suggested that γ-tubulin

is a key component of the pericentriolar protein matrix, itself an important regulator of checkpoint proteins. Additionally, approximately 20% of γ-tubulin is localised to centrosomes. Although the role of γ-tubulin in cancer has yet to be elucidated, centrosome amplification in cancer is linked to poor prognosis and γ-tubulin has been shown to have alterations in expression and localisation in a range of cancers (142). Recent research has suggested that E7 interacts and regulates γ-tubulin in an Rb-independent manner. It has been hypothesised that this interaction allows for centrosome abnormalities that induce genomic instability and subverts other γ-tubulin functions such as cell cycle regulation. Genomic instability has been shown to promote viral integration and therefore cancer progression. As both the induction of genomic instability and cell cycle regulation are key roles of E7, the importance of this interaction may not be fully appreciated or elucidated (143).

Numerous studies have identified the immune evasion properties of E7. This occurs through many mechanisms including dysregulation of innate immune receptors such as toll-like receptor 9 (TLR9). TLR9 are expressed in both plasmacytoid dendritic cells and B cells as well as nonimmune cells such as epithelial cells, localised to the endosomes. TLR9 recognises unmethylated CpG-motifs of microbial DNA. Upon recognition, TLR9 signals interferon and NF-κB dependent inflammatory cytokines through the recruitment of MyD88 and IRAK4 (144). To prevent the triggering of an immune response by HPV, E7 activates the canonical NF-κB pathway to induce formation of a NF-κBp50–p65 complex as well as the recruitment of chromatin modifying enzymes and ERα. This leads to the silencing of TLR9 expression, therefore preventing the triggering of an immune response (145).

This is not the only way E7 modulates the immune response. E7 has been found to bind to Interferon Regulatory Factor-9 (IRF9), the DNA-binding region of the IFN-stimulated gene factor 3 (ISGF3) and IRF1, preventing both IFN-α and IFN-β responses

(65, 146) Additionally, E7 similar to E5, impairs MHC class I antigen processing and presentation through an IRF1, TAP1 and IFN-γ-dependent mechanism (147).

1.8.3.3 E7 targets similar host functions as E6

Although E7 has distinctly different targets to E6, often their functions overlap, leading to them targeting the same process. An example of this is the targeting of DNA methylation through DNMT1 through different mechanisms. E7 targets DNMT1 by two distinct mechanisms. E7 binding to Rb leads to the release of E2F transcription factor, inducing expression of *DNMT1*. Additionally, E7 is able to bind to DNMT1, inducing a conformational change, promoting its activity (148, 149).

E7, like E6 also dysregulates histone modification enzymes such as HDACs to dysregulate the host transcriptome. HDACs remove the acetyl groups from histones, leading to a repression of transcription. E7 has been found to interact with HDACs to both represses transcription and displace HDACs leading to transcription activation (65). Furthermore, many of the host signalling pathways dysregulated by E6 are also dysregulated by E7, through different targets, again showing cooperation between E6 and E7.

1.9 The Hippo signalling pathway

1.9.1 Pathway discovery

Key components of The Hippo signalling pathway were originally discovered in *Drosophila* in 2003 by genetic screens for tumour suppressive genes. Warts, Salvador, Mats and Hippo were all identified in quick succession with loss-of-function mutants, resulting in tissue overgrowths and were found to form a signalling cascade (150-153). Later Yorkie was identified as the target of the kinase cascade through a screen for Warts binding proteins. It was observed that overexpression of Yorkie led to the same phenotype as loss of Hippo signalling (154) and soon, a pathway from plasma membrane to nucleus was elucidated. In 2007 the pathway was discovered to be conserved in

mammals leading to characterisation of the Hippo pathway-mediated regulation of key functions such as cell proliferation, organ size and survival (155).

1.9.2 Mammalian Hippo pathway

In the canonical mammalian Hippo signalling pathway (Figure 1.10), STE20-Like Protein Kinase 3/4 (STK3/4) activation are regulated by upstream proteins including TAO kinases (TAOK) and Ras association domain family (RASSF) proteins, in response to a number of stimuli (156). For example, although the exact mechanism is still unclear, it is hypothesised that TAOK1-3 can activate STK3/4 in response to stimuli from Neurofibromin 2 (NF2) and kidney and brain expressed protein (KIBRA). Studies have shown that NF2 is activated by detachment from the extracellular matrix, cell contact inhibition and loss of growth factor signalling, and these stimuli can activate the Hippo signalling pathway (157). STK3/4 are activated through phosphorylation of residues in their activation loop (Thr183 or Thr180). The Sav/RASSF/Hpo (SARAH) domain of STK3/4 has also been shown to be important in STK3/4 activation, allowing for its dimerisation, resulting in autophosphorylation and activation (156). Some regulators of the Hippo pathway, such as the RASSF proteins, interact with the SARAH domain present in STK3/4 to prevent dimerisation-mediated activation of the kinases. However, RASSF1A has been experimentally observed to promote activation of STK3/4 by binding the SARAH domain, preventing STK3/4 dephosphorylation in response to DNA damage mediated by ATM and ATR (158).

When activated, STK3/4 phosphorylate Large tumour suppressor kinase 1/2 (LATS1/2) and MOB kinase activator 1 (MOB1) with the help of the scaffolding protein Salvador homolog 1 (Sav) (159). MOB1 phosphorylation enhances the ability of STK3/4 to phosphorylate LATS1/2, leading to its activation. Active LATS1/2 can then phosphorylate serine 127 of Yes associated protein (YAP) and S89 of Transcriptional Co-Activator With PDZ-Binding Motif (TAZ) transcription factors, leading to the binding of YAP/TAZ to 14-3-3 proteins and their cytoplasmic retention. Cytoplasmic localised

YAP/TAZ cannot interact with nuclear partners including members of the TEAD, SMAD and RUNX transcription factor families (159). YAP/TAZ are also phosphorylated at S397 and S311 respectively by LATS1/2, promoting their ubiquitination and proteasomal degradation (160).

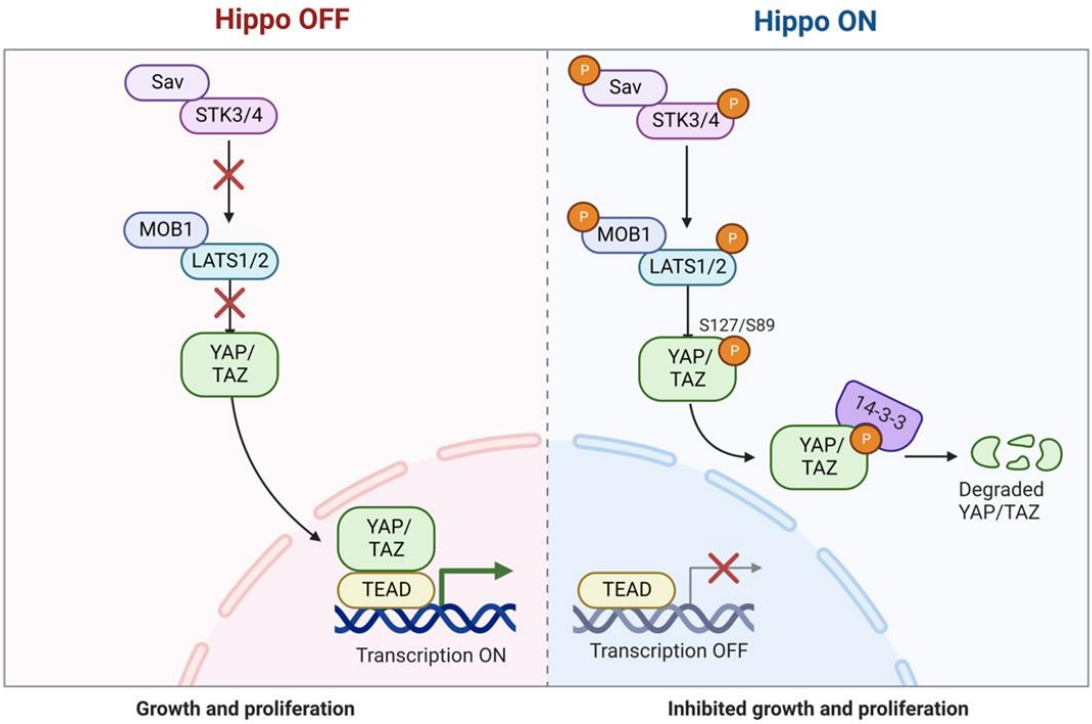

Figure 1.10 The mammalian Hippo signalling pathway. Schematic of the mammalian Hippo signalling pathway. When the pathway is off, YAP and TAZ are free to enter the nucleus and interact with transcription factors such as TEAD to promote transcription of pro-proliferative genes. When activated, STK3/4 phosphorylate and therefore activate LATS1/2 with the help of SAV and MOB1. LATS1/2 go on to phosphorylate YAP/TAZ, leading to their cytoplasmic retention and degradation (created with biorender).

1.10 STK4

1.10.1 Ste20 family

The Sterile 20 (Ste20) family is a group of closely related but functionally distinct kinases first described as serine/threonine kinases in the 1990s. It is formed of roughly 30 serine/threonine kinases, split into p21-activated kinase (PAKs) and germinal centre kinases (GCKs) subfamilies dependent on overall and catalytic domain architecture. The

family is well conserved with homologues identified in *Drosophila* and *Caenorhabditis elegans* (161). 6 PAK members have been identified, split into two small groups composed of PAK1, 2, 3 and then PAK4, 5, 6. PAKs are effector proteins of Rho GTPases and have been identified to have roles in development and cancer (162). Research has shown that generally GCKs activated MAPK cascades, transmitting signals from extracellular signals to regulate gene expression and includes members such as STK3, STK4, thousand and one amino acid kinase 1 (TAO1) and TAO3. Furthermore, several stable binding partners have been identified for Ste20 kinases, acting as substrate adaptors (such as MOB1) (161).

1.10.2 MST subfamily

A prominent subfamily of Ste20 kinases are the Mammalian Sterile20-like family kinases with homologues first identified in Saccharomyces *cerevisiae* and their functions first characterised in *Drosophila*. The subfamily includes 5 mammalian members but is highly conserved, with homologues found across the eukaryotic kingdom. This subfamily is divided into two groups containing STK3 and STK4 (considered GCKII) and then STK24, 25 and 26 (considered GCK III). The functions of STK kinases remain fairly conserved across eukaryotes with roles including regulation of cell division and cell polarity (163). Although STK3/4 are the key regulators of the Hippo signalling pathway, the functions of other STK kinase members until recently appeared to be Hippo pathway independent. A recent paper published by Lim et al has identified STK25 as an activator of LATS1 in response to cytoskeletal tension, through an RNAi screen (164).

1.10.3 STK4 structure

STK3 and 4 share a 95% similarity in amino acid sequence in their catalytic domains and both contain 3 domains: an N-terminal kinase domain and a C-terminal regulatory region containing an autoinhibitory domain and a SARAH domain. The C-terminal regulatory region contains two nuclear export sequences (NES) at 361-370 and 441-451, which retain STK4 in the cytoplasm (156). STK4 also contains two caspase

cleavage sites at N326 and N349, producing a 36 kDa and a 41 kDa cleavage product. Upon cleavage, the kinase domain of STK4 is activated, losing its autoinhibitory domain and translocates to the nucleus where it induces apoptosis (165).

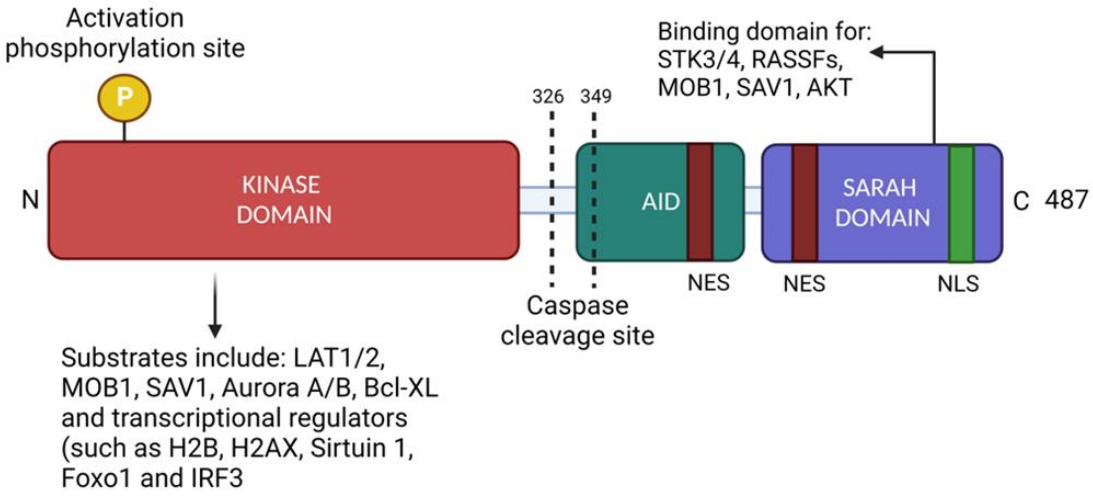

Figure 1.11 STK4 structure. Schematic of STK4 structure including the kinase domain, the autoinhibitory domain (AID) and SARAH domain. Numbers refer to amino acid positions (created with biorender).

1.10.4 Hippo pathway independent STK4 functions

Apart from activation of the Hippo signalling pathway, STK4 has many well characterised functions in apoptosis through a multitude of cellular interactions including with p53, H2B, c-Jun N-terminal kinase (JNK) and FOXO3. Additionally, STK4 can contribute to apoptosis through interactions with BH3-only protein Beclin-1. A study by Maejima et al showed that Beclin-1, with key roles in apoptosis and autophagy, is phosphorylated at Thr 108 by STK4. This phosphorylation increases the Beclin-1-Bcl-2 and Beclin-1-Bcl-xl interactions which antagonise the anti-apoptotic activity of Bcl-2 and Bcl-xl. It has also been suggested that apoptosis occurs due to protein accumulation due to inhibiting autophagy, as beclin-1 can induce apoptosis independently of Bax and Bak activity (166). Another substrate of STK4 is Bcl-xl. This phosphorylation prevents Bcl-xl binding to Bax, increasing Bax activity, therefore promoting apoptosis (167).

1.11 YAP and TAZ

1.11.1 Discovery and structure

YAP was first identified associating with Src family non-receptor tyrosine kinase Yes in 1994 (168) with TAZ identified as a 14-3-3 binding partner later in 2000 (169). Sequence analysis showed that YAP and TAZ are paralogs but neither of their functions were understood until they were identified as homologues for Drosophila protein Yorkie, the downstream effector of the Drosophila Hippo pathway (154). YAP and TAZ share several domains but there are differences in structure, with TAZ lacking an N-terminal proline-rich region, an SH3 binding domain and a second WW domain (Figure 1.12). Although they share some functions, recent research has indicated that the previous assumption that they are functionally redundant is incorrect. YAP has been characterised to a greater extent than TAZ but differences in regulation depending on tissue type has been identified (170).

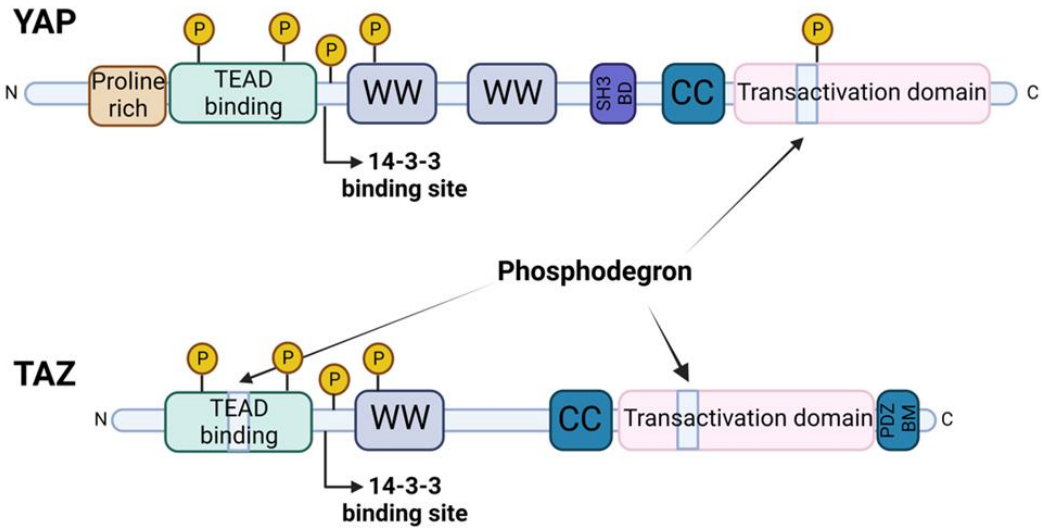

Figure 1.12 YAP and TAZ structure. Schematic of YAP and TAZ structure including LATS1/2 phosphorylation sites (P) (created with biorender).

1.11.2 Shared functions of YAP and TAZ

Although YAP/TAZ bind to a variety of transcription factors, the best characterised binding partners are TEAD1-4. TEAD1-4 share a TEA DNA binding domain but have distinct roles and expression patterns. Mouse studies have shown TEADs to be important for developmental processes (171, 172) and overexpression of TEAD transcription factors, particularly TEAD1 and TEAD 4 has been linked to tumourigenesis. Expression of genes ampiregulin (AREG), connective tissue growth factor (CTGF), and cysteine-rich angiogenic inducer 61 (CYR61) are regulated by YAP/TAZ and TEAD activity and promote a variety of cellular processes including proliferation. Although YAP and TAZ are both vital for development, overexpression and increased activity is strongly linked to cancer (173-176).

1.11.3 Differences between YAP and TAZ

Although YAP and TAZ have a high protein sequence similarity, there are significant variations, alluding to differences in function. While both contain WW domains which mediate protein-protein interactions, for example with LATS1/2, TAZ only contains one WW domain while YAP contains two (177). Additionally, while both YAP and TAZ contain TEAD binding domains, only YAP contains an additional PXXOP loop (178). TAZ also lacks regions such as the N-terminal proline rich region and SH3-binding motif, found in YAP. (179). Interestingly, the domains are not interchangeable as a study by Lu et al showing that replacing the coiled coil (CC) domain of TAZ with the coiled coil (CC) domain of YAP causes a loss of the ability of TAZ to induce nuclear puncta (180). Moreover, it has been indicated that YAP and TAZ protein stability is regulated by different proteins. A recent study suggests that only TAZ is phosphorylated by GSK3β, creating a second phosphodegron, allowing for more dynamic regulation of protein stability(181). In general YAP is more stable and remains expressed long term whereas TAZ is seen to be highly dynamic. This is highlighted by the ability of TAZ liquid-liquid phase separation (LLPS) condensates, a highly dynamic process, by interacting with paraspeckle protein Non-POU domain-containing octamer-binding protein (NONO) (182).

It is not just the regulation and structure of the proteins that differs, it is also the expression of target genes. Although currently poorly understood, an RNA-seq in HEK293 cells with YAP and TAZ individually knocked out, suggested that even though YAP and TAZ target the same transcription factors, different genes are expressed. It has been suggested that this is due to TAZ forming a hetrotetramer with TEAD that may affect DNA target selectivity (183). Despite this, difference in YAP and TAZ functions are poorly elucidate, with research primarily focusing on YAP function, leaving most of TAZ function to be inferred.

1.12 The Hippo pathway in disease

Extensive studies have shown that the Hippo pathway has tumour suppressive function with dysregulation observed in many cancers. Aberrant YAP/TAZ activity and nuclear localisation resulting from mutations or dysregulation of Hippo pathway components such as STK4 and LATS1, or amplification of *YAP1* or *WWTR1* (the gene name for TAZ) have been observed in most solid cancers and is often linked to poor prognosis. In most cancers, low expression of Hippo pathway components or high expression of YAP/TAZ has been linked to a poor overall outcome (184, 185). Hippo pathway dysregulation by oncogenic viruses, such as Hepatitis B virus and HPV, has also been observed (173, 186). Loss of key regulators of YAP activity such as STK4 is also linked to poor disease outcome (187).

Sustained nuclear YAP/TAZ promotes cancer stem cell properties such as proliferation, apoptosis evasion and metastasis (188). YAP/TAZ dependent genes promote various hallmarks of cancer and have been observed to be overexpressed in many cancers. Overexpression of Bcl-2 an anti-apoptotic YAP/TAZ dependent gene, suppresses mitochondrial-mediated apoptosis induced by apoptotic signals such as Fas expression. The oncogene myc is another YAP/TAZ/TEAD dependent gene. Overexpression of myc has been seen in many cancers and has been linked to the promotion of proliferation and cell cycle disruption (189).

Another hallmark of cancer that YAP/TAZ activity promotes is metastasis. There is evidence for increased YAP/TAZ activity promoting most steps of metastasis including: EMT, invasion/migration, intravasion, extravasation and metastatic growth. For example, increased nuclear YAP/TAZ is associated with a loss of epithelial architecture which is one of the first events in EMT. This forms a positive feedback loop as EMT inactivates the Hippo pathway, resulting in increased YAP and TAZ activity (190).

However, the full extent of Hippo pathway disruption in many cancers is still unknown. In most cases, immunohistochemistry is used to show increased nuclear YAP/TAZ, but the underlying reasons are often not investigated. Frequently it is not known whether this is due to the amplification of YAP/TAZ genes themselves or if this is due to disruption of an upstream Hippo pathway component resulting in decreased Hippo pathway signalling. In prostate cancer, multiple mechanisms lead to increases in YAP mRNA and protein expression. For example, Heat shock protein 27 (Hsp27) degrades STK4, leading to increased nuclear YAP and ETS-regulated gene transcription factor increases *YAP* promoter activity (191, 192). Not only does this make clear the importance of YAP in prostate cancer, but it also highlights the variety of mechanisms in YAP/TAZ modulation in a single type of cancer. Elucidating such mechanisms and understanding how the Hippo signalling pathway is dysregulated in cancer could be the key to developing new therapeutic treatments.

The Hippo pathway also plays roles in diseases other than cancer. YAP lessens lung inflammation in bacterial pneumonia by inhibiting NFκB, circumventing the continuous recruitment of immune cells to prevent persistent lung inflammation (193). Loss of function mutations or deletion of NF2 results in neurofibromatosis type 2, a disease characterised by the development of usually benign tumours termed bilateral vestibular schwannomas as well as other symptoms such as deafness (194).

1.12.1 The Hippo pathway and HPV

Currently Hippo pathway dysregulation in HPV-driven cancers is not well-elucidated. Although YAP has been observed to be increased in cervical cancer, its role is not yet fully understood, despite evidence suggesting YAP overexpression alone is sufficient to induce cervical dysplasia (173, 195). Recent work by Hatterschide et al showed YAP is activated by HPV E7 through degradation the of YAP inhibitor PTPN14 in HPV-positive oropharyngeal cancers and clearly demonstrating the necessity of YAP in HPV infection and carcinogenesis (196). Furthermore, aberrant YAP activity facilitates HPV infections in transgenic mice, likely through both increase HPV receptors and inhibiting type 1 IFN signalling (195).

However, there is conflicting evidence of the role of TAZ in cervical cancer with studies citing it as a tumour suppressor and an oncogene (197, 198). Furthermore, most Hippo pathway components have not been investigated in cervical disease.

1.12.2 Targeting YAP and TAZ in disease

Given the important role Hippo pathway components play in many solid cancers, targeting the Hippo pathway therapeutically has been a focus of research. The most common approach has been to disrupt YAP/TAZ and TEAD interactions. While initial YAP-TEAD inhibitor verteporfin had cytotoxicity issues, in more recent years more viable therapeutics have been developed. Most recently, drug design has focused on targeting palmitoylation sites of TEAD. However, very few therapeutics target YAP or TAZ directly, mostly due to the disordered and flexible nature of the proteins. Even though the many existing anti-cancer compounds are kinase inhibitors, few clinically viable kinase activators are currently available, none of which are known to activate Hippo pathway upstream components (199).

Targeting downstream targets of YAP and TAZ may be a better therapeutic option such as PD-L1, inhibitors of which have been shown to be promising in many cancers (200).

1.13 MicroRNA

1.13.1 Biogenesis

MicroRNAs (miRNAs) are often dysregulated in cancer, including HPV-related cancers (174, 201, 202). Since their discovery in the 1990s, it has been apparent that miRNAs play key roles in the regulation of cellular processes and could be used as biomarkers for certain diseases (203-205). miRNAs are ~22 nucleotide long, short non-coding RNA species expressed in nearly all eukaryotes. Most miRNAs are transcribed by RNA polymerase II in the form of primary miRNAs (pri-miRNAs) and can be encoded in the introns of protein-coding genes (intronic), in individual genes (monocistronic) or as gene clusters (polycistronic). pri-miRNAs are then processed to single hairpin loops called precursor miRNAs (pre-miRNAs) by a complex called the microprocessor containing Drosha and DiGeorge Syndrome Critical Region 8 (DGCR8) proteins (Figure 1.13). Next the pre-miRNAs are exported to the cytoplasm and processed by Dicer to a dsRNA loop 20-22nt long (this is the mature RNA sequence). In the last step of processing an Argonaute (AGO) protein family member selects one strand of the duplex, known as the guide strand and the other strand is discarded (206). This is known as the RNA-Induced Silencing Complex (RISC).

1.13.2 miRNA function

Mature miRNAs act as post-transcriptional repressors through binding to mRNA through complementary sequences. Most commonly miRNAs bind to the 3’UTR of an mRNA transcript, leading to translational repression by targeting the mRNA for storage in P-bodies or degradation. However, miRNAs can also bind to the 5’UTR of target mRNA to act in a transcriptional repressive manner (203).

Mature miRNAs carry out their functions by binding with AGO proteins, usually Ago2, by its middle domain and P-element induced wimpy tests (PIWI) domain binding to the 5’ of the miRNA and Piwi-Argonaute-Zwille (PAZ) domain binding to the 3’ end. When a miRNA binds to a target with full complementarity while also bound to Ago2, it leads to Ago2 cleaving the target mRNA. Although there are 4 AGO proteins encoded in the human genome, Ago2 is the best characterised and is the main AGO protein with the ability to cleave target mRNA (207, 208). Nucleotides 2-8 of the miRNA sequence are key for the targeting of mRNA transcripts and form the seed sequence. However, targets with a 2-7 or 3-8 nucleotide complementarity can also be targeted but to a weaker extent (209). miRNAs can not only cleave target mRNAs, but they can inhibit their translation to prevent protein expression. This likely occurs the release of eukaryotic initiation factors 4 A-I and A-II (eIF4A-I and eIF4A-II) and mediating mRNA decay by promoting decapping of mRNA transcripts leading to mRNA decay. Although there is debate about how eIF4A-I and eIF4A-II are released, one hypothesis suggests the mature RNA-induced silencing complex (mRISC) induces the release from the target mRNA, inhibiting ribosome scanning and the formation of the eIF4F translation initiation complex (210).

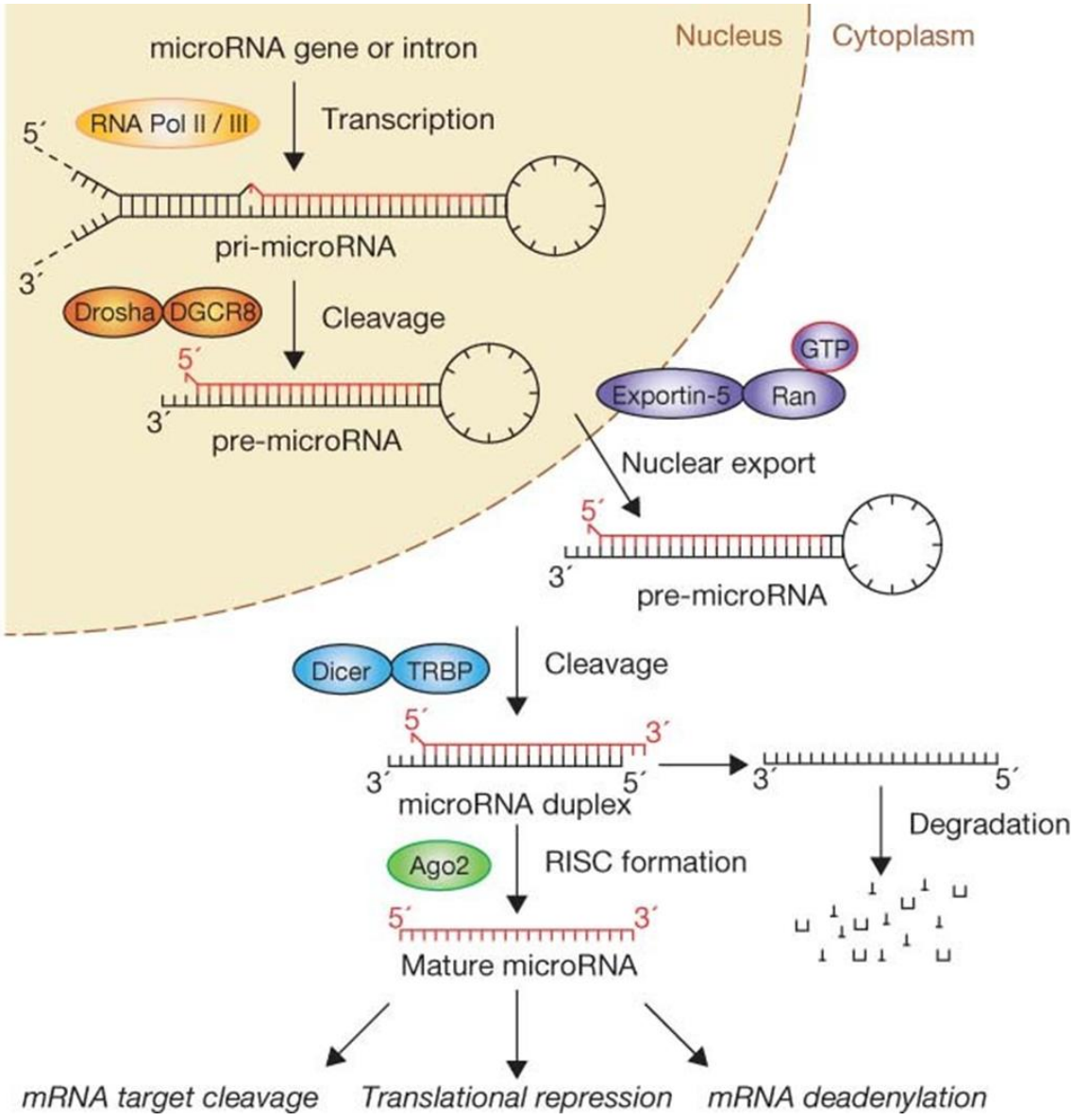

Figure 1.13 miRNA biogenesis pathway. Schematic of the miRNA biogenesis pathway. After transcription, pri-miRNAs are processed into pre-miRNAs by the microprocessor before the pre-miRNAs are transported out of the nucleus. The Dicer complex then cleaves the pre-miRNA and the guide strand is selected by AGO forming the mature mi-RNA (211).

1.13.3 Regulation of microRNAs

Regulation of microRNA expression is highly complex, it can be on either a transcriptional or post-transcriptional level, including regulation of biogenesis and post-processing regulation. Additionally, regulation can be specific to certain microRNAs or can affect the global microRNA expression. MicroRNAs transcriptional regulation occurs

in a similar manner to protein-coding genes, including epigenetic silencing through DNA methylation. For example, miR-203 a tumour suppressive miRNA has been observed to be downregulated in many cancers with low expression linked to EMT and oncogenesis (212). The promoter region of miR-203 contains several CpG islands which are methylated in cancer, suppressing the expression of miR-203 (213).

Another way microRNAs can be regulated is sequestering by competing endogenous RNA (ceRNAs). ceRNAs act as miRNA sponges, binding to miRNA preventing them from binding to their mRNA targets. Pseudogenes, lncRNAs and circRNAs have ceRNA activity and have been reported to have dysregulated expression in cancer, altering miRNA expression and activity.

1.13.4 MicroRNA and malignancy

1.13.4.1 MicroRNAs in cancer

Dysregulation of miRNAs in cancer was first reported in 2002 when miR-15 and miR-16 were found to be frequently deleted in chronic lymphocytic leukaemia (214). Since then many miRNAs have been identified to be dysregulated, with dysregulated miRNAs found to be both tumour suppressive and oncogenic. With more miRNAs and their interactions being discovered in diseases, the importance of understanding their interactions is evident. As miRNA expression is very tissue dependent, it can be used to differentiate between different cellular subtypes, as it has been shown for both prostate and leukemic (215, 216). Additionally, miRNAs could be used as biomarkers for metastasis, with certain miRNAs strongly linked to promoting various steps in metastasis (217). Clinical trials currently underway are largely aim to utilise miRNA profiles for tumour classification or for markers of prognosis but the potential for therapeutic targeting miRNAs is great.

1.13.4.2 MicroRNAs and viral infection

Dysregulation of host microRNAs occurs commonly upon virus infection as a method to dysregulate host cellular processes. This includes viruses such as: Kaposi's

sarcoma-associated herpesvirus (KSHV), Herpes simplex virus type 1, hepatitis C virus (HCV), Epstein Barr Virus (EBV) and Dengue virus (218-221). For example, EBV encode- latent membrane protein 1 (LMP1) induces miR-146a expression leading to microRNA-mediated suppression of IFN response genes hence dysregulating the immune response in latency. LMP1 mimics constituently active tumour necrosis factor receptor and activates transcription factors such as NF-κB inducing miR-146a expression through 2 NF-κB binding sites in the miR-146a promoter (218).

1.13.4.3 MicroRNAs and HPV

Numerous cellular miRNAs have already been determined to be dysregulated by HR-HPV however, the function of many of the miRNAs dysregulated remains unknown (201). Not only has the alteration of miRNA expression been observed to promote oncogenesis in HPV-related cancer, but they can also play a role in the virus lifecycle (202, 222, 223). For instance, upregulation of miR-9, miR-21 and miR-155 has been linked to the promotion of metastasis and proliferation and as such they have been suggested as biomarkers in HPV-driven cervical cancer (224, 225). However, miRNA expression profiles are often cell type specific and vary between cancer subtypes, therefore it remains unknown if miRNAs dysregulated by HPV are virus-specific, specific to the site of the cancer. In recent years, many mechanisms of miRNA dysregulation by HPV have been suggested with both E6 and E7 reported to play roles (174).

1.13.5 miR17-92 cluster

The miRNA-17-92 cluster is an example of an oncogenic polycistronic miRNA cluster that has been seen to be widely expressed in prostate, breast, lung and pancreatic cancer. The cluster is composed of 6 miRNAs; 17, 18a, 19a, 20a, 19b-1 and 92a-1, that are transcribed as one pri-miRNA but form individual mature miRNAs (226, 227). All the mature members of this cluster have been linked to tumourigenesis and certain members such as miR-18a and miR-19 have also been linked to regulation of developmental processes. Although oncogenes such as MYC have been linked to the

transcriptional upregulation of the cluster, it is theorised that post transcriptional processing plays a role in the upregulation of the mature miRNA (226). The miR-17-92 cluster has two highly conserved paralog clusters; miR-106b-25 and miR-106a-363 containing 15 miRNAs. The miR-17-92 cluster is split into 4 groups based on sequence, and currently there are more than 30 confirmed targets of the cluster including *PTEN, E2F1* and *BIM* with many more predicted (228-231). Although each member has different cellular targets, all have been evidenced to be oncogenic.

The cluster also plays key roles in normal development, found to be highly expressed in embryonic cells and deletion of the cluster in mice led to perinatal lethality with embryos expressing severe skeletal abnormalities (232). The mice embryos also had less developed lungs and a reduced number of pre-B cells indicating problems with epithelial proliferation, branching and B-cell maturation (232, 233). The mice embryos with deleted miR-17-92 cluster exhibited a phenotype similar to Feingold syndrome in humans, a disease characterised by multiple skeletal abnormalities in fingers and toes, microcephaly and short stature. A study found that patients with Feingold syndrome were found to have deletions in the *MIR17HG* locus, the gene that encodes the miR-17-92 cluster (234).

1.13.5.1 miR-18a

miR-18a is considered to be the most oncogenic member of the cluster, evidenced to promote oncogenesis and angiogenesis. It is one of them most highly expressed miRNAs and has been observed to be upregulated in many cancers including; HNSCC, breast cancer, prostate cancer and hepatocellular carcinoma. Additionally, overexpression of miR-18a has been linked with poor prognosis and has been suggested to be used as a blood-based biomarker to screen patients (235). In NSCLC, miR-18a is significantly upregulated and targets *IRF2*. *IRF2* plays a key role in regulating cellular responses in tumourigenesis, apoptosis and migration and therefore miR-18a has been suggested as a therapeutic target (236).

Another target of miR-18a is a STK4, as previously discussed, a key regulator of the Hippo signalling pathway. In prostate cancer cells, overexpression of miR-18a led to targeting of STK4, leading to promoting of proliferation and colony formation. The same study also stated that increased targeting of STK4 led to enhanced AKT phosphorylation. It has been suggested that miR-18a promotes tumourigenesis both *in vitro* and *in vivo*, suggesting antagonising miR-18a could be a therapeutic strategy in prostate cancer (237).

In gastric cancer, overexpression of miR-18a led to the increased targeting of *protein inhibitor of activated STAT3* (PIAS3), a negative regulator of oncogene STAT3, leading to enhanced expression of downstream STAT3 targets. miR-18a plays a vital role in the development of gastric cancer. Targeting of *PIAS3* was also observed in malignant mesothelioma by miR-18a, with miR-18a expression negatively correlated with patient survival (238, 239). Furthermore, miR-18a has been seen to be upregulated in cervical cancer in one study, suggesting miR-18a indirectly upregulated PD-L1, an immune receptor overexpressed in cervical cancer. Additionally, they also suggested miR-18a targets the well-characterised tumour suppressor *PTEN* (240).

1.13.5.2 Regulation of the miR17-92 cluster

As with other microRNAs, regulation of the miR-17-92 cluster can occur on two levels; regulation of transcription or post transcriptional, which includes the regulation of miRNA processing. As the cluster is transcribed as one, transcription regulates the whole cluster, whereas post-transcriptional regulation can regulate individual miRNA members. Although several transcription factors have been indicated to regulate the cluster, one of the best characterised regulators of miR-17-92 transcription. Depletion of c-myc in HeLa cells led to reduction in the expression of miR-17-92 cluster members (241). Another members of the myc family, N-myc control miR-17-92 expression through activation by sonic hedgehog/patched signalling pathway (242). In prostate cancer SOX4, a developmental transcription factor and oncogene, transcriptionally upregulates the miR-

17-92 cluster to promote cancer progression (243). Although it is well documented that transcription factors regulate the expression of the cluster, other post-transcriptional mechanisms are equally important including the tertiary structure of the pri-miR-17-92 cluster. The folded RNA means certain regions are accessible and inaccessible to Drosha, for example, normal folding means that access to miR-19b and miR-92a (the 3' core) is impaired and disruption can lead to dysregulated miR-92 expression (244).

Certain mechanisms of post-transcriptional regulation can be specific to certain members of the cluster. Although this regulation has not been completely elucidate and is complex, an example of this is the regulation of miR-18a by Heterogeneous nuclear ribonucleoproteins A1 (hnRNP A1). hnRNP A1 is a nucleo-cytoplasmic shuttling protein linked to mRNA metabolism and has functions in alternative splicing regulation (245, 246). However, hnRNPA1 can bind specifically to stem-loop structure of pri-miR-18a to facilitate the processing of the miRNA by maintaining secondary structures for Drosha recognition and to possibly prevent binding of unknown factors (247).

Other cofactors such as cleavage and polyadenylation specificity factor subunit 3 (CPSF3) and the spliceosome associated ISY1 splicing factor homolog (ISY1) specifically associate with the cleavage site of pri-17-92, promoting processing of all cluster members apart from miR-92, increasing their expression (248, 249).

Staphylococcal nuclease and Tudor domain containing 1 gene (SND1) is a key component of the RISC complex that has been linked to the degradation of miRNAs as well as splicing activities. However, SND1 can bind to all members of the miR-17-92 cluster in pri, pre and mature forms and is a modulator cluster processing. A study showed that when SND1 was knocked down in the presence of a hypoxia mimicking iron chelator DFO, the ratio mature:pre miRNA was significantly decreased, but the exact mechanism of how SND1 regulates the cluster processing is not known (250).

Although AGO2 has canonical roles in the biogenesis of all miRNAs, it has specific roles for maturation of miR-17-92 cluster members. Acetylation of AGO2 at three specific sites K720, K493, and K355 increased maturation of miR-19b, specifically in the pre to mature step of biogenesis. This led to increased recruitment and therefore processing of miR-19b due to a UGUGUG motif. P300/CBP can acetylate AGO2 while HDAC7 can deacetylate it, leading to a fine control of the final step of the miRNA biogenesis pathway, leading to increased mature miR-19b levels (251).

Another mechanism of post-transcriptional regulation often dysregulated in cancer is sponging by non-coding RNAs. Unlike other mechanisms, non-coding RNAs do not regulate miRNA processing but instead can bind to the mature miRNA and acting as a sponge, preventing mature miRNA activity. lncRNA cancer susceptibility candidate 2 (CASC2) is a tumour suppressive lncRNA in glioma cells due to its ability to target miR-18a. The loss of this lncRNA leads to overexpression of miR-18aand increased targeting of miR-18a-5p targets. Loss of such ceRNAs is a commonly seen mechanism in cancer, leading to overexpression of the mature miRNAs without any changes in biogenesis (252).

Thesis aims

HPV is the causative agent for the vast majority of cervical cancer, a disease which remains a major global health issue despite available vaccines. Even with ongoing research there are currently no specific therapeutics for HPV-driven cancers. To develop such treatments, a better understanding of how HPV transforms cells is crucial. Recent work in the Macdonald group has highlighted how the dysregulation of signalling pathways is important in cervical cancer tumourigenesis and found in particular that the Hippo signalling pathway is pivotal in transformation. Preliminary data found STK4, the key kinase of the Hippo signalling pathway to be lost in cervical cancer but the mechanism of how this occurred remained elusive. Furthermore, recent studies by others have focused mainly on the critical role of YAP in HPV-driven cancer, I contrast both the roles and regulation of other Hippo pathway components such as TAZ has been less clear. With this in mind the objectives of this work are:

1) Elucidate the mechanism of *STK4* dysregulation in HPV+ cervical cancers

2) Investigate the regulation of YAP paralog TAZ in cervical cancers

3) Characterise the role of TAZ in HPV-driven cervical cancers

4) Identify and characterise TAZ-dependent genes in cervical cancers

Chapter 2. Material and Methods

2.1 Bacterial cell culture

2.1.1 Bacterial growth and storage

DH5α Escherichia *coli* strain (NEB, USA) were grown on semisolid medium (agar in Luri--Bertani (LB) Medium) and in liquid shaking cultures (LB medium: 10 g/L tryptone soya broth, 10 g/L NaCl, 5 g/L yeast extract), overnight (o/n) at 37°C with appropriate antibiotic; 50 µg/µL Kanamycin or 100 µg/µL Ampicillin for selection. For long-term storage, cells were frozen at -80ºC in 1:1 ratio of 50% glycerol to liquid broth.

2.1.2 Transformation of competent bacteria with plasmid DNA

To transform DH5α bacteria, 50 µl of bacteria were incubated with 1 µl plasmid DNA on ice for 20 minutes before undergoing heat shock treatment at 42ºC for 45 seconds. Cultures were incubated on ice for 5 minutes before the addition on 949 µl of LB medium and 1 hr incubation at 37ºC shaking at 180rpm. Cultures were then streaked onto selective semisolid medium. Plasmids used can be found in table 1 in Appendix.

2.1.3 Preparation of plasmid DNA

For small scale plasmid purification, 10 ml of selective LB medium were inoculated with a single colony grown on selective semisolid medium and then incubated o/n at 37ºC shaking at 180 rpm. Cells were centrifuged at 4000 x g for 30 mins at 4ºC to harvest before plasmid DNA was purified using sodium dodecyl sulfate (SDS)-alkaline denaturation method employed by the Wizard® Plus SV Minipreps DNA Purification System (Promega, UK) following manufacturer's protocol. Plasmid DNA was eluted with 100 µl ddH_2O.

For large scale plasmid purification, 20 ml of selective LB medium was inoculated with a single colony grown on selective semisolid medium and then incubated for 8hrs at 37ºC shaking at 180 rpm. Following this 80 ml of selective LB medium was added and cultures were incubated o/n at 37ºC shaking at 180rpm. Cells were centrifuged at 4000

x g for 30 mins at 4ºC to harvest before plasmid DNA was purified Plasmid Maxikit (Qiagen, Germany) following to the manufacturer's protocol. Plasmid DNA was eluted with 200- 1000 µl ddH2O

Concentration of plasmid DNA was determined using a Nanodrop spectrophotometer (Thermo Fisher Scientific, USA).

2.2 Molecular cloning

2.2.1 Plasmid DNA vectors and oligonucleotides

A list of oligonucleotides used and plasmid vectors can be found in the appendix (table 2). Primers were designed using NCBI Blast and IDT "The OligoAnalyzer™ Tool" was used to avoid unwanted complementarity.

2.2.2 PCR (Q5)

DNA target sequences were amplified using Q5 high-fidelity DNA polymerase (NEB, M0491) in 50 µl reactions. Each reaction contained 200 µM dNTPs, 0.5 µM of forward and reverse primers, 20 ng template DNA, 1x Q5 reaction buffer, 1.5 µl DMSO and 0.02 U/µl Q5 high-fidelity polymerase. All reactions were prepared on ice before the following protocol was used; 98ºC 30 seconds, 35 cycles of 98ºC for 10 seconds, 50-72ºC for 30 seconds and 72ºC for 30 seconds/kb before 72ºC for 2 minutes. Annealing temp was determined using NEB Tm calculator. DNA integrity was confirmed by agarose gel electrophoresis.

2.2.3 Agarose Gel Electrophoresis

0.8-2% agarose gels were prepared (0.8-2% w/v agarose in Tris-acetate-EDTA buffer (TAE, 40 mM Tris base, 20 mM Acetic acid and 1 mM ethylenediamine tetraacetic acid (EDTA))) with 1 x SYBR safe DNA gel stain (Invitrogen, S33102). 5 µl of DNA was added in 1x Gel loading dye (NEB, B7025S) alongside 6 µl of prestained DNA ladder. Electrophoresis was used to separate out DNA at 70 V for 1 hr in TAE buffer. The agarose gel was then imaged using a Syngene InGenius gel documentation system

(Syngene Bioimaging). The PCR product was then purified with the Monarch PCR and DNA cleanup kits per manufacturer's instructions.

2.2.4 Restriction digest

For restriction digestion, plasmids and purified PCR products were digested with appropriate restriction digest enzymes (NEB). Both single and double digestions were carried out to access efficiency of digestion reaction. Each reaction contained 1 µg of DNA, 1 x CutSmart buffer and 10 units of appropriate restriction digest enzymes in a total reaction volume of 50 µl. Reactions were incubated first at 37ºC for 1 hr and then at 65ºC for 20 minutes to heat inactivated the enzymes (when possible).

2.2.5 Shrimp alkaline phosphatase treatment

Linearised plasmid vectors were treated with 1 unit of recombinant shrimp alkaline phosphatase and incubated 37 ºC for 30 minutes and then at 65 ºC for 5 minutes to heat inactivated the enzymes.

2.2.6 DNA ligation

T4 DNA ligase (NEB, M0202S) was used to insert digested PCR products into digested and phosphatase treated plasmids. Each reaction contained 1 x T4 DNA ligase buffer, 100 ng of digested plasmid with the insert in a 1:3 ratio and 200 units of T4 ligase buffer in a total reaction volume of 50 µl. Reactions were incubated at 16 ºC o/n before transformation into chemically competent DH5α (2.1.2).

2.2.7 Colony PCR

To confirm correct ligation, several single colonies were selected and incubated for 4 hrs in 1 mL of LB media. Colony PCR was conducted using BLANK according to manufactures protocols. Each reaction 1 x Green Go Taq Reaction Buffer, 0.2 mM of each dNTP, 0.2 µM of forward and reverse primers, 1.25 units of GoTaq G2 DNA polymerase and bacterial culture in a total volume reaction of 50 µl. Each reaction was run on an agarose gel (2.2.3).

2.2.8 Sequencing

2.2.9 shRNA design

21-mer optimal targeting sequence was designed against (preferably) the non-coding region of the gene of interest. Rules followed while designing include: G-C content of less than 50%, no repeats of 4 or more nucleotides (especially T) and an A or T between positions 15-19. IDT “The OligoAnalyzer™ Tool” was used to avoid unwanted complementarity. Primer sequences can be found in the appendix.

2.2.10 shRNA cloning

pLKO.1-TRC cloning vector (Addgene) was digested with AgeI and EcoR1-HF restriction digest enzymes (NEB) to remove 1.9kb stuffer. Each reaction 3 µg of plasmid, 1 unit of appropriate digest enzyme and 1x CutSmart buffer in a total volume of 20 µl. The reactions were incubated for 3 hours and then ran on a 0.8% agarose gel in 1x loading dye (NEB) until 2 distinct bands could be observed. The 7kb band was cut from the gel and extracted using Monarch® DNA Gel Extraction Kit as per manufacturer’s instructions.

shRNA oligos were annealed by incubating each reaction at 95ºC for 4 minutes, 70ºC for 10 minutes and then slowly cooling to room temperature over several hours in a water bath. Each reaction contained 5 µl of both forward and reverse 20 µM oligos and 1x NEB buffer 2 in a total volume of 50 µl.

Annealed oligos and digested pLKO.1-TRC cloning vector were ligated using T4 DNA ligase (Promega). Each reaction contained 2 µl annealed oligos, 20ng of digested pLKO.1-TRC cloning vector, 1x NEB T4 DNA ligase buffer (Promega), 1 µl T4 DNA ligase in a total final volume of 20 µl. Reactions were incubated overnight at 16ºC before transformation into competent DH5α cells.

2.3 Protein biochemistry

2.3.1 Cell lysis

Media was aspirated and mammalian cells were washed twice with phosphate buffered saline (PBS) and lysed in 200/400/1,000 µl for 6 well, 6 cm^2 and 10 cm^2 dishes respectively of RIPA buffer (150 mM NaCl, 1% Nonidet P-40 (v/v), 0.5% sodium deoxycholate (w/v), 0.1% sodium dodecyl sulfate (SDS) (w/v) and 25 mM Tris-HCl pH 7.4, plus 1x Protease inhibitor cocktail, EDTA-Free (Roche, Switzerland)). Cells were incubated on ice for 20 minutes before cells were scraped and transferred into eppendorfs. Cells were then centrifuged at 17,000 x g for 10 minutes to removed insoluble precipitates and supernatant was transferred to a fresh Eppendorf tube. Samples were stored at -20ºC.

2.3.2 Protein bicinchoninic acid assay (BCA) for protein concentration

Protein concentrations were calculated using a BCA assay following the manufacturer's protocol (Thermo Fisher Scientific, USA). Standard dilutions 0 µg/ml to 2 µg/ml of bovine serum albumin were prepared in appropriate matched lysis buffer. Cell lysates were 1:40 in assay reagent following manufactures instructions. BCA standards and samples were ran in duplicate in a 96 well plate. After 10 min incubation at 37°C, the absorbance at 562 nm was read on a PowerWave XS2 Microplate Spectrophotometer (BioTek, UK). Absorbance values were calculated by the software (Gen5 1.11, BioTek, UK). Measurements were used to determine samples protein concentration.

2.3.3 SDS polyacrylamide gel electrophoresis (SDS-PAGE)

Equal amounts of protein were loaded onto a 8%, 10%, 12.5% and 15% SDS-polyacrylamide gel (v/v) for the appropriate protein resolutions (separating gel: 8%, 10%, 12.5% and 15% Acrylamide (v/v), 375 mM Tris/Cl, pH 8.8; 0.1% SDS (w/v), 0.1% APS (w/v), 0.01% TEMED (v/v); stacking gel: 6% Acrylamide (v/v), 125 mM Tris/Cl, pH 6.8;

0.1% SDS (w/v), 0.1% APS (w/v), 0.01% TEMED (v/v)). Samples were resuspended in 2 x Laemmli Sample Buffer (32.9 mM Tris.HCl pH 6.8, 13.15% glycerol (v/v),1.1% SDS (w/v), 0.01% bromophenol blue (w/v), 0.1% β-mercaptoethanol (v/v)) in a 1:1 ratio. Protein was separated alongside 2 µl BLUeye Pre-Stained Protein Ladder (Sigma) and separated according to molecular weight using a Mini-PROTEAN Tetra cell (Biorad) at 80-160 V in 1x SDS running buffer (34.7 mM SDS, 250 mM Tris Base, 1.92 M Glycine) until proteins were resolved.

2.3.4 Western blotting

After protein resolution, the SDS-PAGE gels were transferred on to Amersham Protran 0.2 µm pore nitrocellulose, (Amersham BioSciences, 10600001) using a Trans-Blot Turbo Transfer System (BioRAD). Nitrocellulose membranes were then blocked in 5% w/v dried skimmed milk powder in TBS-T (TBS: 25 mM Tris/Cl, pH 7.5; 138 mM NaCl and 0.1% Tween--20)) for 1 hr at room temperature before incubation in primary antibody diluted accordingly (table 3 can be found in the appendix) o/n at 4ºC on a shaking platform. Membranes were washed 4 x 5 minutes in Tris-buffered saline (TBS) with 0.1%Tween (TBS-T) at room temperature before incubation in appropriate secondary antibody (conjugated to horseradish peroxidase diluted in 5% w/v dried skimmed milk (1:5000) for 1 hr at room temperature. Membranes were then washed 4 x 5 minutes in TBS-T at room temperature. To detect chemiluminescent signal, membrane were incubated with Molly-brew™ solution A containing 0.25 mM luminol, 0.396 mM coumanic acid and 10 mM Tris-HCl pH 8.5 and ECL solution B containing 64 µl 30% hydrogen peroxide and 10 mM Tris-HCl pH 8.5 and visualised on X-ray film using Xograph Compact 4 machine.

2.3.5 Densitometry

Western blot films were scanned for digitalisation so protein levels could be quantified using Image J (National Institutes of Health, USA). Protein bands were

selected using the square tool before band intensity was determined with the measure function and the background intensity was deducted.

2.4 RNA work

2.4.1 RNA extraction

To extract total RNA, cells were lysed in 350 µl of TRK lysis buffer and lysates were processed with the E.Z.N.A. Total RNA Kit I (Omega Bio-Tek) following manufactures protocols. RNA was eluted in 40 µl nuclease-free H_2O and yields were determined using a Nanodrop spectrophotometer (2.1.3).

2.4.2 One-step Quantitative Real-time PCR

Real time PCR reactions were performed using GoTaq Taq 1-Step RT-qPCR System (Promega) and a CFX connect Real-Time System (Biorad). Reactions contained 10ng RNA, 5 µl GoTaq qPCR Master Mix, 0.2 µl GoScript™ RT Mix and 0.4 µM of each specific forward and reverse primer for each gene (table 4 can be found in the appendix) in a total volume of 10 µl with nuclease-free H_2O.The PCR was conducted as follows: 50ºC for 10 minutes, 95ºC for 5 minutes to allow for reverse transcription then a two-step cycle of denaturation 95ºC for 10 seconds followed by a combined annealing and extension 60ºC for 30 seconds which was then repeated 39 times. Data generated was analysed using ΔΔCt method with U6 used as a housekeeper control.

2.4.3 miScript RT

For microRNA analysis, RNA was processed with miScript II RT kit (Qiagen). 1000ng of RNA, 10x miScript Reverse Transcriptase Mix, 10x miScript Nucleic Mix and 5x miScript HiSpec Buffer were combined in a total volume of 20 µl at room temperature before incubation at 37ºC for 1 hour followed but 5 minutes at 95ºC to inactivate the reverse transcriptase. Resultant cDNA was diluted in nuclease-free water in a 1:10 ratio.

2.4.4 miScript Real-time quantitative PCR

For real time quantitative PCR of microRNAs, reactions were performed with miScript SYBR Green PCR Kit (Qiagen) and a CFX connect Real-Time System (Biorad). Reactions contained 10 µl 2xSYBR, 2 µl 10x miScript universal primer, 2 µl 10x miScript primer assay specific to miRNA of interest and 1 µl cDNA equals (62.5 ng of cDNA) in a total reaction volume of 20 µl with nuclease-free H_2O. The PCR was conducted as follows: an initial activation step at 95ºC for 15 minutes followed by 40 3-step cycles of a denaturing step at 94ºC for 15 seconds, an annealing step at 55ºC for 30 seconds and an extension step at 70ºC for 30 seconds. Data generated was analysed using ΔΔCt method with SNORD68 used as a housekeeper control.

2.5 Trizol extraction

2.5.1 Lysis

To lyse cells, 1 ml of Trizol (Thermo Fisher Scientific, USA) was added per $5x10^6$ cells before homogenisation, followed by a 5 minute incubation at room temperature. 0.2 mls of chloroform (Thermo Fisher Scientific, USA) was added and samples were vigorously mixed before incubation at room temperature for 3 minutes. Samples were then centrifuged at 12,000g for 15 minutes at 4ºC to separate out the phases. At this point the aqueous phase was transferred to a new Eppendorf tube, taking care to not disturb phases.

2.5.2 RNA precipitation

To precipitate RNA 10 µg of glycogen was added to the aqueous phase alongside 0.5 ml of isopropanol (stored at -80ºC before use) before mixing and incubation at room temperature for 10 minutes. Samples were then centrifuged 10 minutes at 12,000g at 4°C, with the RNA forming a white pellet. The supernatant was then discarded.

2.5.3 RNA wash and solubilisation

RNA pellets were resuspended in 1 ml of 75% ethanol per 1 ml of Trizol, Samples were vortexed briefly before centrifugation at 7500g for 5 minutes at 4ºC. The supernatant was then discarded and the sample was air dried before resuspension in 20 µl of Nuclease-free water.

2.5.4 DNase treatment

To remove DNA from the samples, samples were processed using DNase treatment kit (Thermo Fisher Scientific, USA) following manufacturer's instructions.

2.5.5 Protein extraction

Any remaining aqueous phase was removed before the addition of 0.3 mls of 100% ethanol per 1 ml of Trizol reagent. Samples were inverted several times before incubation at room temperature for 3 minutes and centrifugation at 2000 g for 5 minutes at 4ºC. Supernatant was transferred to a new tube and 1.5 ml of 100% isopropanol was added before incubation at room temperature for 10 minutes. Samples were then centrifuged for 10 minutes at 12,000 g at 4ºC and the supernatant was discarded. Pellets were resuspended in 2 mls of 0.3M guanidine hydrochloride 95% ethanol (heated to 50ºC before use dissolved any precipitates) before incubation at room temperature for 20 minutes and centrifugation at 7500 g for 5 minutes at 4ºC. The supernatant was discarded and pellets were washed twice more. Pellets were then resuspended in 2mls of 100% ethanol and vortexed before incubation at room temperature for 20 minutes. Samples were centrifuged at 7500 g for 5 minutes at 4ºC and the supernatant was discarded. Pellets were air dried and then lysed in 100 µl of RIPA lysis buffer. Insoluble material was not removed via centrifugation and samples were stored at -80ºC.

2.5.6 Trizol LS

To extract RNA and protein from liquid samples, 750 µl of Trizol LS was used per 250 µl of liquid sample. Samples were then homogenised using a 19-gauge syringe

before incubation at room temperature for 15 minutes. Samples were then processed following usual method (2.5-2.5.4)

2.6 Mammalian cell culture

2.6.1 Cell lines and maintenance

HaCaT (Human immortalized keratinocytes), C33A (HPV negative cervical squamous carcinoma cells), SiHa (HPV16 positive cervical squamous carcinoma cells), CaSKi (HPV16 positive cervical squamous carcinoma cells), SW756 (HPV18 positive cervical squamous carcinoma cells) and HeLa (HPV18 positive cervical epithelial adenocarcinoma) cell lines obtained from ATCC were grown in DMEM supplemented with 10% fetal bovine serum (GIBCO, UK) and 50 U/mL Pen/Strep (Lonza, Switzerland). MS751 (HPV18 positive cervical squamous cell carcinoma derived from lymph node) cell line obtained from ATCC was grown in Eagle's Minimum Essential Medium supplemented with 10% fetal bovine serum and 50 U/ml Pen/Strep. C4-I (human squamous carcinoma of the uterine cervix) cell line obtained from ATCC was grown in Waymouth's MB 752/1 medium supplemented with 10% fetal bovine serum and 50 U/ml Pen/Strep. Primary normal human keratinocytes (NHKs) were grown in serum free media (GIBCO, UK) with 25 µg/mL bovine pituitary extract (GIBCO, UK) and 0.2 ng/mL recombinant EGF (GIBCO, UK) (Grown and pelleted by Dr David Kealy). Cells were all grown at 37°C and 5% CO_2 (Sanyo, USA). All cell lines were kept in 75 cm^2 flasks (T75) (Sarstedt, Germany) and all cell culture work was conducted in an Airstream Class II Biological Safety cabinet (ESCO, UK).

2.6.2 Passaging of cell lines

Upon reaching 80-90%, cell medium was aspirated and cells were washed once with sterile phosphate buffered saline (PBS) before detachment with 1% trypsin at 37ºC and 5% CO_2 for the appropriate amount of time. The trypsin was then deactivated with complete DMEM media and then re-seeded into a T75 flask at a 1:8 ration of cell suspension: fresh DMEM or seeded into the appropriate flask at the required density.

2.6.3 Transfections with Lipofectamine 2000

For transfection of HeLa, SiHa, CaSKi or C33A cells were seeded into 12 well, 6 well, 60 mm or 100 mm cell culture plate (Corning, USA) at a density of 5 x 10^5, 1 x 10^6, 2 x 10^6 or 5 x 10^6 cells/mL respectively and incubated overnight at the aforementioned conditions. The required amount of plasmid DNA was incubated in 200 µl of 1 x Opti-MEM (GIBCO, UK) for 5 minutes at RT while in a separate tube, the required amount of Lipofectamine 2000 was incubated with 1 x Opti-MEM (GIBCO, UK) for 5 minutes at RT before tubes were combined. The mixture was incubated for a further 20 minutes at RT. Complete media in culture dishes was aspirated and replaced with Reduced Serum Media (GIBCO, UK) and mixture was added and cells were incubated overnight in aforementioned conditions. Media was replaced with fresh complete media and incubated for the appropriate length of time.

2.6.4 Transfection of siRNA or miRNA mimic or antagonist with Lipofectamine 2000

For transfection of HeLa, SiHa, CaSKi with siRNA, miRNA mimic or miRNA antagonist, cells were seeded into either 6-well dish at a density of 1 x 10^5 or 60 mm dishes at 2 x 10^5 cells/mL. siRNA, miRNA mimic or miRNA antagonist at the appropriate concentration was incubated in 200 µl of 1 x Opti-MEM (GIBCO, UK) for 5 minutes at RT while in a separate tube, the required amount of Lipofectamine 2000 was incubated with 1 x Opti-MEM (GIBCO, UK) for 5 minutes at RT before tubes were combined. The mixture was incubated for a further 20 minutes at RT. Complete media in culture dishes was aspirated and replaced with Reduced Serum Media and the mixture was added dropwise and cells were incubated overnight. Media was replaced with fresh complete media and incubated for the appropriate length of time.

2.6.5 Transient transfection with polyethylenimine

To transfect HEK293TTs, cells were seeded into either a 6 well culture plate at a density of 1 x 10^6 cells/mL or 100 mm culture dish at 2 x 10^6 cell/mL respectively before incubation overnight (2.5.1). The required amount of plasmid DNA was incubated in 200

µl of 1 x Opti-MEM (GIBCO, UK) for 5 minutes at RT before polyethylenimine (PEI; 23966, Polyscience Inc.) was added in a 4:1 ratio. The mixture was then incubated for a further 30 minutes at RT. Complete media in culture dishes was aspirated and replaced with Reduced Serum Media and the mixture was added dropwise and cells were incubated overnight. Media was replaced with fresh complete media and incubated for the appropriate length of time.

2.7 Generation of stable cell lines

2.7.1 Production of lentiviruses for gene transduction

pPAK2, pVSVG and the shRNA plasmid were transfected into HEK293TTs in a ratio of 0.65:0.65:1.2 respectively. shRNA sequences used can be found in table 5 in the appendix.

72 hours post transfection, complete DMEM media containing lentivirus was removed and filtered with a 0.45 µm regenerated cellulose filter (Sartorius, 16555-K). If not needed immediately, aliquots were frozen on dry ice and stored at -80ºC.

2.7.2 Virus transduction

Appropriate cells were seeded at a density of $7.5x10^5$ in s 100mm culture dish and incubated overnight. Media was aspirated and lentivirus containing media was added in a 1:1 ratio with fresh complete DMEM media to cells along with 4 µg/µl Polybrene (Santa Cruz, sc-134220) and 20 mM HEPES. Cells were then incubated for 72 hours.

2.7.3 Selection and production monoclonal cell line

72 hrs post transduction, media was aspirated from cells and replaced with fresh complete DMEM media containing 2 µg/ml of puromycin (InvivoGen, ant-pr-1). Cells were passaged when appropriate and selected with puromycin for 2 weeks post transduction before puromycin concentration was lowered to 1 µg/ml to sustain cell line. Cells were then washed in PBS before detachment with 1% trypsin at 37ºC and 5% CO2

for the appropriate amount of time. The trypsin was then deactivated with complete DMEM media and cells were counted. 4095 cells were seeded into each well of column 1 of a 96-well plate in 200ul of media. Serial dilutions of 1 in 2 using complete DMEM media were performed across the 96-well plate. Wells were then checked and marked if contained a single cell. Only cells from marked wells were passaged when appropriate, gradually increasing dish size until cells could be pelleted and screened.

2.8 Immunofluorescence

2.8.1 Cell seeding

Cells were seeded onto coverslips (400-08-26; glass coverslips, Dia. 19. Academy Science, UK) at a density of 1x 10^5 and were transfected 24 hours later as required. Cells taken forward for staining were approximately 70% confluent.

2.8.2 Fixation and permeabilisation

Cells were fixed with 4% paraformaldehyde for 10 minutes, which was then removed and cells were washed twice in PBS for 3 minutes while rocking. Cells were then permeabilised with 0.10% Triton for 15 minutes before removal and cells were washed in PBS 3 times for 3 minutes while rocking.

2.8.3 Immunolabelling

After cells were permeabilised, cells were incubated for forty-five minutes at room temperature in 4% BSA/PBS to block. After blocking, cells were immediately incubated overnight in 4% BSA/PBS with primary antibodies inverted at 4ºC. Primary antibodies were used at a concentration of 1:300. Cells were then washed in PBS 4 times for 5 minutes before incubation in secondary antibodies Alexa 594 and Alexa 488 (1:400) (Invitrogen) in PBS with 4% BSA for 2 hours. DAPI was used to visualise nuclei. Coverslips were then mounted onto slides with Prolong Gold (Invitrogen).

2.8.4 Microscopy

Labelled cells were then imaged using LSM880 upright (Zweiss, Germany) under an oil-immersion 63 x objective lens. Images were processed in Zen black (Zweiss, Germany).

2.8.5 TAZ immunofluorescence

To visualise TAZ, cells were seeded onto coverslips at a density of $1x10^5$ and incubated for 24 hours. Cells were then fixed in 4% paraformaldehyde for 10 minutes at room temperature before washing twice in PBS at room temperature for 3 minutes while rocking. Cells were then permeabilised with 0.3% Triton/PBS for 10 minutes at room temperature. Permeabilised cells were then washed 3 times with PBS while rocking for 1 minute at room temperature. Cells were then blocked in 10% BSA/0.1%Triton/PBS (10%BSA/PBS-T) at room temperature 1 hour. Cells were immediately inverted and incubated in anti-TAZ primary antibody (1:100) in 2% BSA/PBST overnight in a humid chamber at 4ºC. Cells were treated following usual immunofluorescence protocol.

2.9 Cancer cell assays

2.9.1 Growth curve assays

At the experiment end point treated cells were reseeded in 6 well plate at a density of 5×10^5 or in a 12 well plate at a density of 2.5×10^5 depending on the experiment. Each condition was seeded and counted in duplicate. Cells were harvested daily and counted manually using a haemocytometer (Thermo Fisher Scientific, USA). Cells were harvested for 5 days post seeding.

2.9.2 Colony formation assay

Cells were transfected as required. 48 hour after transfection, cells were trypsinised and reseeded in a six well plate at 500 cells per well and left to incubate for 14-21 days. Colonies were then stained using staining solution (1% crystal violet, 25% methanol) and colonies were counted manually. Each experiment was repeated at least 3 times unless stated otherwise.

2.9.3 Soft agar assay

Cells were transfected as required. 60mm dishes were coated with a layer of 1% agarose (Thermo Fisher Scientific, USA) in 2X DMEM (Thermo Fisher Scientific, USA) supplemented with 20% FBS and 100U/ml Pen/Strep. 48 hours after transfection, cells were trypsinised and cells were added to 0.7% agarose in 2X DMEM (Thermo Fisher Scientific, USA) supplemented with 20% FBS at 1000 cells/mL in a 1:1 ratio. Once set, normal DMEM was added. The plates were then incubated for 14-21 days. Each experiment was repeated at least three times unless stated otherwise. Visible colonies were counted manually.

2.9.4 Wound healing assay

Cells were seeded at a density of $5x10^5$ and grown until fully confluent. When 100% confluent cells were wounded with a p200 pipette tip. Media was then aspirated before cells were washed in PBS to remove any detached cells and fresh complete DMEM media was added before imaging using EVOS Auto 2 Microscope. Cells were the incubated for a further 24 hours before reimaging. Each condition was imaged 3 times at each time point. Images were analysed in FIJI (FIJI Is Just Image J).

2.9.5 Migration assay

Cells were transfected as required. 48 hours post transfection, cells were trypsinised and reseeded at a density of 2.5 $x10^4$ in the cell culture insert of a Transwell assay in serum free media. Fresh complete DMEM media was added to the well (below the permeable membrane). Cells were then incubated a further 24 hours before all media was aspirated and all non-migrated cells (which remain above the membrane) were removed with a cotton swab without puncturing the membrane. Migrated cells were then stained before the membrane were imaged using EVOS. Images were analysed in FIGI.

2.9.6 Invasion assay

Cells were transfected as required. 48 hours post transfection, cells were trypsinised and reseeded at a density of 2.5 $x10^4$ in the cell culture insert of a Transwell

assay with matrix in serum free media. Fresh complete DMEM media was added to the well (below the permeable membrane). Cells were then incubated a further 24 hours before all media was aspirated and all non-invasive cells (which remain above the membrane) were removed with a cotton swab without puncturing the membrane. Invasive cells were then stained before the membrane were imaged using EVOS. Images were analysed in FIJI

2.10 Small molecule inhibitors

A list of inhibitors used can be found in the Appendix (table 6).

2.11 Subcellular fractionation

HeLa cells were seeded into 10cm dishes and grown to 70% confluency before harvested and washed with PBS. Cells were then incubated on ice in 150 µl of cytoplasmic lysis buffer 10 minutes before centrifugation at 800 g for 10 minutes. The supernatant was kept as the cytoplasmic fraction (20 mM Tris pH 7.5, 100 mM NaCl, 0.5 mM EDTA, 0.5% NP-40, and protease inhibitor cocktail) and the pellet was resuspended and centrifuged at 800 g 3 times. Remaining pellet was lysed in 100 µl of RIPA buffer (50 mM Tris pH 7.5, 150 mM NaCl, 1% NP-40, 0.5% sodium deoxycholate, 0.1% SDS, protease inhibitor cocktail) with 1 µl of benzonase (EMD Millipore) for 30 minutes to obtain the nuclear fraction.

2.12 Luciferase assay

C33A, HeLa and CaSKi cells were seeded at the appropriate density for 70% confluence 24 hours post seeding in 12 well culture plates and were transfected using Lipofectamine (2.5.3) with a *firefly* reporter plasmid and a separate constitutively expressing *Renilla* luciferase plasmid for transfection efficiency. pEZX-PL01 plasmid vector contained both a *firefly* reporter plasmid and a constitutively expressing *Renilla* luciferase. psiCheck2 plasmids contained both *Renilla* luciferase reporter and a constitutively expressing *firefly* luciferase for transfection efficiency. Transfected cells

were incubated for the appropriate length of time before media was aspirated and cells were washed with PBS before aspirating followed by lysis Passive Lysis Buffer (Promega) (150 µl per well) at room temperature for 20 minutes, rocking. Samples were assayed for luciferase activities using Dual luciferase Stop and Glo reagent (Promega) and a luminometer (EG&G Berthold). Fold activity was calculated by dividing the relative luciferase activity of stimulated cells by that of mock--treated cells

2.13 HPV positive biopsy samples

Archival paraffin-embedded cervical biopsy samples were obtained with informed consent. Subsequent analysis of these samples was performed in accordance with approved guidelines, which were approved by Glasgow Royal Infirmary: RN04PC003. HPV presence was confirmed by PCR using GP5+/GP6+ primers. RNA and protein was extracted by Trizol extraction.

2.14 RNA sequencing

2.14.1 Sample preparation and sequencing

Total RNA was extracted for all 14 samples sent for sequencing. Samples consisted of 2 controls (NEG), 2 TAZ A KDs, 2 TAZ B KDs, 2 YAP A KDs, 2 YAP B KDs, 2 Y/T KD, therefore each cell line was sequenced in duplicate. Library preparation and Human Whole Transcriptome Sequencing was performed by NovaSeq (PE150& SE5 for mRNA and lncRNA.

2.14.2 RNAseq analysis

Analysis of RNAseq was performed by Dr Chinedu Anene and Joseph Cogan. Trimmomatic was used to filter raw reads to remove low-quality reads and adaptors. These processed reads were aligned using human reference genome GRCh38/hg38 assembly using HISAT (v2.1.0). Expression counts across genomic features were generated using HTSeq (v0.11.1) on human GRCh38 reference annotation (GENCODE release 32). Then R package edgeR was used to perform differential gene expression

analysis. Firstly raw expression counts were normalised for counts per million (CPM) using trimmed mean of M values (TMM) method. CPM of genes were filtered to remove genes with low expression across all samples. Next quasi-likelihood F-test for DGE analysis was performed by fitting generalised linear model (GLM). The Benjamini-Hochberg method was used to calculate False Discovery Rates (FDR) and P-values were corrected for multiple testing. DGE analysis was performed on individual shRNA in the following contrasts: Neg vs TAZ-S1= A1, Neg vs TAZ-S2= A2, Neg vs YAP-S1= B1, Neg vs YAP-S2= B2 and Neg vs Y/T-S1=C. Extracted genes which were, significantly altered in both A1 and A2, and not significantly altered in B1 and B2 were identified for further analysis.

2.15 Statistical analysis

Statistical analysis was used where appropriate using two-tailed unpaired Student's T-test. P value < 0.05 = *, P value < 0.01=**, P value < 0.005 = ***. Error bars were calculated using standard deviation. Error bars represent the mean +/- standard deviation. *P<0.05, **P<0.01, ***P<0.005 (Student's t-test).

Chapter 3- STK4 is targeted by miR-18a in HPV+ cervical cancer

3.1 Introduction

The Hippo signalling pathway is a key regulator of organ size and development, controlling the transcription of genes involved in cell growth and proliferation. Although many inputs feed into the pathway, the core kinase cascade consists of STK4/3 and LATS1/2 (together with SAV1 and MOB1) and ends with phosphorylation and subsequent inactivation/degradation of YAP/TAZ (253). Research has highlighted the importance of this pathway in cancer with YAP found to be frequently overexpressed and aberrantly activated in many solid tumours including (184, 185, 254, 255).

The current role of HR-HPV oncogenes in the disruption of the Hippo pathway is poorly understood. Recent studies have shown that both HR-HPV E6 and E7 promote YAP stabilisation and activation, highlighting the key role of YAP in cervical cancer (173, 196). Additionally, HPV8 E6 (of the β genus) induces YAP dependent transcriptional activity, potentially through reducing activity of LATS of the Hippo pathway (256). Furthermore, Hippo pathway dysregulation in cervical cancer is a major driving feature of carcinogenesis as hyperactivation of YAP is sufficient to the drive development of cervical squamous cell carcinoma (CSCC) without the HPV oncoproteins (195). With YAP clearly displayed as a key oncogene in cervical cancer, understanding how HPV dysregulates other key pathway components is vital to understanding HPV-induced carcinogenesis.

Preliminary data has identified STK4 as a novel host protein that is downregulated in cervical cancer, suggesting that E6 and E7 downregulate STK4 expression to promote proliferation. This is of importance as it highlights STK4 as a tumour suppressor and as a potential therapeutic target in HPV-associated cancers (Figure 3.1). However, the mechanism of STK4 dysregulation remains unknown.

STK4 dysregulation has been reported to occur through multiple mechanisms including decreased expression due to DNMT1 activity and targeting by oncomiR miR-18a in prostate cancer (237, 257). miR-18a is a member of the oncogenic miR17-92 cluster with members known to play pivotal roles in range of cancers and have been found to be highly expressed in cervical cancer (240, 258). Although miR-18a has been shown to be highly expressed in cervical cancer and promote proliferation, the role of this miRNA remains poorly elucidated. Additionally, it remains unclear how miR-18a activity is driven by HPV, it is known that E6 and E7 are both capable of modulating miRNA expression.

The aim of this chapter is to elucidate how STK4 expression is suppressed in cervical cancer through miR-18a and DNMT1 activity.

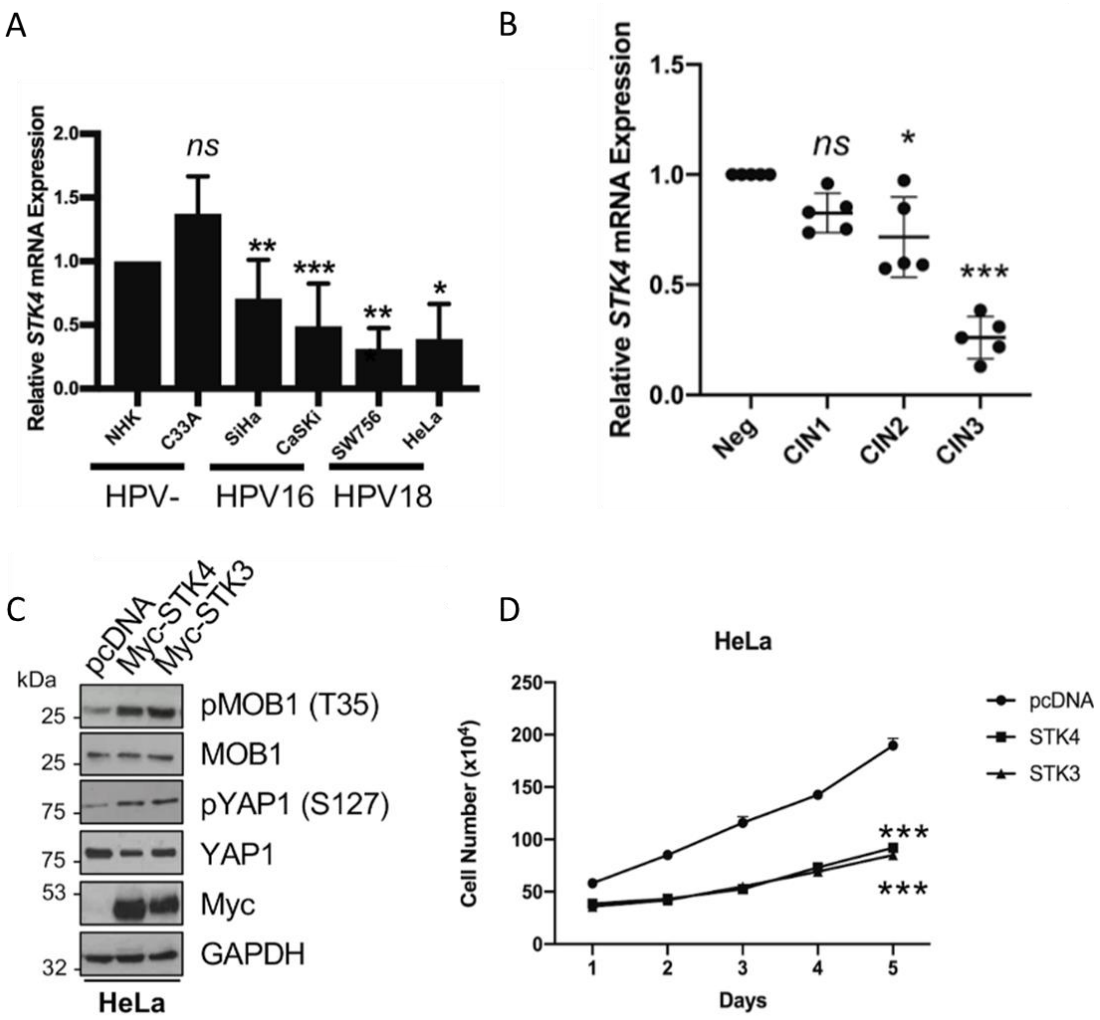

Figure 3.1 STK4 is downregulated in cervical cancer and reintroduction suppressed proliferation A) qRT-PCR analysis of STK4 expression in HPV-, HPV16+ or HPV18+ cell lines. U6 transcript levels were used as a loading control. **B)** qRT-PCR analysis of STK4 expression in panel of cytology samples. (Neg, CIN 1–3) U6 transcript levels were used as a loading control (Performed by Dr Ethan Morgan) **C)** Representative western blots of HeLa cell lysates with STK3/4 overexpression (24 hours). Cell lysates were probed for Myc (to show successful transfection and expression of myc tagged proteins), pMOB1 T35, total MOB1, pYAP1 S127 and total YAP1. GAPDH was used as a loading control. D) Growth curve analysis of HeLa cells transfected with STK3/4 (for 24 hours).

3.2 Results

3.2.1 miR-18a is upregulated in cervical cancer

Bioinformatics analysis of the *STK4* 3'UTR sequence revealed a putative miR-18a binding site (pairing with the seed sequence of miR-18a) suggesting that miR-18a could regulate *STK4* mRNA expression as previously seen in other cancer (237) (Figure 3.2 A red indicates binding site). As the binding site is predicted to be a perfect match with no 'wobble' this is predicted to lead to the cleavage and degradation of STK4 mRNA (259). This could result in the downregulation of *STK4* expression seen in HPV+ cervical cancer (Figure 3.1 A-B).

To confirm the expression of mature miR-18a in cervical cancer cells, qRT-PCR was used to analyse expression levels in a panel of cervical cancer cell lines compared with NHK cells as a non-transformed control. The data showed that whilst there was no significant difference between NHK and the HPV- cervical cancer C33A cell line, both the HPV16+ and HPV18+ cell lines showed significantly increase levels of miR-18a (Figure 3.2 B). However, as these cell lines have been adapted to grow in tissue culture, miR-18a expression was analysed in cervical liquid cytology samples from patients with HPV16+ disease. These samples represented cervical disease progression from CIN1 to CIN3 and were collected by the Scottish HPV archive alongside HPV- normal cervical tissue samples. Analysis of miR-18a levels by qRT-PCR showed a significant inverse correlation between disease progression and miR-18a expression (Figure 3.2 C). Further investigation of microarray datasets also revealed miR-18a expression was significantly increased in either cervical cancer or CIN 2-3 (HSIL) samples in both datasets used (Figure 3.2 D).

Together these data suggests that mature miR-18a is overexpressed in HPV+ cervical cancer cell lines and expression correlates with disease progression in cervical disease.

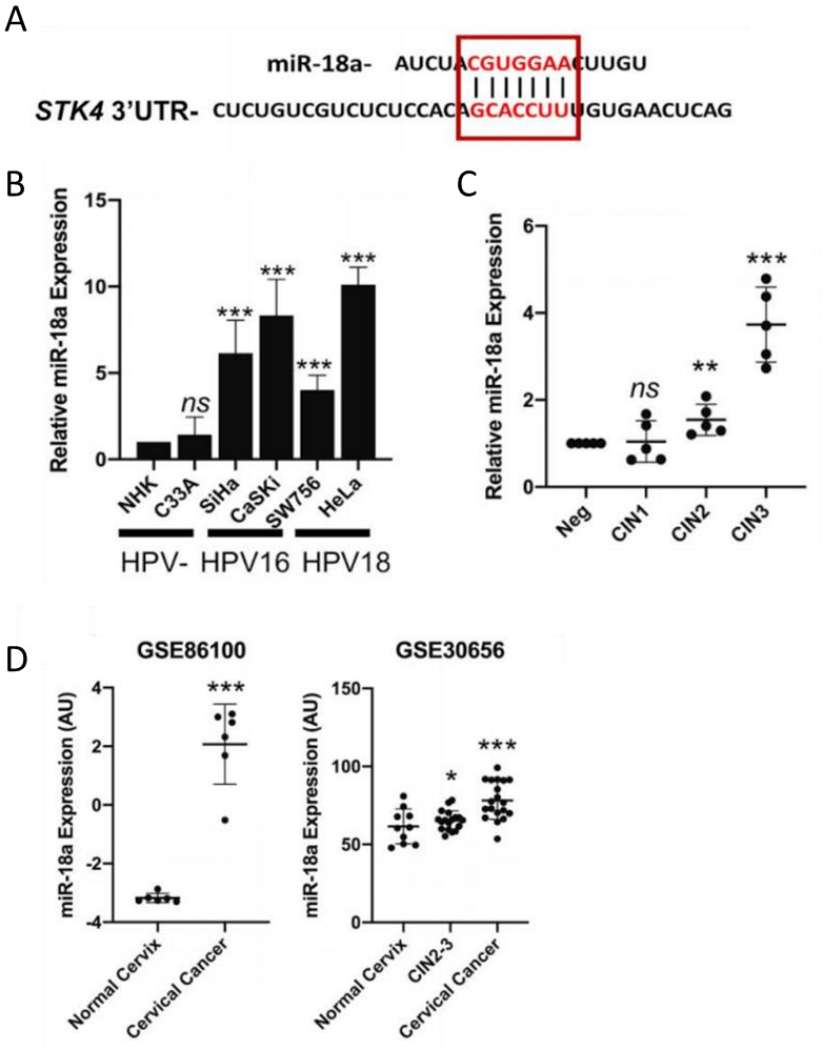

Figure 3.2 miR-18a is upregulated in cervical cancer A) Schematic of STK4 3'UTR with miR-18a binding site highlighted. **B)** Mature miR-18a expression analysed by miScript and qPCR in a panel of HPV- and HPV+ cervical cancer cell lines. snORD68 expression was used as a loading control. **C)** miScript and qPCR analysis of mature miR-18a expression in patient cervix liquid cytology samples from different CIN grades (n=5 from each grade) (performed by Dr Ethan Morgan and Emma Ryder). snORD68 was used as a loading control. **D)** Scatter plot from GSE86100 (normal cervix n=26 and cervical cancer n=30). Arbitrary expression values for miR-18a was plotted for each sample. **E)** Scatter plot from GSE30656 (normal cervix n=10, CIN2-3 n=18, cervical cancer n=19). Arbitrary expression values for miR-18a was plotted for each sample.

3.2.2 Only the mature form of miR-18a is upregulated

miRNA processing is a complicated multi-step process with the potential for modulation of miRNA levels to occur at several stages. To investigate if the increase in mature miR-18a levels observed in cervical cancer was due to an increase in the transcription of the miRNA or changes in processing, levels of *pre-miR18a*, a partially processed intermediate product, were analysed using qRT-PCR. Interestingly, *pre-miR18a* levels were significantly decreased in both the HPV16+ and HPV18+ cell lines, the opposite of mature miR-18a levels (Figure 3.3 A).

As miR-18a is part of the miR17-92 cluster that is transcribed as a single pri-RNA transcript, levels of *pre-miR92a* were analysed. This miRNA was chosen as it has been previously shown that mature miR-92a is increased in cervical cancer (201). When expression of *pre-miR92a* were analysed using qRT-PCR, the same trend of expression was observed that was seen in *pre-miR18a*, with *pre-miR92a* significantly decreased in both HPV16+ and HPV18+ cell lines.

Together this suggest that miR-18a levels are not increased due to an increase in the cluster transcription but likely to be due to increased processing of the *pre-miR18a* transcript. It is also likely that other members of the cluster such as miR-92a are regulated in a similar way.

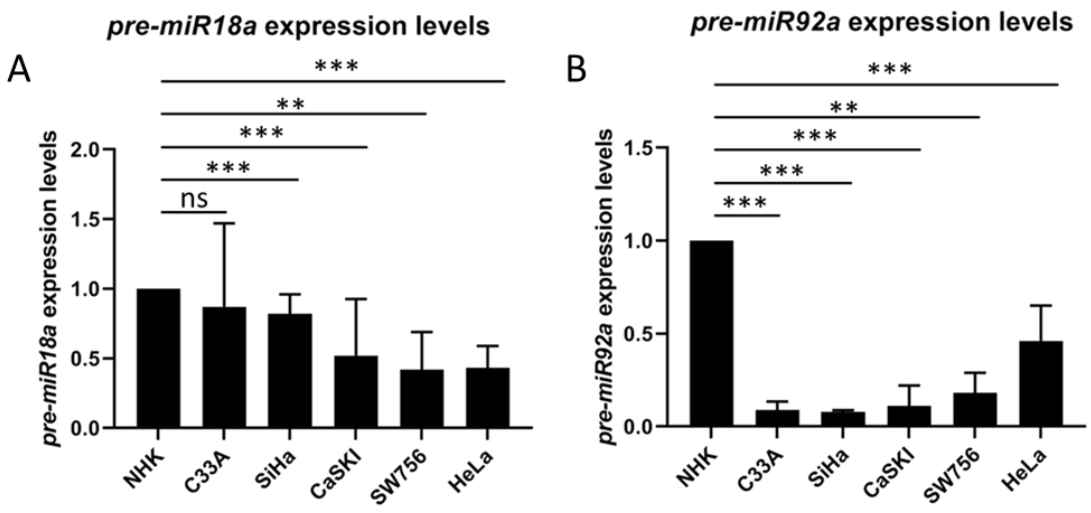

Figure 3.3 pre-miRNA levels for miR17-92 cluster are not increased in HPV+ cervical cancer cell lines. A) qRT-PCR analysis of pre-miR18a transcript levels in a panel of HPV- and HPV+ cervical cancer cell lines. U6 transcript levels were used a loading control. **B)** qRT-PCR analysis of pre-miR92a transcript levels in a panel of HPV- and HPV+ cervical cancer cell lines. U6 transcript levels were used a loading control.

3.2.3 miR-18a directly targets STK4 3'UTR

Although miR-18a levels was increased in cervical cancer (Figure 3.2) and has been previously reported to target *STK4*, given that miRNAs are capable of targeting multiple and distinct mRNAs in different cell types it was important to verify if miR-18a was targeting *STK4* in cervical cancer. Firstly, the expression of mature miR-18a and *STK4* was compared in matched samples of cervical liquid cytology samples and were found to be inversely correlated (Figure 3.4 A), which suggested a possible functional link in their expression.

To investigate if miR-18a activity was responsible for the downregulation of *STK4* observed in HPV+ cervical cancer cell lines, a miR-18a antagomir, which acts by sterically the interaction between blocking miR-18a's with mRNA targets, was transfected into HeLa cells at doses ranging from 40 nM to 120 nM. Analysis by either qRT-PCR or western blotting showed inhibition of miR-18a activity led to a significant dose dependent increase in *STK4* mRNA and protein expression respectively, (Figure 3.4 B and C compare lane 2 to lanes 3-5).

It was important to investigate if miR-18a was directly binding to the predicted binding site in the 3'UTR of *STK4* to decrease expression. For this, a reporter construct was generated with the *STK4* 3'UTR fused after a *renilla* luciferase gene. A mutant variant, where the miR-18a binding site was disrupted was also created (Figure 3.4 D). Analysis of luciferase expression in either HeLa or CaSKi cells upon miR-18a activity inhibition showed a significant increase in luciferase expression (Figure 3.4 E and F compare black bars). This suggests that the 3'UTR of *STK4* is no longer targeted for degradation. However, when the predicted binding site is mutated, luciferase expression is unaffected by inhibition of miR-18 activity.

Further investigation revealed miR-18a only targets *STK4* in HPV+ cervical cancer cells as qRT-PCR analysis of *STK4* expression in C33A cells following transfection of the miR-18a inhibitor showed no significant change (Figure 3.4 G).

Taken together these data suggest that miR-18a is directly targeting the 3'UTR of *STK4*, via the predicted binding site, leading to its degradation.

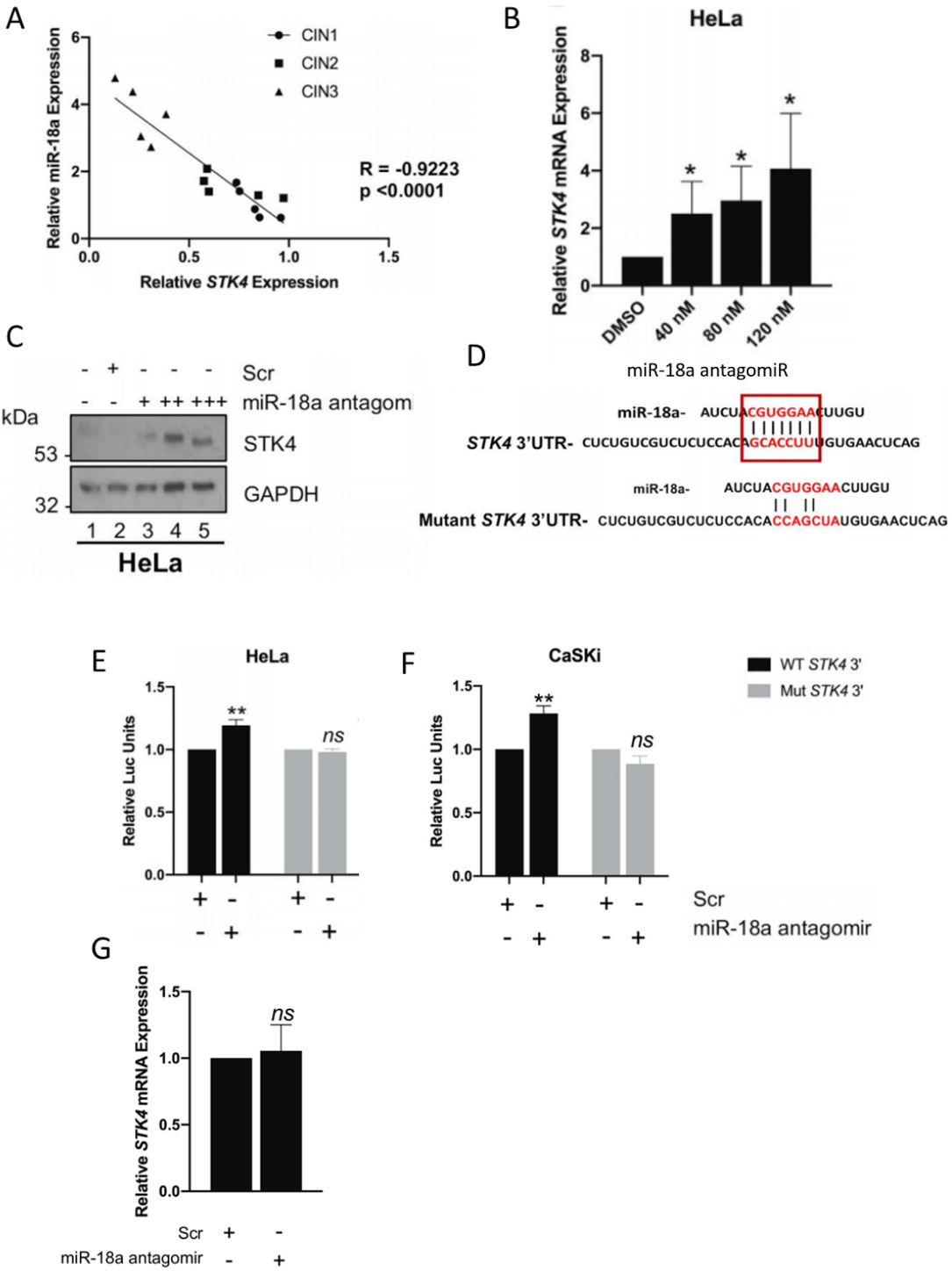

Figure 3.4 miR-18a directly targets STK4. A) Graph showing correlation between miR-18a and STK4 expression in matched patient samples of cervical disease (n = 15) (Performed by Dr Ethan Morgan). **B)** qRT-PCR analysis of STK4 transcript levels in HeLa cells with increasing doses of miR-18a antagomir ranging from 40-120nM 24 hours post transfection. U6 transcript levels were used a loading control. **C)** Representative western blot of HeLa cell lysate with increasing doses

of miR-18a antagomir ranging from 40-120nM 24 hours post transfection. Lysates were probed for STK4. GAPDH was used as a loading control. **D)** Schematic of STK4 3'UTR with miR-18a binding site highlighted compared with the mutated STK4 3'UTR sequence. **E)** Luciferase reporter assay in HeLa cells. Cells were transfected with 120nM of miR-18a antagomir and either a wild-type STK4 3'UTR reporter plasmid or a mutant that lacks the putative miR-18a binding site for 24 hours. Internal firefly luciferase was used as a loading control. **F)** Luciferase reporter assay in CaSKi cells. Cells were transfected with 120nM of miR-18a antagomir and either a wild-type STK4 3'UTR reporter plasmid or a mutant that lacks the putative miR-18a binding site for 24 hours. Internal firefly luciferase was used as a loading control. **G)** qRT-PCR analysis of STK4 transcript levels in C33A cells with 120nM of miR-18a antagomir 24 hours post transfection. U6 transcript levels were used a loading control.

3.2.4 E6/E7 suppression of STK4 expression is mediated by miR-18a

HPV-encoded oncoproteins E6 and E7 are the primary drivers of transformation in HPV+ cervical cancer cells and preliminary data ((174) Figure 5) suggested both oncoproteins were required for downregulation of *STK4* expression. As, both E6 and E7 have been linked to modulation of miRNA expression, it was hypothesised that oncoprotein regulation of *STK4* was miR-18a-mediated. To investigate this, firstly we analysed expression of miR-18a upon E6/E7 knockdown in both HPV16+ (CaSKi) and HPV18+ (HeLa) cells transfected with a pool of siRNAs directly targeting E6 and E7. Not only were miR-18a levels significantly reduced but we confirmed that STK4 *mRNA* levels also significantly increased upon oncoprotein depletion. It was possible to recover suppression of *STK4* expression by transfecting in 20 nM of a miR-18a mimic (a chemically modified double strand RNA molecule designed to mimic activity of endogenous miR-18a) (Figure 3.5 A and B). The same result was observed on protein level when analysed by western blotting in both HPV16+ and HPV18+ cell lines (Figure 3.5 C and D).

Next, it was important to confirm that the changes in *STK4* expression observed was due to changes in the targeting of the 3'UTR. This was investigated utilising the *STK4* 3'UTR luciferase assay described in 3.2.3. When the oncoproteins were depleted with siRNA, there was a significant increase in luciferase expression, suggesting a decrease in targeting of the 3'UTR. Importantly, this increase in luciferase was ablated after re-introduction of miR-18a activity with the miR-18a mimic in both CaSKi and HeLa cells (Figure 3.5 E and F).

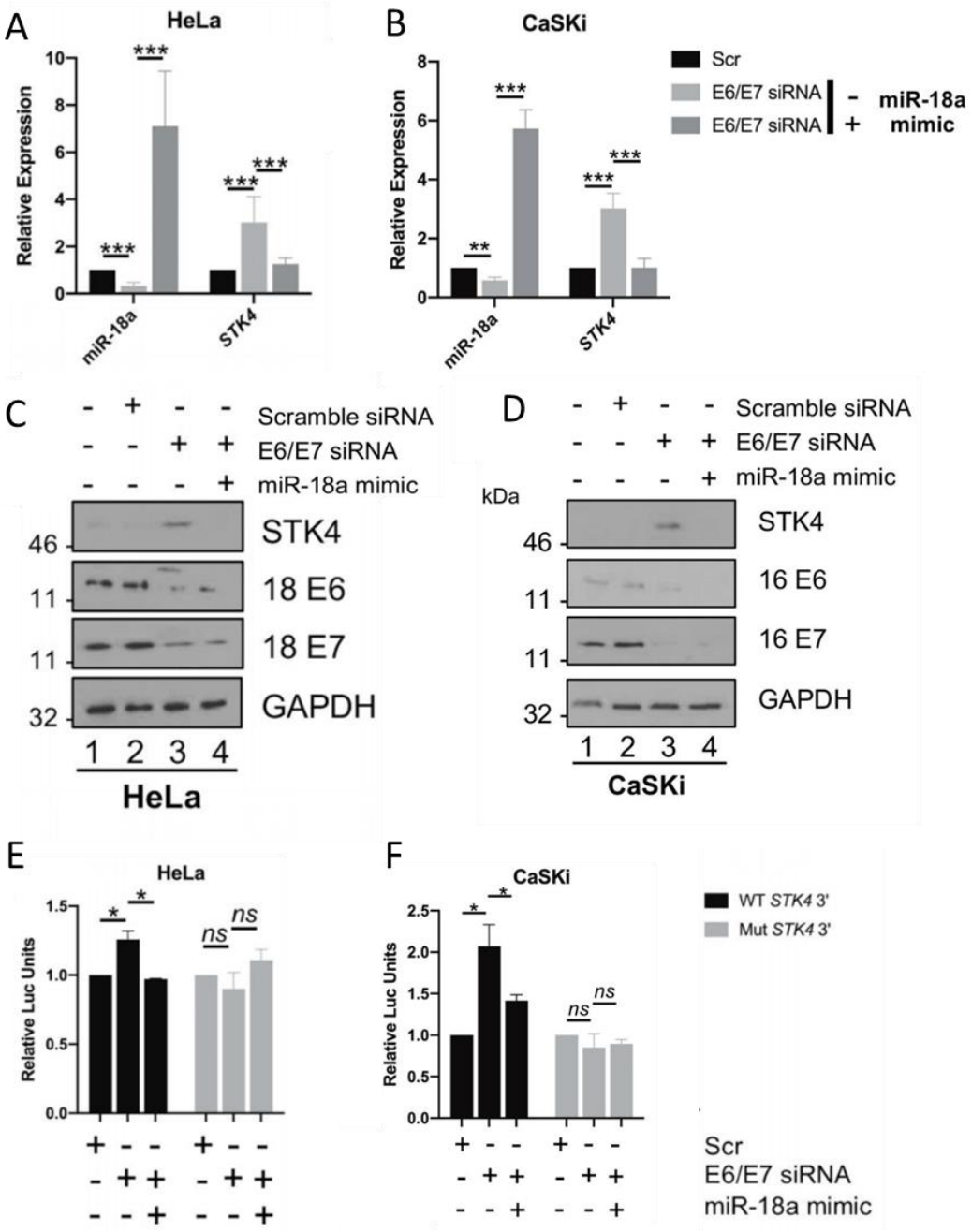

Figure 3.5 E6/E7 downregulation of STK4 is miR-18a mediated. A) Mature miR-18a expression analysed by miScript and qPCR in HeLa cells transfected with E6/E7 targeting siRNA (for 72 hours) with or without 20nM of miR-18a mimic (for 24 hours). snORD68 was used as a loading control. **B)** Mature miR-18a expression analysed by miScript and qPCR in CaSKi cells transfected with E6/E7 targeting siRNA (for 72 hours) with or without 20nM of miR-18a mimic (for 24 hours). snORD68 was used as a loading control. **C)** Representative western blot of HeLa cell lysate with E6/E7 targeting siRNA (for 72 hours) with or without 20nM of miR-18a mimic (for 24

hours). Cell lysate was probed for STK4, HPV18 E6 and HPV18 E7 expression. GAPDH was used as a loading control. **D)** Representative western blot of CaSKi cell lysate with E6/E7 targeting siRNA (for 72 hours) with or without 20nM of miR-18a mimic (for 24 hours). Cell lysate was probed for STK4, HPV16 E6 and HPV16 E7 expression. GAPDH was used as a loading control. **E)** Luciferase reporter assay in HeLa cells. Cells were transfected with E6/E7 targeting siRNA (for 72 hours) with or without 20nM of miR-18a mimic (for 24 hours) along with either a wild-type STK4 3'UTR reporter plasmid or a mutant that lacks the putative miR-18a binding site for 24 hours. Internal firefly luciferase was used as a loading control. **F)** Luciferase reporter assay in CaSKi cells. Cells were transfected with E6/E7 targeting siRNA (for 72 hours) with or without 20nM of miR-18a mimic (for 24 hours) along with either a wild-type STK4 3'UTR reporter plasmid or a mutant that lacks the putative miR-18a binding site for 24 hours. Internal firefly luciferase was used as a loading control.

3.2.5 Inhibition of miR18a leads to activation of the Hippo signalling pathway in an STK4 dependent manner

STK4 is the key activator of the Hippo signalling pathway, a tumour suppressive pathway that leads to the phosphorylation and degradation of YAP and TAZ oncogenes. Preliminary data showed overexpression of either STK4 or paralogue STK3 (which shares many functions with STK4) led activated the pathway and inhibition of YAP transcriptional activity (Figure 3.1 C). As data suggested that miR-18a was a key regulator of STK4 expression, the effect of miR-18a on the Hippo signalling pathway was investigated. To assess pathway activation, phosphorylated MOB1 (T35), direct substrate of STK4 kinase activity was probed for. Downstream target phosphorylated YAP S127 was also probed for, as this phosphorylation is key in the regulation of the subcellular localisation of YAP (260). Total MOB1 and total YAP1 were also analysed so it could be ascertained if there were actual changes in the phosphorylated form of each protein and not just the total levels of the proteins. Antagomir-mediated inhibition of miR-18a increased both MOB1 and YAP1 phosphorylation, indicating that Hippo signalling pathway is activated (Figure 3.6 A lane 2 compared with lane 3). As miR-18a is reported to target multiple genes, it was essential to confirm that the increased activity in the Hippo pathway we observed was because of the increase in STK4 expression and not mediated by an additional target. Depletion STK4 using a pool of siRNA in cells treated with the miR-18a antagomir reduced levels of both MOB1 and YAP1 phosphorylation in comparison with miR-18a antagomir treatment alone (Figure 3.6 A lane 3 compared with lane 4). This effect was observed in both HPV16+ and HPV18+ cell lines. This indicated that the Hippo pathway activation seen upon miR-18a inhibition is STK4-dependent.

As Hippo pathway activation leads to cytoplasmic YAP, YAP transcription activity was analysed following miR-18a antagomir treatment. Analysis of the expression levels of canonically YAP-dependent genes; *AREG*, *CYR61*, *PROM1* and *CCND1* by qRT-PCR revealed miR-18a depletion led to a significant decrease in expression (Figure 3.6 B).

Further investigation revealed that the loss of YAP-dependent gene expression was STK4 dependent as depletion of STK4 levels alongside miR-18a led to a recovery of gene expression in both HeLa and CaSKi cell lines (Figure 3.6 B).

Together this suggests that miR-18a inactivates the Hippo signalling pathway in a STK4-dependent manner, leading to increased YAP transcriptional activity.

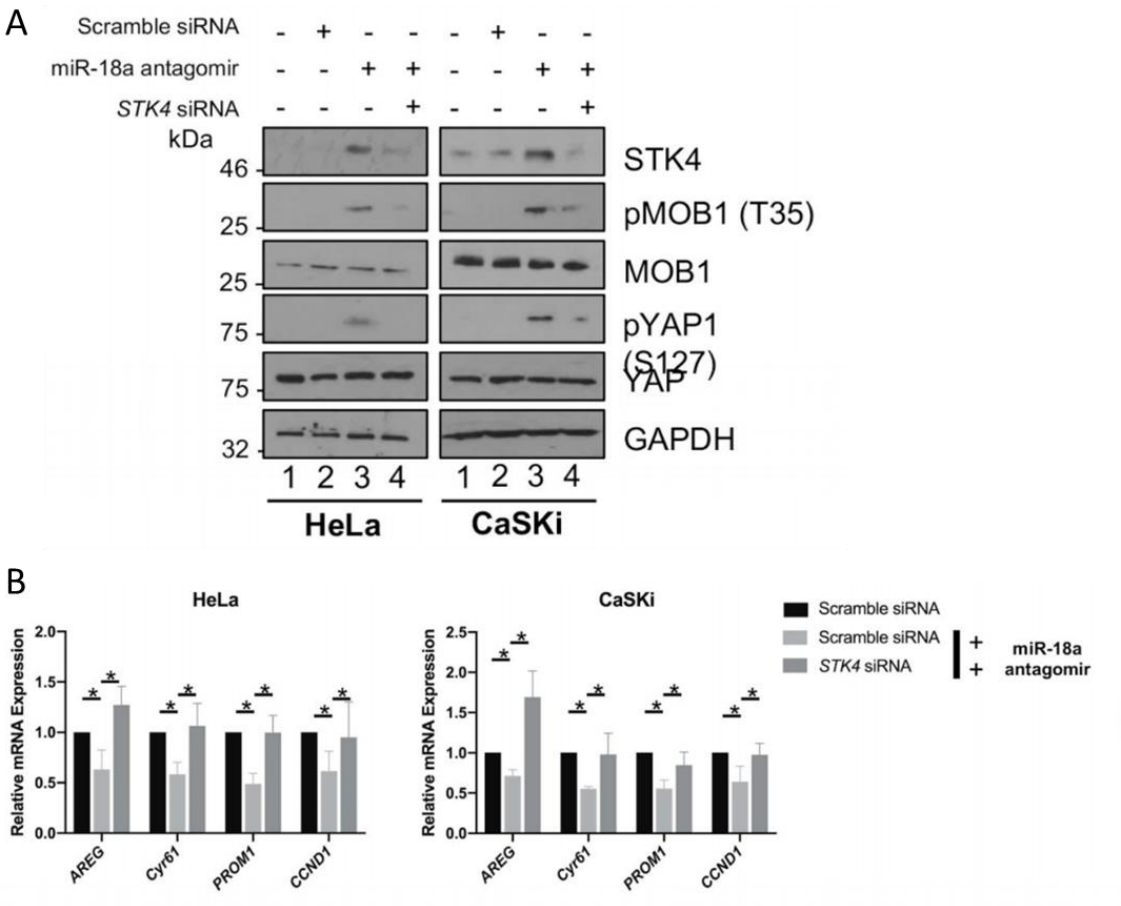

Figure 3.6 miR-18a inhibits Hippo pathway activation through targeting STK4. A) Representative western blots Hela or CaSKi cell lysate with 120nM of miR-18a antagomir (for 24 hours) with or without STK4 targeting siRNA (for 72 hours). Cell lysates were probed for STK4, pMOB1 T35, total MOB1, pYAP1 S127 and total YAP1. GAPDH was used as a loading control. **B)** qRT-PCR analysis of YAP dependent gene transcripts (AREG, Cyr61, PROM1, and CCND1) in HeLa or CaSKi cells transfected with 120nM of miR-18a antagomir (for 24 hours) with or without STK4 targeting siRNA (for 72 hours) U6 transcript levels were used a loading control.

3.2.6 The proliferative defect upon miR-18a inhibition is partially dependent on increased STK4 protein expression

miR-18a has been frequently described in literature as an 'oncomiR', a miRNA that promotes cancerous phenotypes (235-237). Additionally, preliminary data suggested that reintroduction of STK4 into cervical cancer led to a reduction in proliferation and colony forming ability (Figure 3.1 C and (174) Figure 2). This, alongside the ability of miR-18a to inhibit the tumour suppressive Hippo signalling pathway, led it to be hypothesised that miR-18a promoted proliferation in cervical cancer cells. To investigate this a growth assay was used to measure the proliferative ability of cervical cancer cells upon inhibition of miR-18a activity. Both HeLa and CaSKi cells proliferation after miR-18a antagomir treatment (Figure 3.7 A and B). Depletion of STK4 with a pool of *STK4*-targting siRNA alongside inhibiting miR-18a led to a partial restoration in growth ability compared to miR-18a inhibition alone in both HPV16+ and HPV18+ cell lines (Figure 3.7 A and B).

Given the significant role of miR-18a on growth, the effect of miR-18a on colony forming ability in an anchorage-dependent manner in both HeLa and CaSKi cell lines was also investigated. Treatment with the miR-18a antagomir led to a reduction in the ability to form colonies in both cell lines (Figure 3.7 C and D). Furthermore, this was seen to be partially dependent on STK4 as transfection of a pool of siRNA targeting STK4 alongside the miR-18a antagomir led to an increase in the number colonies (Figure 3.7 C and D). A similar trend was observed in anchorage-independent colony forming ability. While inhibition of miR-18a activity alone led to a reduction in anchorage-independent colony formation, additional depletion of STK4 led to a partially recovery in colony forming ability (Figure 3.7 E and F). This was observed both in HeLa and CaSKi cells

Together these data suggests that miR-18a promotes proliferation in HPV+ cervical cancer cells partially due to targeting STK4.

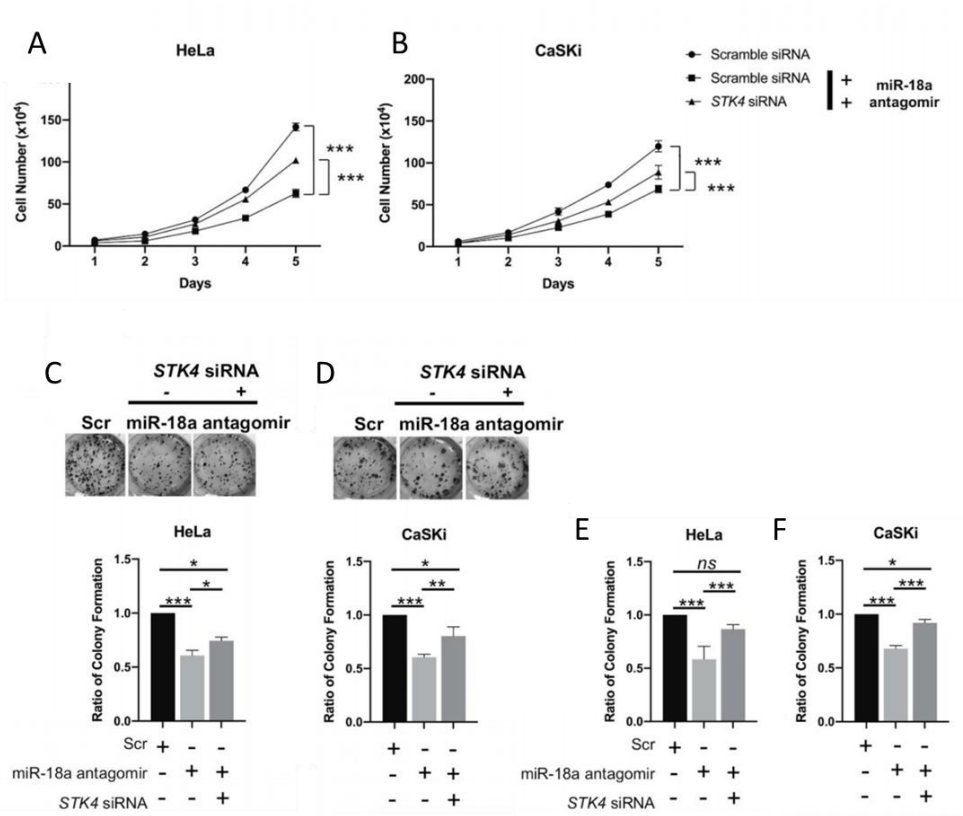

Figure 3.7 miR-18 promotes proliferation in a partially STK4-dependent manner A) Growth curve analysis of HeLa cells transfected with 120nM of miR-18a inhibitor (for 24 hours), with or without STK4 siRNA (for 72 hours). **B)** Growth curve analysis of CaSKi cells transfected with miR-18a inhibitor (for 24 hours), with or without STK4 siRNA (for 72 hours). **C)** Colony formation assay (analysis anchorage dependent growth) of HeLa cells transfected with 120nM of miR-18a inhibitor (for 24 hours), with or without STK4-targeting siRNA (for 72 hours). **D)** Colony formation assay (analysis anchorage dependent growth) of CaSKi cells transfected with 120nM of miR-18a inhibitor (for 24 hours), with or without STK4-targeting siRNA (for 72 hours). **E)** Soft agar assay (analysis anchorage independent growth) of HeLa cells transfected with 120nM of miR-18a inhibitor (for 24 hours), with or without STK4-targeting siRNA (for 72 hours). **F)** Soft agar assay (analysis anchorage independent growth) of CaSKi cells transfected with 120nM of miR-18a inhibitor (for 24 hours), with or without STK4-targeting siRNA (for 72 hours).

3.2.7 DNMT1 activity may contribute to STK4 suppression in cervical cancer in a miR-18a dependent manner

DNMT1 is a DNA-methyltransferase that transfers a methyl group to alternate cytosines predominantly at CpG islands. Epigenetic silencing of tumour suppressive genes through dysregulation of DNA methylation has been frequently observed in multiple types of cancer. It is common for tumour suppressive genes to have aberrantly hypermethylated CpG containing sequences resulting in gene silencing. Furthermore, this has been observed in cervical cancer and several candidate methylation markers suggested in both cervical squamous cell carcinoma and adenocarcinoma (261). In both HNSCC and soft tissue sarcoma, the promoter of STK4 has been observed to be hypermethylated. Therefore, it was hypothesised that DNMT1 activity may also contribute to the suppression of STK4 expression in cervical cancer.

To inhibit DNMT1 activity, HeLa and CaSKi cells were treated with DNA methyltransferase inhibitor 5-aza-2'-deoxycytidine (DAC). Successful DAC treatment was observed by the loss of DNMT1 protein expression and was observed by western blotting (Figure 3.8 A). DAC treatment in either HeLa or CaSKi cells led to a significant decrease in STK4 protein levels (Figure 3.8 A quantification in Figure 3.8 B). Furthermore, analysis of *STK4* expression showed a significant increase in mRNA expression following DAC treatment in both HeLa and CaSKi cells (Figure 3.8 C).

Next, to confirm these results and to confirm that the observations were not due to any off-target effects following DAC treatment, a pool of siRNAs was used to deplete DNMT1 expression. Western blot analysis of cell lysates showed a significant increase of STK4 expression upon knockdown of DNMT1 (Figure 3.8 D). Quantification of densitometry showed that this was a significant increase in both HeLa and CaSKi cells (Figure 3.8 E quantification of Figure 3.8 D). Further investigation of *STK4* mRNA expression upon DNMT1 siRNA-mediated knockdown showed significant increase.

Little is known on the effect of DNA-methylation on miR-18a expression but one study has suggested an inverse correlation in hepatocellular carcinoma (262). To elucidate if the control of STK4 expression by DNMT1 was miR-18-dependent, mature miR-18a levels were analysed by qRT-PCR. Interestingly, treatment of HeLa cells with DAC led to a significant reduction in miR-18a expression (Figure 3.9 A).

Together these data suggests DNMT1 contributes to the suppression of *STK4* in HPV+ cervical cancer, potentially through regulation of mature miR-18a expression.

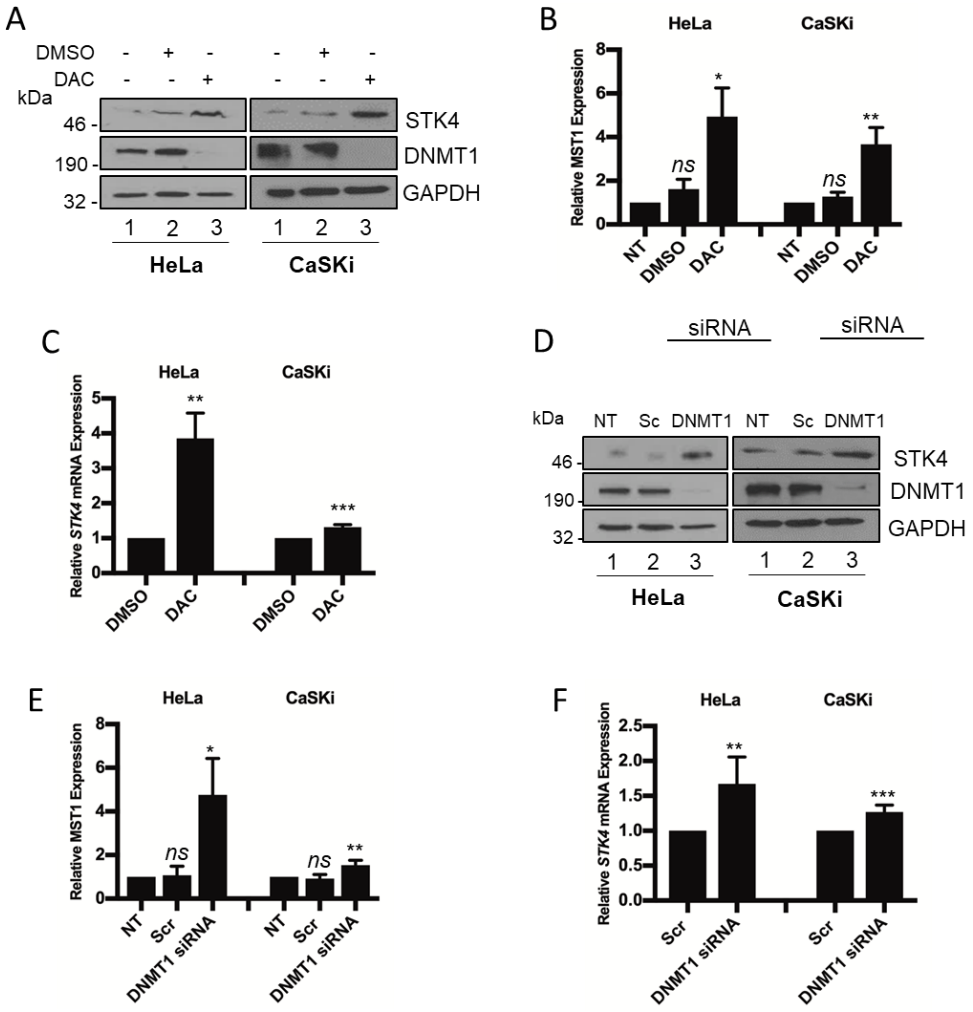

Figure 3.8 Inhibition of DNMT1 activity rescues STK4 expression. A) Representative western blots Hela or CaSKi cell lysate after DNA methylation inhibitor 5-aza-2'-deoxycytidine DAC treatment (for 72 hours). Cell lysates were probed for STK4 and DNMT1. Expression of DNMT1 was probed for a positive control of DNMT1 inhibition. GAPDH was used as a loading control. **B)** Quantification of A from three independent experiments. **C)** qRT-PCR analysis of STK4 transcript in HeLa or CaSKi cells after 72 hour DAC treatment. U6 transcript levels were used as a loading control. **D)** Representative western blots Hela or CaSKi cell lysate after transfection of DNMT1 specific siRNA (72 hours). Cell lysates were probed for STK4 and DNMT1. Expression of DNMT1 was probed for a positive control of DNMT1 knockdown. GAPDH was used as a loading control. **E)** Quantification of D from three independent experiments. **F)** qRT-PCR analysis of STK4 transcript in HeLa or CaSKi cells after transfection of DNMT1 specific siRNA (72 hours). U6 transcript levels were used as a loading control.

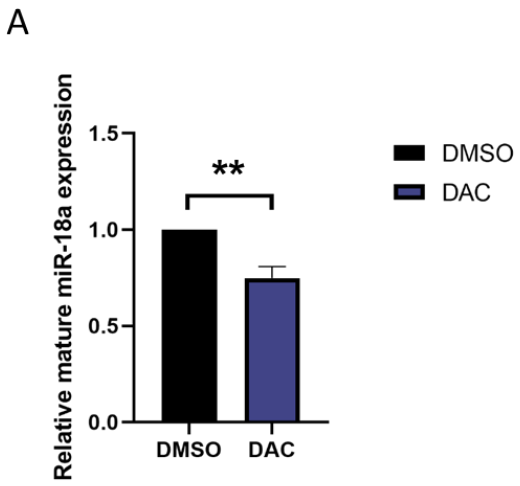

Figure 3.9 Inhibition of DNMT1 activity reduces miR-18a expression. A) Mature miR-18a expression analysed by miScript and qPCR in HeLa cells after DAC treatment (72 hrs). snORD68 expression was used as a loading control.

3.2.8 Genotoxic stress does not induce STK4 expression

Inhibition of either E6 or E7 is known to lead to the induction of apoptosis. Furthermore, as both miR-18a and DNMT1 are both promoters of proliferation, loss of either of their activity could also lead to apoptosis. STK4 is a key mediator of apoptosis and activates DNA damage response pathways and therefore, it is possible that STK4 was simply increased upon depletion of E6/E7, inhibition of miR-18a or inhibition of DNMT1 as a response to genotoxic stress. To confirm whether was the case, apoptosis and DNA damage pathways were induced and *STK4* mRNA expression was assessed. STK4 protein expression was not assessed as STK4 protein is cleaved upon induction of apoptosis and therefore would be expected to decrease with genotoxic stress.

Firstly, staurosporine was used to induce apoptosis. qRT-PCR analysis showed that there was no significant change in *STK4* expression with staurosporine treatment (Figure 3.10 A). Next, DNA damage was induced in HeLa cells with treatment of H_2O_2 and no significant change was observed in *STK4* when mRNA was analysed (Figure 3.10 B). Furthermore, analysis of *STK4* mRNA showed no significant change in expression following low dose etoposide treatment to induce senescence following DNA damage (Figure 3.10 C). Additionally, p53 overexpression led to no significant change in *STK4* mRNA (Figure 3.9 D).

Collectively, these data suggests that the upregulation of STK4 expression observed upon depletion of E6/E7, inhibition of miR-18a or DNMT1 does not occur simply due to genotoxic stress.

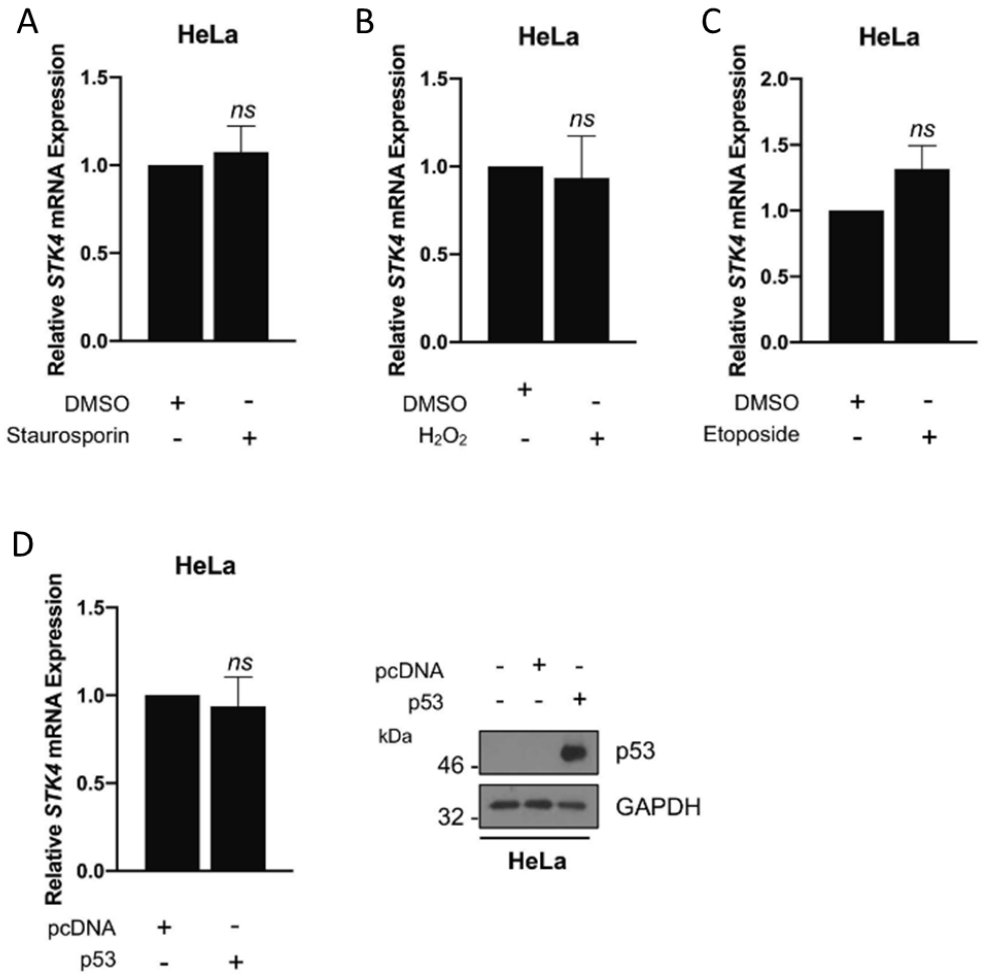

Figure 3.10 Genotoxic stress does not increase STK4 expression. A) qRT-PCR analysis of STK4 transcript in HeLa cells after 48 hour Staurosporine (50 µM) treatment. U6 transcript levels were used as a loading control. **B)** qRT-PCR analysis of STK4 transcript in HeLa cells after 48 hour H_2O_2 (200 µM) treatment. U6 transcript levels were used as a loading control. **C)** qRT-PCR analysis of STK4 transcript in HeLa cells after 48 hour Etoposide (2 µM) treatment. U6 transcript levels were used as a loading control. **D)** qRT-PCR analysis of STK4 transcript in HeLa cells after 48 hour post transfection with pcDNA3-p53. U6 transcript levels were used as a loading control. Representative western blot of HeLa cells 48 hour post transfection with pcDNA3-p53. Cell lysates were probed for the expression of p53. GAPDH was used as a loading control.

3.3 Discussion

This study identifies miR-18a as an upregulated miRNA in cervical cancer. Relative expression of mature miR-18a was measured using a combination of miScript and qPCR to confirm previous studies suggesting miR-18a is highly expressed in invasive cervical cancer. Our data suggests miR-18a is significantly overexpressed in both HPV16+ and HPV18+ cell lines compared to HPV- cell lines. Our data also suggests that miR-18a is overexpressed in clinical biopsies of CIN2 and CIN3 patient samples but not in CIN1. This confirmed that miR-18a is upregulated in clinically relevant samples and not just in cell lines adapted for tissue culture growth. Further analysis of online microarray datasets agreed with this, with miR-18a significantly increased in cervical cancer in GSE86100 and in both CIN2-3 and cervical cancer in GSE30656. Taken together it was concluded that miR-18a is upregulated in cervical cancer.

The biogenesis pathway of miRNAs is complex and has multiple steps before mature miRNA is produced. To investigate the mechanism behind the upregulation of miR-18a, pre-miR18a levels were assessed via qRT-PCR. Interestingly, *pre-miR18a* level were found to be decreased in all HPV+ cell lines tested and furthermore *pre-miR92a*, another member for the miR17-92 cluster previously seen to be increased in cervical cancer, showed a similar trend. This suggests that the increase in mature miR-18a observed is not due to an increase in transcription of the cluster, but likely due to increased processing of the cluster however this should be confirmed by investigating pri-miRNA levels. Although several components of the miRNA biogenesis pathway are reported to be dysregulated in cervical cancer, several host cell factors play roles specifically in processing of the miR17-92 cluster. For example, Heterogeneous nuclear ribonucleoprotein A1 (hnRNP A1) has been shown to facilitate processing of pre-miR18a and therefore cell factors such as this should be investigated in the context of cervical cancer (247).

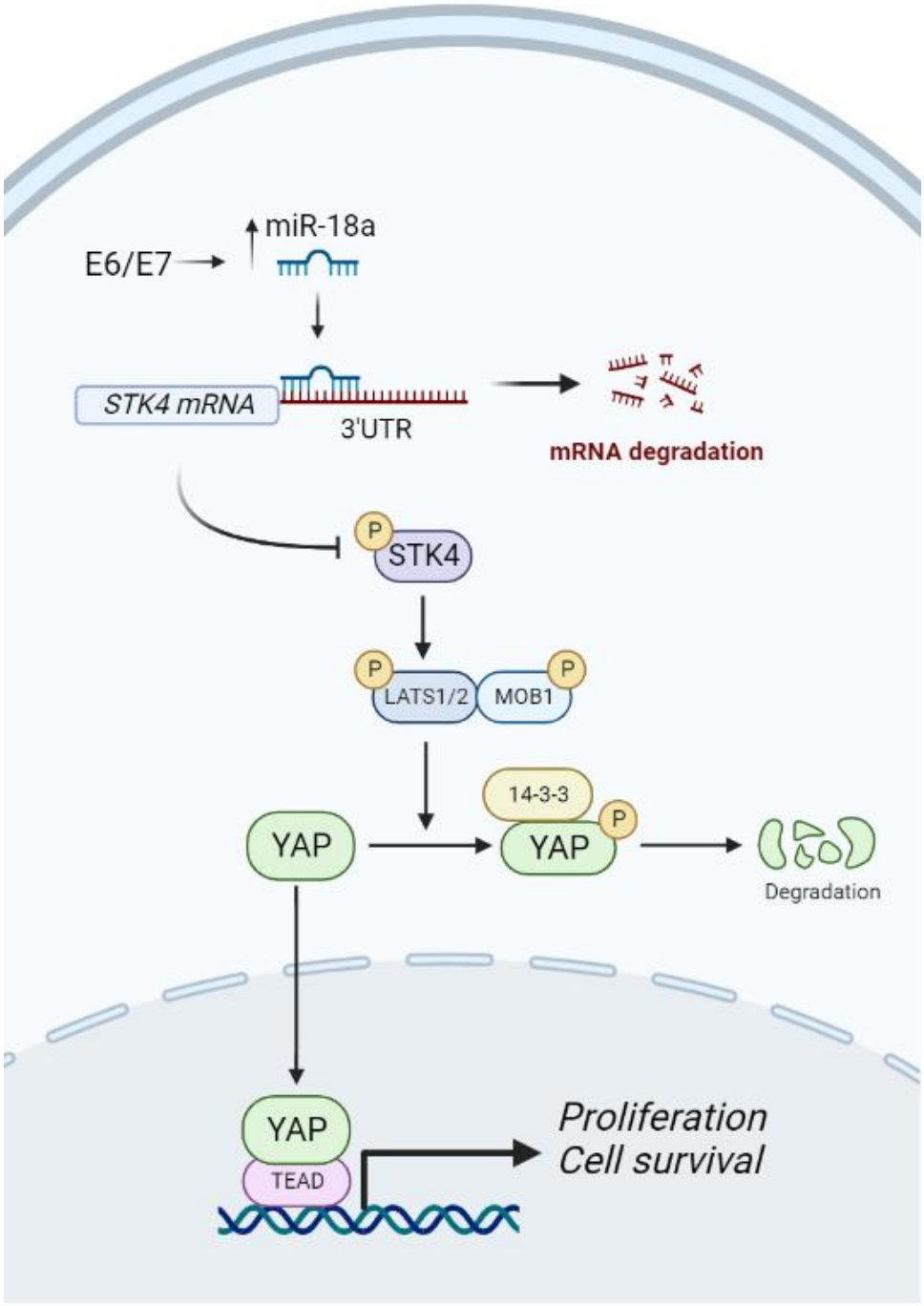

Figure 3.11 Summary of miR-18a/STK4. HPV oncoproteins upregulate mature miR-18a to target STK4, preventing Hippo pathway activation and therefore promoting proliferation (created with biorender).

When patient samples were matched, miR-18a was found to inversely correlate with *STK4* expression. As miR-18a is not changed in CIN1 compared to higher CIN grades, this suggests that while miR-18a is upregulated in cervical cancer, levels are not significantly changed with HPV infection alone, suggesting miR-18a overexpression is a cancer-specific phenotype.

Our data suggests that despite miR-18a having multiple targets, STK4 is an important target of miR-18a in cervical cancer as not only does inhibition of miR-18a using an antagomir lead to restoration of STK4 gene expression, but this occurs specifically through the predicted binding site. Although this was confirmed with a luciferase reporter assay, RNA immunoprecipitation pulldown of miR-18a could have been used to confirm STK4 as a miR-18a target. This same method could be used in the future to identify further miR-18a targets in the context of HPV+ cervical cancer. In contrast, *STK4* was only determined to be a target of miR-18a in HPV-driven cervical cancer, as inhibition of miR-18a in C33A cells led to no changes in *STK4* expression, demonstrating cell specific effects of the miRNA.

Although an in-depth mechanism was not investigated, it was determined that miR-18a was responsible for E6/E7 control of STK4 expression. While E6 and E7 are well known to target tumour suppressors p53 and Rb respectively, our data alongside other studies demonstrates loss of these tumour suppressors alone insufficient for transformation, and also that virus-mediated cervical cancer progression is more complex. Not only does this suggest that perturbation of multiple host factors is needed for cervical cancer transformation but that this perturbation occurs through multiple mechanisms, such as via control of miRNA expression or by dysregulation of DNMT1 activity, which we also demonstrate to be a regulator of STK4 expression. Even though it has been reported that certain host cell factors are targeted by multiple mechanisms in cervical cancer, our data suggest a potentially complex pathway with E6 and E7 potentially regulating mature miR-18a expression through DNMT1 activity. As we

determined miR-18a to not be dysregulated on a transcriptional level, DNMT1 is likely to be controlling a host cell factor involved in processing of miR-18a, but further investigation is required to confirm this.

The data demonstrates a clear functional depletion of STK4 by miR-18a. Inhibition of miR-18a led to the restoration of STK4 expression and therefore activation of the Hippo pathway, loss of YAP activity and subsequent reduction in proliferation in both HPV16 and HPV18+ cervical cancer cells. Even though it has been reported that HPV oncoproteins increase YAP activity in cervical cancer through separate mechanisms, the suppression of Hippo pathway signalling by miR-18a highlights the pathways importance in cervical cancer.

Interestingly, it is likely that miR-18a has multiple targets in cervical cancer cells, as depletion of STK4 after miR-18a inhibition did not fully restore the loss of proliferation. Further investigation should be undertaken to identify additional tumour suppressors targeted by miR-18a.

Together this study identifies STK4 as a prominent target of miR-18a in cervical cancer. While seemingly not upregulated in HPV infection (CIN1), miR-18a plays a key role in HPV-driven cervical cancer. It also highlights the oncogenic ability of miR-18a in cervical cancer is partially dependent on the depletion of STK4. This study also suggests DNMT1 plays a role in the regulation of miR-18a expression by HPV oncoproteins E6 and E7.

Chapter 4- TAZ expression is increased by the E7 oncoprotein in HPV18+ cervical cancers using an EGFR-SP1 signalling pathway

4.1 Introduction

The previous chapter studied upstream regulation of the Hippo pathway and the effects upon the most well-characterised effector and transcriptional regulator downstream of the pathway, YAP. In contrast to YAP, less is known about the role of the YAP paralogue TAZ in cancers, as until recently it had been assumed to play a redundant role to YAP in driving pro-oncogenic transcription. However, as more recent studies have identified ever increasing YAP-independent functions of TAZ, the need to understand this oncogene is clear.

Whilst a small number of previous studies have analysed the role of TAZ in cervical cancer, their findings are controversial. Some studies have shown that TAZ expression is decreased in cervical cancer compared with normal tissue (197). In contrast, others suggest that TAZ is oncogenic and regulates proliferation, invasion and apoptosis whilst upregulating PD-L1, a prominent regulator of T-cell evasion (198). In addition to these contrasting findings, no study has explained how TAZ expression is regulated in cervical cancer.

This chapter aims to clarify how TAZ expression is regulated in cervical cancer and begin to elucidate a mechanism for its regulation.

4.2 Results

4.2.1 TAZ expression is increased in HPV18+ cervical cancer

TAZ protein expression was analysed in a panel of cervical cancer cell lines. This panel included HPV- HaCaT (immortalized human keratinocytes) and C33a cells, HPV16+ SiHa and CaSKi cells and HPV18+ SW756, HeLa, C4-I and MS751 cells. We have previously been reported that YAP protein expression was increased in all cell lines (174), but interestingly TAZ protein was only increased in the HPV18+ cell lines (Figure 4.1 A).

Previous studies have shown that the increase in YAP increased in HPV-driven cancers is due to an increase in protein stability (173, 196) . To investigate if TAZ protein was likewise stabilised, a cycloheximide (CHX) chase was performed over an 8-hour period to measure the half-life of TAZ in HPV18+ HeLa cells. Past studies have suggested the unstabilised TAZ has a half-life of roughly 2 hours (263, 264). The half-life of TAZ was also measured in HPV16+ SiHa cells for comparison. Analysis of YAP expression with CHX treatment revealed very little change in expression in both cell lines with CHX treatment, agreeing with reports on its increased stability. In contrast, TAZ protein expression was lost upon CHX treatment with densitometry analysis suggesting a half-life of roughly 3 hours in both HPV16+ and HPV18+ cells (Figure 4.1 B with densitometry analysis in Figure 4.1 C). As there was no difference in TAZ half-life between HPV16+ and HPV18+ cells despite increased TAZ expression in the HPV18+ cells, this suggested TAZ was unlikely to be stabilised on a protein level like YAP. The slight increase in both HeLa and SiHa cells compared to other studies may due to little normal Hippo pathway activation due to the loss of STK4 expression (174).

Further investigation revealed that TAZ was degraded in a proteasomal-mediated manner as CHX treatment followed by treatment with the proteasome inhibitor MG132 restored TAZ protein levels. Treatment with the lysosome inhibitor following CHX

treatment led to no change in TAZ levels indicating TAZ was not degraded in a lysosome-mediated manner (Figure 4.1 D).

As TAZ was not stabilised on a protein level, the levels of *WWTR1,* (the gene encoding TAZ) mRNA were examined. Analysis showed *WWTR1* mRNA expression was not significantly changed in the HPV16+ cell lines while SW756, HeLa and MS756 cells all had significantly increased *WWTR1* mRNA expression compared to HaCaT cells. C4-1 also showed increased *WWTR1* mRNA, although this was not significant (Figure 4.1 E).

Together these data suggested that TAZ was increased on an mRNA level in HPV18+ cervical cancer cell lines. However, as these cell lines were adapted for tissue culture growth, *WWTR1* mRNA expression was investigated in a panel of cervical liquid cytology samples. Samples were obtained from the Scottish HPV archive and taken from patients with a healthy cervix as well as from HPV16+ and HPV18+ positive patients representing cervical disease progression from CIN1 to CIN3. qRT-PCR analysis showed significantly increase *WWTR1* mRNA in CIN2 and CIN3 from HPV18+ patients only (Figure 4.2 A). These data allied with an analysis of *WWTR1* mRNA expression in an online dataset of cervical cancer samples (Figure 4.2 B). Analysis of *WWTR1* mRNA expression between cervix squamous epithelium and cervical adenocarcinoma (a cervical cancer subset predominantly caused by HPV18) also showed significantly increased expression (Figure 4.2 C). Analysis of the Cervical Squamous Cell Carcinoma and Endocervical Adenocarcinoma (TCGA, Firehose Legacy) dataset using cBioportal showed WWTR1was frequently altered in cervical cancer (in 20%). Interestingly, YAP and TAZ were found to be altered in different samples (Figure 4.2 D). Further analysis of the TCGA dataset for multiple cancers suggested TAZ was frequently altered in many cancers, but most often in squamous cell carcinomas (Figure 4.2 E). Together these data suggested TAZ was increased in cervical cancer on an mRNA level.

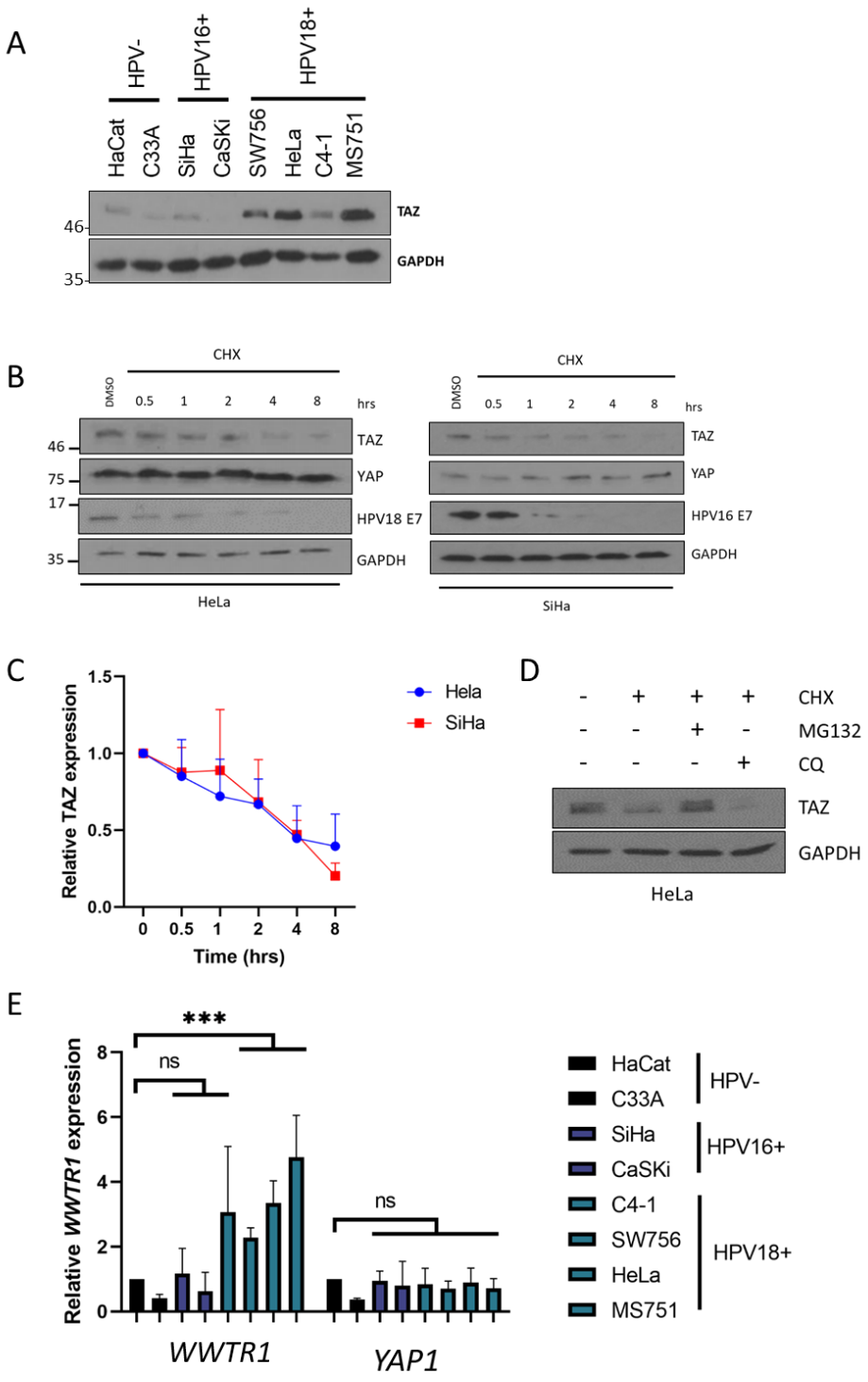

Figure 4.1 TAZ is overexpressed in HPV18+ cervical cancer cells A) Representative western blot of lysate from HPV-, HPV16+ and HPV18+ cell lines. Lysates were probed for TAZ and YAP, GAPDH was used as a loading control. **B)** Representative western blot of HeLa and SiHa lysate over a time course of 8 hours following treatment with CHX. Lysates were probed for TAZ and YAP. E7 was used as a positive control of CHX treatment. GAPDH was used as a loading control.

C) Densitometry analysis of TAZ expression in B from 3 independent repeats. **D)** Representative western blot of HeLa lysates 8 hours post treatment with a combination of DMSO, CHX, MG132 or CQ. Lysates were probed for TAZ. GAPDH was uses as a loading control. **E)** qRT-PCR analysis of WWTR1 or YAP expression in HPV-, HPV16+ or HPV18+ cell lines. U6 transcript levels were used as a loading control.

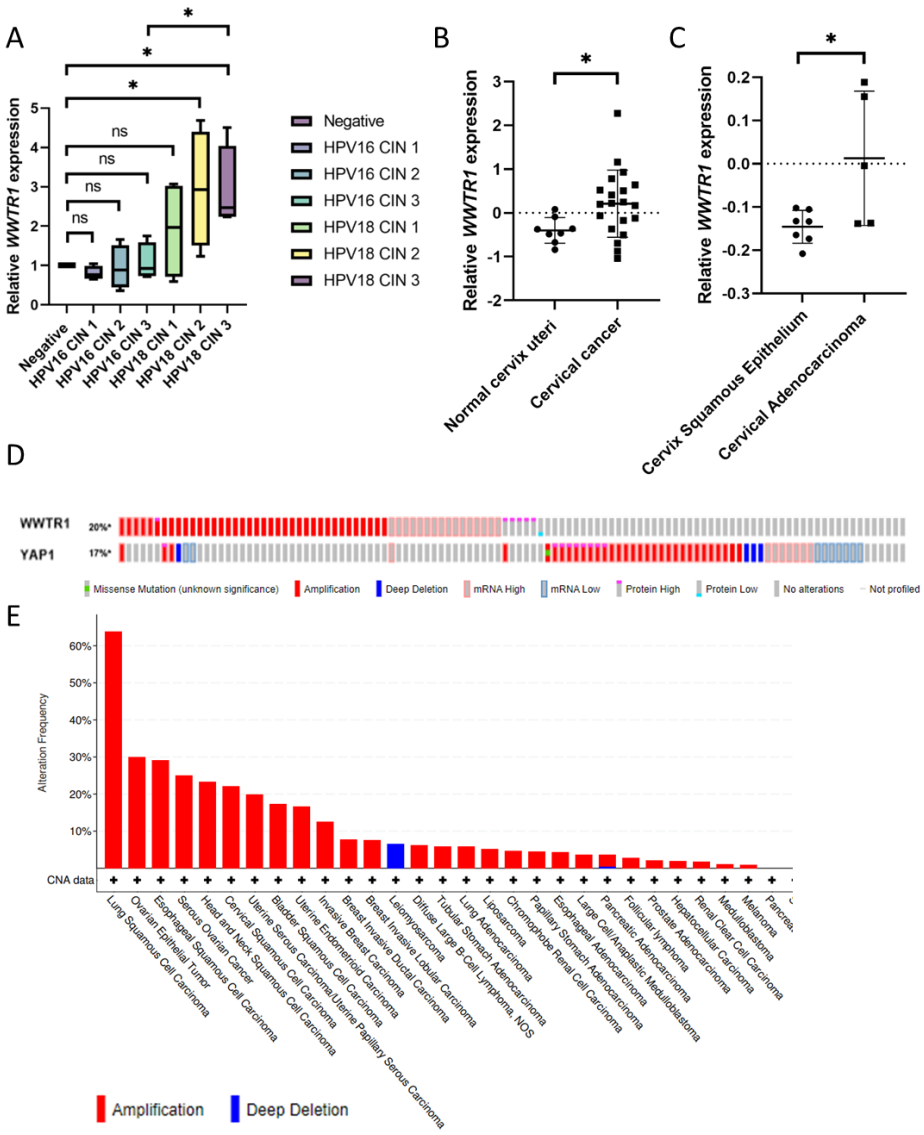

Figure 4.2 TAZ is overexpressed in cervical cancer A) qRT-PCR analysis of *WWTR1* expression in negative, HPV16 or HPV18+ patient cervix liquid cytology samples from different CIN grades (n=4 from each grade). U6 was used as a loading control. **B)** Scatter plot from GSE9750. Arbitrary expression values for *WWTR1* was plotter for each sample. **C)** Scatter plot of GSE6791. Arbitrary expression values for *WWTR1* was plotter for each sample. **D)** WWTR1 and YAP1 expression in Cervical Squamous Cell Carcinoma and Endocervical Adenocarcinoma (TCGA, Firehose Legacy) dataset for mutations, putative copy-number alterations, mRNA expression z-scores relative to diploid samples (RNA Seq V2 RSEM) and Protein expression z-scores (RPPA). **E)** *WWTR1* expression in Pan-cancer analysis of whole genomes (ICGC/TCGA, Nature 2020) for Consensus putative gene level copy-number calls.

4.2.2 Knockdown of E6/E7 in HPV18+ cells decreases TAZ expression

To investigate if E6 and E7 were responsible for the upregulation of TAZ, E6 and E7 expression was knocked down in HPV18+ cells using a pool of siRNA and this resulted in a decrease in TAZ mRNA and protein expression (Figure 4.3 A-B). An approach to target both E6 and E7 together was taken as knockdown of one often leads to knockdown of the other.

As many factors can regulate mRNA levels including transcription and mRNA stability, WWTR1 mRNA transcript stability was measured. Actinomycin D (an inhibitor of transcription) treatment was performed over a course of 24 hours and both TAZ protein and mRNA levels were investigated. Treatment led to reduction in TAZ protein levels and *WWTR1* mRNA expression (Figure 4.3 C-D). As *WWTR1* mRNA was not stabilised, further analysis was performed to study if the *WWTR1* promoter was activated by HPV. For this a reporter plasmid was generated in which the *WWTR1* promoter was cloned upstream of firefly luciferase. In these assays, a plasmid encoding renilla luciferase was used as a transfection control. Knockdown of HPV18 E6 and E7 in HeLa cells significantly reduced firefly luciferase levels, suggesting a reduction in *WWTR1* promoter activity. Together these data suggests that E6/E7 upregulate *WWTR1* promoter activity in HPV18+ cervical cancer cells though as neither E6 nor E7 have DNA binding activity this is indirect.

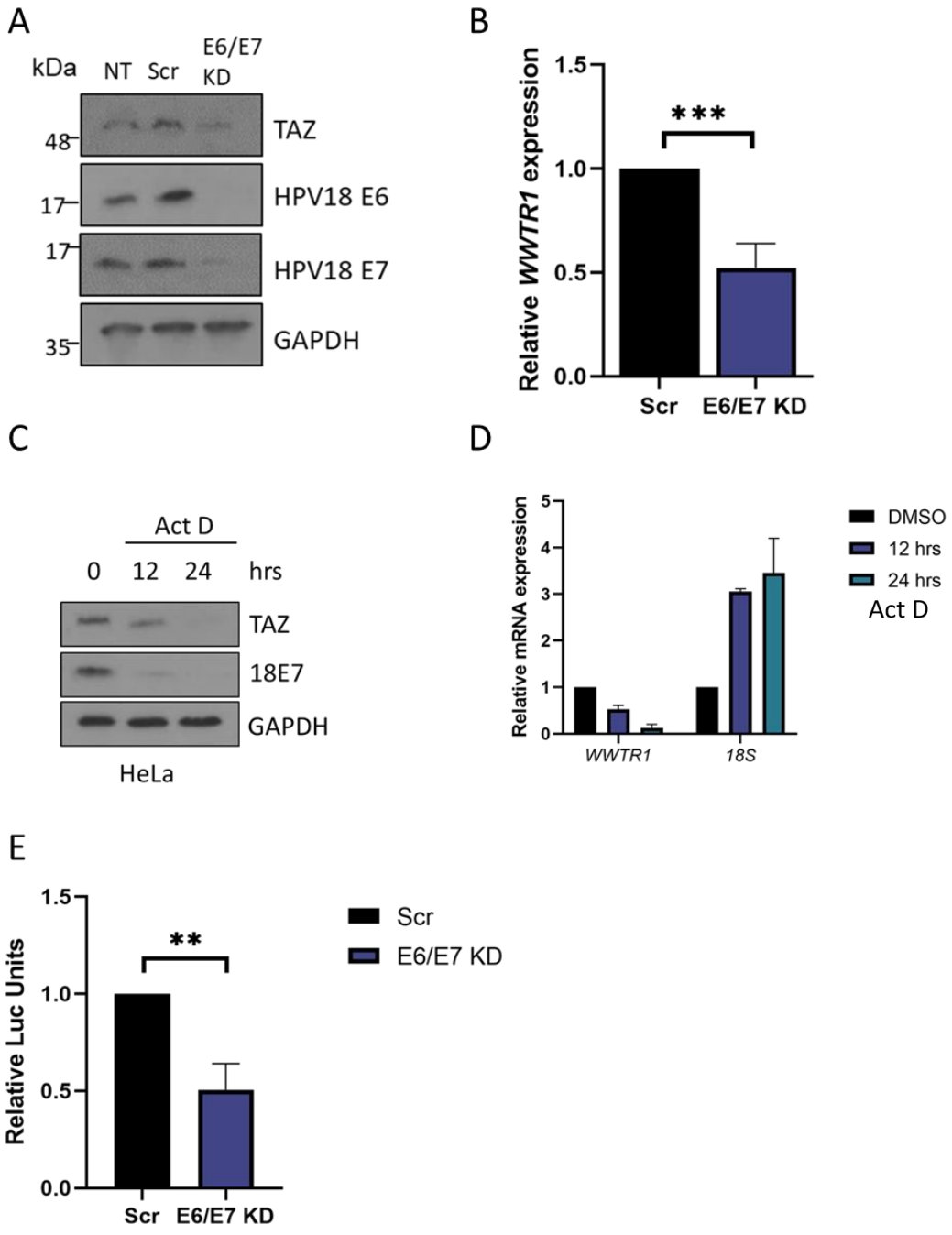

Figure 4.3 HPV18 E6/E7 knockdown reduces TAZ promoter activity A) Representative western blot of HeLa cell lysate with E6/E7 targeting siRNA (for 72 hours). Cell lysates were probed for TAZ. HPV18 E6 and HPV18 E7 were probed for to show successful knockdown of E6 and E7. GAPDH was used as a loading control. B) qRT-PCR analysis of *WWTR1* expression in HeLa cells with E6/E7 targeting siRNA (for 72 hours). *U6* was used as a loading control. **C)** Representative western blot of HeLa cell lysate following Act D treatment over a 24 hour time course. Cell lysates were probed for TAZ. HPV18 E7 was probed for to show successful Act D

treatment. GAPDH was used as a loading control. **D)** qRT-PCR analysis of *WWTR1* expression in HeLa cells following Act D treatment over a 24 hour time course. *18S* expression was used to show successful ActD treatment. *U6* was used as a loading control (n=2). **E)** Luciferase reporter assay in HeLa cells with E6/E7 targeting siRNA (for 72 hours) and then *WWTR1*-promoter luciferase reporter (for 24 hours). Internal renilla luciferase was used as a loading control.

4.2.3 HPV18 E7 upregulates TAZ expression

As the siRNA used in Figure 4.3 target both HPV18 E6 and E7, further investigations were carried out to determine which oncoprotein was responsible. HA-tagged HPV18 E6 or HPV18 E7 were stably overexpressed in HPV- C33A cells in a puromycin resistant vector and *WWTR1* promoter activity was assessed using the *WWTR1* luciferase reporter outlined in 4.2. Only HPV18 E7 expression led to a significant increase in luciferase activity (Figure 4.4 A). *WWTR1* mRNA expression was also increased by HPV18 E7 compared to the empty vector control (Figure 4.4 B). Crucially, HPV18 E7 expression also led to a significant increase in TAZ protein expression. Oncoprotein expression was confirmed by western blotting and probing for HPV18 E6 or HPV18 E7 (Figure 4.4 C).

To confirm that the expression of HPV18 E7 was leading to increase *WWTR1* promoter activity and not increased protein stability, the mechanism seen in regulation of YAP, HPV18 E7-expressing C33A cells were treated with CHX and TAZ protein expression was analysed. CHX treatment led to a reversal of the increase in TAZ expression seen with HPV18 E7 expression alone (Figure 4.4 D lane 3 compared with lane 2) suggesting HPV18 E7 did not lead to stabilisation of TAZ protein degradation.

Furthermore, to confirm HPV18 E7 was not stabilising *WWTR1 mRNA*, HPV18 E7 expressing C33A cells were treated with actinomycin D and *WWTR1* mRNA expression was analysed using qRT-PCR. Analysis showed that treatment with actinomycin D led to a reversal of the increase in *WWTR1* mRNA expression seen with HPV18 E7 expression. Even though it was not a complete reversal, the increase between the empty vector and HPV18 E7 expressing cells after actinomycin D treatment was not significant. Similarly, treatment reverse the increase in TAZ protein observed with HPV18 E7 expression.

As increased TAZ expression was only seen in HPV18+ cell lines (4.2.1), it was hypothesised that HPV16 E7 would lack the ability to increase TAZ levels. To investigate this, C33A cells were generated stably expressing HA-tagged HPV16 E7 and *WWTR1* promoter activity was measured using the *WWTR1*-promoter luciferase reporter. Importantly, these assays demonstrated clearly that HPV16 E7 was not able to increase *WWTR1* promoter activity compared with HPV18 E7 (Figure 4.5 A). Furthermore, analysis of *WWTR1* mRNA and TAZ protein expression confirmed that expression of HPV16 E7 did not lead to any significant change (Figure 4.5 B-C). HPV16 E7 was probed to confirm successful expression, the double band observed is likely due to cleavage of the HA tag (Figure 4.5 C).

To confirm these results observed were not a cell type specific phenotype to C33A cells, HPV18 E7 was expressed in the immortalised keratinocyte HaCaT cell line. Measuring promoter activity showed HPV18 E7 was still able to increase *WWTR1* promoter activity (Figure 4.6 A). Furthermore HPV18 E7 also significant increased *WWTR1 mRNA* expression and TAZ protein expression (Figure 4.6 B-C). As this matched the data observed in C33A, it was concluded that the effects seen were not a cell specific phenotype. Together, these data suggest HPV18 E7 increase *WWTR1* promoter activity leading to an increase in both mRNA and protein levels.

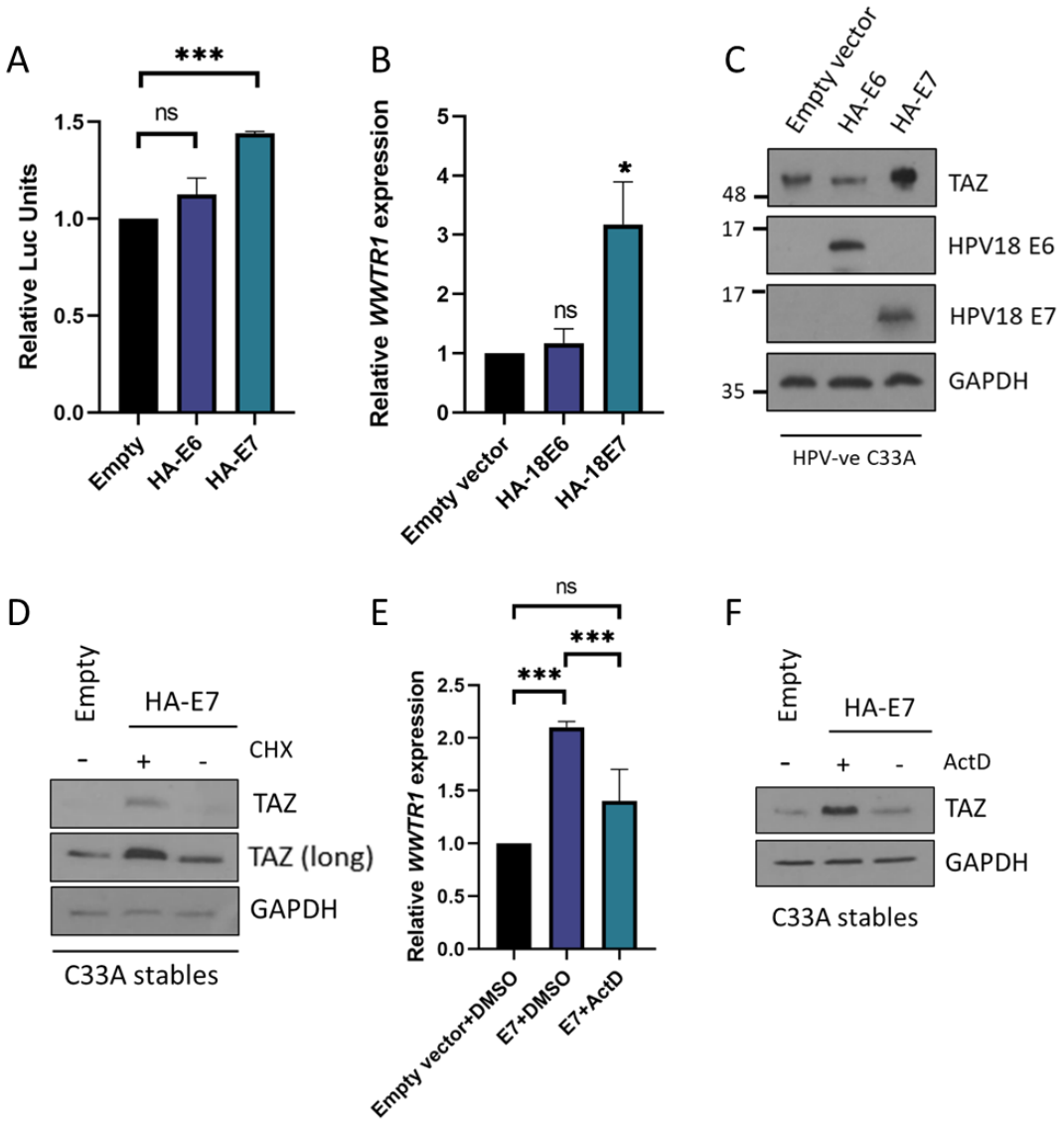

Figure 4.4 HPV18 E7 upregulates TAZ promoter activity A) Luciferase reporter assay in C33A cells stably expressing either HA-HPV18 E6 or HA-HPV18 E7 transfected with WWTR1-promoter luciferase reporter (for 24 hours). Internal renilla luciferase was used as a loading control. **B)** qRT-PCR analysis of *WWTR1* expression in C33A cells stably expressing either HA-HPV18 E6 or HA-HPV18 E7. U6 was used as a loading control. **C)** Representative western blot of C33A cell lysate stably expressing either HA-HPV18 E6 or HA-HPV18 E7. Cell lysate was probed for TAZ. HPV18 E6 and HPV18 E7 were probed for to confirm successful expression. GAPDH was used as a loading control. **D)** Representative western blot of C33A stably expressing HA-HPV18 E7 with or without treatment of CHX. Cell lysate was probed for TAZ. GAPDH was used as a loading control. **E)** qRT-PCR analysis of WWTR1 expression in C33A stably expressing HA-HPV18 E7 with or

without treatment of Act D. U6 was used as a loading control. **F)** Representative western blot of C33A stably expressing HA-HPV18 E7 with or without treatment of Act D. Cell lysate was probed for TAZ. GAPDH was used as a loading control.

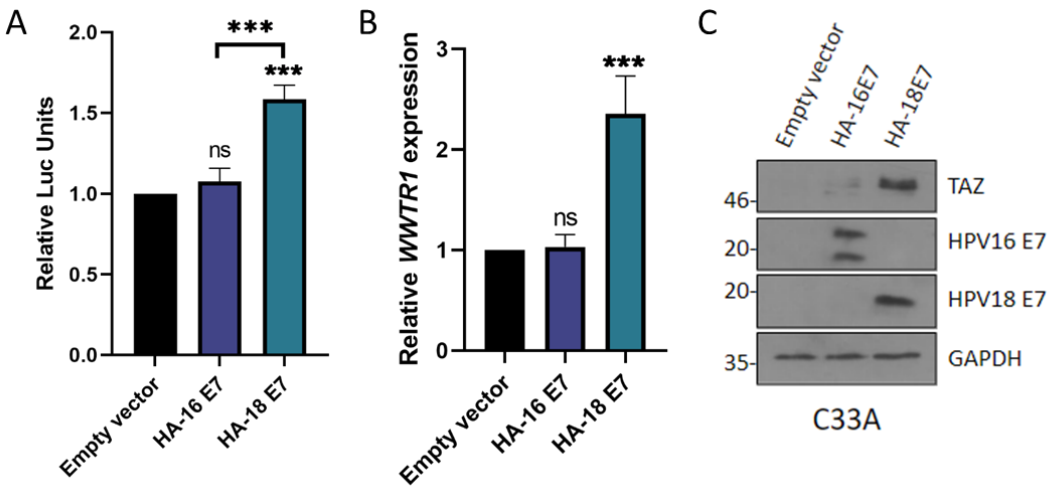

Figure 4.5 HPV16 E7 does not increase *WWTR1* promoter activity A) Luciferase reporter assay in C33A cells stably expressing either HA-HPV16 E7 or HA-HPV18 E7 transfected with WWTR1-promoter luciferase reporter (for 24 hours). Internal renilla luciferase was used as a loading control. **B)** qRT-PCR analysis of *WWTR1* expression in C33A cells stably expressing either HA-HPV16 E7 or HA-HPV18 E7. *U6* was used as a loading control. **C)** Representative western blot of C33A cell lysate stably expressing either HA-HPV18 E6 or HA-HPV18 E7. Cell lysate was probed for TAZ. HPV16 E7 and HPV18 E7 were probed for to confirm successful expression. GAPDH was used as a loading control.

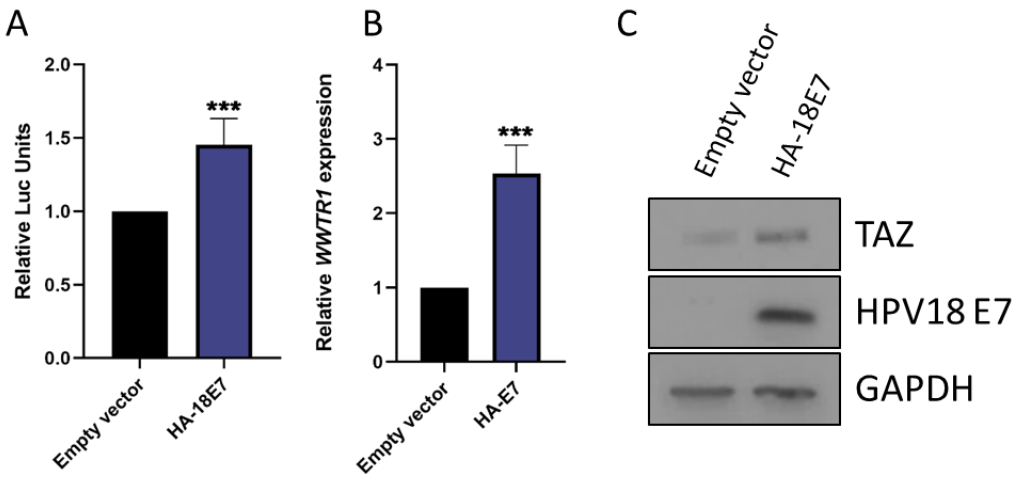

Figure 4.6 HPV18 E7 in HaCaT increases *WWTR1* promoter activity A) Luciferase reporter assay in HaCaT cells stably expressing HA-HPV18 E7 transfected with WWTR1-promoter luciferase reporter (for 24 hours). Internal renilla luciferase was used as a loading control. **B)** qRT-PCR analysis of *WWTR1* expression in HaCaT cells stably expressing HA-HPV18 E7. *U6* was used as a loading control. **C)** Representative western blot of HaCaT cell lysate stably expressing HA-HPV18 E7. Cell lysate was probed for TAZ. HPV16 E7 and HPV18 E7 were probed for to confirm successful expression. GAPDH was used as a loading control (n=2).

4.2.4 Transcription factor specificity protein 1 (SP1) controls TAZ expression

As HPV18 E7 does not have any DNA binding ability, it was hypothesised that the upregulation of *WWTR1* promoter activity seen must be through a host transcription factor. Online analysis of the *WWTR1* promoter region revealed 2 SP1 binding sites (Figure 4.7 A). Previous studies showed that SP1 plays a crucial role in HPV18-mediated transformation and high SP1 correlates with metastasis and invasion in cervical cancer (265). Therefore it was hypothesised that HPV18 E7 could be driving the increase the *WWTR1* promoter activity through SP1.

To investigate the effect of SP1 on TAZ expression, a small molecular inhibitor Mithramycin A (Mith A) which acts by displacing SP1 from binding sites was used (266). Treatment of HeLa cells led to a dose-dependent decrease in both *WWTR1*-promoter driven luciferase levels and *mRNA* expression (Figure 4.7 B-C). *CCND1* expression was used to confirm successful Mith A treatment (267). Crucially, Mith A treatment caused a dose-dependent decrease in TAZ protein expression (Figure 4.7 D). To confirm SP1 was binding to the *WWTR1* promoter through the predicted SP1 binding sites (Figure 4.7 A), site directed mutagenesis was used to delete each of the binding sites. Deletion of either of the binding sites led to a significant decrease in promoter activity in HeLa cells (Figure 4.7 E).

Together this, suggests SP1 regulates TAZ expression in HeLa cells. To confirm this was not a HeLa-specific phenotype, two additional HPV18+ cell lines were treated with Mith A and analysis revealed this led to a significant dose-dependent reduction in *WWTR1* mRNA in both SW756 (Figure 4.8 A) and MS751 (Figure 4.8B) cells. *YAP* mRNA was assessed in both these cell lines following Mith A treatment, as qRT-PCR analysis showed no significant change in *YAP* expression, it was concluded this was a mechanism specifically for regulation of TAZ expression.

Inhibitors such as Mith A often have off-target effects, so to confirm specifically that SP1 inhibition leads to a reduction in TAZ expression, an SP1 mutagenesis strategy was performed in parallel. For this, an expression plasmid was generated containing a truncated Flag tagged SP1 (Trunc SP1) that is capable of binding to SP1 binding sites in target promoters but that cannot activate transcription, therefore acting as a dominant negative (Figure 4.9 A). Expression of Trunc SP1 led to a significant decrease in *WWTR1*-promoter luciferase reporter levels, *WWTR1* mRNA expression and TAZ protein expression in HeLa cells. (Figure 4.9 B-D).

As HPV18 E7 increase *WWTR1* promoter activity, it was hypothesised that HPV18 E7 was acting through SP1. To investigate this GFP-HPV18 E7 was transfected into C33A cells. GFP-HPV18 E7 was used as Mith A treatment did not affect the expression of the construct. Mith A treatment of GFP-HPV18 E7 transfected C33A cells led to a reversal of significant increase in *WWTR1* promoter activity seen with GFP-HPV18 E7 transfection alone (Figure 4.10 A). Furthermore, treatment with Mith A reversed the significant increase in *WWTR1* mRNA expression seen with GFP-HPV18 E7 overexpression alone (Figure 4.10 B) and the same trend was observed TAZ protein expression. Probing for GFP confirmed Mith A treatment did not affect GFP-HPV18 E7 expression (Figure 4.10 C). These data suggests that HPV18 E7 upregulates TAZ expression in a SP1-dependent manner.

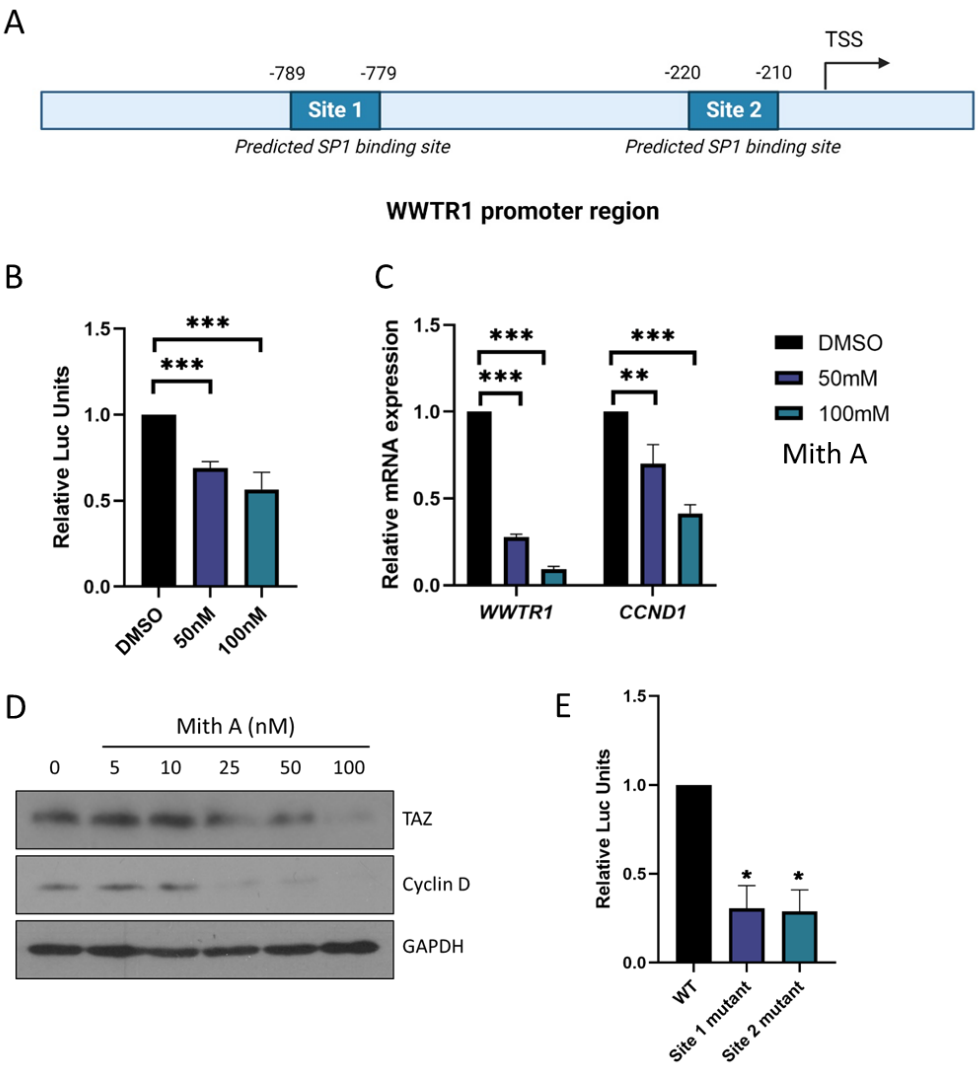

Figure 4.7 SP1 controls TAZ expression A) Schematic of *WWTR1* promoter with predicted SP1 binding sites highlighted. **B)** Luciferase reporter assay in HeLa cells following Mith A treatment (24 hours) and transfection of *WWTR1*-promoter luciferase reporter (48 hours). Internal renilla luciferase was used as a loading control. **C)** qRT-PCR analysis of *WWTR1* expression in HeLa cells following Mith A treatment. CCND1 transcript levels were used to show successful Mith A treatment. U6 was used as a loading control. **D)** Representative western blot of HeLa cells following Mith A treatment. Cell lysate was probed for TAZ. Cyclin D was probed for to show successful Mith A treatment. GAPDH was used as a loading control. E) Luciferase reporter assay in HeLa cells following transfection of the WWTR1-promoter luciferase reporter or SP1 binding site 1 or binding site 2 mutants (24 hours). Internal renilla luciferase was used as a loading control.

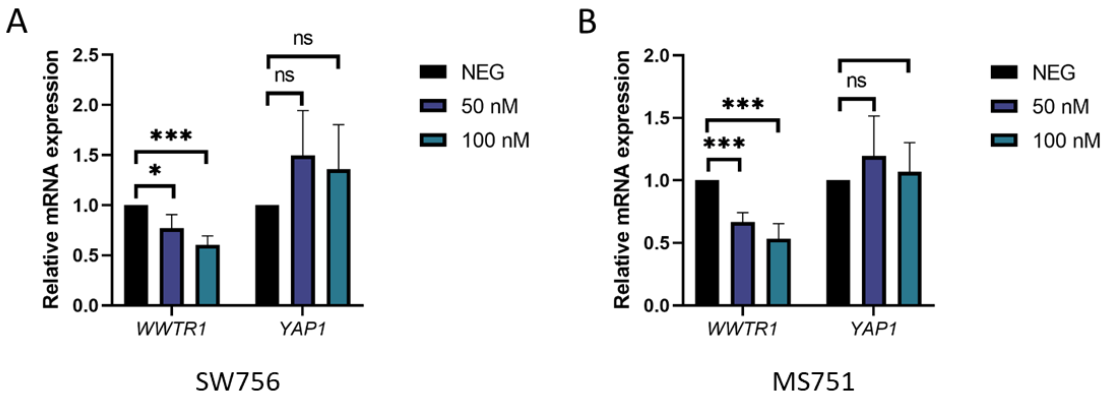

Figure 4.8 Inhibition of SP1 leads to a reduction in *WWTR1* expression in other HPV18+ cell lines A) qRT-PCR analysis of *WWTR1* expression in SW756 cells following Mith A treatment. U6 was used as a loading control. **B)** qRT-PCR analysis of WWTR1 expression in MS751 cells following Mith A treatment. U6 was used as a loading control.

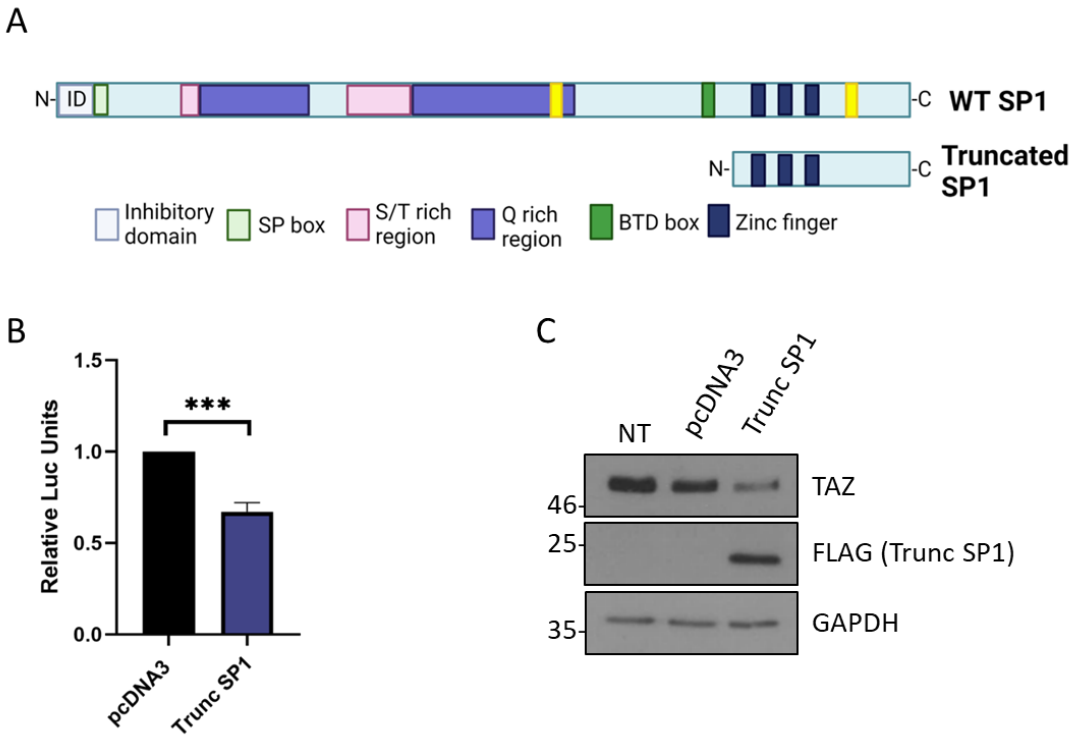

Figure 4.9 Dominant negative SP1 inhibits TAZ expression A) Schematic demonstrating Trunc SP1 feature compared to full length SP1. **B)** Luciferase reporter assay in HeLa cells following transfection of Trunc SP1 and *WWTR1*-promoter luciferase reporter (24 hours). Internal renilla luciferase was used as a loading control. **C)** qRT-PCR analysis of *WWTR1* expression in HeLa cells following transfection of Trunc SP1 (24 hours). U6 was used as a loading control. **D)** Representative western blot of HeLa cells following transfection of Trunc SP1 (24 hours). Cell lysate was probed for TAZ. FLAG was probed for to show successful transfection of Trunc SP1. GAPDH was used as a loading control.

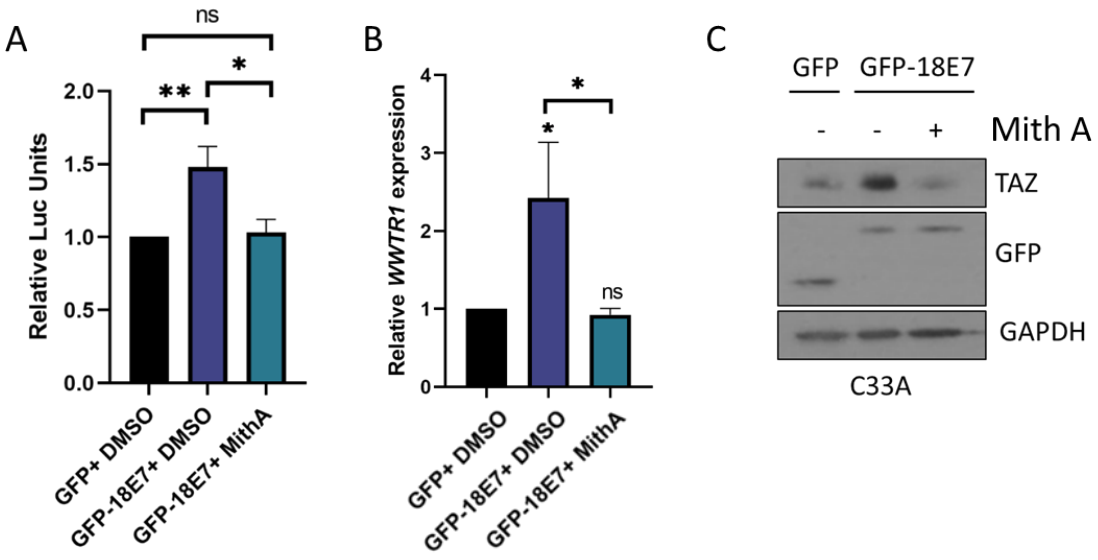

Figure 4.10 Upregulation of TAZ by HPV18 E7 is SP1-dependent A) Luciferase reporter assay in C33A cells following transfection of GFP-HPV 18 E7 and *WWTR1*-promoter luciferase reporter (48 hours) with or without Mith A treatment (24 hours). **B)** qRT-PCR analysis of *WWTR1* expression in C33A cells following transfection of GFP-HPV 18 E7 (48 hours) with or without Mith A treatment (24 hours). U6 was used as a loading control. **C)** Representative western blot of C33A lysate following transfection of GFP-HPV 18 E7 (48 hours) with or without Mith A treatment (24 hours). Cell lysate was probed for TAZ. GFP was probed for to show successful transfection of GFP-HPV 18 E7. GAPDH was used as a loading control.

4.2.5 The ERK1/2 signalling pathway regulates TAZ expression

Literature suggests SP1 activity is regulated by phosphorylation by many kinases. However, two phosphorylation sites, T453 and T739 (Figure 4.11 A), have been linked to ERK1/2 signalling activity, which is a pathway aberrantly activated by HPV E7 (268, 269). Therefore, it was hypothesised that ERK1/2 signalling is involved in the regulation of TAZ expression.

ERK1/2 signalling was inhibited by treatment with U0126, an MKK1/2 inhibitor, preventing ERK1/2 phosphorylation and activation (270). Treatment with U0126 led to a significant dose-dependent reduction in *WWTR1* promoter activity and WWTR1 expression (Figure 4.11 B-C). Analysis of *YAP* mRNA showed no significant change in expression, demonstrating this mechanism of regulation is specific to TAZ (Figure 4.11 C).

To investigate if E7 was activating ERK1/2 in the context of SP1 driven TAZ expression HPV18 E7 stable expressing C33A cells were treated with U0126. Analysis of the *WWTR1*-promoter luciferase reporter assay revealed a complete reversal of luciferase expression, indicating inhibition of ERK1/2 reversed the increase in *WWTR1* promoter activity seen with HPV18 E7 expression. Furthermore, U0126 treatment reversed the increase in *WWTR1* mRNA seen with HPV18 E7 overexpression alone (Figure 4.11 E).

SP1 is not solely activated by ERK, other MAPK pathways such as JNK are known regulators and is aberrantly activated in HPV+ cancer (271). Interestingly, treatment with JNK signalling inhibitor JNK-IN-8 actually increased *WWTR1* promoter activity, indicting it is not a regulator of *WWTR1* expression (Figure 4.11 F). Taken together, these data suggests ERK1/2 signalling is a regulator of TAZ expression.

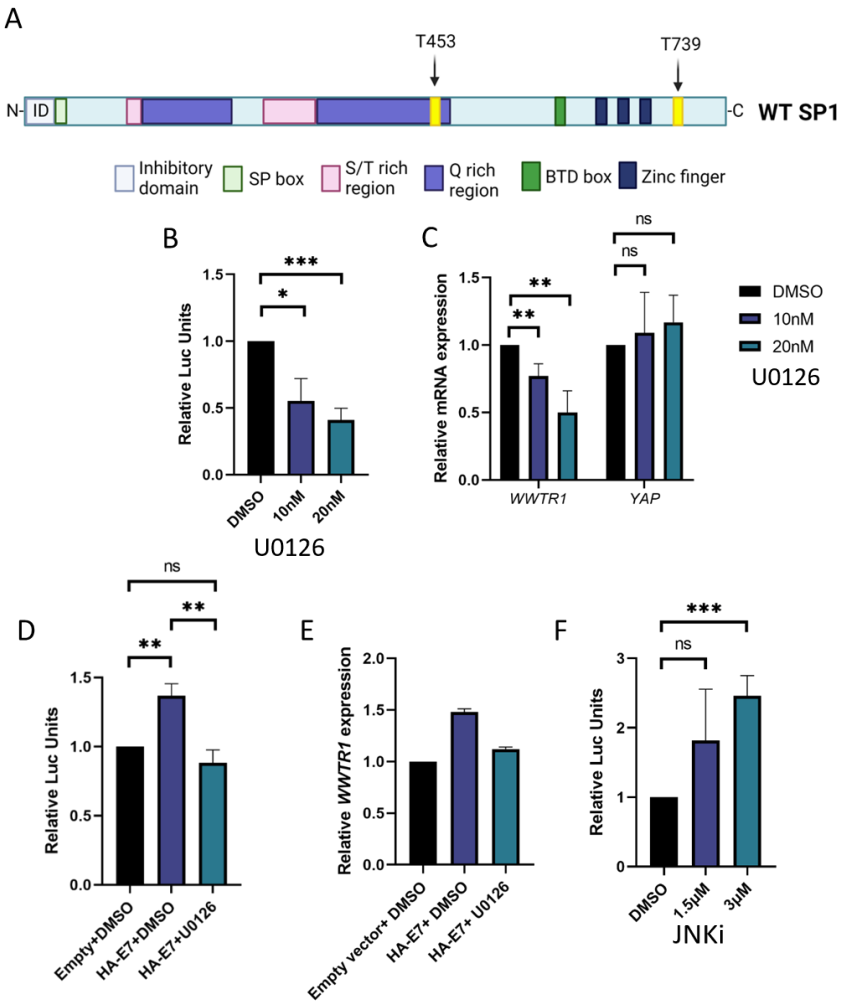

Figure 4.11 HPV 18 E7 control of WWTR1 expression is ERK1/2 signalling dependent A) Schematic demonstrating SP1 phosphorylation sites phosphorylated by ERK1/2 signalling. **B)** Luciferase reporter assay in HeLa cells following U0126 treatment (24 hours) and transfection of *WWTR1*-promoter luciferase reporter (48 hours). Internal renilla luciferase was used as a loading control. **C)** qRT-PCR analysis of *WWTR1* and *YAP* expression in HeLa cells following Mith A treatment. U6 was used as a loading control. D) Luciferase reporter assay in C33A cells following transfection of GFP-HPV 18 E7 and *WWTR1*-promoter luciferase reporter (48 hours) with or without U0126 treatment (24 hours). **E)** qRT-PCR analysis of *WWTR1* expression in C33A cells following transfection of GFP-HPV 18 E7 (48 hours) with or without U0126 treatment (24 hours). U6 was used as a loading control. **F)** Luciferase reporter assay in HeLa cells following JNK-IN-8 treatment (24 hours) and transfection of *WWTR1*-promoter luciferase reporter (48 hours). Internal renilla luciferase was used as a loading control.

4.2.6 HPV18 E7 regulates *WWTR1* mRNA expression in a EGFR-ERK1/2-dependent manner

EGFR signalling is a major activator of ERK1/2 signalling and also is regularly seen to be activated by E7 (272). Furthermore, in glioblastoma, EGFR signalling also increased TAZ expression (273). Therefore, it was hypothesised that EGFR was activating the ERK1/2 signalling pathway leading to increase TAZ expression.

Firstly, it was investigated if activation of EGFR signalling led to an increase in TAZ by stimulating serum-starved HeLa cells with EGF. Analysis revealed EGF-stimulation of serum starved HeLa cells led to an increase *WWTR1 mRNA* expression over the 8 hour time course (Figure 4.12 A).

Next, the effect of inhibiting the EGFR signalling pathway was investigated using PD153035 (PD) (274). PD treatment in HeLa cells showed EGFR inhibition led to a significant dose-dependent decrease in WWTR1 promoter activity (Figure 4.12 B) and *WWTR1* mRNA expression. Additionally, analysis of *YAP* mRNA expression showed no significant changes, highlighting that this mechanism was TAZ specific (Figure 4.12 C).

As E7 is both a known regulator of EGFR signalling and the regulator of TAZ in HPV18+ cells, it needed to be determined if the effect of HPV18 E7 on TAZ was EGFR-dependent. PD treatment reversed the increase WWTR1 promoter activity seen with HPV18 E7 expression alone (Figure 4.12 D). Likewise, PD treatment reversed the increase in *WWTR1* mRNA seen with HPV18 E7 expression alone, suggesting HPV18 E7 regulates TAZ expression in an EGFR-dependent manner (Figure 4.12 E).

To assess if the effect of EGFR signalling on TAZ is through activation of ERK1/2 signalling, serum starved HeLa cells were stimulated with EGF and then treated with U0126. Analysis showed U0126 treatment reversed the increase in both promoter activity and mRNA expression seen with EGF stimulation (Figure 4.12 F-G)

As ERK1/2 phosphorylates SP1 at two key residues indicated in Figure 4.11 A, an SP1 mutagenesis strategy was performed in parallel with both sites were mutated to be phosphomimetic, producing a constituently active SP1 that does not require ERK1/2 activation known as SP1 2TD. Depletion of HPV18 E6 and E7 in HeLa cells followed by expression of SP1 2TD restored WWTR1 expression (Figure 4.13 A). E6 and E7 mRNA expression was analysed by qRT-PCR to show changes in WWTR1 mRNA expression following SP1 2TD were not due to changes in oncogene expression (Figure 4.13 B-C).

Together these data identify that HPV18 drives TAZ expression through a pathway requiring the growth factor dependent activation of the SP-1 transcription factor.

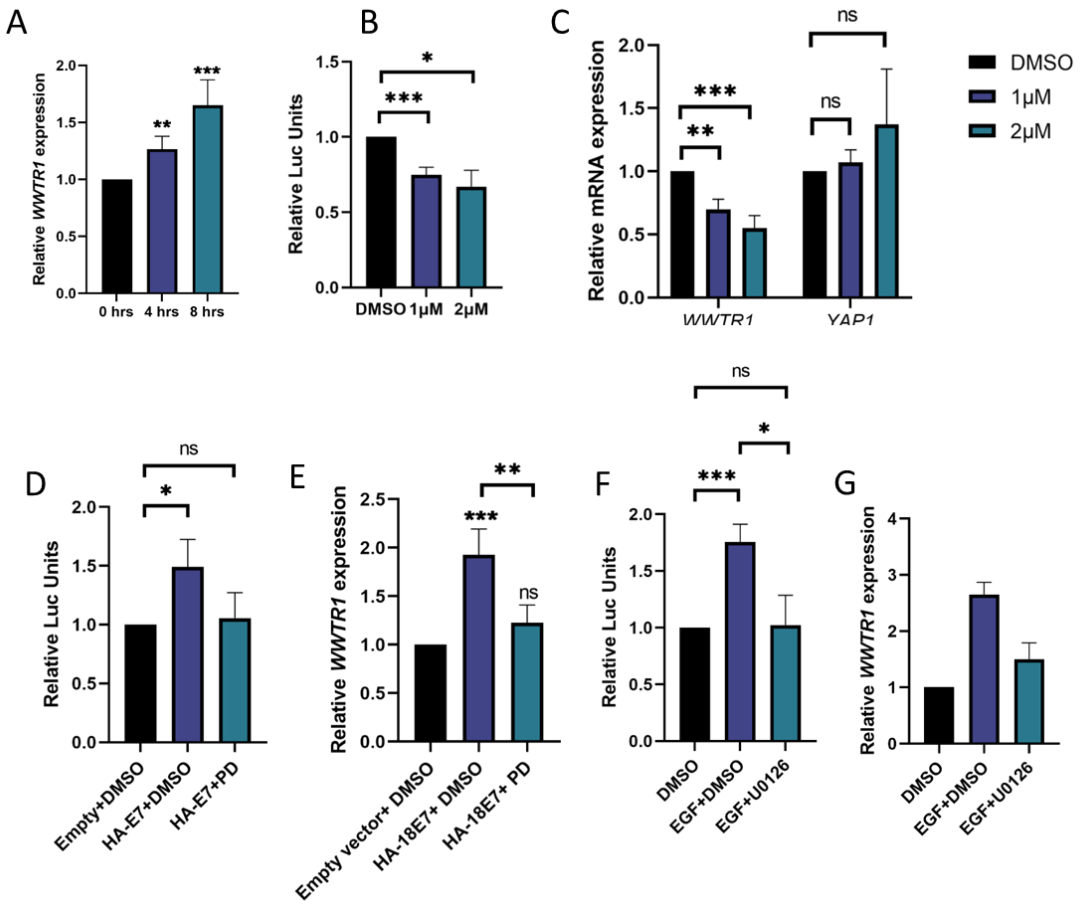

Figure 4.12 HPV 18 E7 control of WWTR1 expression is dependent on EGFR-ERK1/2 signalling axis A) qRT-PCR analysis of WWTR1 expression in HeLa cells following EGF stimulation (4 and 8 hrs). U6 was used as a loading control. **B)** Luciferase reporter assay in HeLa cells following PD treatment (24 hours) and transfection of WWTR1-promoter luciferase reporter (48 hours). Internal renilla luciferase was used as a loading control. **C)** qRT-PCR analysis of WWTR1 and YAP expression in HeLa cells following PD treatment. U6 was used as a loading control. **D)** Luciferase reporter assay in C33A cells following transfection of GFP-HPV 18 E7 and WWTR1-promoter luciferase reporter (48 hours) with or without PD treatment (24 hours). **E)** qRT-PCR analysis of WWTR1 expression in C33A cells following transfection of GFP-HPV 18 E7 (48 hours) with or without PD treatment (24 hours). U6 was used as a loading control. **F)** Luciferase reporter assay in HeLa cells following EGF stimulation and transfection of WWTR1-promoter luciferase reporter (24 hours) with or without U0126 treatment (24 hours). **G)** qRT-PCR analysis of WWTR1 expression in HeLa cells following EGF stimulation with or without U0126 treatment (24 hours) (n=2).

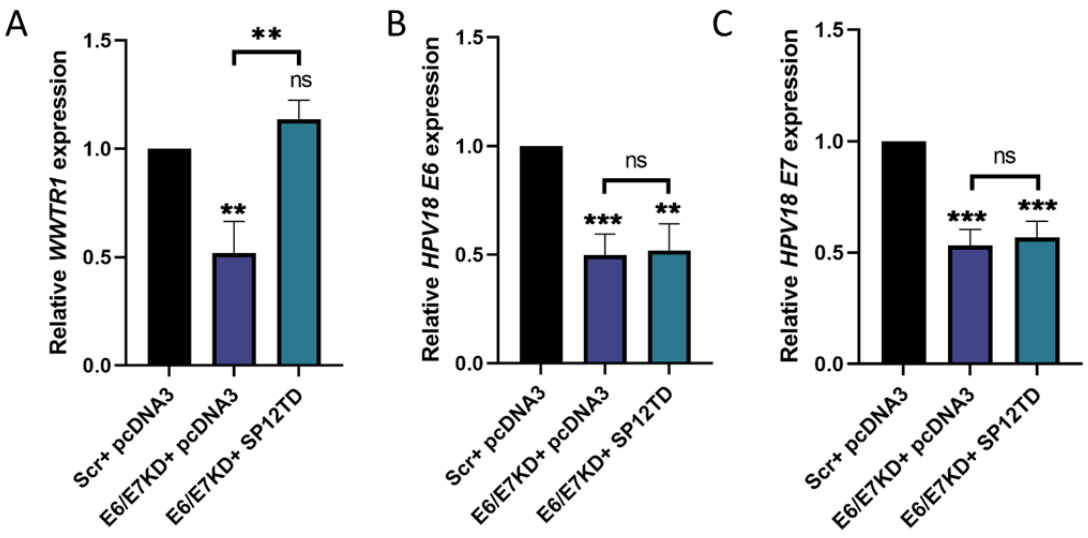

Figure 4.13 Active SP1 rescues loss of WWTR1 expression after E6/E7 knockdown A) qRT-PCR analysis of WWTR1 expression in HeLa cells with E6/E7 targeting siRNA (for 72 hours) with or without SP1 2TD transfection (24 hours). HPV 18 E6 **(B)** and HPV 18 E7 **(C)** levels were analysed to confirm successful knockdown. U6 was used as a loading control.

4.2.7 EGFR-ERK1/2 signalling regulates TAZ in a SP1 dependent manner.

Next, it was investigated if EGFR and ERK1/2 signalling were regulating TAZ expression through SP1 activity. Serum starved HeLa cells stimulated with EGF and then treated with Mith A showed Mith A treatment reversed the significant increase in promoter activity caused by EGF stimulation (Figure 4.14 A). Similar results were observed upon transfection of Trunc SP1 with transfection reversing the increase in *WWTR1* promoter activity seen with EGF stimulation alone (Figure 4.14 B). Additionally, the phosphomimetic SP1, SP1 2TD, was able to increase *WWTR1* promoter activity without need for EGFR/ERK1/2 signalling (Figure 4.14 C).

It was next assessed if SP1 2TD could rescue the loss of TAZ promoter activity seen after treatment with PD. SP1 2TD led to a complete recovery of *WWTR1* promotor activity in PD treated HeLa cells (Figure 4.14 D). Additionally, SP1 2TD transfection in PD treated HeLa cells recovered the decrease in *WWTR1* mRNA expression seen with PD treatment alone (Figure 4.14 E) indicating SP1 activity is necessary for EGF-induced *WWTR1* expression.

Lastly it was investigated if SP1 activity could recover the loss in *WWTR1* expression seen after ERK1/2 signalling inhibition. Expression of SP1 2TD in U0126-treated HeLa cells led to a recovery of *WWTR1* promoter activity (Figure 4.14 F) and subsequently led to a complete recovery of the reduction of *WWTR1* expression (Figure 4.14 G). This suggested SP1 activity is crucial for ERK-mediated regulation of *WWTR1* expression

Together these data suggests that EGFR and ERK1/2 signalling are regulating TAZ expression through SP1 activity.

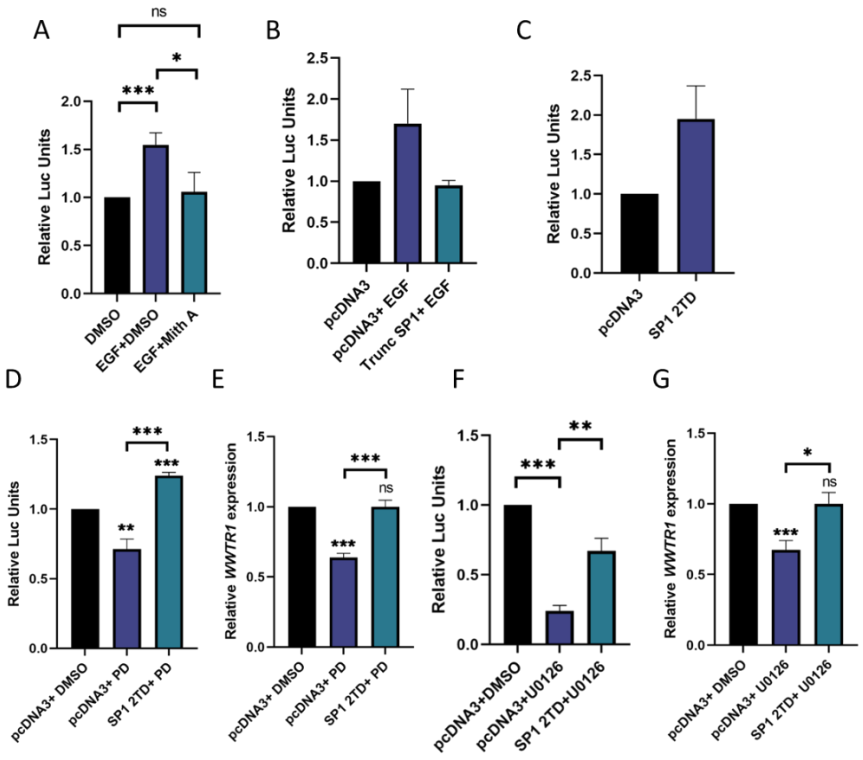

Figure 4.14 EGFR/ERK1/2 regulation of WWTR1 expression is SP1-dependent A) Luciferase reporter assay in HeLa cells following EGF stimulation and transfection of *WWTR1*-promoter luciferase reporter (24 hours) with or without Mith A treatment (24 hours). **B)** Luciferase reporter assay in HeLa cells following EGF stimulation and transfection of *WWTR1*-promoter luciferase reporter (24 hours) with or without Trunc SP1. Internal renilla luciferase was used as a loading control. **C)** Luciferase reporter assay in serum-starved HeLa cells following transfection of SP1 2TD and *WWTR1*-promoter luciferase reporter (24 hours). **D)** Luciferase reporter assay in HeLa cells following PD treatment (24 hours) and transfection of *WWTR1*-promoter luciferase reporter (24 hours) with or without SP1 2TD transfection (24 hours). Internal renilla luciferase was used as a loading control. **E)** qRT-PCR analysis of *WWTR1* expression in HeLa cells following PD treatment (24 hours) with or without SP1 2TD transfection (24 hours). U6 was used as a loading control. **F)** Luciferase reporter assay in HeLa cells following U0126 treatment (24 hours) and transfection of *WWTR1*-promoter luciferase reporter (24 hours) with or without SP1 2TD transfection (24 hours). Internal renilla luciferase was used as a loading control. **G)** qRT-PCR analysis of *WWTR1* expression in HeLa cells following U0126 treatment (24 hours) with or without SP1 2TD transfection (24 hours). U6 was used as a loading control.

4.3 Discussion

This chapter aimed to investigate levels of TAZ expression in HPV+ cervical cancer and the mechanism of regulation. While YAP is known to be overexpressed in both HPV16 and HPV18+ cervical cancer, analysis of cervical cancer cell lines revealed TAZ was only overexpressed in HPV18+ cell lines. Furthermore, we demonstrated clear differences between YAP and TAZ regulation by HPV. While YAP protein is increased in cervical cancer by protein stabilisation, we clearly established TAZ was not stabilised in HPV18+ cells as when analysed the half-life of TAZ was similar to that in HPV16+ cells. Furthermore, we confirmed that TAZ was degraded in a proteasome-mediated manner in these cells. Investigation revealed *WWTR1* mRNA to be increased not only in HPV18+ cell lines but also in CIN 2 and CIN3 patient samples from HPV18+ patients. Analysis of online datasets agreed with our data, suggesting TAZ is overexpressed in cervical cancer. Interestingly, analysis of the TCGA dataset suggested YAP and TAZ were largely overexpressed in different samples. Although this is not a phenotype we observe in cervical cancer cell lines, further analysis of *YAP1* expression the panel of patient samples could be undertaken to see if this can be replicated.

Intriguingly, we did not see a significant change in *WWTR1* mRNA in our panel of patient samples in CIN1 despite confirmed HPV expression in these samples. This suggests the upregulation of TAZ does not occur in HPV infection but is a cancer-specific phenotype. This phenotype should be further investigated by comparing *WWTR1* and TAZ expression in NHK cells with and without the HPV18 genome.

It was determined that HPV18 E7 was responsible for upregulating the expression of TAZ through increasing promoter activity. We did not observe any stabilisation of TAZ protein expression, agreeing with the unchanged TAZ half-life between HPV16+ and HPV18+ cells. This was surprising as E7 has been shown to stabilise YAP expression by targeting PTPN14 for degradation in HNSCC. Furthermore, we did not see any stabilisation of TAZ mRNA expression with E7 expression, supporting

our hypothesis that the upregulation in TAZ stems from an increase in promoter activity. HPV18 E7 was found to be able to increase WWTR1 promoter activity in both C33A and HaCaT cells. Results could have been further validated in NHKs but it was determined HaCaTs were a better option due to simpler growth requirements. Furthermore HPV18 E7 was established to increase WWTR1 promoter activity through an EGFR-ERK1/2-SP1 signalling axis.

SP1 was determined to be a major regulator of TAZ expression as inhibition of SP1 activity through multiple ways led to a significant loss of TAZ expression, WWTR1 mRNA and promoter activity across multiple HPV18+ cervical cancer cell lines. Furthermore, deletion of SP1 binding sites led to a reduction in basal *WWTR1* promoter activity in HeLa cells. In addition to this constituently active SP1 (SP1 2TD) restored WWTR1 expression in E6/E7 knockdown cells. Even though various MAPK signalling pathways have been reported to activate SP1, we determined that activation of SP1 by E7 was largely due to ERK1/2 signalling as inhibition of JNK signalling did not lead to a loss of *WWTR1* promoter activity. JNK signalling is largely E6 regulated and therefore unsurprisingly does not regulated WWTR1 promoter activity in this system, however it may play a role in other cancers. Furthermore, inhibition of ERK1/2 signalling following E7 expression led to a near complete reversal of *WWTR1* promoter activity and. similar results were observed with EGFR signalling, with inhibition of ERK1/2 also completely reversing the increased promoter activity. Although PD153035 is a well characterised EGFR inhibitor, as targeting of EGFR is recently a common therapeutic option for cancer treatments, the effects of other, more clinically relevant EGFR inhibitors should be investigated (275). It is worth noting that as the change in WWTR1 promoter activity is relatively small (but consistent) there may be other unknown mechanisms of TAZ regulation occurring.

Even though other studies have reported phosphorylation of SP1 at residues T453 and T739 by ERK1/2, further investigations should be carried out to confirm HPV18

E7 expression leads to increased phospho-SP1 and therefore increased SP1 activity. Additionally, despite the luciferase data remaining consistent with our hypothesis, our results could be confirmed utilising Chromatin Immunoprecipitation (ChIP). This could be used to confirm SP1 binding at the regions in the *WWTR1* promoter specified.

HPV16 E7 expression did not led to changes in TAZ expression, agreeing the lack of changes in TAZ expression in both HPV16+ cervical cancer cell lines and patient samples. This also explains why many online datasets did not show an increase in TAZ expression as many of these datasets are skewed to HPV16+ samples, especially in cervical squamous cell carcinoma.

Even though our data is clear that HPV18 E7 is regulating TAZ through this EGFR-ERK1/2-SP1 signalling axis, it is currently unknown why HPV16 E7 cannot increase TAZ expression. Many studies have documented the ability of HPV16 to activate these same pathways, making it unclear how HPV18 E7 only does this. Further investigation into this should be undertaken and the ability of other both high and low HPV E7s to upregulate TAZ should be assessed. Although to sequence analysis reveals subtle difference between HPV16 and HPV18 E7, the functional differences between the two are unclear. Generating a panel of HPV16/18 E7 chimeras could be used to clarify which region of HPV18 E7 specifically is needed to regulate TAZ.

Chapter 5- TAZ is essential and promotes proliferation in a YAP-independent manner in cervical cancer

5.1 Introduction

Identifying novel therapeutic targets, such as oncogenes, is a priority for HPV-driven cancers. Although YAP has been shown to be clearly oncogenic in cervical cancer, TAZ has been reported to both be oncogenic and tumour suppressive in cervical cancer and therefore further elucidation is needed. Additionally a detailed investigation comparing the role of YAP and TAZ in cervical cancer is currently lacking. This need is highlighted given the differences in YAP and TAZ expression highlighted in chapter 4. YAP and TAZ are the targets of various therapeutics currently in clinical trials, with the mechanism of action generally focusing on disrupting YAP/TAZ/TEAD interactions. Therefore, if the role of YAP/TAZ is better understood, there is a potential for these therapeutics to be used in HPV-driven cervical cancer.

In this chapter the effect of TAZ on proliferation and EMT was investigated in both HPV16 and HPV18+ cervical cancer cell lines. Furthermore, it was assessed if YAP and TAZ played non-redundant roles in the regulation of proliferation.

5.2 Results

5.2.1 TAZ promotes proliferation in HeLa cells

To begin to investigate its role in HPV18+ cervical cancer cells, HeLa cells were treated with two TAZ inhibitors. The first inhibitor, 6079510, was characterised to prevent the nuclear localisation of TAZ by promoting an interaction between importin α5 and CSE1L, preventing the binding of importin α5 to TAZ (276). Ivermectin was used to inhibit both YAP and TAZ nuclear import and is thought to act in a similar manner, by inhibiting importins (277). As both inhibitors are acting on cellular factors other than YAP and TAZ, immunofluorescence was used to confirm the ability of both drugs to regulate YAP and TAZ in the assumed manner. Imaging showed while treatment of Ivermectin led to a loss of both YAP and TAZ nuclear localisation, 6079510 treatment only resulted in the loss of nuclear TAZ, leaving YAP unaffected (Figure 5.1 A and B). As the images suggested that TAZ was not just relocalised to the cytoplasm, but levels were generally lower, western blotting and probing for TAZ was used to assess overall protein levels. Analysis showed TAZ expression was slightly decreased with either inhibitor treatment while analysis of YAP levels showed no change. Both inhibitors were taken forward for further investigations due to the clear effects observed by immunofluorescence (Figure 5.1 C).

As TAZ has been linked to promoting proliferation in multiple cancers, the effect of TAZ inhibition was assessed with a growth assay. Treatment of HeLa cells with either inhibitor led to a significant reduction in growth over the 5 days of the assay (Figure 5.1 D). Analysis showed a slight additional reduction in growth when both YAP and TAZ were inhibited compared to inhibition of TAZ alone. Given the significant results observed, the effect of TAZ inhibition was assessed for colony forming ability. Investigation of both anchorage-dependent and anchorage-independent colony forming ability showed a significant reduction in the ability of HeLa cells to form colonies following treatment of either inhibitor (Figure 5.1 E and F).

As neither of the inhibitors used acted on TAZ or YAP directly, it was possible that the results observed were due to off-target effects. Therefore, TAZ expression was knocked down with stable expression of short hairpin RNAs (shRNAs) in HeLa cells in a puromycin resistant vector. qRT-PCR analysis was used to confirm a stable reduction in *WWTR1* expression without reducing *YAP1* expression when compared to a non-targeting control (NEG) (Figure 5.2 A). The ability of two shRNAs targeting different sequences to target *WWTR1* was assessed and both were confirmed to reduce *WWTR1* expression below 50%. To ensure consistent knockdown of *WWTR1*, the cell lines used were grown from a single cell in each case (making the cell lines monoclonal). Analysis showed *YAP1* expression was actually increased in both TAZ KD cell lines, inversely correlating with *WWTR1* expression levels. This suggested a possible feedback between TAZ and YAP expression.

It was also confirmed that this led to a significant reduction in TAZ protein expression in both TAZ KD cell lines. Further probing for HPV18 E6 and E7 showed little change in expression of either oncoprotein (Figure 5.2 B). This result was not surprising as previous work in the group showed activation of the Hippo signalling pathway led to no changes in expression of either oncoprotein (Data generated by MBiol student not shown). Next the proliferative ability of the TAZ KD cells was assessed. A growth assay showed knockdown of TAZ led to a significant reduction in growth over 5 days. Further analysis of colony forming ability showed TAZ knockdown led to a significant reduction in the ability of HeLa cells to form both anchorage-dependent and anchorage-independent colonies.

Together this suggested inhibition of TAZ activity led to a significant reduction in proliferation.

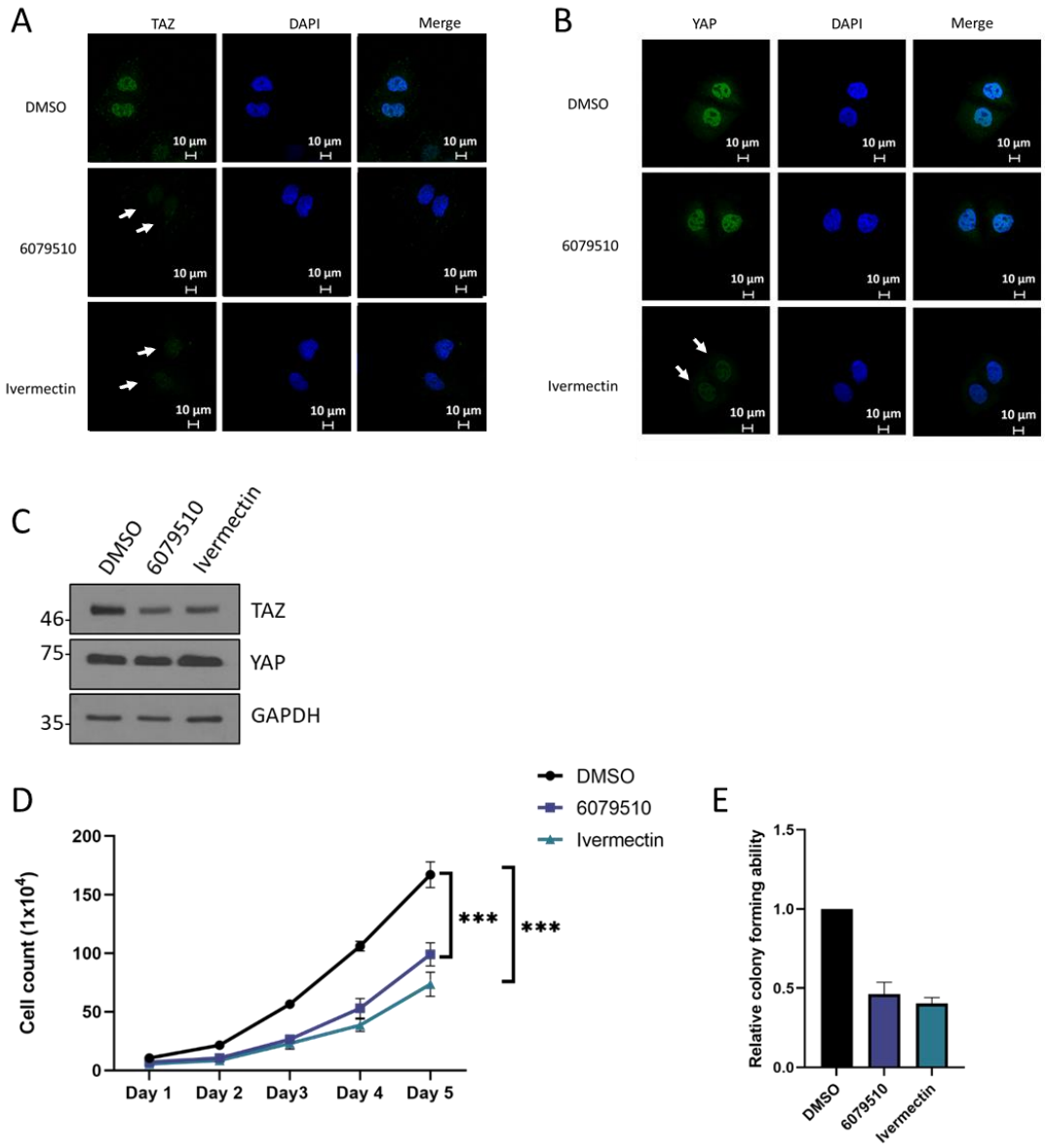

Figure 5.1 Inhibition of TAZ or YAP/TAZ reduces proliferation in HeLa cells A) Immunofluorescence microscopy analysis loss of nuclear TAZ (green) in HeLa cells with treatment of either 6079510 or Ivermectin. DAPI stained nuclei (blue). Scale bar 10 µm. **B)** Immunofluorescence microscopy analysis loss of nuclear YAP (green) in HeLa cells with treatment of Ivermectin only. DAPI stained nuclei (blue). Scale bar 10 µm. **C)** Representative western blot of HeLa cell lysates following treatment with either 6079510 (16 hours) or Ivermectin (24 hours). Cells lysate was probed for TAZ or YAP. GAPDH was used as a loading control (n=2). **D)** Growth curve analysis of HeLa cells treated with either 6079510 (16 hours) or Ivermectin (24 hours). **E)** Colony formation assay (analysis of anchorage dependent growth of HeLa cells treated with either 6079510 (16 hours) or Ivermectin (24 hours) (n=2).

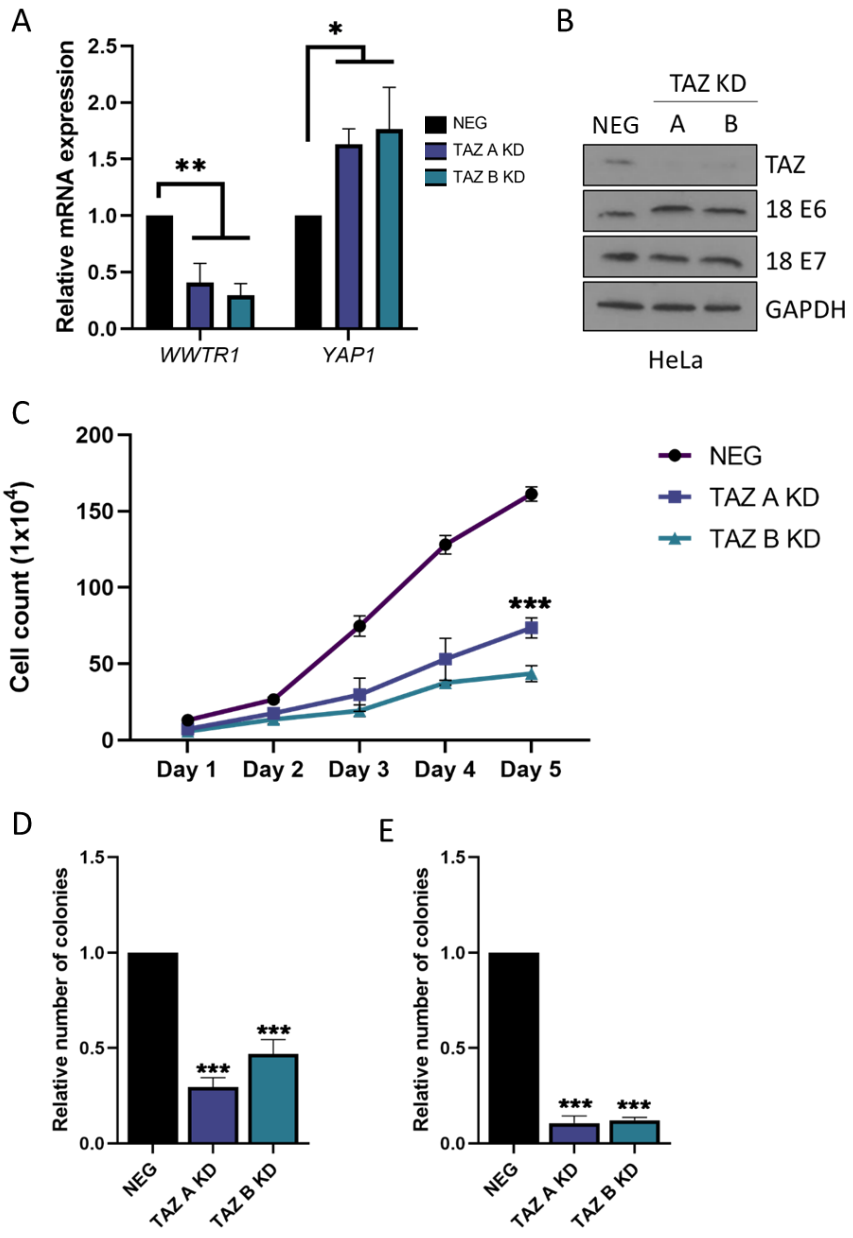

Figure 5.2 Knockdown of TAZ using shRNA in HeLa cells reduces proliferative ability A) qRT-PCR analysis of *WWTR1* or *YAP1* expression in monoclonal shRNA-mediated TAZ knockdown HeLa cells. U6 was used as a loading control. **B)** Representative western blot of monoclonal shRNA-mediated TAZ knockdown HeLa cells. Cell lysates were probed for TAZ, HPV18 E6 or HPV18 E7. GAPDH was used as a loading control. **C)** Growth curve analysis of monoclonal shRNA-mediated TAZ knockdown HeLa cells. **D)** Colony formation assay (analysis anchorage dependent growth) monoclonal shRNA-mediated TAZ knockdown HeLa cells. **E)** Soft agar assay (analysis anchorage-independent growth) in monoclonal shRNA-mediated TAZ knockdown HeLa cells.

5.2.2 TAZ knockdown reduces proliferation in other HPV18+ cell lines and plays a key role in E7-mediated proliferation

Even though it was clear TAZ promoted proliferation in HeLa cells, this may have been a cell-specific phenotype and not a true representative of the function of TAZ in HPV18+ cervical cancer. Therefore the role of TAZ in two other HPV18+ cervical cancer cell lines, SW756 and MS751 was investigated. Both these cell lines were chosen as they showed consistent high TAZ expression (Chapter 4 Figure 1). Polyclonal TAZ knockdown cell lines were generated using the same two shRNA plasmids used in HeLa cells. Successful knockdown of *WWTR1* expression was confirmed with qRT-PCR analysis in both SW756 and MS751 cells when compared to the NEG cell line in each case (Figure 5.3 A and B). Analysis of YAP mRNA expression showed little change upon *WWTR1* knockdown. Western blotting and probing for TAZ protein levels was used to demonstrate the loss of *WWTR1* led to a loss of TAZ protein expression in SW756 and MS751 cells when compared to the NEG cell line in each case (Figure 5.3 C and D).

After it was confirmed that polyclonal TAZ KD SW756 and MS751 cell lines were generated, the proliferative ability was investigated. Assessment of growth showed a significant reduction upon TAZ knockdown in both KDs in each cell line after 5 days (Figure 5.3 E and F). Furthermore, both the ability for form anchorage-dependent colonies was reduced upon TAZ knockdown in both SW756 and MS751 cells (Figure 5.3 G and H). Anchorage independent colony forming ability was not assessed due to poor ability of both SW756 and MS751 to form colonies under normal conditions.

Together this data suggests TAZ promotes proliferation in HPV18+ cell lines, beyond HeLa cells.

As results in Chapter 4 showed TAZ expression is regulated by HPV18 E7, it was hypothesised that TAZ played a role in the cancerous phenotype promoted by HPV18 E7. To investigate this, anchorage dependent colony forming ability was assessed in

C33A cervical cancer cells stably expressing HPV18 E7 with and without treatment with 6079510 to inhibit TAZ activity. Analysis showed while expression of HPV18 E7 alone roughly double the number of colonies, treatment with 6079510 led to a strong but not complete reversal of the increase (Figure 5.4 A). Similar results were observed in HaCaT keratinocyte cells expressing HPV18 E7 with and without treatment with 6079510 (Figure 5.4 B). This suggested that TAZ plays a key role in HPV18 E7-mediated colony forming ability.

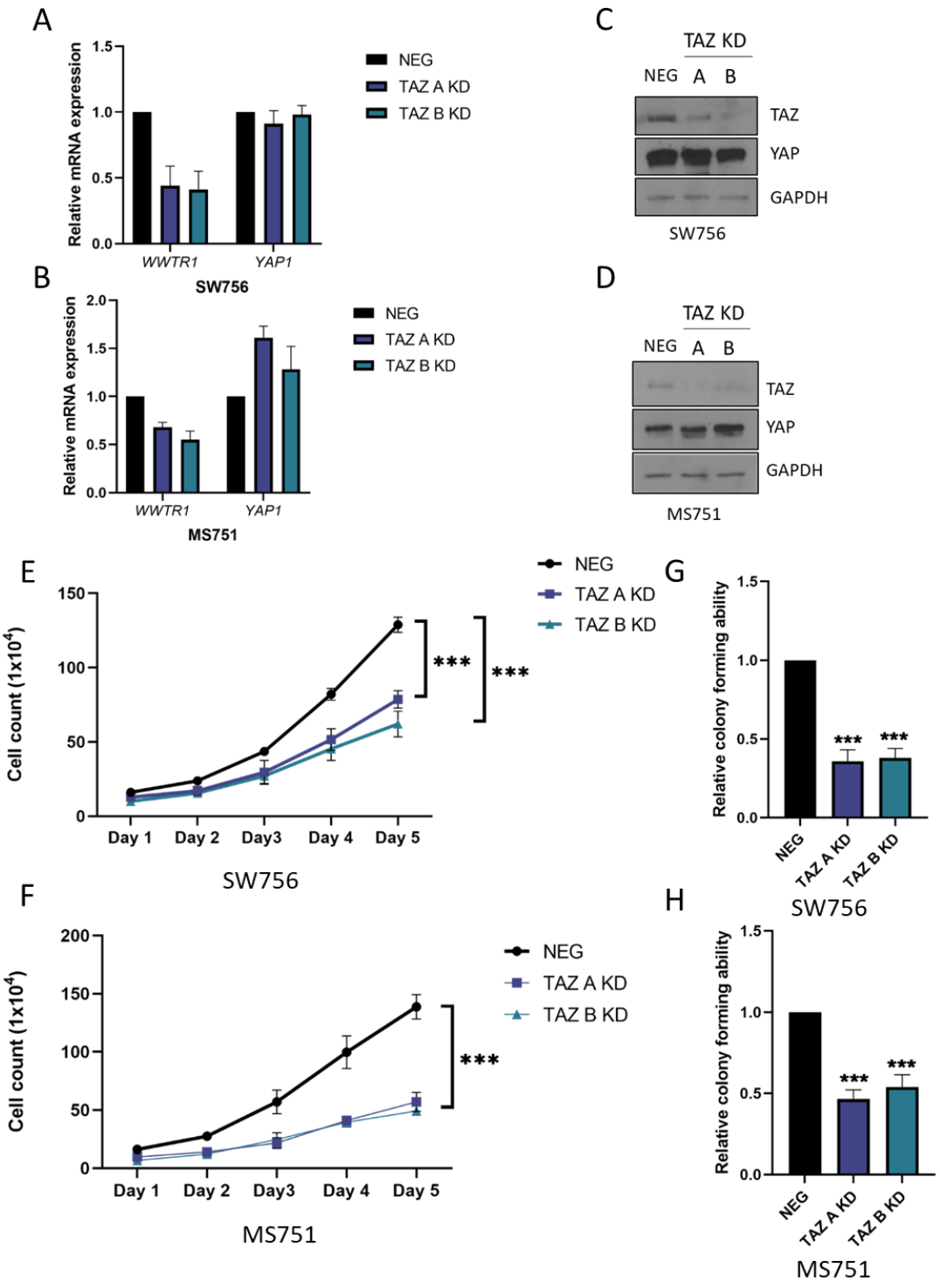

Figure 5.3 Knockdown of TAZ using shRNA in other HPV18+ cervical cancer cells reduces proliferation A) qRT-PCR analysis of *WWTR1* or *YAP1* expression in polyclonal shRNA-mediated TAZ knockdown SW756 cells. U6 was used as a loading control. **B)** qRT-PCR analysis of *WWTR1* or *YAP1* expression in polyclonal shRNA-mediated TAZ knockdown SW756 cells. U6 was used as a loading control **C)** Representative western blot of polyclonal shRNA-mediated TAZ

knockdown SW756 cells. Cell lysates were probed for TAZ and YAP. GAPDH was used as a loading control. **D)** Representative western blot of polyclonal shRNA-mediated TAZ knockdown MS751 cells. Cell lysates were probed for TAZ and YAP. GAPDH was used as a loading control **E)** Growth curve analysis of polyclonal shRNA-mediated TAZ knockdown SW756 cells. **F)** Growth curve analysis of polyclonal shRNA-mediated TAZ knockdown MS751 cells. **G)** Colony formation assay (analysis anchorage dependent growth) polyclonal shRNA-mediated TAZ knockdown SW756 cells. **H)** Colony formation assay (analysis anchorage dependent growth) polyclonal shRNA-mediated TAZ knockdown SW756 cells.

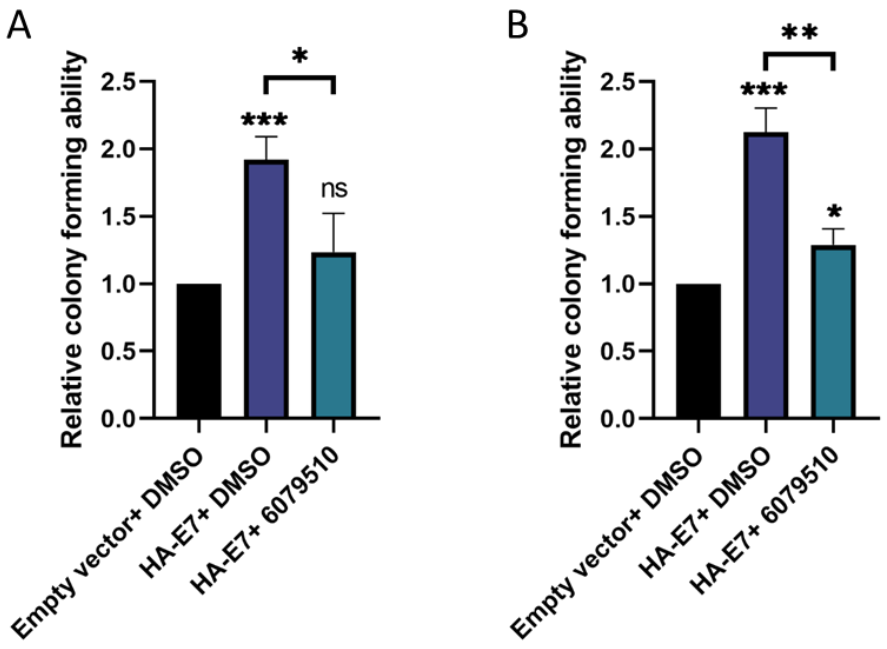

Figure 5.4 Inhibition of TAZ reduce HPV18 E7-mediated colony formation A) Colony formation assay (analysis anchorage dependent growth) in C33A cells stably expressing HA-HPV18 E7 with or without 6079510 treatment (16 hours). **B)** Colony formation assay (analysis anchorage dependent growth) in HaCaT cells stably expressing HA-HPV18 E7 with or without 6079510 treatment (16 hours).

5.2.3 TAZ is tumour suppressive in HPV16+ cell lines

Given the effect of TAZ inhibition in HPV18+ cells, the role of TAZ in HPV16+ SiHa cells that expressed low levels of TAZ was investigated. Firstly, SiHa cells were treated with both 6079510 and Ivermectin and growth was assessed. Treatment with Ivermectin, inhibiting both YAP and TAZ nuclear localisation, led to a reduction in growth over 5 days when compared to a DMSO control, inhibiting TAZ alone with 6079510 had no significant effect, likely was TAZ expression in low in these cells (Figure 5.5 A). Further investigation revealed Ivermectin reduced the ability to form anchorage dependent colonies while 6079510 treatment actually increased colony forming ability (Figure 5.5 B). As this was such a distinct effect to what was observed in HPV18+ cells, this was investigated further by overexpressing YAP or TAZ.

Firstly, the effect of overexpressing either YAP or TAZ in HeLa was assessed. Western blotting and probing for the FLAG epitope used to confirm successful expression of FLAG-YAP or FLAG-TAZ (Figure 5.6 A). Analysis of growth over a 5-day period showed overexpression of either YAP or TAZ led to a small but significant increase in growth in HeLa cells (Figure 5.6 B). Further investigation also showed overexpression of either YAP or TAZ led to the increased ability to form anchorage dependent or independent colonies (Figure 5.6 C and D).

However, this was not the case in SiHa cells. When growth was analysed over a 5-day period, analysis showed while YAP overexpression (Successful expression was confirmed in Figure 5.7 A) led to a similar significant increase in growth as seen in HeLa cells, overexpression of TAZ led to a significant reduction in growth (Figure 5.7 B). Furthermore, while YAP overexpression increased colony forming ability, TAZ overexpression reduced it (Figure 5.7 C-D).

To further investigate the role of YAP and TAZ in SiHa cells, a panel of monoclonal knockdown cell lines were generated with shRNAs targeting TAZ, YAP or

both YAP/TAZ simultaneously (termed Y/T) stably expressed in a puromycin-resistant vector. Appropriate successful knockdown of TAZ and YAP was confirmed by using qRT-PCR to analyse *WWTR1* and *YAP1* mRNA levels (Figure 5.8 A). Then the proliferative ability of TAZ, YAP and dual knockdown SiHa was assessed using growth and colony formation assays. Analysis of growth over a 5-day period showed that while knockdown of YAP alone or in combination with TAZ led to a significant reduction in growth, knockdown of TAZ alone led to significant increase (Figure 5.8 B). Further investigation demonstrated a similar trend in the ability of SiHa cells to form both anchorage dependent or independent colonies (Figure 5.8 C-D).

These findings suggest that while TAZ is oncogenic in HPV18+ cells, it may possibly be tumour suppressive in HPV16+ SiHa cells. Crucially, analysis of online datasets supports the hypothesis that TAZ may only be oncogenic in HPV18+ cells, with high *WWTR1* correlating with poor overall survival only in HPV18+ cervical cancers. Conversely, there was little change with high *WWTR1* expression in non-HPV18+ cervical cancers (Figure 5.9).

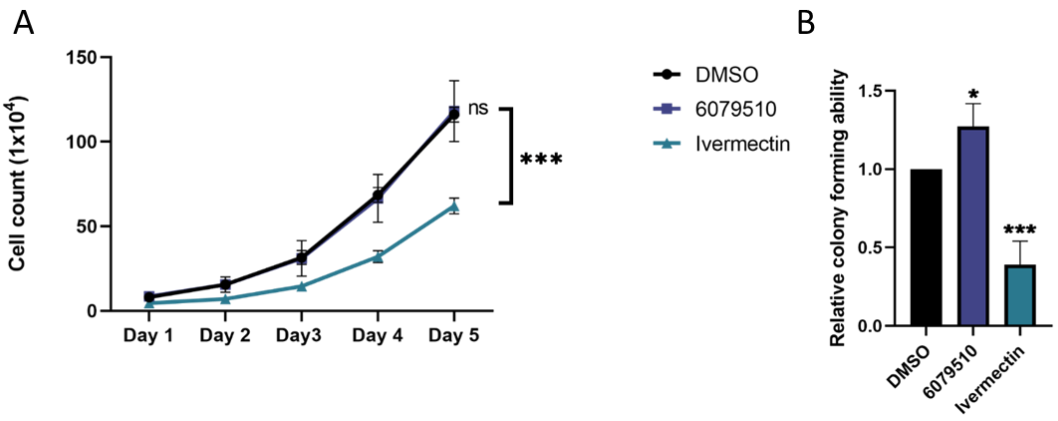

Figure 5.5 Inhibition of TAZ in SiHa does not reduce proliferation A) Growth curve analysis of SiHa cells treated with either 6079510 (16 hours) or Ivermectin (24 hours). **B)** Colony formation assay (analysis of anchorage dependent growth of SiHa cells treated with either 6079510 (16 hours) or Ivermectin (24 hours).

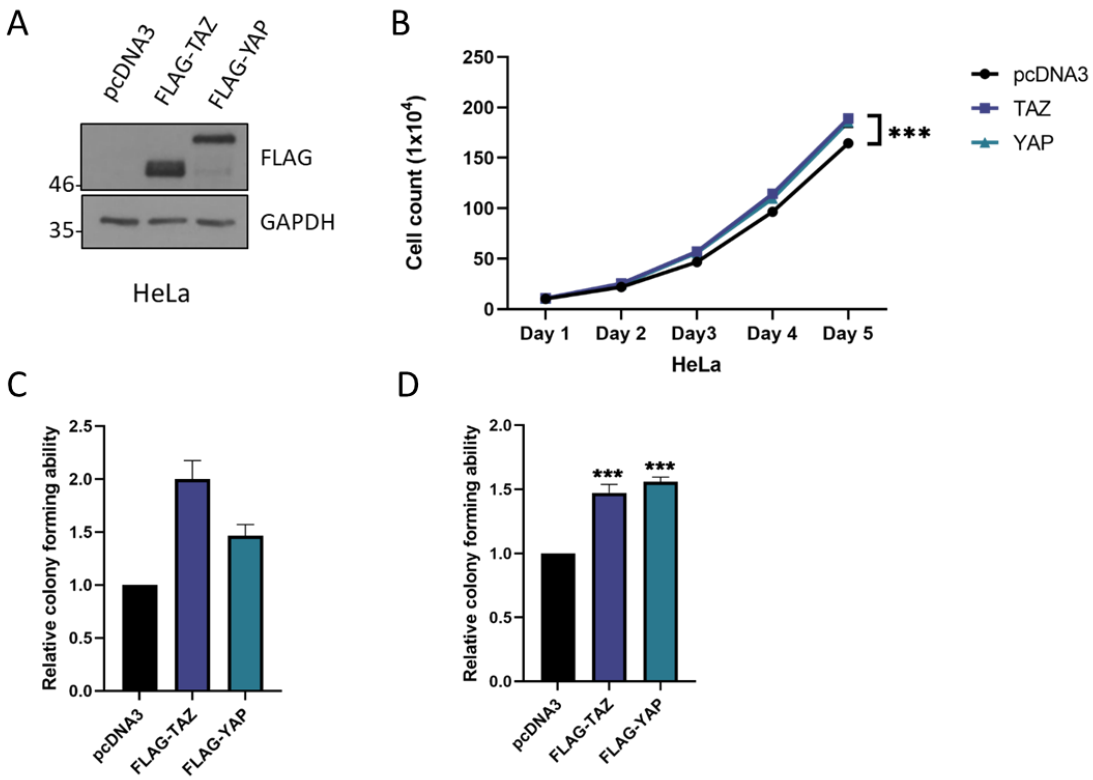

Figure 5.6 Overexpression of either YAP or TAZ is HeLa cells increases proliferation A) Representative western blot of HeLa cells transfected with FLAG-TAZ or FLAG-YAP (48 hours). Cell lysates were probed for FLAG. GAPDH was used as a loading control. **B)** Growth curve analysis of HeLa cells transfected with FLAG-TAZ or FLAG-YAP (48 hours). **C)** Colony formation assay (analysis anchorage dependent growth) of HeLa cells transfected with FLAG-TAZ or FLAG-YAP (48 hours) (n=2). **D)** Soft agar assay (analysis anchorage-independent growth) in HeLa cells transfected with FLAG-TAZ or FLAG-YAP (48 hours).

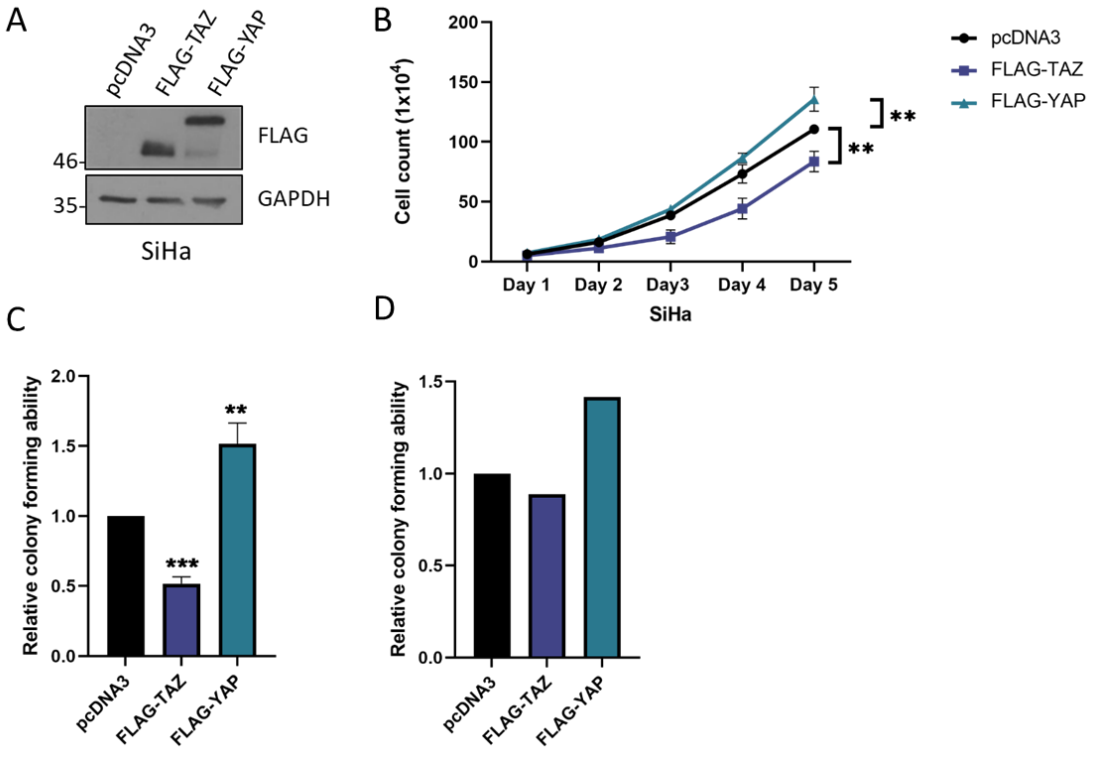

Figure 5.7 Overexpression of TAZ in SiHa cells decreases proliferation A) Representative western blot of SiHa cells transfected with FLAG-TAZ or FLAG-YAP (48 hours). Cell lysates were probed for FLAG. GAPDH was used as a loading control. **B)** Growth curve analysis of SiHa cells transfected with FLAG-TAZ or FLAG-YAP (48 hours). **C)** Colony formation assay (analysis anchorage dependent growth) of SiHa cells transfected with FLAG-TAZ or FLAG-YAP (48 hours) (n=2). **D)** Soft agar assay (analysis anchorage-independent growth) in SiHa cells transfected with FLAG-TAZ or FLAG-YAP (48 hours) (n=1).

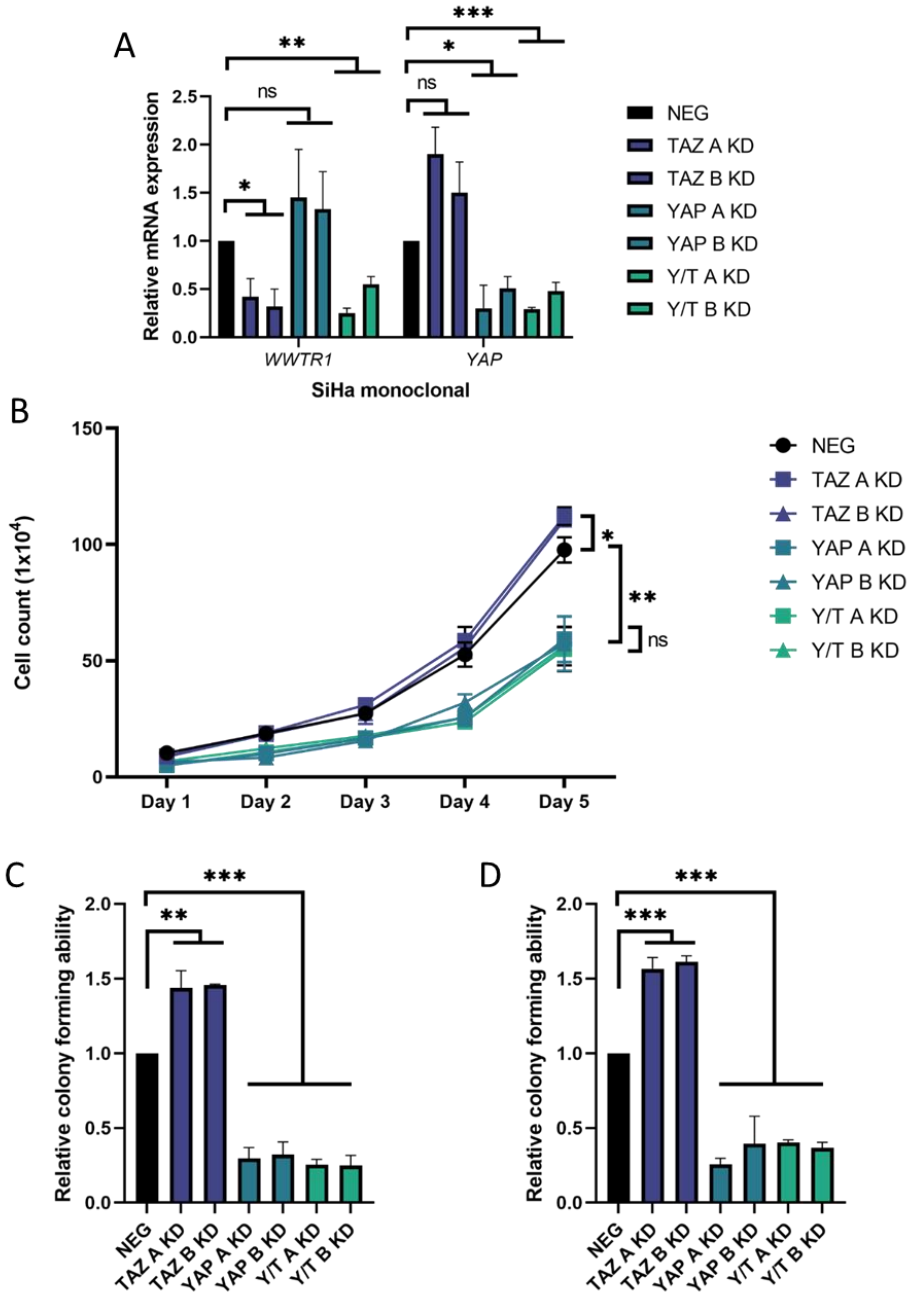

Figure 5.8 Knockdown of YAP but not TAZ reduces proliferation in SiHa cells A) qRT-PCR analysis of *WWTR1* or *YAP1* expression in monoclonal shRNA-mediated TAZ, YAP or YAP/ TAZ (Y/T) knockdown SiHa cells. U6 was used as a loading control. **B)** Growth curve analysis of monoclonal shRNA-mediated TAZ, YAP or YAP/ TAZ (Y/T) knockdown SiHa cells. **C)** Colony formation assay (analysis anchorage dependent growth) of shRNA-mediated TAZ, YAP or YAP/ TAZ (Y/T) knockdown SiHa cells. **D)** Soft agar assay (analysis anchorage-independent growth) of monoclonal shRNA-mediated TAZ, YAP or YAP/ TAZ (Y/T) knockdown SiHa cells.

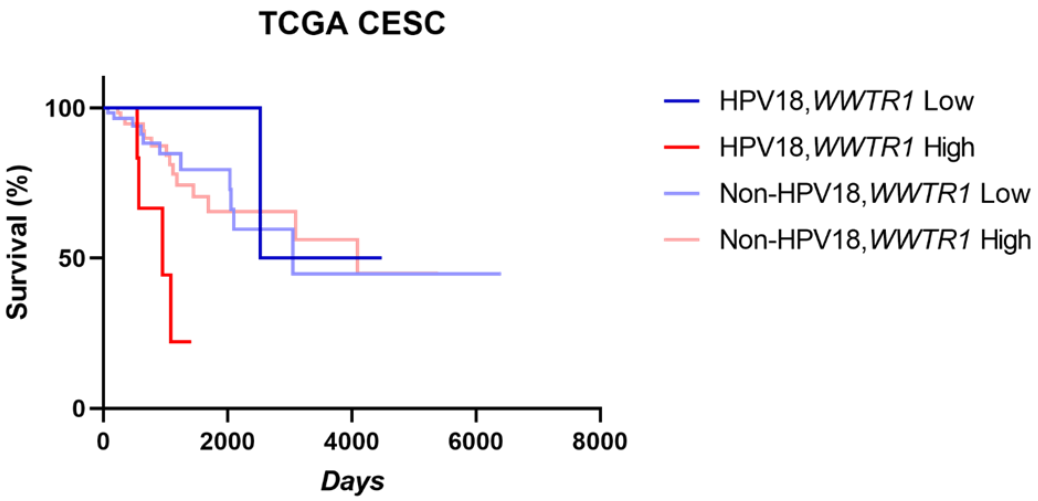

Figure 5.9 High TAZ correlated with reduced survival in HPV18+ cervical cancer. Kaplan-Meier curves showing overall survival in cervical cancer stratified by HPV18+ or non-HPV18+. Survival was compared using the log-rank test (performed by Dr Ethan Morgan)

5.2.4 TAZ is required for epithelial to mesenchymal transition in HPV18+ cervical cancer cells

TAZ has been linked to invasion in many types of cancer (278-280) so it was investigated if TAZ is required for the invasive phenotype of HPV18+ cervical cancer cells. Firstly, the expression of a panel of common EMT markers was analysed by qRT-PCR. Analysis showed while expression of EMT-associated transcription factors such as *SNAIL, SLUG* and *TWIST1* increased with TAZ knockdown in HeLa cells, expression of mesenchymal markers vimentin (*VIM*) and N-cadherin (*CDH2*) decreased. In opposition, epithelial marker ZO-1 (*TJP1*) increased with TAZ knockdown (Figure 5.10 A). Analysis of protein levels of Snail, Slug and vimentin via western blotting was consistent with mRNA levels (Figure 5.10 B).

Both Slug and Snail are known to interact with TAZ to promote transcription. Therefore, it was hypothesised that although levels of both were increased with TAZ knockdown, activity may not be. To investigate this, mRNA levels of two Snail/Slug dependent genes, *SPARC* and *MMP2*, were analysed and showed TAZ knockdown led to significant decreases in both *SPARC* and *MMP2* expression, suggesting a decrease in Snail/Slug activity (Figure 5.10 C and D). Although Slug and Snail activity still requires further investigation, data overall suggested a decrease in EMT-potential with TAZ knockdown, so therefore wound healing ability was investigated.

When wound healing ability was analysed with scratch assays, it was observed TAZ knockdown led to a significant decrease in the percent of wound healed after 24 hours (Figure 5.10 E with analysis in Figure 5.10 F). Next, migration and invasion ability were investigated using Transwell assays with (to test invasion) and without matrix (to test migration). Analysis showed TAZ knockdown led to a significant reduction in the ability of HeLa cells to migrate or invade (Figure 5.10 G and H).

As it was clear there was a loss of metastatic phenotype with TAZ, it was hypothesised that there may be a disruption of the actin cytoskeleton reorganisation that is associated with cell motility. To investigate this, cells were stained with Rhodamine-Phalloidin which selectively binds to F-actin allowing structures such as filopodia (Thin structures consisting of tight bundles of F-actin) to be visualised. Staining of TAZ knockdown HeLa cells followed by imaging and analysis revealed TAZ knockdown reduces both the length of filopodia-like structures and the overall number per cell (Figure 5.11 A-C).

Together, these data suggest TAZ is a key regulator of EMT and cell motility in HPV18+ cervical cancer cells.

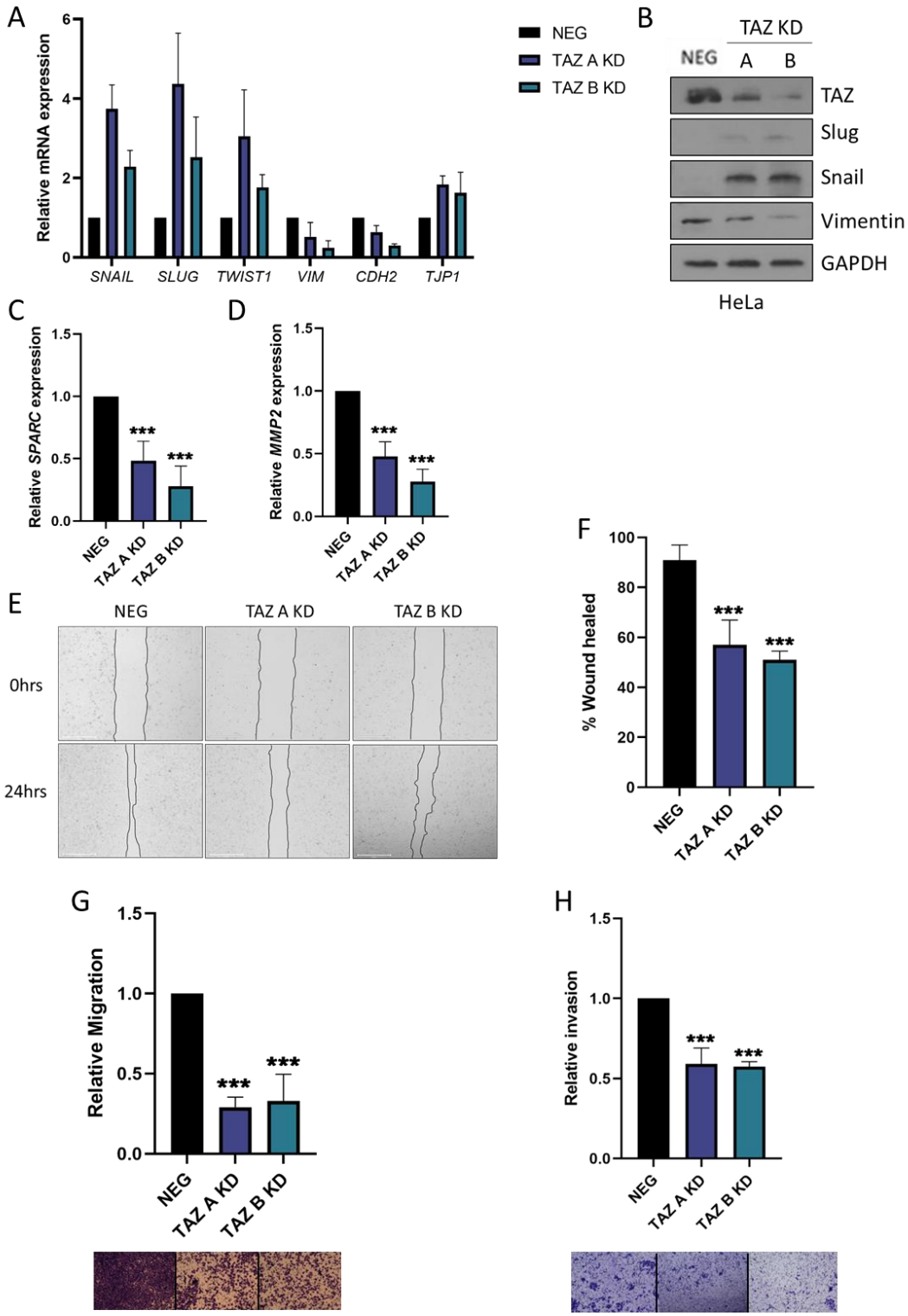

Figure 5.10 TAZ knockdown in HeLa cells reduces EMT potential A) qRT-PCR analysis of *SNAIL, SLUG, TWIST1, VIM, CDH2* and *TJP1* mRNA expression in monoclonal shRNA-mediated TAZ knockdown HeLa cells. U6 was used as a loading control. **B)** Representative western blot of monoclonal shRNA-mediated TAZ knockdown HeLa cell lysate. Cell lysates were probed for TAZ,

Slug, Snail and Vimentin. GAPDH was used as a loading control. **C)** qRT-PCR analysis of SPARC mRNA expression in monoclonal shRNA-mediated TAZ knockdown HeLa cells. **D)** qRT-PCR analysis of MMP2 mRNA expression in monoclonal shRNA-mediated TAZ knockdown HeLa cells. **E)** EVOS analysis of scratch assays. Confluent monolayers of monoclonal shRNA-mediated TAZ knockdown HeLa cells were scratched with a pipette tip and imaged. Cells were then reimaged after 24 hours (images shown). Black line indicates edge of wound. **F)** Analysis of % wound closure calculate from **(E)**. **G)** Transwell migration assay of monoclonal shRNA-mediated TAZ knockdown HeLa cells. **H)** CHEMICON Cell Invasion assay of monoclonal shRNA-mediated TAZ knockdown HeLa cells.

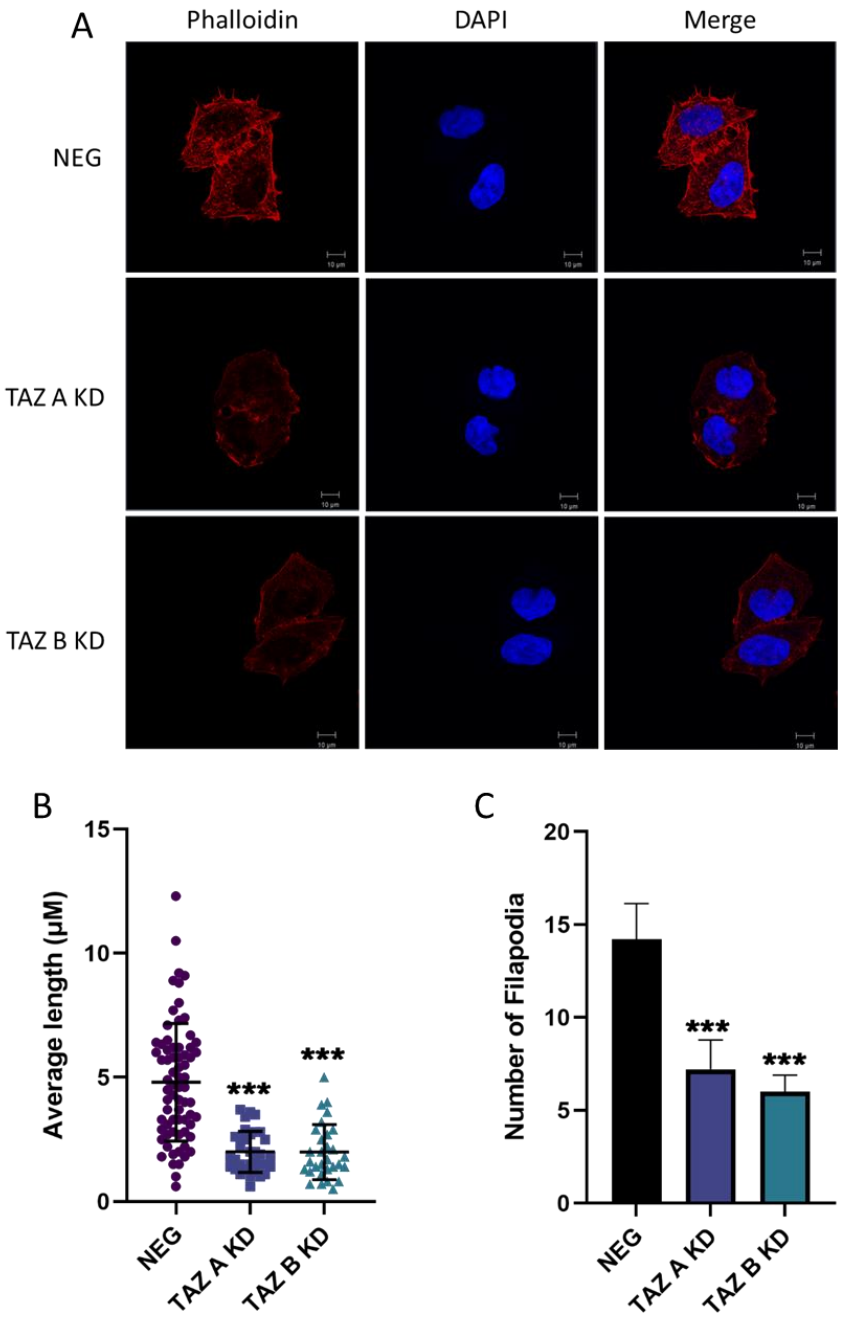

Figure 5.11 TAZ knockdown reduces filopodia length and number in HeLa cells A) Immunofluorescence microscopy analysis of Rhodamine-Phalloidin staining (red) monoclonal shRNA-mediated TAZ knockdown HeLa cells. DAPI stained nuclei (blue). Scale bar 10 µm. **B)** Measurement of filopodia length in monoclonal shRNA-mediated TAZ knockdown HeLa cells. **C)** Average number of filopodia per cell in monoclonal shRNA-mediated TAZ knockdown HeLa cells.

5.2.5 YAP and TAZ both promote proliferation in HPV18+ cells

Both YAP and TAZ have oncogenic potential in many cancer types. While it was clear from these studies that TAZ played a role in promoting proliferation in HPV18+ cells, YAP expression is also high and has been previously shown to be essential for cervical cancer (173, 195, 196). The role of YAP compared to TAZ in promoting proliferation was investigated in HeLa cells through generating stable monoclonal knockdowns of YAP and dual YAP/TAZ (termed Y/T) through use of shRNAs in a puromycin-resistant vector. To confirm successful appropriate knockdowns, qRT-PCR was used to analysed *WWTR1* and *YAP1* mRNA levels. Analysis showed successful knockdown of YAP alone (each knockdown had YAP expression of below 50%), however, knockdown of both YAP and TAZ together led a poorer knockdown of each (Figure 5.12 A). These cell lines were still taken forward for use as it was hypothesised this dual knockdown would be hard to achieve if both YAP and TAZ were required for growth. Successful knockdown of YAP and TAZ protein was confirmed through use of western blotting (Figure 5.12 B).

After it was confirmed that successful knockdowns were generated, the proliferative ability of the cells was assessed using a combination of growth and colony formation assays. Analysis of cell growth over a 5-day period showed knockdown of either YAP or TAZ alone or in combination led to a significant reduction in growth. However, there was no observable combined effect after YAP and TAZ simultaneous knockdown (Figure 5.12 C). Analysis of both anchorage dependent and independent colony forming ability showed knockdown of either YAP or TAZ led to a significant loss in the ability to form colonies. Yet again, there was no observable combined effect of upon simultaneous knockdown of YAP and TAZ (Y/T).

These results suggested both YAP and TAZ promoted growth in HeLa cells.

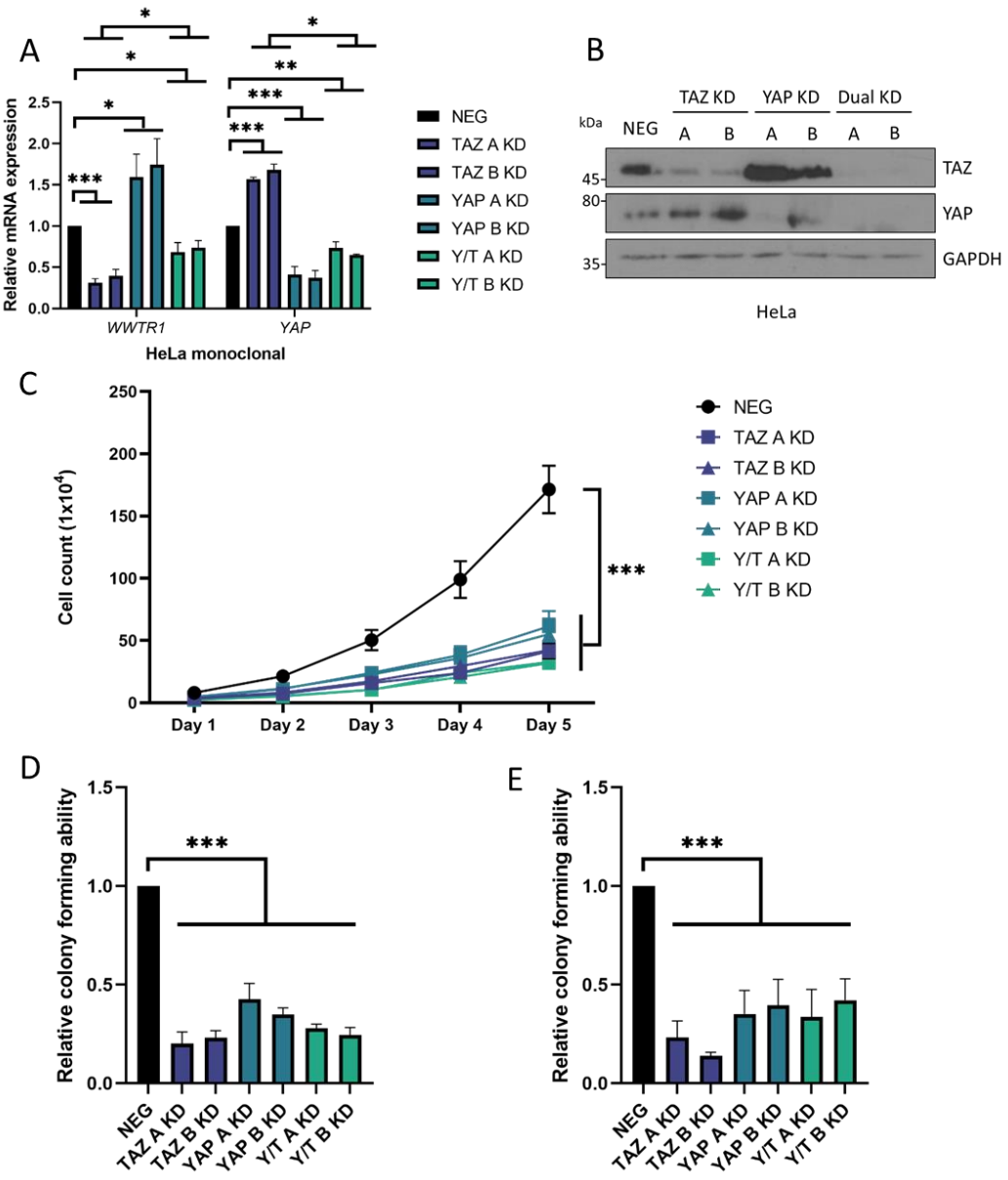

Figure 5.12 Knockdown of either YAP or TAZ reduces proliferation in HeLa cells A) qRT-PCR analysis of WWTR1 or YAP1 expression in monoclonal shRNA-mediated TAZ, YAP or YAP/ TAZ (Y/T) knockdown HeLa cells. U6 was used as a loading control. **B)** Representative western blot of in monoclonal shRNA-mediated TAZ, YAP or YAP/ TAZ (Y/T) knockdown HeLa cell lysate. Cell lysate was probed for TAZ and YAP. GAPDH was used as a loading control. **C)** Growth curve analysis of monoclonal shRNA-mediated TAZ, YAP or YAP/ TAZ (Y/T) knockdown HeLa cells. **D)** Colony formation assay (analysis anchorage dependent growth) of shRNA-mediated TAZ, YAP or YAP/ TAZ (Y/T) knockdown HeLa cells. **E)** Soft agar assay (analysis anchorage-independent growth) of monoclonal shRNA-mediated TAZ, YAP or YAP/ TAZ (Y/T) knockdown HeLa cells.

5.2.6 YAP and TAZ play non-redundant roles in promoting proliferation

As it was observed that both YAP and TAZ can promote proliferation in HeLa cells and as paralogues, are often reported to play the same role in cells, it was investigated if YAP and TAZ do actually play non-redundant functions. For this, FLAG-tagged TAZ and YAP were overexpressed in TAZ knockdown HeLa cells (Figure 5.13 A). Firstly it was investigated if YAP or TAZ could recover the loss of proliferation seen with TAZ knockdown. Analysis of growth over a 5-day period showed that overexpression of TAZ in the TAZ knockdown cells led to an almost complete recovery of growth (Figure 5.13 B, green line is TAZ overexpression in TAZ knockdown cells compared to black line of NEG cells transfected with pcDNA3). In contrast, YAP overexpression in the TAZ knockdown cells had no effect on growth compared to pcDNA3 expression alone (Figure 5.13 B, red line is YAP overexpression in TAZ knockdown cells, blue line is pcDNA3 in TAZ knockdown cells). Further investigation demonstrated a similar trend in the ability of cells to form both anchorage-dependent and independent colonies (Figure 5.13 C and D).

The need for TAZ-TEAD interactions was also investigated with the overexpression of a mutant TAZ without the ability to bind to TEAD. Analysis of growth over a 5-day period showed little change between the growth of TAZ knockdown cells with or without the expression of the TEAD binding defective TAZ (Figure 5.13 B yellow line). Additionally, there was little recovery of growth following transfection of TAZ S89D (a TAZ mutant incapable of nuclear import) in TAZ knockdown cells. Additionally, while expression of TAZ S89D led to no significant recovery in either anchorage-dependent or anchorage independent colony forming ability, there was a slight recovery when TEAD binding defective TAZ was expressed, although this was very little when compared to the WT TAZ (Figure 5.13 C-D).

In summary, TAZ and YAP play non-redundant roles by promoting proliferation. Furthermore, TAZ promotes proliferation in a largely TEAD-dependent manner.

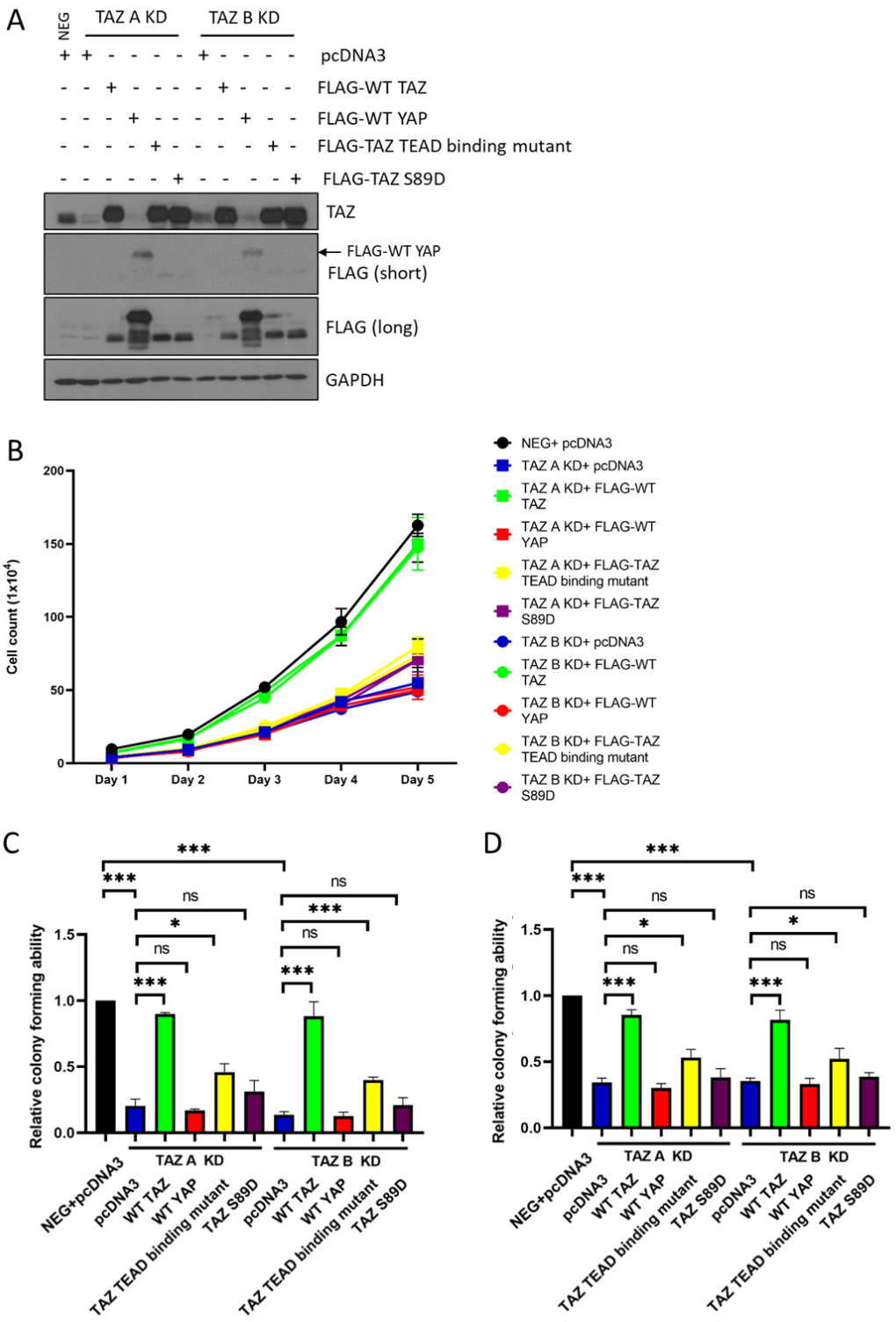

Figure 5.13 YAP or TEAD-defective binding TAZ cannot rescue loss of proliferation seen with TAZ knockdown in HeLa cells A) Representative western blot of monoclonal shRNA-mediated TAZ knockdown HeLa cell lysates transfected with either pcDNA3, FLAG-WT TAZ, FLAG-WT YAP, FLAG-TAZ TEAD binding mutant and FLAG-TAZ S89D (48 hours). Cell lysate

was probed for TAZ and FLAG. GAPDH was used as a loading control. B) Growth curve analysis of monoclonal shRNA-mediated TAZ knockdown HeLa cell lysates transfected with either pcDNA3, FLAG-WT TAZ, FLAG-WT YAP, FLAG-TAZ TEAD binding mutant and FLAG-TAZ S89D (48 hours). C) Colony formation assay (analysis anchorage dependent growth) of monoclonal shRNA-mediated TAZ knockdown HeLa cell lysates transfected with either pcDNA3, FLAG-WT TAZ, FLAG-WT YAP, FLAG-TAZ TEAD binding mutant and FLAG-TAZ S89D (48 hours). **D)** Soft agar assay (analysis anchorage-independent growth) of monoclonal shRNA-mediated TAZ knockdown HeLa cell lysates transfected with either pcDNA3, FLAG-WT TAZ, FLAG-WT YAP, FLAG-TAZ TEAD binding mutant and FLAG-TAZ S89D (48 hours).

5.2.7 YAP and TAZ promote transcription of distinct transcriptional programmes

As results suggested YAP and TAZ were promoting proliferation through different mechanisms, it was hypothesised this was because they were promoting the transcription of distinct target genes. Investigation showed that YAP knockdown (either alone or alongside TAZ) led to a significant decrease in the expression of a panel of canonically YAP-dependent genes (*AREG*, *CCND1*, *CD133* and *CYR61)* (Figure 5.14 A-D). Interestingly, knockdown of TAZ alone actually led to a significant increase in all 4 genes assessed (Figure 5.14 A-D).

Figure 5.13 suggested TEAD was important for TAZ-dependent proliferation, so it was further investigated if TAZ was still able to promote transcription of TEAD dependent genes in HeLa cells. Cells treated with either 6079510 or Ivermectin were transfected with a TEAD luciferase reporter plasmid (8xGTIIC-luciferase). This plasmid contains multiple TEAD binding sites (ACATTCCA) preceding a firefly luciferase gene. Analysis showed inhibition of TAZ or YAP/TAZ led to a significant decrease in luciferase expression, suggesting a loss of TEAD transcription activity (Figure 5.14 E). This was confirmed by transfecting the TEAD luciferase reporter plasmid into TAZ, YAP or YAP/TAZ knockdown HeLa cells. Analysis of luciferase expression showed significant decreases in all knockdown cell lines, suggesting all had reduced TEAD transcriptional activity (Figure 5.14 F).

These studies suggests that while TAZ likely promotes a different transcriptional profile to that of YAP, this is not due to failing to promote transcription of TEAD-dependent genes.

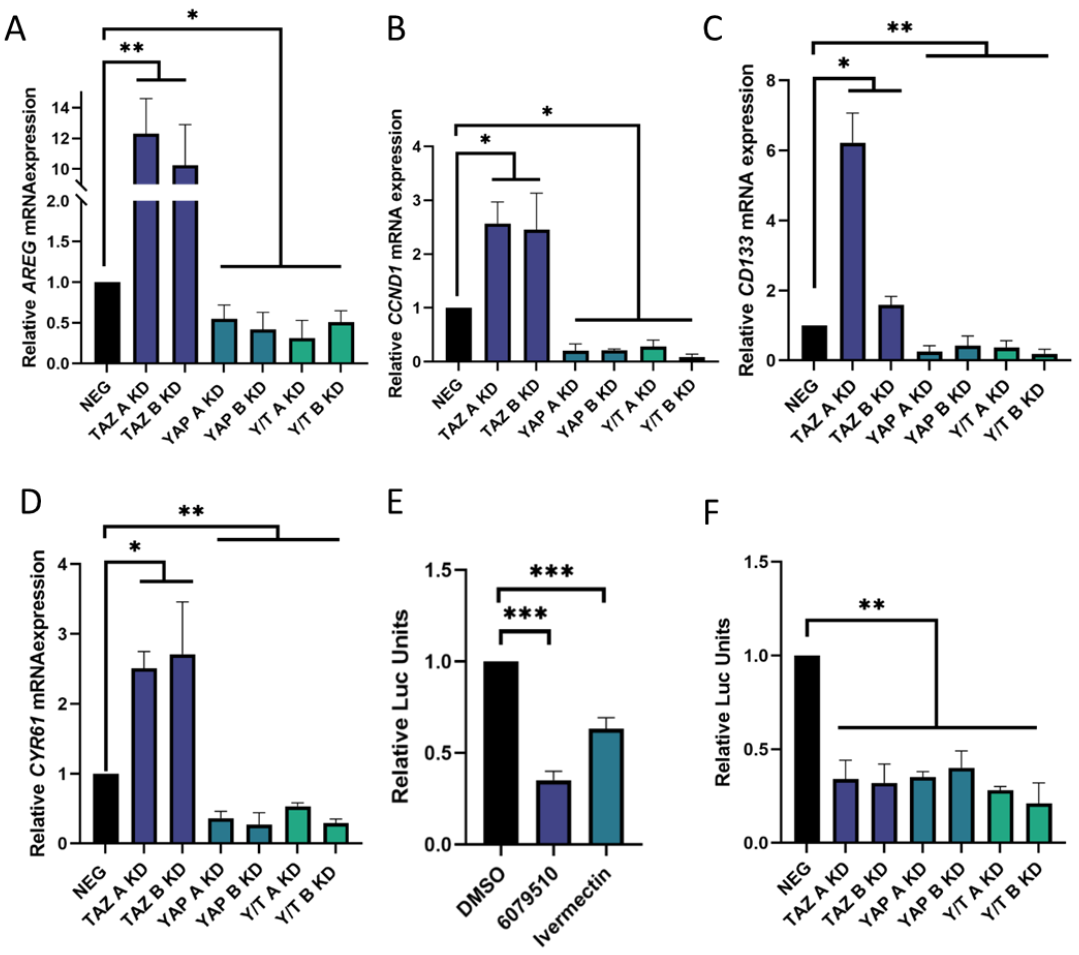

Figure 5.14 TAZ does not promote transcription of YAP dependent genes but still promotes TEAD dependent gene transcription A) qRT-PCR analysis of *AREG* expression in monoclonal shRNA-mediated TAZ, YAP or YAP/ TAZ (Y/T) knockdown HeLa cells. U6 was used as a loading control. **B)** qRT-PCR analysis of *CCND1* expression in monoclonal shRNA-mediated TAZ, YAP or YAP/ TAZ (Y/T) knockdown HeLa cells. U6 was used as a loading control. **C)** qRT-PCR analysis of *CD133* expression in monoclonal shRNA-mediated TAZ, YAP or YAP/ TAZ (Y/T) knockdown HeLa cells. U6 was used as a loading control. **D)** qRT-PCR analysis of *CYR61* expression in monoclonal shRNA-mediated TAZ, YAP or YAP/ TAZ (Y/T) knockdown HeLa cells. U6 was used as a loading control. E) Luciferase reporter of HeLa cells treated with 6079510 (16 hours) or Ivermectin (24 hours). Cells were transfected with 8xGTIIC-luciferase plasmid for 24 hours. pRL-TK (Renilla) was transfected in as a loading control.

5.3 Discussion

This chapter aimed to investigate the role of TAZ in HPV+ cervical cancer. While it is known that YAP strongly promotes an oncogenic phenotype in cervical cancer cells, reports on the function of TAZ have been conflicting. Through use of small molecule inhibitors it was demonstrated that TAZ promotes proliferation in HPV18+ cervical cancer cell line HeLa cells. Furthermore, this was confirmed with use of shRNA knockdowns in HeLa cells as well as two other HPV18+ cell lines. Further analysis of available online data also revealed high TAZ expression correlates with to reduced survival in HPV18+ cervical cancer.

The results in this chapter also demonstrate that both YAP and TAZ promote proliferation in HeLa cells while only YAP promotes proliferation in SiHa cells. TAZ shRNA-mediated knockdown led to an increase of proliferation in SiHa cells and conversely, TAZ overexpression inhibited growth. It is unclear why TAZ is playing a tumour suppressive role in SiHa cells, one possible explanation is that TAZ serves as a negative regulator for YAP. This is supported by data showing that TAZ knockdown led to increased YAP expression (non-significant in SiHa cells but significant in HeLa cells). As TAZ was lowly expressed in SiHa cells compared with HPV18+ cells, the cells do not rely on any TAZ-specific activity and therefore when TAZ is overexpressed it could be simply reducing YAP activity. This could be tested by investigating if the TAZ-TEAD binding mutant negatively affects YAP activity. Presumably if it is due to competition, this TAZ mutant will not serve as a tumour suppressor. Another possible explanation is TAZ interacts with different transcription factors in SiHa cells and HeLa cells and therefore promotes different transcription profiles in each cell line, an oncogenic profile in HeLa cells and a tumour suppressive profile in SiHa cells. This theory could be tested by using proteomics to elucidated TAZ interactors and comparing the cell lines or by comparing the transcriptome resulting from TAZ knockdown in SiHa to HeLa cells. On the other hand, TAZ may be promoting the same transcription profile in HeLa cells and SiHa cells

but TAZ-dependent genes are tumour suppressive in SiHa cells. Further investigations are needed to determine which explanation is more likely and could include comparing the transcriptional profile of TAZ-dependent genes in SiHa cells and HeLa cells. Furthermore, analysis of TAZ binding proteins could be compared between cell lines using immunoprecipitation and mass spectrometry.

One important conclusion that can be drawn from the findings of this chapter is YAP and TAZ play non-redundant roles in HPV18+ cervical cancer cell lines. This is key as much of the YAP and TAZ literature implies they have the same function or that TAZ has lesser of a role than YAP. Not only does the data show TAZ is a strong promoter of proliferation in HPV18+ cervical cancer, but overexpressing YAP in TAZ knockdown cells does not recover any function that was tested in this study, leading us to conclude TAZ has key YAP-independent functions in HPV18+ cervical cancer cells. Further investigations could involve used of YAP/TAZ chimeras, panels of YAP/TAZ mutants with domains between the two swapped to identify which domain of TAZ is important for YAP distinct function.

Analysis of proliferation between TAZ, YAP and YAP/TAZ knockdown cells initially seems to contradict this, as there was no additional reduction of proliferation upon simultaneous knockdown of YAP and TAZ compared to each oncogene alone. However, analysis of TAZ and YAP levels reveals the simultaneous knockdown of both YAP and TAZ does not achieve as successful of a knockdown as knocking down each individually. This may be due to multiple reasons including target sequences for shRNA to target both YAP and TAZ were hard to design as the mRNA sequences vary largely between the oncogenes despite high similarities in the protein sequences or simply the cells with the best knockdown of YAP and TAZ do not survive in the long term. This second theory is supported with the use of Ivermectin, which was found to be much more toxic to the cells than treatment with 6079510. Either way, the less than ideal knockdown of TAZ and YAP levels in the dual knockdowns compared to the control is theorised to be the main reason

why a combined effect on proliferation is not observed. Future investigation should try using siRNA to knockdown both YAP and TAZ simultaneously in a short term manner, which may enable a more successful knockdown of both.

The effect of TAZ on proliferation in these cells is not simply due to changes in E6 and E7 expression as levels of both remained unchanged with TAZ knockdown. Although this may seem unusual at first, this is in line with previous data suggesting the Hippo signalling pathway does not affect expression of either E6 or E7. Furthermore, as TAZ knockdown does not lead to a reduction in canonical YAP-dependent gene expression, the genes which TAZ promotes the transcription of to promote proliferation remain unknown and require further investigation to elucidate. Furthermore, despite the indicating TAZ plays a YAP-independent role, the ability of TAZ to interact with TEAD remains critical for TAZ-mediated proliferation. This can be concluded from results showing TEAD-defective TAZ cannot fully rescue the loss of proliferation seen with TAZ knockdown and TAZ knockdown leading to a reduction in TEAD transcription activity. However, it is possible that because the TEAD binding-defective TAZ mutant has multiple point mutations, these mutations are disrupting other interactions.

Additionally, apart from promoting proliferation, the results in this chapter show TAZ also plays a key role in EMT. Analysis of EMT markers suggested while TAZ knockdown causes a loss of mesenchymal markers such as Vimentin and N-cadherin and a corresponding increase in epithelial marker ZO-1, this is not due to changing levels of EMT-associated transcription factors. However, while there is not a loss of Snail or Slug expression, there may be a loss of activity as Snail/Slug/YAP/TAZ complex have been seen to be key in regulate gene expression. Analysis of two Snail/Slug dependent genes supports this both *SPARC* and *MMP2* expression were significantly decreased with TAZ knockdown. TAZ knockdown not only led to changes in expression of EMT-markers but also led to reduced wound healing, migration and invasion. It is hypothesised this could be due to loss of filopodia-like structures both in length and

overall number per cell. How TAZ is linked to the regulation of filopodia has yet to be elucidated and requires further investigation.

Overall, this chapter demonstrated TAZ is an oncogene in HPV18+ cervical cancer cells and plays essential roles in promoting proliferation and EMT in a YAP-independent manner.

Chapter 6- TAZ has novel YAP-independent targets in HPV18+ cervical cancer that are important for proliferation and EMT

6.1 Introduction

This chapter aims to elucidate TAZ-only target genes and the role they play in proliferation to clarify the distinct way TAZ promotes proliferation independently of YAP. Although most previous studies have considered YAP and TAZ to be functionally redundant this study, alongside recent others, shows this to be incorrect. The distinct transcriptional profile of TAZ compared to YAP is poorly understood and it is unknown which targets make contributions towards the oncogenic phenotype observed in HPV18+ cervical cancer. This chapter aims to not only identify novel TAZ target genes but to also elucidate the role they play in TAZ-mediated proliferation.

One way which TAZ regulates proliferation independently of YAP is through paraspeckles. TAZ interacts with paraspeckle protein NONO to achieve liquid-liquid phase separation to compartmentalise transcription factors/enhancers for transcription. Although YAP can bind to NONO it does not promote liquid-liquid phase separation (182). Therefore, as a TAZ-specific method of transcription regulation, this chapter also investigates if TAZ performs this role in HPV18+ cervical cancer cells and if this regulates TAZ-dependent genes. As this TAZ-NONO interaction regulates TEAD transcription, it may provide an explanation of how TEAD is necessary for TAZ-dependent proliferation despite YAP also interacting with TEAD.

6.2 Results

6.2.1 RNA sequencing analysis identifies distinct YAP and TAZ driven transcriptional profiles

To investigate how YAP and TAZ were promoting proliferation, the panel of shRNA TAZ and YAP and Y/T (YAP/TAZ) knockdown cell lines were sent for mRNA/lncRNA sequencing. Two different cell lines (with the target knocked down with two different shRNAs) for TAZ, YAP and Y/T and each cell line was sequenced in duplicate and compared to the NEG control (HeLa cells stable expressing a non-targeting control shRNA). Z-score analysis of the RNA-seq revealed large changes in the transcriptome between NEG, TAZ KD and YAP KD cell lines. It was clear that while YAP knockdown leads to large scale downregulation of genes, TAZ knockdown seems to lead to more upregulated genes, indicating TAZ plays a larger role in transcriptional repression. Surprisingly, there seemed to be few genes that were regulated by both YAP and TAZ and furthermore there seems to be more YAP-specific genes than TAZ-specific genes (Figure 6.1 A).

Genes were then separated into groups according to if they were TAZ or YAP specific, for example an upregulated TAZ-specific gene is a gene that is significantly up compared to the NEG control in at least 1 of the TAZ knockdown cell lines (in both repeats) but not in either of the YAP knockdown cell lines. It was decided that genes didn't have to be significantly changed in both the TAZ knockdown cell line in this example to allow for more potential TAZ-specific genes. When genes were sorted into these groups, 87 upregulated and 21 downregulated potential TAZ specific genes were identified (Figure 6.1 B). Further investigation of the functions of upregulated TAZ-specific genes showed potential roles in wound healing, extracellular matrix organisation, skin development, defence response to viruses and cell-substrate junction organisation to name a few (Table 6.1). In fact, many of the gene ontology groups suggested that TAZ-specific upregulated genes may play a role in EMT, aligning with

Description	p.adjust	Count
endodermal cell differentiation	0.004227765	4
endoderm formation	0.004227765	4
wound healing, spreading of epidermal cells	0.004227765	3
wound healing	0.004227765	8
endoderm development	0.011177447	4
skin development	0.016202744	6
epiboly	0.016202744	3
positive regulation of receptor-mediated endocytosis	0.028802548	3
cell-substrate adhesion	0.028802548	6
MDA-5 signaling pathway	0.028802548	2
positive regulation of phagocytosis, engulfment	0.028802548	2
positive regulation of membrane invagination	0.028802548	2
positive regulation of epithelial cell differentiation	0.030518752	3
negative regulation of peptidase activity	0.031375814	5
glycerolipid metabolic process	0.031375814	6
positive regulation of vascular endothelial growth factor receptor signaling pathway	0.034036995	2
positive regulation of hair follicle development	0.039113274	2
defense response to virus	0.05113354	5
defense response to symbiont	0.05113354	5
regulation of apoptotic cell clearance	0.05113354	2
positive regulation of release of cytochrome c from mitochondria	0.066045572	2
epidermal growth factor receptor signaling pathway	0.067439218	3
epidermis development	0.067439218	5
collagen metabolic process	0.067439218	3
blood coagulation	0.067439218	4
negative regulation of hydrolase activity	0.067439218	5
anoikis	0.067439218	2
ERBB signaling pathway	0.067439218	3
coagulation	0.067439218	4
regulation of hair cycle	0.067439218	2
hemostasis	0.067439218	4
regulation of body fluid levels	0.067439218	5
response to virus	0.085874573	5

Table 6.1- Upregulated TAZ-specific gene ontology analysis (performed by Joseph Cogan).

results from 5.2.4 in which it was showed TAZ knockdown lead to a reduction in EMT potential. Gene ontology analysis was not performed on the TAZ-specific downregulated genes due to the lower number of potential targets.

Although several genes were tested (data not shown), three genes were chosen for further analysis based upon the trend in expression in the knockdown cell lines and known biological function of encoded proteins. *TOGARAM2* was chosen as a downregulated-TAZ specific gene as it was identified to be TAZ-specific in both TAZ A KD and TAZ B KD cell lines. Additionally, it had not been linked to either YAP or TAZ previously. Furthermore, it was a very poorly characterised gene, as of time of writing, there had been no molecular studies on the potential functions of *TOGARAM2*, including in the context of cancer. However a study has suggested that *TOGARAM2* (aka *FAM179A*) was significantly overexpressed in relapsing ALK-Positive Anaplastic Large Cell Lymphoma. *SSTR5* was chosen as an upregulated TAZ-specific gene as it has not been linked to either YAP or TAZ activity and has been suggested to be tumour suppressive or downregulated in multiple types of cancer including adrenocortical carcinoma and laryngeal squamous cell carcinoma (281). Moreover, although there are studies in cervical cancer focused on the lncRNA derived from SSTR5 (lncSSTR5-AS1), SSTR5 itself has not been investigated. Firstly both genes were confirmed to be TAZ-specific genes using qRT-PCR. Analysis showed, compared to the NEG control, HeLa cells with TAZ knockdown (both individually and dual KD) expressed very little *TOGARAM2*, while HeLa cells with YAP knockdown actually showed a significant increase in expression (Figure 6.2 A). Analysis of *SSTR5* expression in showed TAZ knockdown in HeLa cells led to a significant decrease in expression while YAP knockdown led to no significant change (Figure 6.2 B).

Another potential upregulated gene *IFIT2* was investigated. Although analysis of the RNA sequencing suggested *IFIT2* may be regulated by both YAP and TAZ, qRT-

PCR analysis showed while knocking down either YAP or TAZ led to an increase in IFIT2 expression, TAZ knockdown led to a far greater upregulation. Given TAZ knockdown (both individually and with YAP) led to a significant increase in IFIT2 compared to YAP alone, it was still taken forward as a TAZ-specific gene (Figure 6.2 C). Taken together, these results suggest TAZ promotes a different transcription profile to that of YAP in HeLa cells and *TOGARAM2*, *SSTR5* and *IFIT2* are potential novel TAZ-dependent genes.

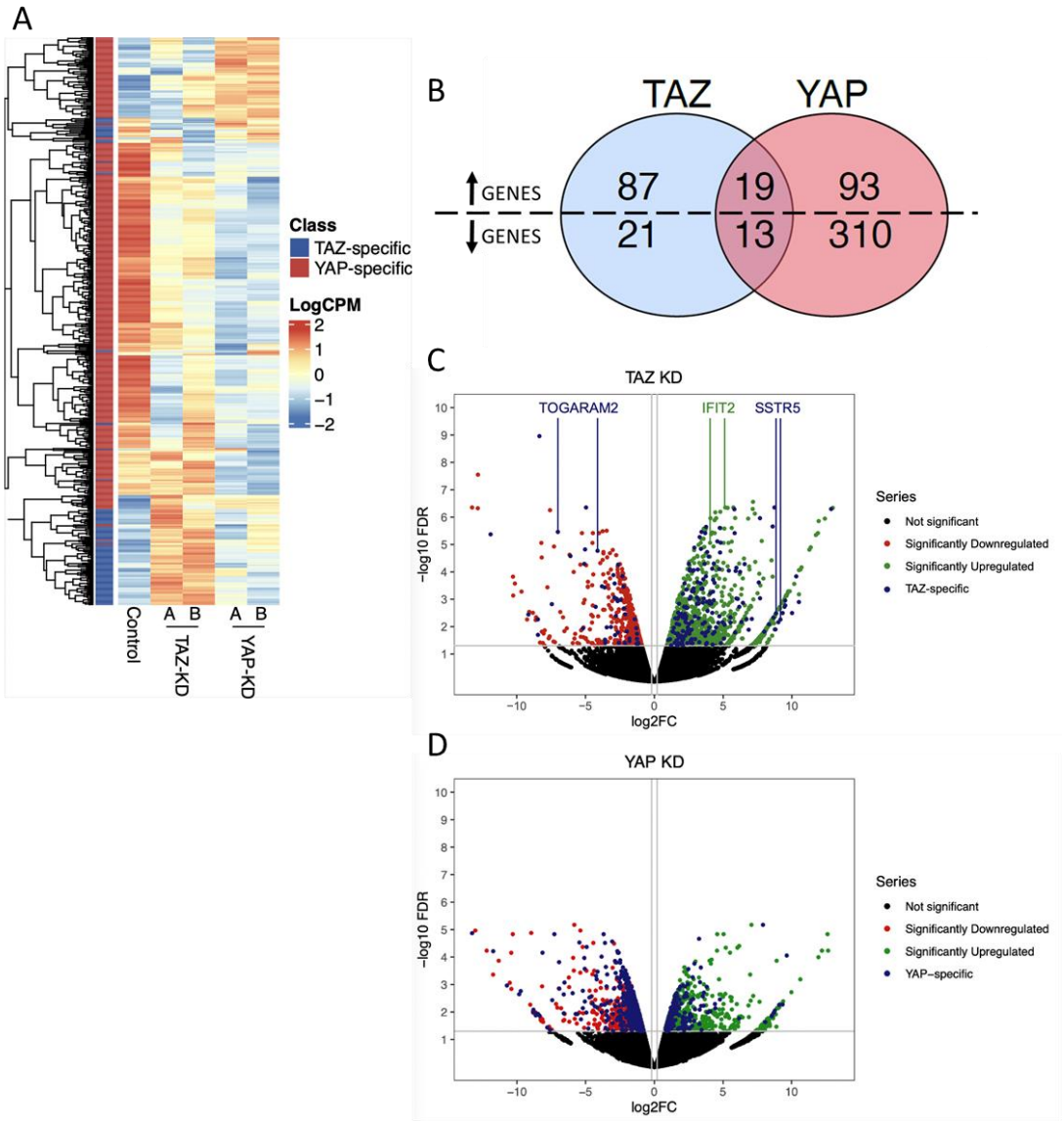

Figure 6.1 TAZ and YAP have different transcription profiles in HPV18+ cervical cancer cells A) Heat map of differentially expressed mRNAs and lncRNAs in TAZ KD (A and B KD cell lines) and YAP KD (A and B KD cell lines) HeLa cell lines (n=2) with T-test analysis. **B)** Venn diagram of TAZ-specific and YAP-specific genes from **A**. **C)** Volcano plot of TAZ knockdown RNA-seq in HeLa cells at adjusted P value < 0.05 with TOGARAM2, SSTR5 and IFIT2 highlighted. TAZ-specific genes are highlighted in blue. **D)** Volcano plot of YAP knockdown RNA-seq in HeLa cells at adjusted P value < 0.05. YAP-specific genes are highlighted in blue. Analysis was performed by Joseph Cogan.

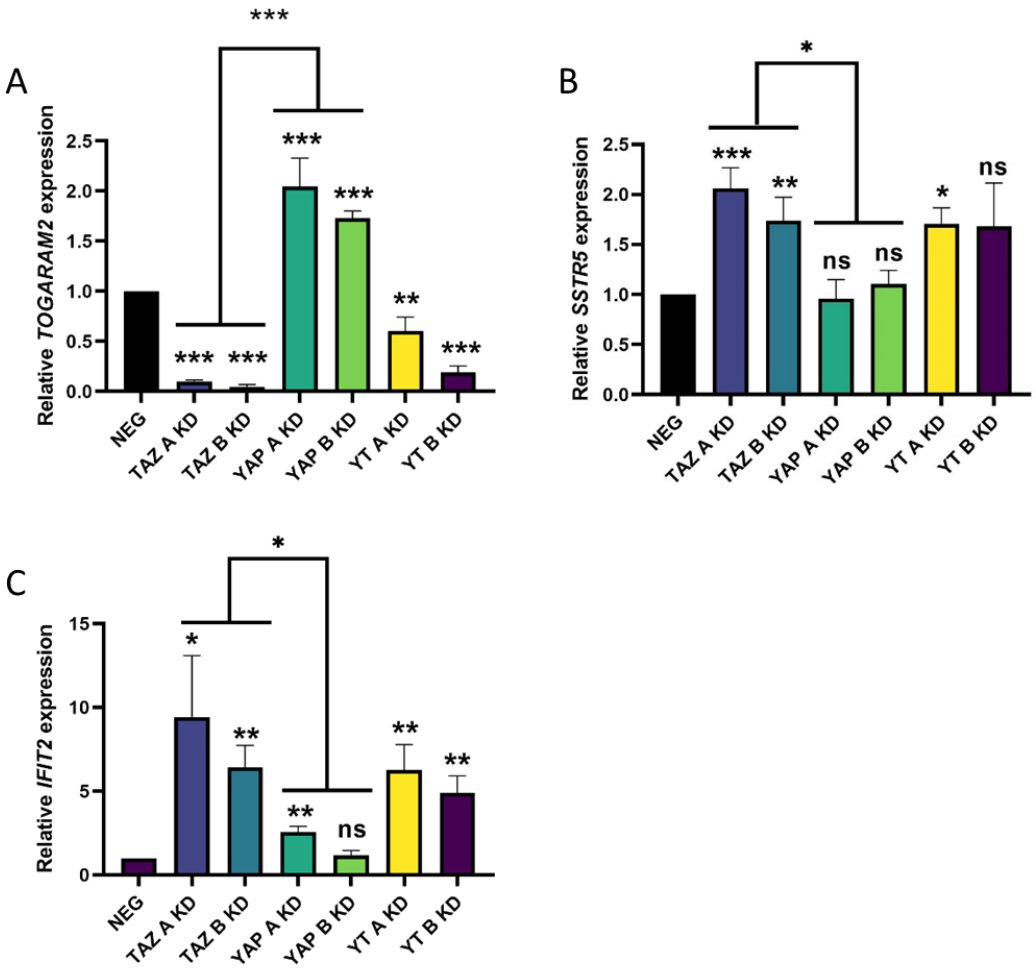

Figure 6.2 Validation of TAZ-specific genes suggested by RNA-seq analysis A) qRT-PCR analysis of *TOGARAM2* expression in monoclonal shRNA-mediated TAZ, YAP or YAP/ TAZ (Y/T) knockdown HeLa cells. U6 was used as a loading control. **B)** qRT-PCR analysis of *SSTR5* expression in monoclonal shRNA-mediated TAZ, YAP or YAP/ TAZ (Y/T) knockdown HeLa cells. U6 was used as a loading control. **C)** qRT-PCR analysis of *IFIT2* expression in monoclonal shRNA-mediated TAZ, YAP or YAP/ TAZ (Y/T) knockdown HeLa cells. U6 was used as a loading control.

6.2.2 TOGARAM2 expression is controlled by TAZ in HPV18+ cervical cancer

The potential for *TOGARAM2* to be a TAZ-dependent gene was further investigated. Firstly, the expression of *TOGARAM2* mRNA in the panel of cervical cancer cell lines was assessed using qRT-PCR. Analysis showed *TOGARAM2* was significantly overexpressed in all HPV18+ cell lines tested while expression did not differ significantly from the control in either HPV16+ cell lines (Figure 6.3 A). As this pattern of expression was very similar to that observed for TAZ, further analysis revealed when *TOGARAM2* expression was compared to *WWTR1* expression in each sample, there was a significant positive correlation (Figure 6.3 B). As all of these cell lines have been adapted for tissue culture use, the expression of *TOGARAM2* was investigated in a panel of cervical liquid cytology samples. These samples represented cervical disease progression from CIN1 to CIN3 and were collected from patients with either HPV16+ or HPV18+ disease alongside HPV- normal cervical tissue samples. *TOGARAM2* expression was significantly increase in CIN2 and 3 of HPV18+ patients (Figure 6.3 C). Furthermore, *TOGARAM2* was found to significantly positively correlate with *WWTR1* expression in matched samples (Figure 6.3 D).

To confirm that *TOGARAM2* was not just a TAZ-dependent gene in HeLa cells, *TOGARAM2* expression was investigated in other HPV18+ cervical cancer cell lines; SW756 and MS751. TAZ knockdown led to a significant reduction in *TOGARAM2* expression compared to the NEG control in both cell lines (Figure 6.3 E and F). Additionally, *TOGARAM2* expression significantly decreased upon inhibition of TAZ activity with 6079510 or Ivermectin treatment, showing that the decrease in *TOGARAM2* expression was not an off-target effect of shRNA treatment (Figure 6.3 G).

Given TAZ was found to be regulated by HPV18E7, it was hypothesised that *TOGARAM2* was as well. Firstly, it was investigated if depletion of HPV18 E6/E7 with in siRNAs led to a decrease in *TOGARAM2* expression. qRT-PCR analysis revealed *TOGARAM2* expression was significantly decrease following E6/E7 knockdown (Figure

6.3 H). Additionally, *TOGARAM2* mRNA levels significantly increase following HPV18 E7 expression (Figure 6.3 I).

TOGARAM2 may be regulated by multiple mechanism, so it was investigated if the increase in *TOGARAM2* with HPV18 E7 expression was TAZ-dependent. HPV18 E7 was stable overexpression in C33A cells before treatment with 6079510. Led to a significant increase in *TOGARAM2* (Figure 6.3 J).

Finally, as results previously showed TAZ-promotes proliferation in a largely TEAD-dependent manner, it was investigated if *TOGARAM2* was TEAD dependent. Investigation revealed *TOGARAM2* expression was significantly decreased in HeLa cells treated with verteporfin (a well characterised TEAD inhibitor) (Figure 6.3 K).

Together these results suggest TOGARAM2 is a TAZ-dependent gene in HPV18+ cervical cancer that is regulated by TAZ in a TEAD-dependent manner.

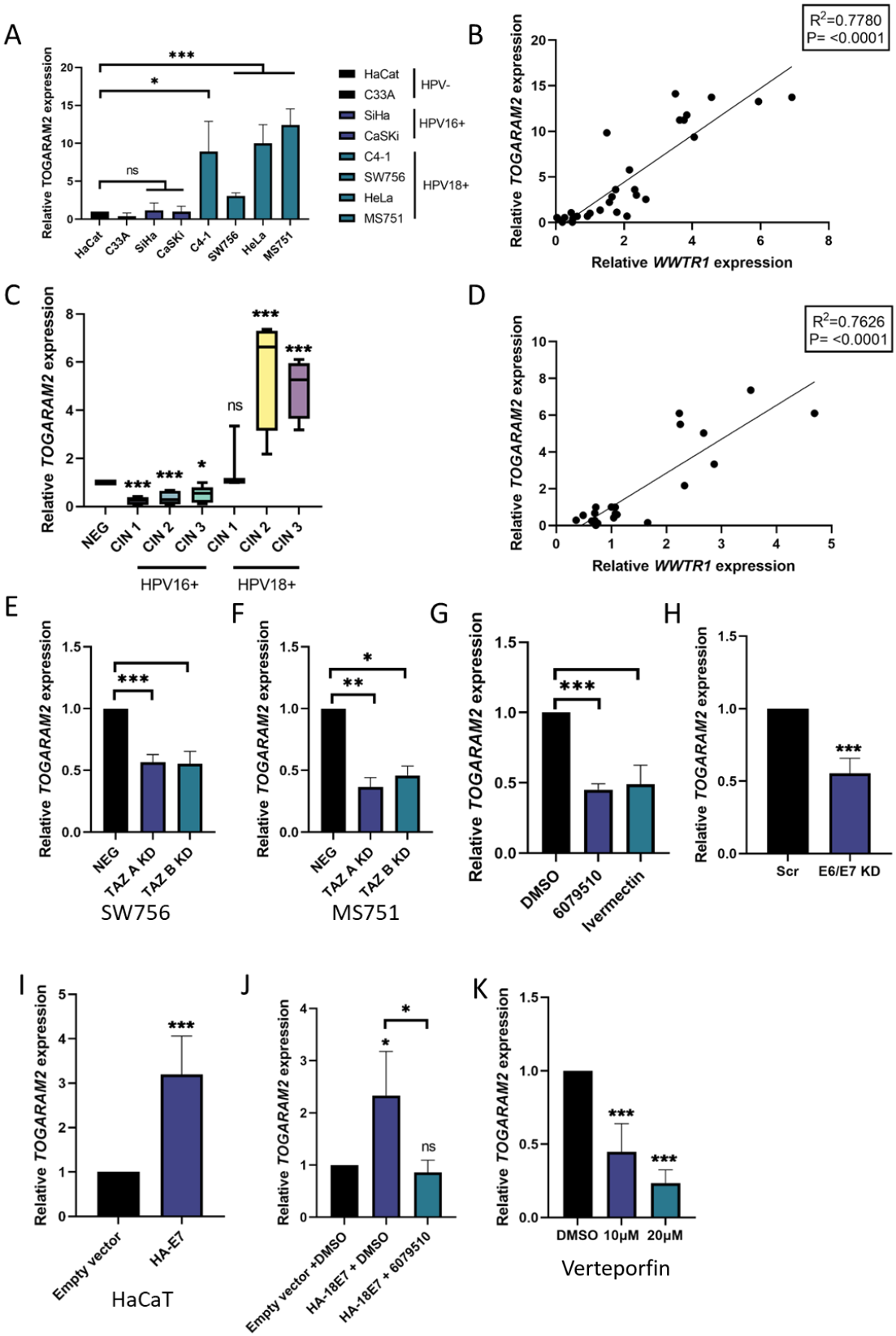

Figure 6.3 TOGARAM2 is a TAZ-dependent gene A) qRT-PCR analysis of TOGARAM2 mRNA expression in HPV-, HPV16+ or HPV18+ cell lines. U6 transcript levels were used as a loading

control. **B)** Graph showing correlation between *TOGARAM2* and *WWTR1* expression from A. **C)** qRT-PCR analysis of *TOGARAM2* expression in negative, HPV16 or HPV18+ patient cervix liquid cytology samples from different CIN grades (n=4 from each grade). U6 was used as a loading control. **D)** Graph showing correlation between *TOGARAM2* and *WWTR1* expression from C. **E)** qRT-PCR analysis of *TOGARAM2* mRNA expression in polyclonal shRNA-mediated TAZ knockdown SW756 cells. U6 was used as a loading control. **F)** qRT-PCR analysis of *TOGARAM2* mRNA expression in polyclonal shRNA-mediated TAZ knockdown MS751 cells. U6 was used as a loading control. **G)** qRT-PCR analysis of *TOGARAM2* expression in HeLa cells following either DMSO, 6079510 (16 hours) or Ivermectin (24 hours) treatment. . U6 was used as a loading control. **H)** qRT-PCR analysis of *TOGARAM2* expression in HeLa cells with E6/E7 targeting siRNA (for 72 hours). *U6* was used as a loading control. **I)** qRT-PCR analysis of *TOGARAM2* expression in HaCaT cells stably expressing HA-HPV18 E7. *U6* was used as a loading control. **J)** qRT-PCR analysis of *TOGARAM2* expression in C33A cells stably expressing HA-HPV18 E7 with or without 6079510 treatment (16 hours). *U6* was used as a loading control. **K)** qRT-PCR analysis of *TOGARAM2* expression in HeLa cells following either DMSO or verteporfin (24 hours) treatment. . U6 was used as a loading control.

6.2.3 TOGARAM2 is a novel oncogene in HPV18+ cells and promotes filopodia formation

Although little is known of the biological function of *TOGARAM2*, what is known has been partially elucidated by comparison to TOGARAM1 (aka Crescerin or FAM179B, the closest relative to *TOGARAM2*) and its *C.elegans* counterpart CHE-12. The recent study identified *TOGARAM1* as a key regulator of primary cilia, using TOG domains to promote MT polymerisation. Each TOG domain consists of 6 HEAT repeats, pairs of antiparallel α-helices. Regions between HEAT repeats consist of loops used to bind tubulin. In CLASP the TOG domain is trimeric and functions to stabilise MT whereas in ch-TOG, the TOG domain is pentameric and promotes MT polymerisation (282, 283). Specifically, TOG2 and TOG4 domains increase MT polymerisation rates. As *TOGARAM2* TOG4 domains shares a high similarity to that of TOGARAM1, it is predicted to share similar functions but as time of writing, there is no molecular studies focusing on *TOGARAM2* (284). Although information is limited, recently *TOGARAM2* was found to be among genes significantly overexpressed in relapsing ALK-Positive Anaplastic Large Cell Lymphoma (285). Moreover, *TOGARAM2* was been identified to form a novel, rare fusion gene, FAM179A-ALK, with variants detected in NSCLC and brain cancer metastasis (286, 287). Other related proteins such as chTOG have been linked to poor prognosis in hepatocellular carcinoma (288).

Given what is known and the results that suggested *TOGARAM2* expression was promoted by TAZ in HPV18+ cervical cancer, it was proposed that *TOGARAM2* was an oncogene. Polyclonal *TOGARAM2* knockdown cell lines were generated using two individual shRNAs in HeLa cells (Figure 6.4 A). Whilst the reduction of *TOGARAM2* was relatively poor but still consistent, these cell lines were taken forward for phenotype analysis.

TOGARAM2 knockdown led to a significant reduction in growth over a 5 day period (Figure 6.4 B) and furthermore, led to a significant reduction in the formation of anchorage-dependent and anchorage-independent colonies in HeLa cells (Figure 6.4 C and D). This suggested *TOGARAM2* promotes proliferation and therefore is a potential novel oncogene.

Other proteins related to TOGARAM2 such as TOGARAM1, CLASP1 and chTOG all have microtubule binding domains imparted by their TOG domains. TOGARAM2 is also predicted to have TOG domains, and our predicted structure agrees with is as regions of repeated α-helices with loops between them are clearly visible, alongside large disordered regions (Figure 6.5 A and B). Therefore as it is predicted TOG domains can bind microtubules, it was hypothesised that TOGARAM2 could play a role in the formation of structures such as filopodia. *TOGARAM2* knockdown in HeLa cells led to a decrease in the length of filopodia and the overall number, similar to the observed effects of TAZ knockdown (Figure 6.5 C-D).

As *TOGARAM2* expression was low in HPV16+ cells, it was hypothesised TOGARAM2 was only oncogenic in HPV18+ cells. To investigate this, FLAG-TOGARAM2 was overexpressed in HeLa cells and western blotting was used to confirm successful expression (Figure 6.6 A). Analysis of growth over 5 days showed TOGARAM2 overexpression led to a significant increase in growth and both anchorage-dependent and independent colony formation (Figure 6.6 B- D). Next, FLAG-TOGARAM2 was expressed in SiHa cells with western blotting used to confirm successful transfection (Figure 6.6 E). The overexpression of FLAG-TOGARAM2 led to a significant decrease in growth over a 5 day period and reduced the ability of SiHa cells to from both anchorage-dependent and independent colonies (Figure 6.6 F-H). Furthermore, analysis of online data showed high TOGARAM2 led to reduced survival compared to low TOGARAM2 expression only in HPV18+ cervical cancer supporting the *in vitro* data observed (Figure 6.7). Taken together these data suggest *TOGARAM2* is a

novel oncogene in HPV18+ cervical cancer cells and promotes filopodia formation. However, it also suggests *TOGARAM2* is tumour suppressive in HPV16+ cells.

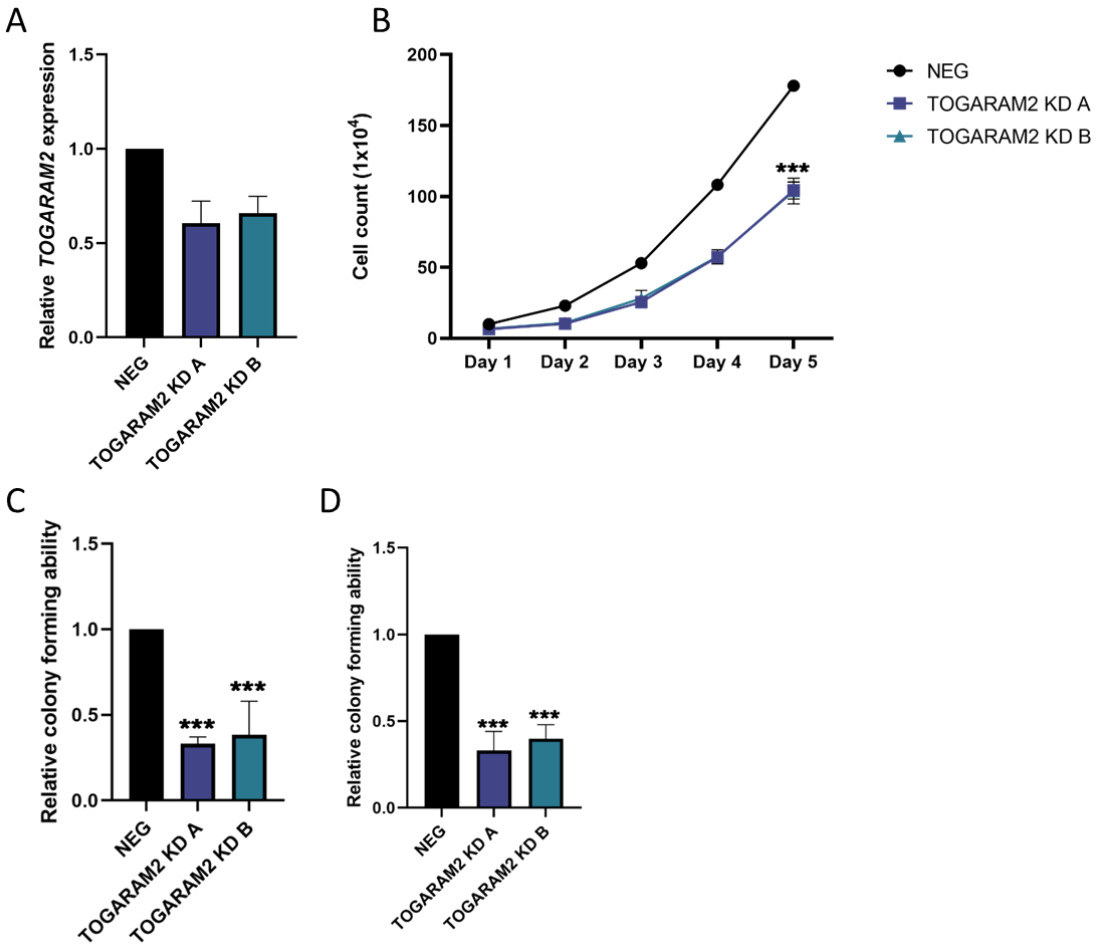

Figure 6.4 TOGARAM2 knockdown reduces proliferation in HeLa cells A) qRT-PCR analysis of *TOGARAM2* mRNA expression in polyclonal shRNA-mediated TOGARAM2 knockdown HeLa cells. U6 was used as a loading control. **B)** Growth curve analysis of monoclonal shRNA-mediated TOGARAM2 knockdown HeLa cells. **C)** Colony formation assay (analysis anchorage dependent growth) monoclonal shRNA-mediated TOGARAM2knockdown HeLa cells. **D)** Soft agar assay (analysis anchorage-independent growth) in monoclonal shRNA-mediated TOGARAM2 knockdown HeLa cells.

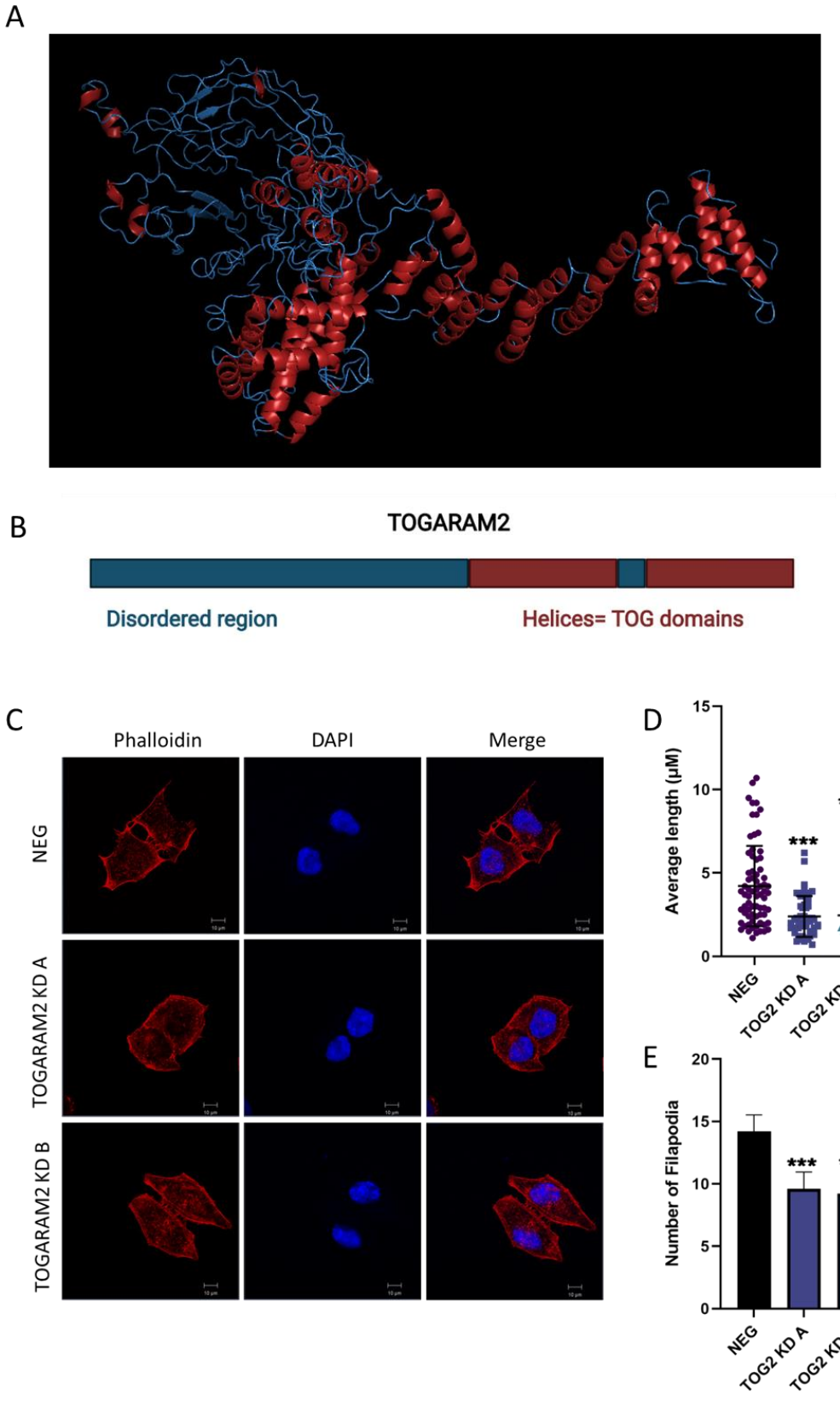

Figure 6.5 TOGARAM2 knockdown impedes filopodia formation A) Predicted structure of TOGARAM2 using Alphafold. α-helices are highlighted in red, disordered region regions such as

coiled coils are highlighted in blue (Generated by Elena Harrington). **B)** Schematic of TOGARAM2 structure with α-helices/TOG domains are highlighted in red, disordered region regions such as coiled coils are highlighted in blue. **C)** Immunofluorescence microscopy analysis of Rhodamine-Phalloidin staining (red) polyclonal shRNA-mediated TOGARAM2 knockdown HeLa cells. DAPI stained nuclei (blue). Scale bar 10 µm. **D)** Measurement of filopodia length in polyclonal shRNA-mediated TOGARAM2 knockdown HeLa cells. **E)** Average number of filopodia per cell in polyclonal shRNA-mediated TOGARAM2 knockdown HeLa cells.

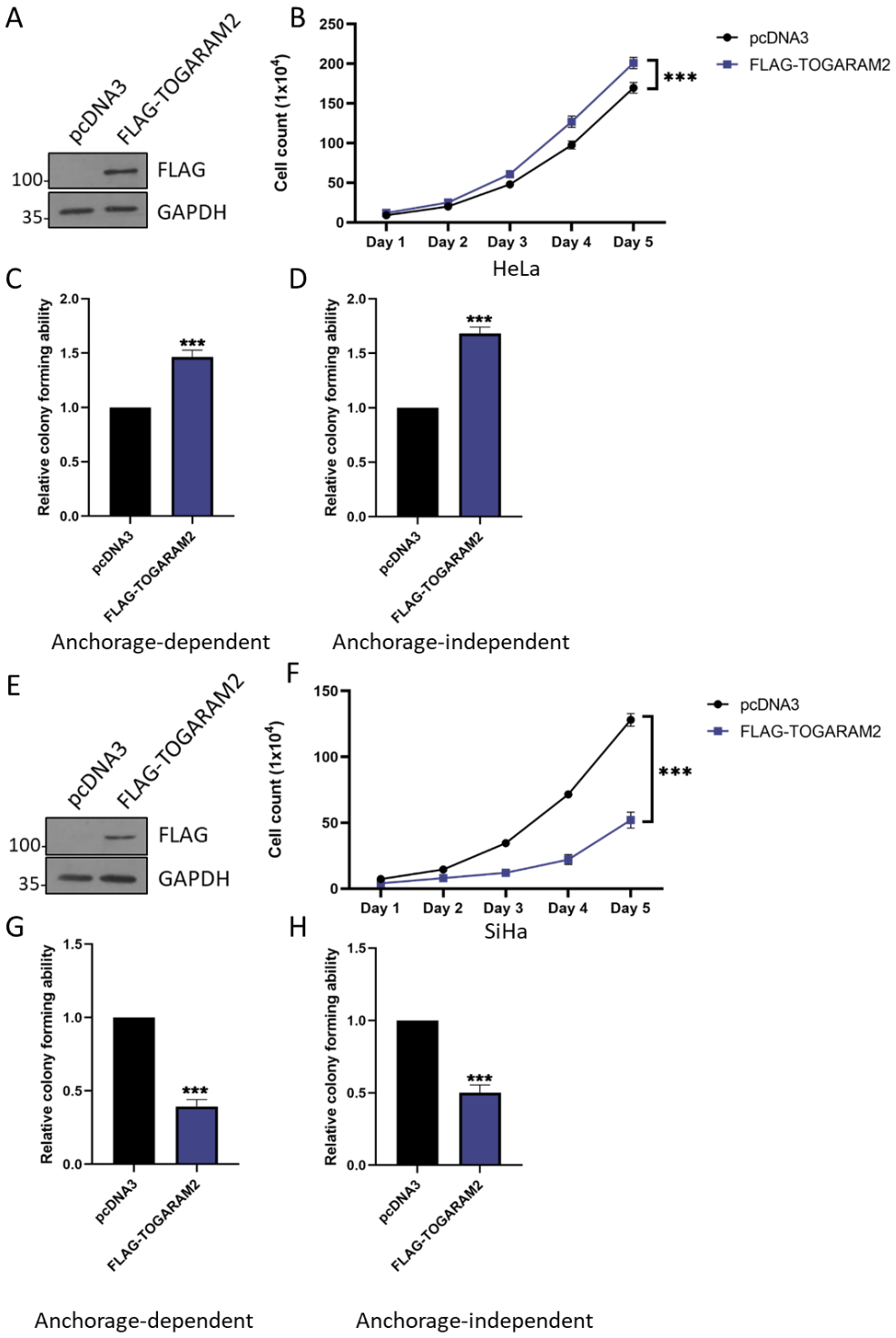

Figure 6.6 TOGARAM2 is not oncogenic in HPV16+ cervical cancer cells A) Representative western blot of HeLa cells transfected with FLAG-TOGARAM2 (48 hours). Cell lysates were probed for FLAG. GAPDH was used as a loading control. **B)** Growth curve analysis of HeLa cells transfected with FLAG-TOGARAM2 (48 hours). **C)** Colony formation assay (analysis anchorage dependent growth) of HeLa cells transfected with FLAG-TOGARAM2 (48 hours). **D)** Soft agar

assay (analysis anchorage-independent growth) in HeLa cells transfected with FLAG-TOGARAM2 (48 hours). **E)** Representative western blot of SiHa cells transfected with FLAG-TOGARAM2 (48 hours). Cell lysates were probed for FLAG. GAPDH was used as a loading control. **F)** Growth curve analysis of SiHa cells transfected with FLAG-TOGARAM2 (48 hours). **G)** Colony formation assay (analysis anchorage dependent growth) of SiHa cells transfected with FLAG-TOGARAM2 (48 hours). **H)** Soft agar assay (analysis anchorage-independent growth) in SiHa cells transfected with FLAG-TOGARAM2 (48 hours).

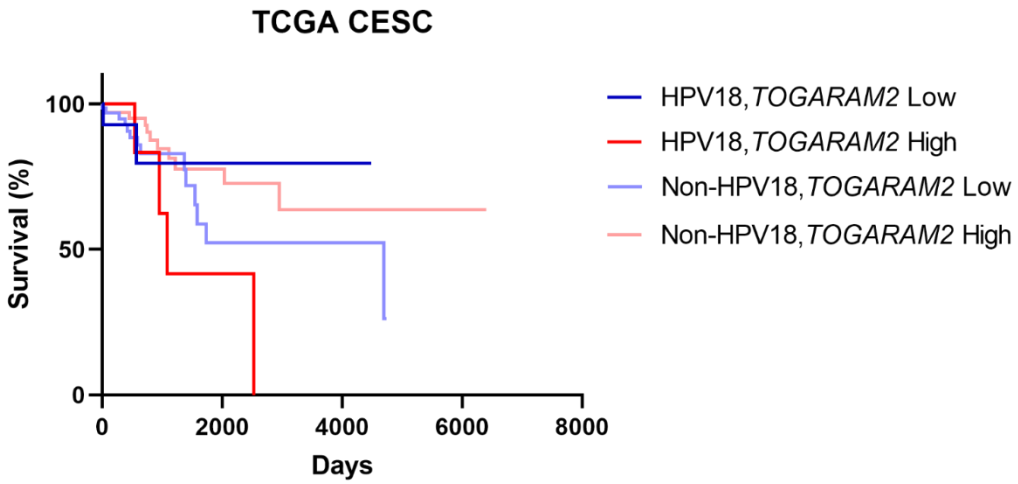

Figure 6.7 High TOGARAM2 expression correlates with reduced survival in HPV18+ cervical cancer. Kaplan-Meier curves showing overall survival in cervical cancer stratified by HPV18+ or non-HPV18+. Survival was compared using the log-rank test (performed by Dr Ethan Morgan)

6.2.4 TOGARAM2 plays a key role in TAZ-dependent proliferation and EMT

As *TOGARAM2* expression was shown to be TAZ-dependent and also oncogenic in HPV18+ cells, it was proposed that *TOGARAM2* played a role in TAZ-mediated proliferation. *TOGARAM2* expression was firstly restored in TAZ knockdown HeLa cells by transfecting in FLAG-TOGARAM2 (Figure 6.8 A). This led to a partial but significant rescue of growth over a 5 day period when compared to TAZ knockdown cells alone and partial rescue of both anchorage-dependent and independent colony forming ability (Figure 6.8 B-D).

Given the effect of *TOGARAM2* knockdown on filopodia, it was hypothesised TOGARAM2 played a role in TAZ-mediated EMT. Analysis of TAZ knockdown cells with TOGARAM2 expression restored showed an almost complete rescue of both migration and invasion compared to TAZ knockdown alone (Figure 6.8 E and F). Taken together, these results suggest TOGARAM not only plays a key role in TAZ-mediated proliferation but is a major mediator of TAZ-mediated EMT.

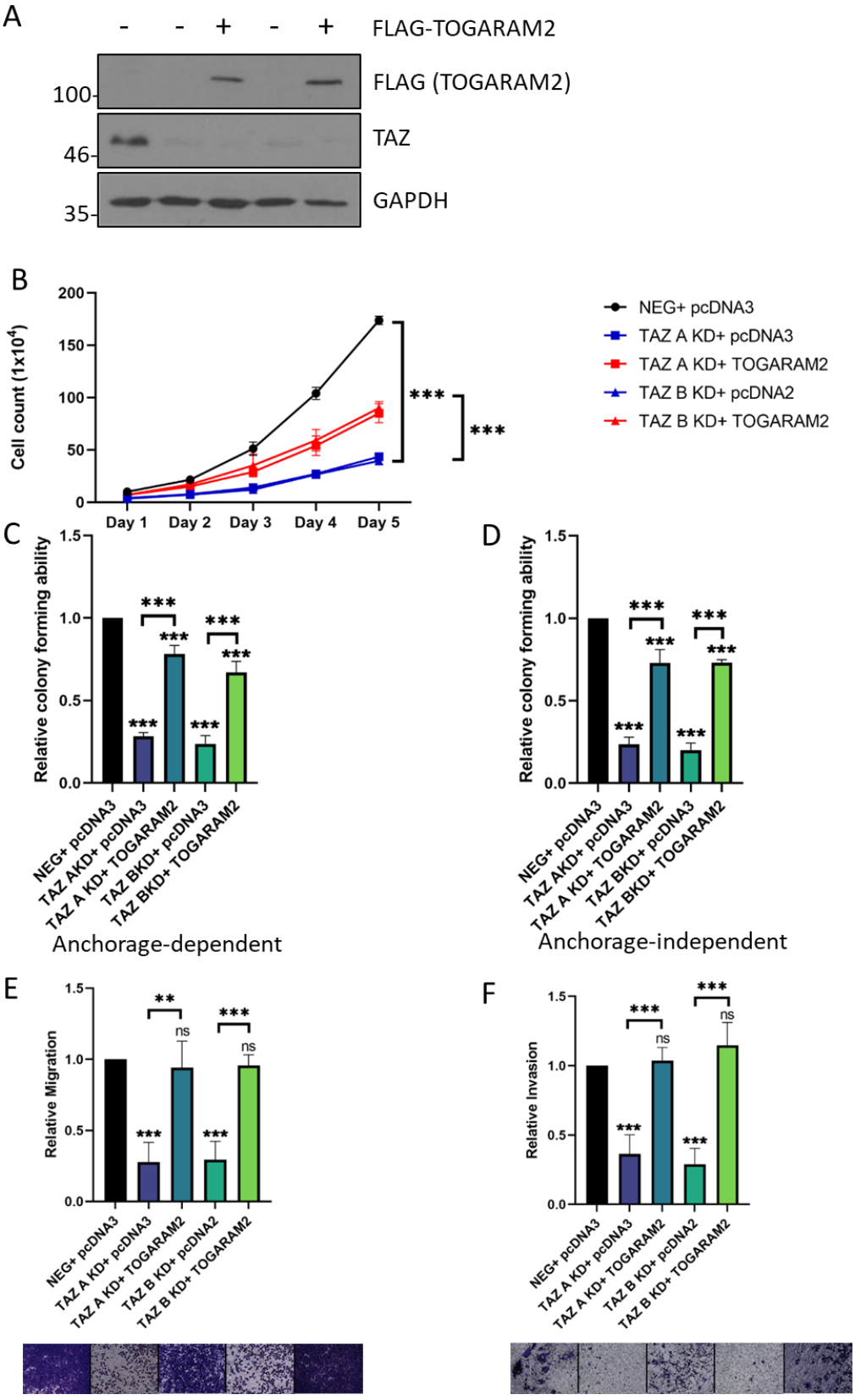

Figure 6.8 TOGARAM2 is critical for TAZ-mediated proliferation and EMT A) Representative western blot of monoclonal shRNA-mediated TAZ knockdown HeLa cell lysates transfected with

either pcDNA3 or FLAG-TOGARAM2 (48 hours). Cell lysate was probed for TAZ and FLAG. GAPDH was used as a loading control. **B)** Growth curve analysis of monoclonal shRNA-mediated TAZ knockdown HeLa cell lysates transfected with either pcDNA3 or FLAG-TOGARAM2 (48 hours). **C)** Colony formation assay (analysis anchorage dependent growth) of monoclonal shRNA-mediated TAZ knockdown HeLa cell lysates transfected with either pcDNA3 or FLAG-TOGARAM2 (48 hours). **D)** Soft agar assay (analysis anchorage-independent growth) of monoclonal shRNA-mediated TAZ knockdown HeLa cell lysates transfected with either pcDNA3 or FLAG-TOGARAM2 (48 hours). Transwell migration assay of monoclonal shRNA-mediated TAZ knockdown HeLa cells transfected with either pcDNA3 or FLAG-TOGARAM2 (48 hours). **F)** CHEMICON Cell Invasion assay of monoclonal shRNA-mediated TAZ knockdown HeLa cells transfected with either pcDNA3 or FLAG-TOGARAM2 (48 hours).

6.2.5 SSTR5 expression is regulated by TAZ in HPV18+ cervical cancer

Despite the significant results observed with *TOGARAM2*, several other genes were shown to be dysregulated by TAZ knockdown and it was clear that other targets were also involved in TAZ-mediated proliferation. Therefore, further investigations were carried out on *SSTR5*, another gene suggested to be TAZ-dependent.

SSTR5 expression in the panel of cervical cancer cell lines showed all HPV16+ and HPV18+ cell lines tested had significantly reduced expression compared to HaCaT cells. Interestingly, C33A cells also had significantly reduced *SSTR5* expression compared to HaCaT cells (Figure 6.9 A). Similarly, *SSTR5* expression was reduced in both HPV16+ and HPV18+ samples in CIN 1-3 (Figure 6.9 B). When the expression of *SSTR5* was compared to *WWTR1* expression in matched patient samples, it was found that expression was only inversely correlated in HPV18+ patient samples (Figure 6.9 C-D). This together with the cell line data suggests while *SSTR5* expression is repressed by TAZ in HPV18+ cells, there is a different method of regulation in the HPV16+ cells.

To confirm that *SSTR5* was not just TAZ-dependent in HeLa cells, expression was investigated in other HPV18+ TAZ KD cell lines. TAZ knockdown led to a significant increase in both SW756 and MS751 (Figure 6.9 E and F). Furthermore, it was confirmed that the increase in *SSTR5* expression was not an off-target effect of TAZ-targeting shRNAs as treatment of HeLa cells with either 6079510 or Ivermectin to inhibit TAZ activity led to a significant increase in *SSTR5* expression (Figure 6.9 G).

It was hypothesised that *SSTR5* expression should be the inverse of HPV18 E7 expression as TAZ in turn is regulated by HPV18E7. *HPV18 E6* and *E7* depletion in HeLa cells led to a significant increase in *SSTR5* expression (Figure 6.9 H). HPV18 E7 stable expression in HaCaT cells also led to a significant decrease in *SSTR5* expression (Figure 6.9 I). Furthermore, C33A cells stably expressing HPV18 E7 treated with 6079510 showed a reversal in the decrease of *SSTR5* levels with HPV18 E7 expression alone

(Figure 6.9 J). Therefore, it was proposed that HPV18 E7 regulates *SSTR5* in a TAZ dependent manner.

Previous chapters suggested TAZ acts in a largely TEAD-dependent manner, and therefore it was not surprising when verteporfin-treated HeLa cells showed a significant dose-dependent increase in *SSTR5* expression (Figure 6.9 K). This demonstrates TAZ represses *SSTR5* expression in a TEAD dependent manner. Taken together, this suggested *SSTR5* is a novel TAZ-dependent gene and is repressed in a TEAD-dependent manner.

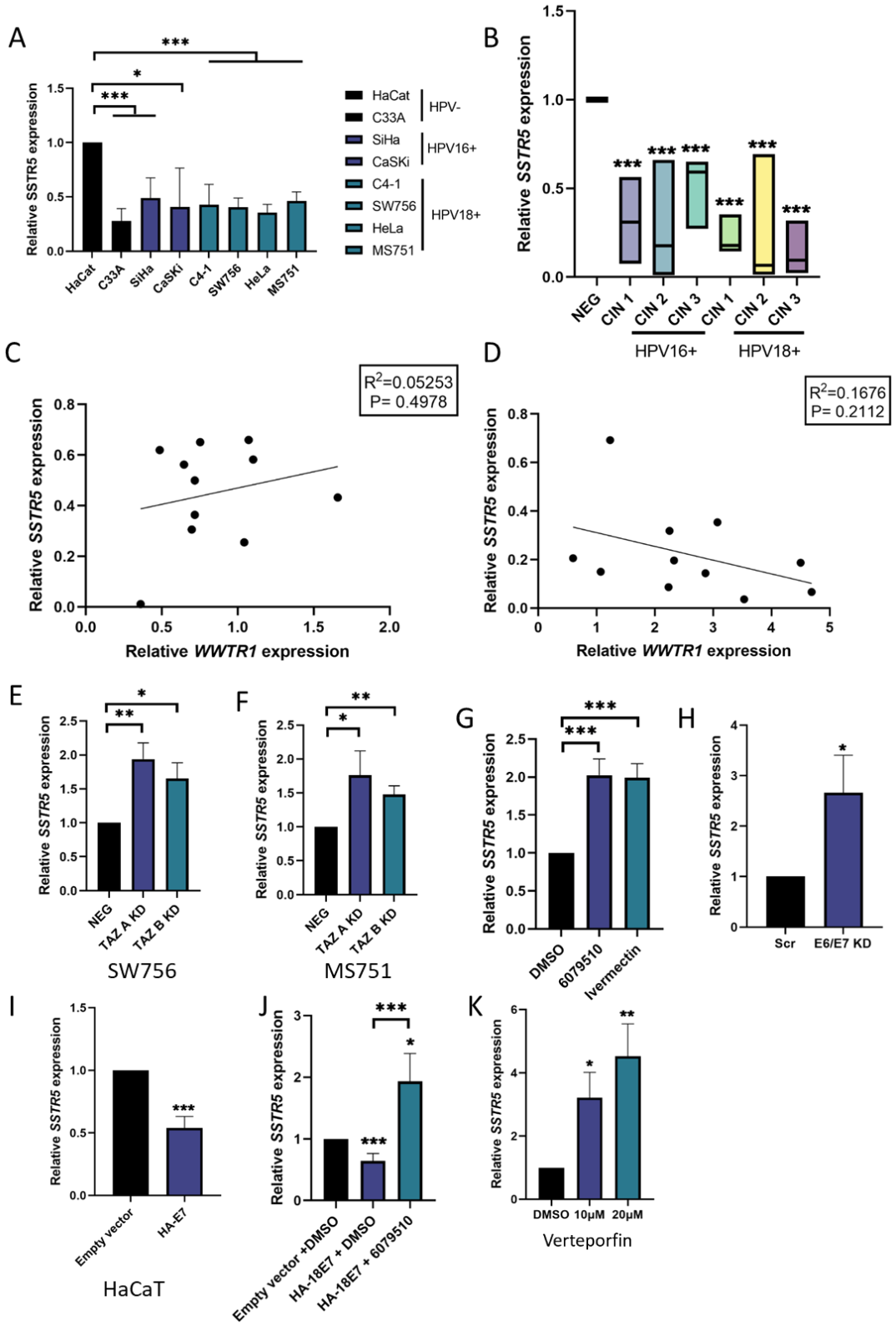

Figure 6.9 SSTR5 is a TAZ-dependent gene A) qRT-PCR analysis of *SSTR5* mRNA expression in HPV-, HPV16+ or HPV18+ cell lines. U6 transcript levels were used as a loading control. **B)** qRT-PCR analysis of *SSTR5* expression in negative, HPV16 or HPV18+ patient cervix liquid

cytology samples from different CIN grades (n=4 from each grade). U6 was used as a loading control. **C)** Graph showing correlation between *SSTR5* and *WWTR1* expression in HPV16+ patient samples from **B**. **D)** Graph showing correlation between *SSTR5* and *WWTR1* expression in HPV18+ patient samples from **B**. **E)** qRT-PCR analysis of *SSTR5* mRNA expression in polyclonal shRNA-mediated TAZ knockdown SW756 cells. U6 was used as a loading control. **F)** qRT-PCR analysis of *SSTR5* mRNA expression in polyclonal shRNA-mediated TAZ knockdown MS751 cells. U6 was used as a loading control. **G)** qRT-PCR analysis of *SSTR5* expression in HeLa cells following either DMSO, 6079510 (16 hours) or Ivermectin (24 hours) treatment. . U6 was used as a loading control. **H)** qRT-PCR analysis of *SSTR5* expression in HeLa cells with E6/E7 targeting siRNA (for 72 hours). *U6* was used as a loading control. **I)** qRT-PCR analysis of *SSTR5* expression in HaCaT cells stably expressing HA-HPV18 E7. *U6* was used as a loading control. **J)** qRT-PCR analysis of *SSTR5* expression in C33A cells stably expressing HA-HPV18 E7 with or without 6079510 treatment (16 hours). *U6* was used as a loading control. **K)** qRT-PCR analysis of *SSTR5* expression in HeLa cells following either DMSO or verteporfin (24 hours) treatment. . U6 was used as a loading control.

6.2.6 SSTR5 is a tumour suppressor in HPV18+ cervical cancer cells and TAZ-mediated proliferation is partially dependent on SSTR5 repression

SSTR5 encodes Somatostatin receptor type 5 (SSTR5) (sometimes referred to in literature as SST5). SSTR5 is part of a small group of G protein couple receptors called SSTs which is further split into Somatostatin 1 and 2 (SRIF1 and SRIF2) based on octreotide (SRIF analogue) with SSTR5 being a SRIF1 member (289).

Although data is limited, it has been reported that SSTR5 acts as a tumour suppressor in laryngeal squamous cell carcinoma, therefore it was proposed that *SSTR5* acts as a tumour suppressor in HPV18+ cervical cancer cells (281). Investigations revealed that FLAG-SSTR5 overexpression in HeLa cells (Figure 6.10 A) led to a significant decrease in growth over a 5 day period (Figure 6.10 B). Furthermore, there was also a significant decrease in both anchorage-dependent and independent colony forming ability (Figure 6.10 C-D). This suggested that SSTR5 was tumour suppressive in cervical cancer cells but it was important to then determine if the repression of *SSTR5* was important for TAZ-mediated proliferation. 6079510 treated HeLa cells were treated with shRNA targeting *SSTR5* (qRT-PCR was used to confirm shRNA treatment reversed the increase in *SSTR5* following 6079510 treatment (Figure 6.11 A)) to determine the role of SSTR5 in TAZ-mediated proliferation. Repression of *SSTR5* in 6079510 treated HeLa cells led to a partial recovery in growth and both anchorage-dependent and independent colony forming ability (Figure 6.11 B-D). This suggested repression of SSTR5 is a necessary step for promotion of proliferation by TAZ. Together these results show SSTR5 have novel tumour suppressive activity in HPV18+ cervical cancer cell and repression is key for TAZ-mediated proliferation.

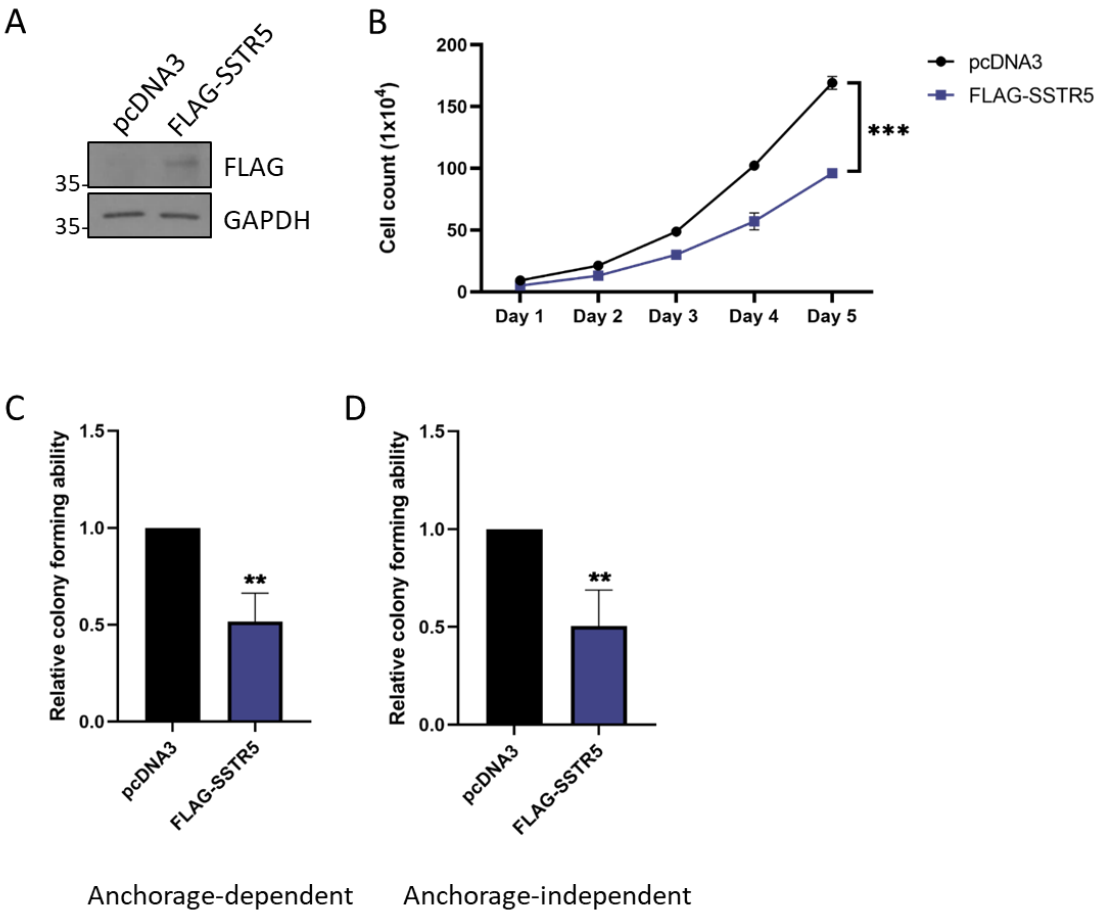

Figure 6.10 SSTR5 is a novel tumour suppressor in HPV18+ cervical cancer cells A) Representative western blot of HeLa cells transfected with FLAG-SSTR5 (48 hours). Cell lysates were probed for FLAG. GAPDH was used as a loading control. **B)** Growth curve analysis of HeLa cells transfected with FLAG-SSTR5 (48 hours). **C)** Colony formation assay (analysis anchorage dependent growth) of HeLa cells transfected with FLAG-SSTR5 (48 hours). **D)** Soft agar assay (analysis anchorage-independent growth) in HeLa cells transfected with FLAG-SSTR5 (48 hours).

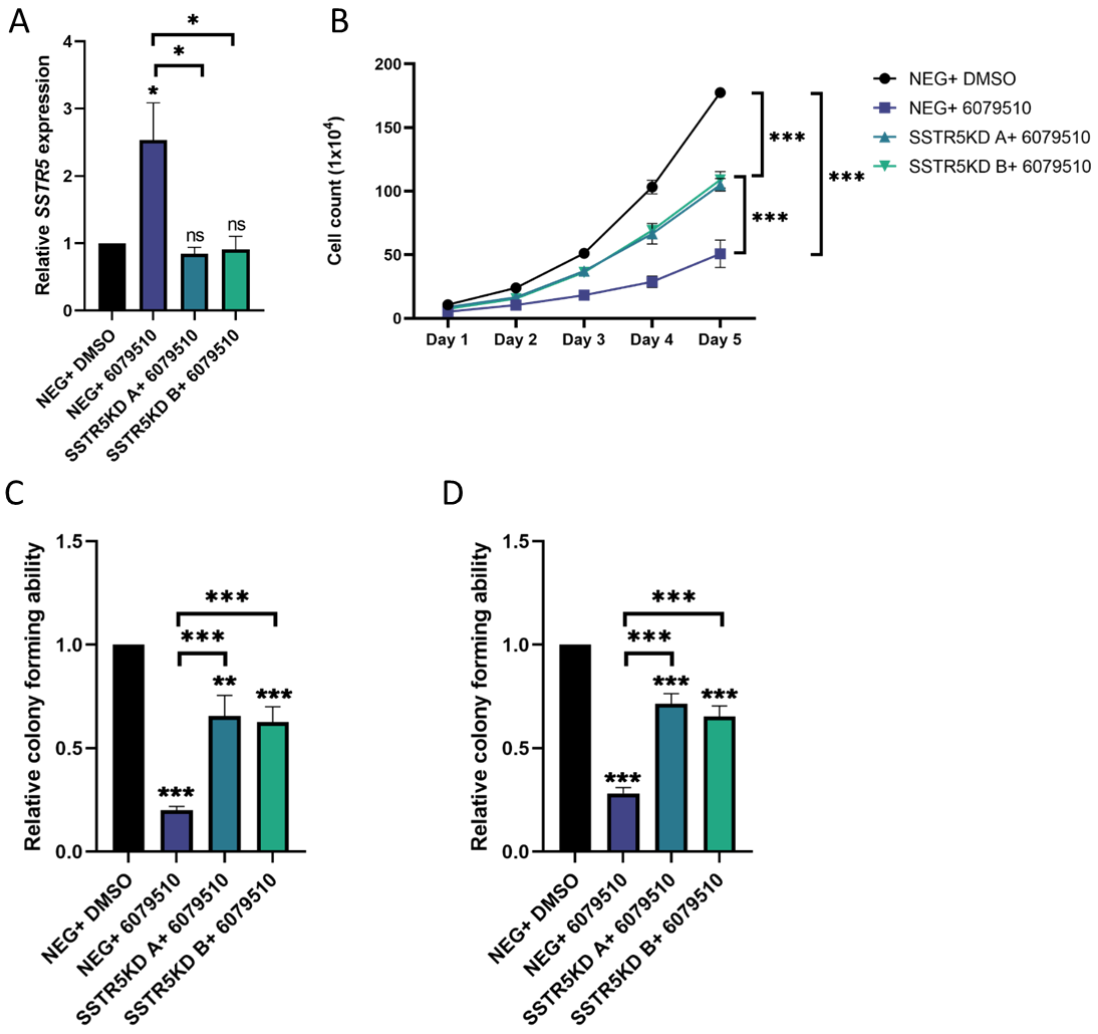

Figure 6.11 SSTR5 repression plays a key role in TAZ-mediated proliferation A) qRT-PCR analysis of *SSTR5* expression of HeLa cells treated with 6079510 (16 hours) with or without stable expression of SSTR5-targeting shRNAs (polyclonal). Cell lysates were probed for FLAG. GAPDH was used as a loading control. **B)** Growth curve analysis of HeLa cells treated with 6079510 (16 hours) with or without stable expression of SSTR5-targeting shRNAs (polyclonal). **C)** Colony formation assay (analysis anchorage dependent growth) of HeLa cells treated with 6079510 (16 hours) with or without stable expression of SSTR5-targeting shRNAs (polyclonal). **D)** Soft agar assay (analysis anchorage-independent growth) in HeLa cells treated with 6079510 (16 hours) with or without stable expression of SSTR5-targeting shRNAs (polyclonal).

6.2.7 *IFIT2* is repressed by TAZ in HPV18+ cervical cancer

Despite *IFIT2* being suggested as a YAP and TAZ dependent gene, qRT-PCR data suggested while knockdown of YAP and TAZ led to an increase in *IFIT2* expression, knockdown of TAZ had a much more profound effect. Therefore, it was further investigated if *IFIT2* was a TAZ-dependent gene in HPV18+ cervical cancer.

Firstly, analysis of *IFIT2* mRNA expression in the panel of cervical cancer cell lines revealed significant reduction in *IFIT2* in all HPV+ cell lines tested. Additionally, *IFIT2* expression was also significantly decreased in HPV- cervical cancer cell line C33A compared to HaCaT cell (Figure 6.12 A). Similar to the cell lines, *IFIT2* expression was reduced in both HPV16+ and HPV18+ samples in CIN 1-3 (Figure 6.12 B). When the expression of *IFIT2* was compared to *WWTR1* expression in the patient samples, it was found that expression was only inversely correlated in HPV18+ patient samples while no correlation was seen in HPV16+ patient samples (Figure 6.12 C-D). Taken together these data suggest that while *IFIT2* is repressed by TAZ in HPV18+ cervical cancer, there is likely another method of regulation in HPV16+ cervical cancer.

To confirm that *IFIT2* repression TAZ-dependency was not a HeLa specific phenotype, *IFIT2* expression was investigated following TAZ knockdown in other HPV18+ cell lines. TAZ knockdown in both SW756 cells and MS751 cells led to a significant increase in *IFIT2* expression (Figure 6.12 E and F). 6079510 and Ivermectin treated HeLa cells showed significantly reduced IFIT2 expression, confirming the reduction is IFIT2 was not an off-target effect of shRNA treatment. Interestingly, a more profound effect was observed upon inhibition of both YAP and TAZ (figure 6.12 G).

It was hypothesised that if *IFIT2* was TAZ-dependent, expression should be affected by HPV18 E7 expression. Depletion of HPV18 E6 and E7 in HeLa cells utilising *E6/E7* targeting siRNA led to a significant increase in *IFIT2* expression (Figure 6.12 H). Conversely, stable expression of HPV18 E7 in HaCaT cells led to a significant decrease

in *IFIT2* expression (Figure 6.12 I). The effect of HPV18 E7 was determined to be due to TAZ as C33A cells stably expressing HPV18 E7 were treated with 6079510 showed a reversal in IFIT2 suppression (Figure 6.12 J). This highlighted that HPV18E7 suppresses IFIT2 expression in a TAZ-dependent manner. Finally it was investigated if TAZ-mediate IFIT2 expression was TEAD dependent. qRT-PCR analysis of HeLa cells showed verteporfin treatment led to no significant change in IFIT2 expression suggesting TAZ regulates IFIT2 in a TEAD-independent manner (Figure 6.12 K).

Taken together these results demonstrate IFIT2 is repressed by TAZ in HPV18+ cervical cancer but in a TEAD-independent manner.

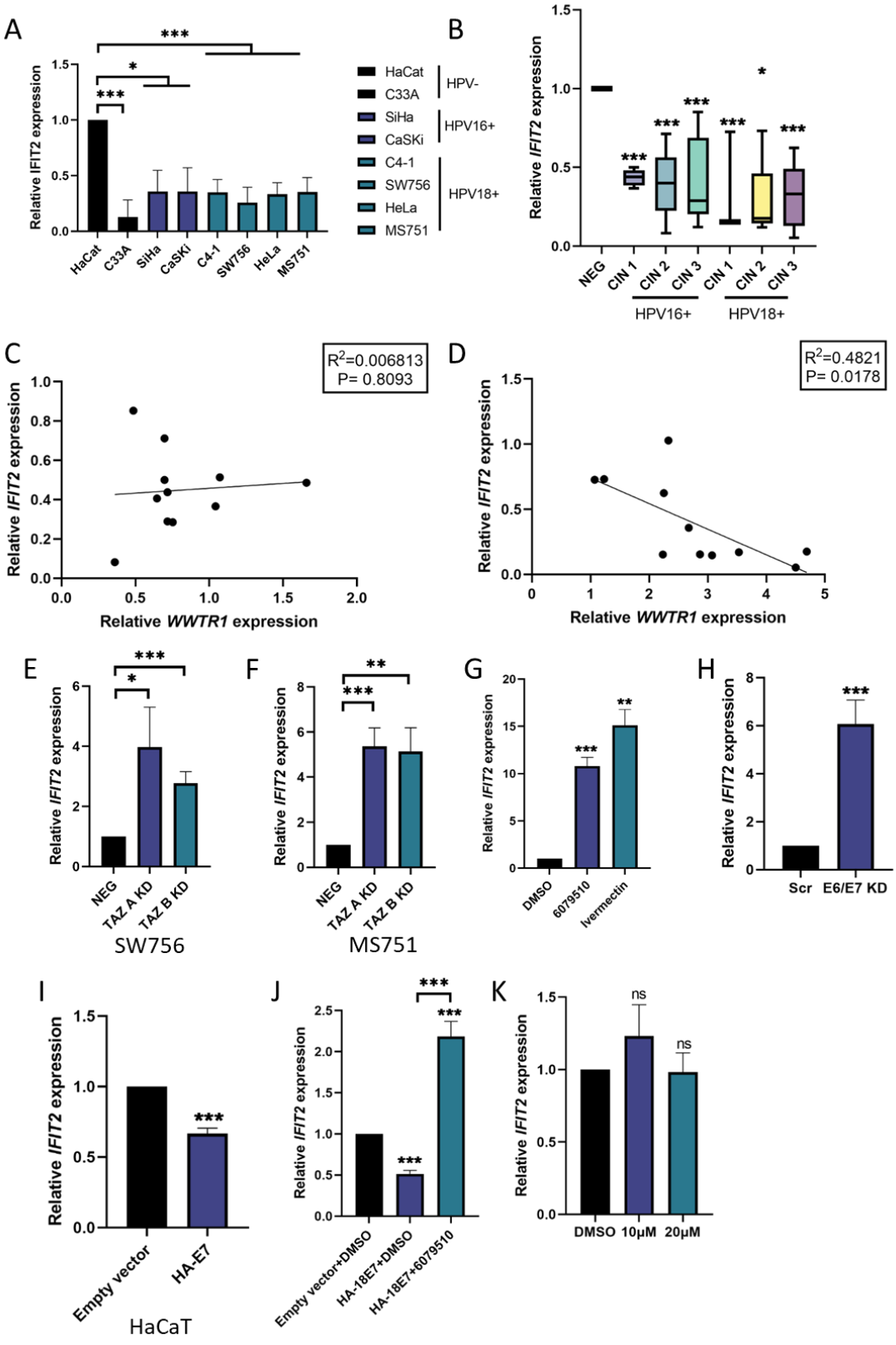

Figure 6.12 IFIT2 is a TAZ-dependent gene A) qRT-PCR analysis of *IFIT2* mRNA expression in HPV-, HPV16+ or HPV18+ cell lines. U6 transcript levels were used as a loading control. **B)**

qRT-PCR analysis of *IFIT2* expression in negative, HPV16 or HPV18+ patient cervix liquid cytology samples from different CIN grades (n=4 from each grade). U6 was used as a loading control. **C)** Graph showing correlation between *IFIT2*and *WWTR1* expression in HPV16+ patient samples from **B**. **D)** Graph showing correlation between *IFIT2* and *WWTR1* expression in HPV18+ patient samples from **B**. **E)** qRT-PCR analysis of *IFIT2* mRNA expression in polyclonal shRNA-mediated TAZ knockdown SW756 cells. U6 was used as a loading control. **F)** qRT-PCR analysis of *IFIT2* mRNA expression in polyclonal shRNA-mediated TAZ knockdown MS751 cells. U6 was used as a loading control. **G)** qRT-PCR analysis of *IFIT2* expression in HeLa cells following either DMSO, 6079510 (16 hours) or Ivermectin (24 hours) treatment. . U6 was used as a loading control. **H)** qRT-PCR analysis of *IFIT2* expression in HeLa cells with E6/E7 targeting siRNA (for 72 hours). *U6* was used as a loading control. **I)** qRT-PCR analysis of *IFIT2* expression in HaCaT cells stably expressing HA-HPV18 E7. *U6* was used as a loading control. **J)** qRT-PCR analysis of *IFIT2* expression in C33A cells stably expressing HA-HPV18 E7 with or without 6079510 treatment (16 hours). *U6* was used as a loading control. **K)** qRT-PCR analysis of *IFIT2* expression in HeLa cells following either DMSO or verteporfin (24 hours) treatment. . U6 was used as a loading control.

6.2.8 IFIT2 is tumour suppressive in HPV18+ cervical cancer cells and repression in crucial for TAZ-mediated proliferation

IFIT2 encodes for the protein IFIT2, a member of the Interferon-induced protein with tetratricopeptide repeats family (IFIT). Unlike, the other potential TAZ-dependent genes investigated in this chapter, the role of IFIT2 in cancer is slightly more elucidated. In gastric cancer, decreased IFIT2 expression was associated with poor prognosis and increase cell survival (290). Other studies have shown increased IFIT2 expression inhibits cancer cell proliferation and migration. Additionally, inhibition of IFIT2 degradation led to its aggregation in the cell centrosome, inducing apoptosis (291, 292). HPV E1 inhibits *IFIT2* expression, likely to dysregulated the immune response but the role IFIT2 in cervical cancer is unknown (293). Given the results showed TAZ repressed IFIT2 expression, it was hypothesised that IFIT2 was tumour suppressive in cervical cancer and is repressed by TAZ.

FLAG-IFIT2 overexpression in HeLa cells led to significant decrease in growth and colony forming ability in anchorage dependent or independent manners, indicating IFIT2 is tumour suppressive in HeLa cells (Figure 6.13 A-D). Next, it was investigated if IFIT2 played a role in TAZ-mediate proliferation. To do this, 6079510-treated HeLa cells were treated with an *IFIT2*-targeting shRNA (qRT-PCR was used to show successful repression of *IFIT2* usually seen to be increased following TAZ inhibition (Figure 6.14 A)) and growth was assessed over a 5 day period. IFIT2 suppression following 6079510 treatment led to a partial recovery of growth compared to 6079510 treatment alone (Figure 6.14 B). Similar effects were seen on both anchorage-dependent and independent colony forming ability (Figure 6.14 C and D) suggesting repression of *IFIT2* is needed for TAZ-mediated proliferation. Taken together these results demonstrate IFIT2 has novel tumour suppressive functions in HPV18+ cervical cancer and repression is crucial for TAZ-mediated proliferation.

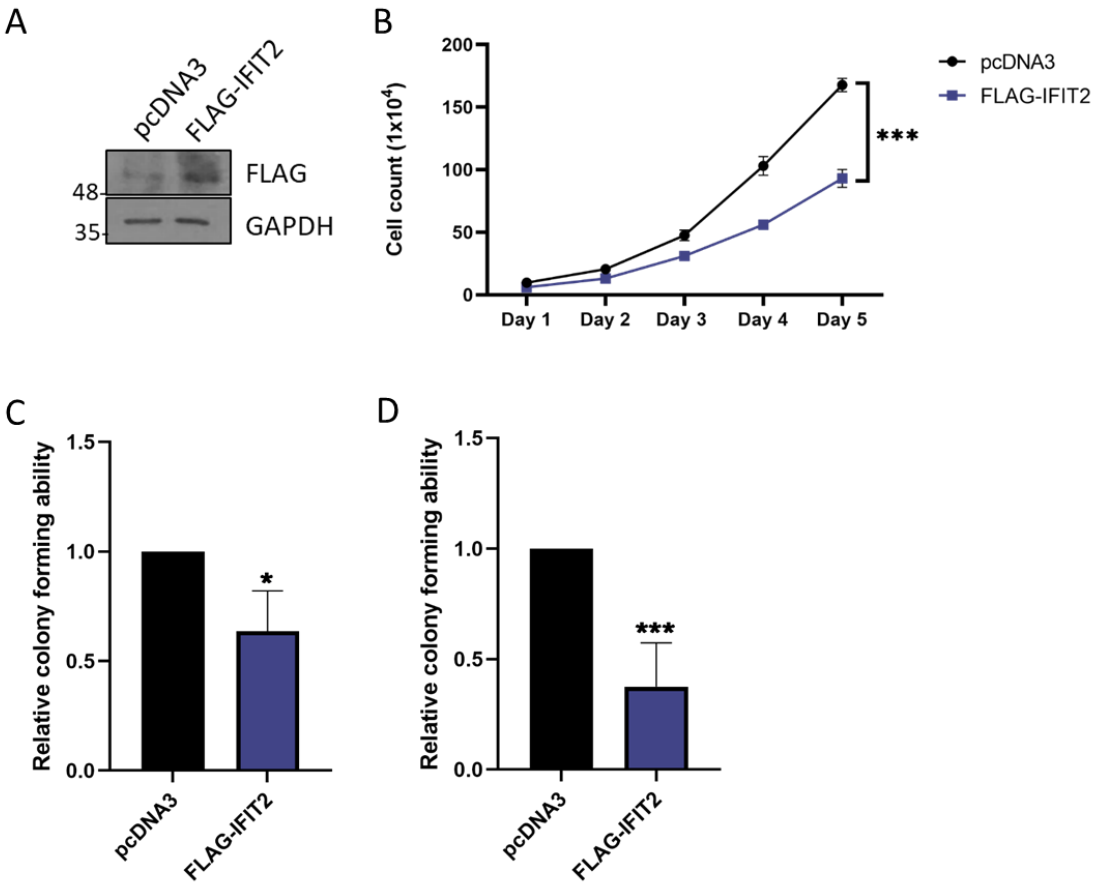

Figure 6.13 IFIT2 is a novel tumour suppressor in HPV18+ cervical cancer cells A) Representative western blot of HeLa cells transfected with FLAG-IFIT2 (48 hours). Cell lysates were probed for FLAG. GAPDH was used as a loading control. **B)** Growth curve analysis of HeLa cells transfected with FLAG- IFIT2 (48 hours). **C)** Colony formation assay (analysis anchorage dependent growth) of HeLa cells transfected with FLAG- IFIT2 (48 hours). **D)** Soft agar assay (analysis anchorage-independent growth) in HeLa cells transfected with FLAG- IFIT2 (48 hours).

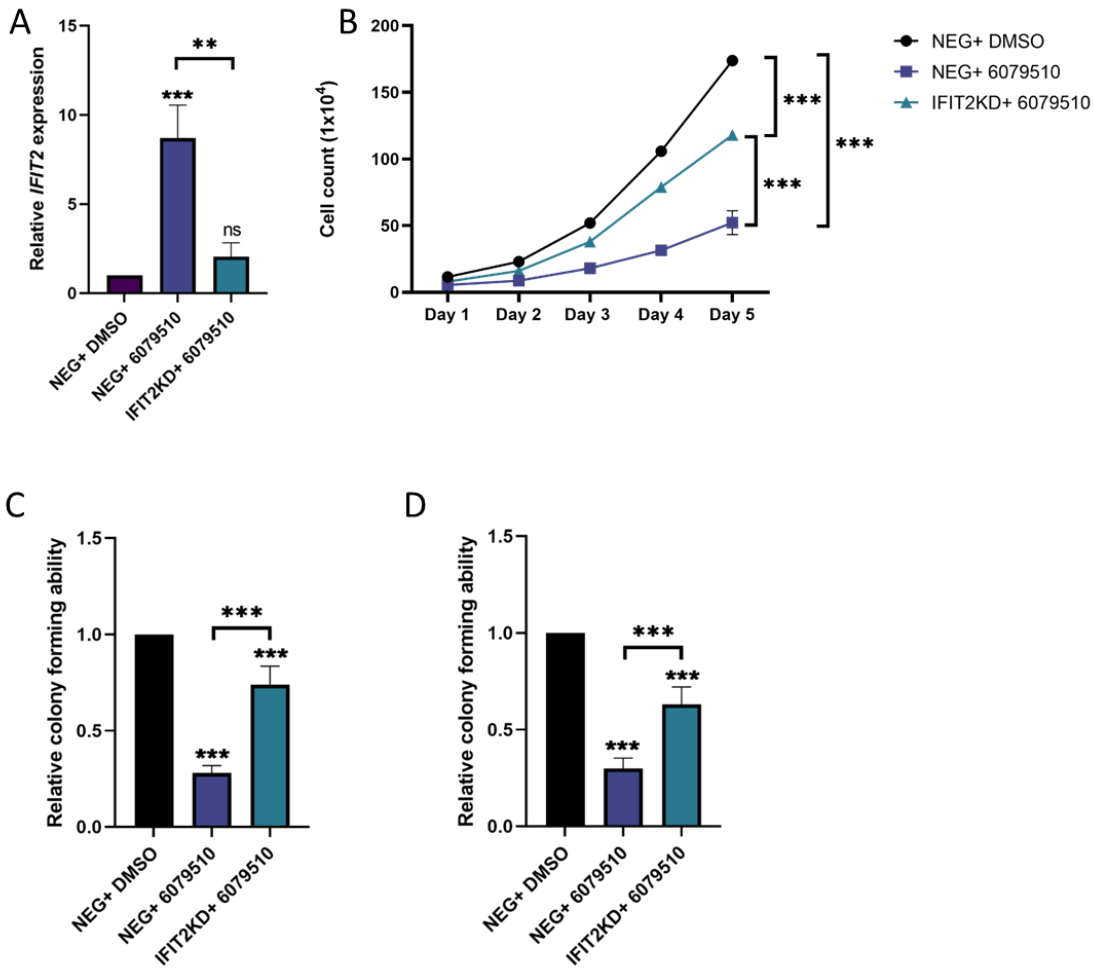

Figure 6.14 IFIT2 repression plays a key role in TAZ-mediated proliferation A) qRT-PCR analysis of *IFIT2* expression of HeLa cells treated with 6079510 (16 hours) with or without stable expression of IFIT2-targeting shRNAs (polyclonal). Cell lysates were probed for FLAG. GAPDH was used as a loading control. **B)** Growth curve analysis of HeLa cells treated with 6079510 (16 hours) with or without stable expression of IFIT2-targeting shRNAs (polyclonal). **C)** Colony formation assay (analysis anchorage dependent growth) of HeLa cells treated with 6079510 (16 hours) with or without stable expression of IFIT2-targeting shRNAs (polyclonal). **D)** Soft agar assay (analysis anchorage-independent growth) in HeLa cells treated with 6079510 (16 hours) with or without stable expression of IFIT2-targeting shRNAs (polyclonal).

6.2.9 SSTR5 and IFIT2 are regulated by YAP in HPV16+ cervical cancer cell and are tumour suppressive

Both *SSTR5* and *IFIT2* expression was significantly reduced in HPV16+ cervical cancer cell lines, which have low TAZ expression (Figure 6.9 A and Figure 6.12 A). Additionally, there was only an inverse correlation with *WWTR1* expression in HPV18+ patient samples (Figure 6.9 C-D and Figure 6.12 C-D). Therefore, it was proposed *SSTR5* and *IFIT2* expression was regulated by other factors such as YAP in HPV16+ cervical cancer cells while *TOGARAM2* expression was solely regulated by TAZ.

TAZ and YAP overexpression in SiHa cells revealed *TOGARAM2* only increased with TAZ and not YAP overexpression, as expected for a TAZ-dependent gene but YAP, but not TAZ overexpression led to a significant reduction in *SSTR5* and *IFIT2* (Figure 6.15 A-C). Therefore, this suggested that while SSTR5 and IFIT2 were TAZ dependent in HPV18+ cervical cancer cells, both are repressed by YAP in HPV16+ cells.

It was then investigated if SSTR5 was tumour suppressive in HPV16+ cells. When growth was assessed over 5 days, SSTR5 overexpression led to a significant reduction in growth and further investigations there was also a significant reduction in both anchorage dependent and independent colony forming ability (Figure 6.16 A-D). This indicates that SSTR5 is a novel tumour suppressor in HPV16+ cervical cancer.

IFIT2 was also revealed to suppress proliferation in SiHa cells. Overexpression of FLAG-IFIT2 in SiHa led to a significant reduction in growth and both anchorage dependent and independent colony formation (Figure 6.16 E- H) suggesting IFIT2 plays a novel tumour suppressive role in these cells. Together this shows both SSTR5 and IFIT2 are tumour suppressive in HPV16+ cells and are likely regulated by YAP in these cells not TAZ.

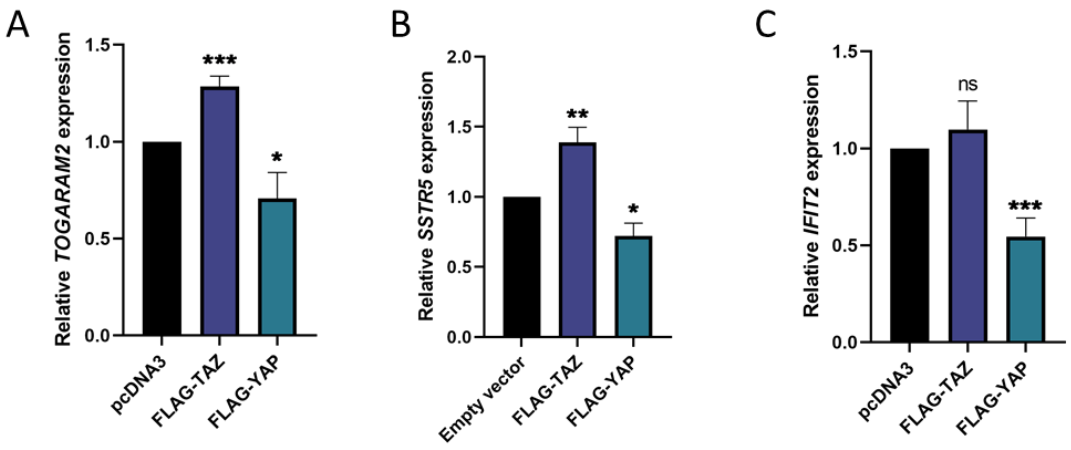

Figure 6.15 SSTR5 and IFIT2 are YAP-dependent genes in HPV16+ cells A) qRT-PCR analysis of *TOGARAM2* expression in SiHa cells transfected with either FLAG-TAZ or FLAG-YAP. U6 was used as a loading control. **B)** qRT-PCR analysis of *SSTR5* expression in SiHa cells transfected with either FLAG-TAZ or FLAG-YAP. U6 was used as a loading control. **C)** qRT-PCR analysis of *IFIT2* expression in SiHa cells transfected with either FLAG-TAZ or FLAG-YAP. U6 was used as a loading control.

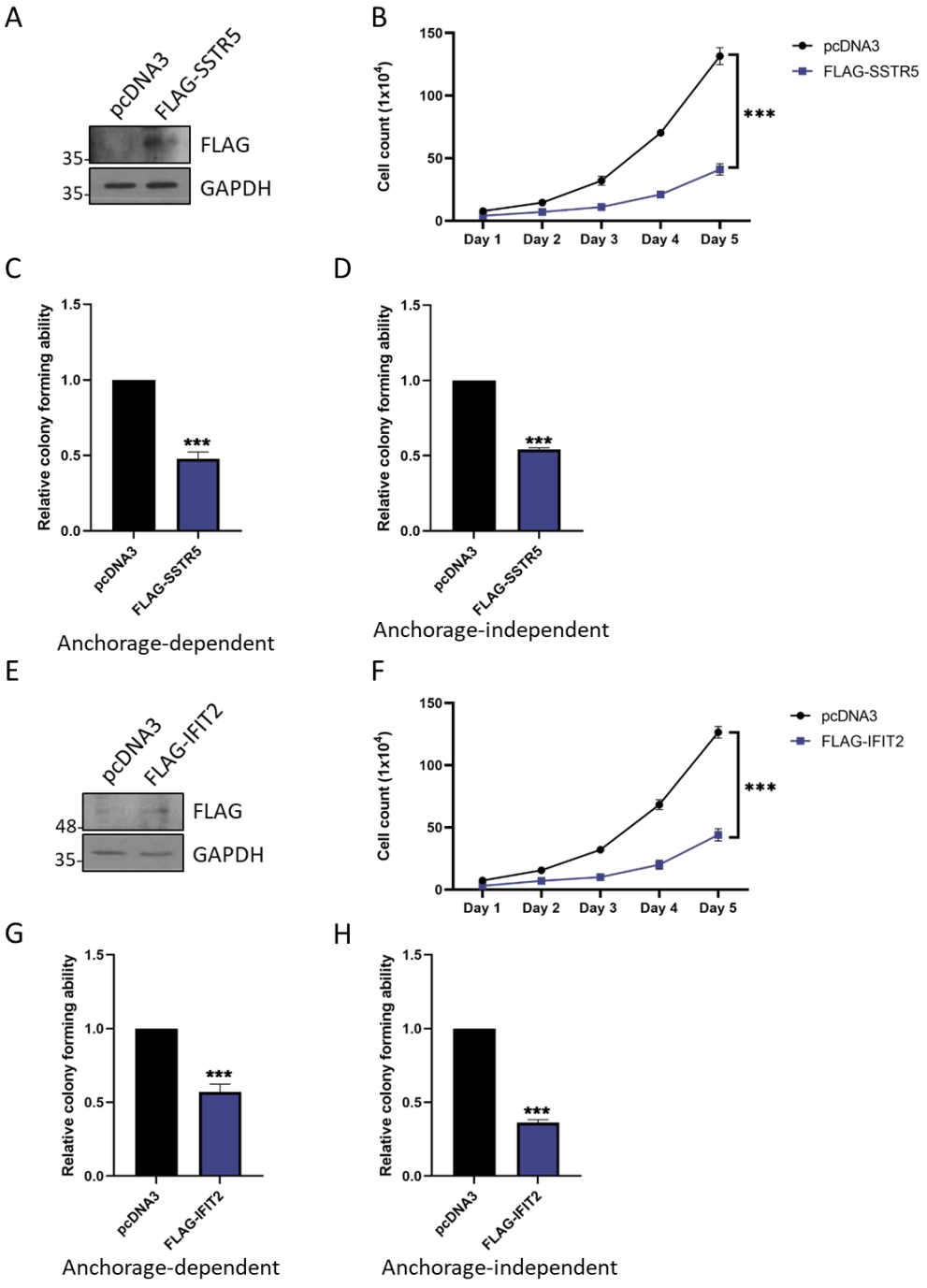

Figure 6.16 SSTR5 and IFIT2 are tumour suppressive in SiHa cells A) Representative western blot of SiHa cells transfected with FLAG-SSTR5 (48 hours). Cell lysates were probed for FLAG. GAPDH was used as a loading control. **B)** Growth curve analysis of SiHa cells transfected with FLAG- SSTR5 (48 hours). **C)** Colony formation assay (analysis anchorage dependent growth) of SiHa cells transfected with FLAG- SSTR5 (48 hours). **D)** Soft agar assay (analysis anchorage-independent growth) in SiHa cells transfected with FLAG- SSTR5 (48 hours). **E)** Representative

western blot of SiHa cells transfected with FLAG-IFIT2 (48 hours). Cell lysates were probed for FLAG. GAPDH was used as a loading control. **F)** Growth curve analysis of SiHa cells transfected with FLAG- IFIT2 (48 hours). **G)** Colony formation assay (analysis anchorage dependent growth) of SiHa cells transfected with FLAG- IFIT2 (48 hours). **H)** Soft agar assay (analysis anchorage-independent growth) in SiHa cells transfected with FLAG- IFIT2 (48 hours).

6.2.10 TAZ phase separation is critical for transcription of TAZ-dependent TOGARAM2 expression

One question that arose from the differences in TAZ and YAP transcriptional profiles was how was TAZ promoting transcription in a YAP-independent manner? When YAP and TAZ were observed with immunofluorescence microscopy, clear differences in nuclear distribution was observed. Whereas YAP expression was diffuse across the nucleus, TAZ was seen to form puncta (Figure 6.17 A). TAZ is known in other cancers to form liquid-liquid phase separation (LLPS) condensates in the nucleus which are enriched with transcription factors to promote transcription (182). Therefore, it was hypothesised that TAZ could be promoting TAZ-specific transcription through these puncta. To confirm that TAZ was able to form these puncta in HeLa cells, FLAG-tagged TAZ and YAP were transfected into HeLa cells at concentrations that would enable low-level expression and imaged by immunofluorescence microscopy. Analysis of these images showed that low levels of TAZ overexpression, but not YAP overexpression, led to puncta formation in HeLa cells (Figure 6.17 B).

To confirm that the puncta formed by TAZ where acting like LLPS condensates, low levels of FLAG-TAZ were expressed into HeLa cells and liquid-liquid phase interactions were disrupted by 1,6-Hexanediol treatment. Immunofluorescence microscopy revealed treatment led to a complete loss of the TAZ puncta seen in the non-treated cells. Additionally, these puncta were very quickly recovered when the drug was removed, highlighting the dynamic nature of liquid-liquid phase interactions (Figure 6.18). The same pattern was also seen when endogenous TAZ was stained for and imaged with immunofluorescence microscopy. Again, 6-Hexanediol treatment led to a disruption of TAZ puncta which were very quickly recovered with removal of the drug and were also protected if cells were fixed with paraformaldehyde (PFA) before treatment (Figure 6.19).

The interaction between TAZ and paraspeckle protein NONO has been shown to be essential for TAZ LLPS activity (182). Therefore it was investigated if NONO was required for transcription of TAZ-dependent genes in cervical cancer cells. Firstly, NONO expression was knocked down in HeLa cells through stable expression of 2 different NONO-targeting shRNAs (confirmed by qRT-PCR (Figure 6.20 A)). As it was theorised NONO was important for the formation of TAZ-puncta, TAZ nuclear localisation was analysed through immunofluorescence microscopy. Imaging showed NONO knockdown led to a significant loss of nuclear TAZ and therefore TAZ puncta (Figure 6.20 B). Furthermore, qRT-PCR analysis showed NONO knockdown led to a significant decrease in *TOGARAM2* expression (Figure 6.20 C). Taken together, these results show TAZ forms puncta with LLPS condensate properties that may be important for regulation of TAZ-specific transcription.

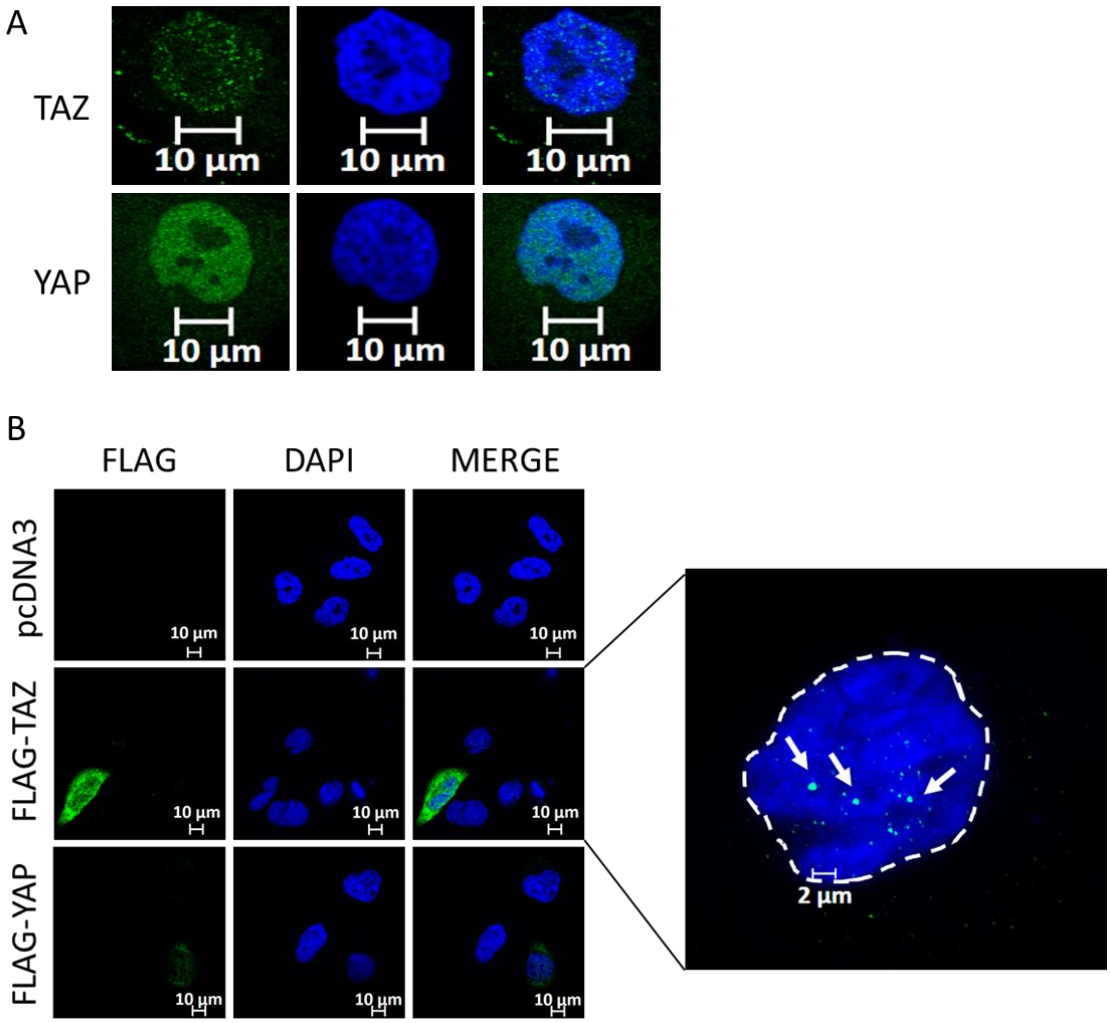

Figure 6.17 TAZ forms puncta in HPV18+ cervical cancer cells A) Immunofluorescence analysis of endogenous TAZ or YAP (green) nuclear localisation. Nuclei were visualised using DAPI. Scale bare 10 µm. **B)** Immunofluorescence analysis of HeLa cells transfected with either FLAG-TAZ or FLAG-YAP. Coverslips were stained for FLAG (green). Nuclei were visualised using DAPI. Scale bare 10 µm.

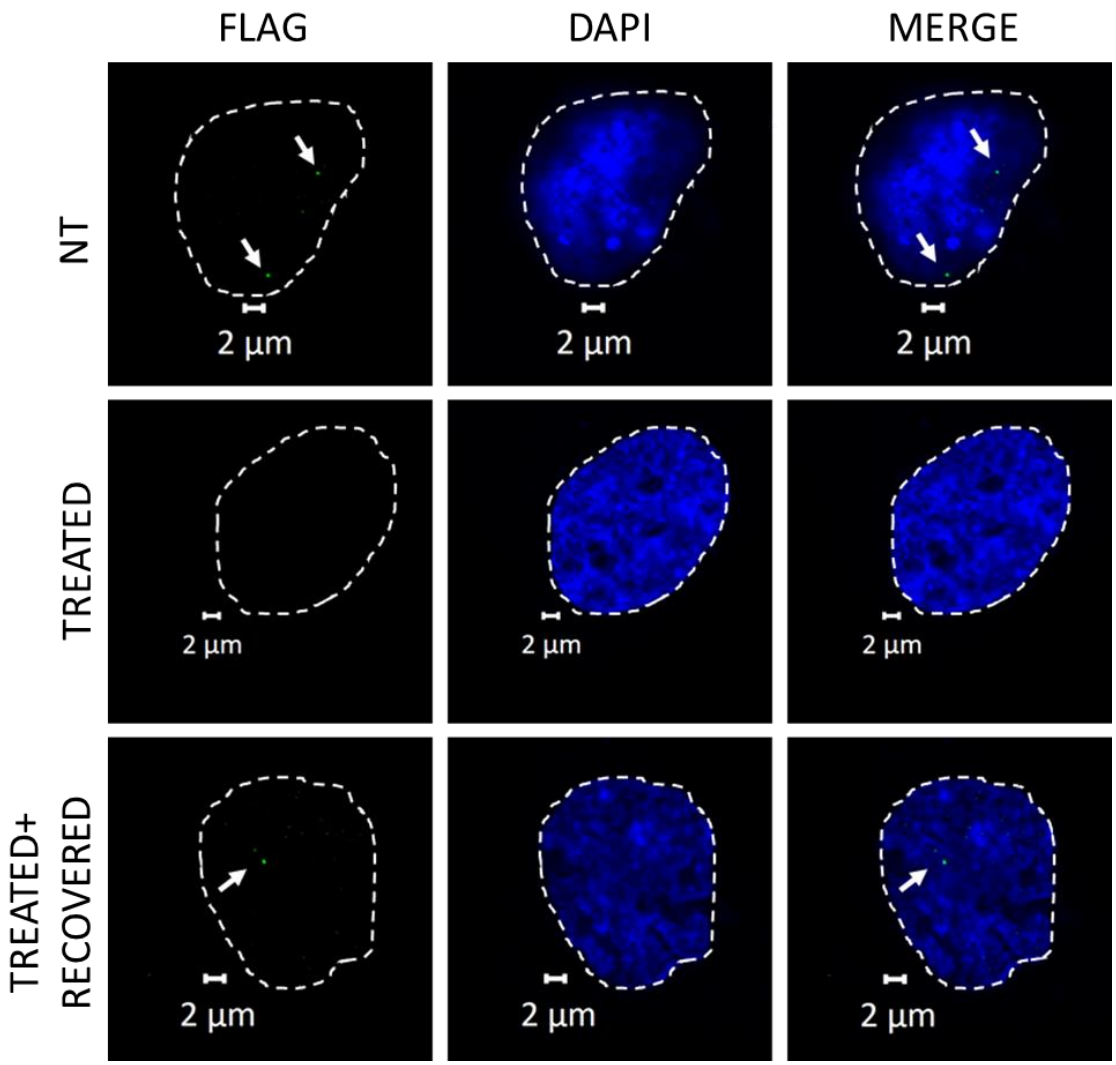

Figure 6.18 Disruption of liquid-liquid interactions prevents exogenous TAZ puncta formation. Immunofluorescence analysis of HeLa cells transfected with low levels of FLAG-TAZ before either 6-Hexanediol treatment or treatment then 30 minutes recovery. Coverslips were stained for FLAG (green). Nuclei were visualised using DAPI. Scale bare 1 µm.

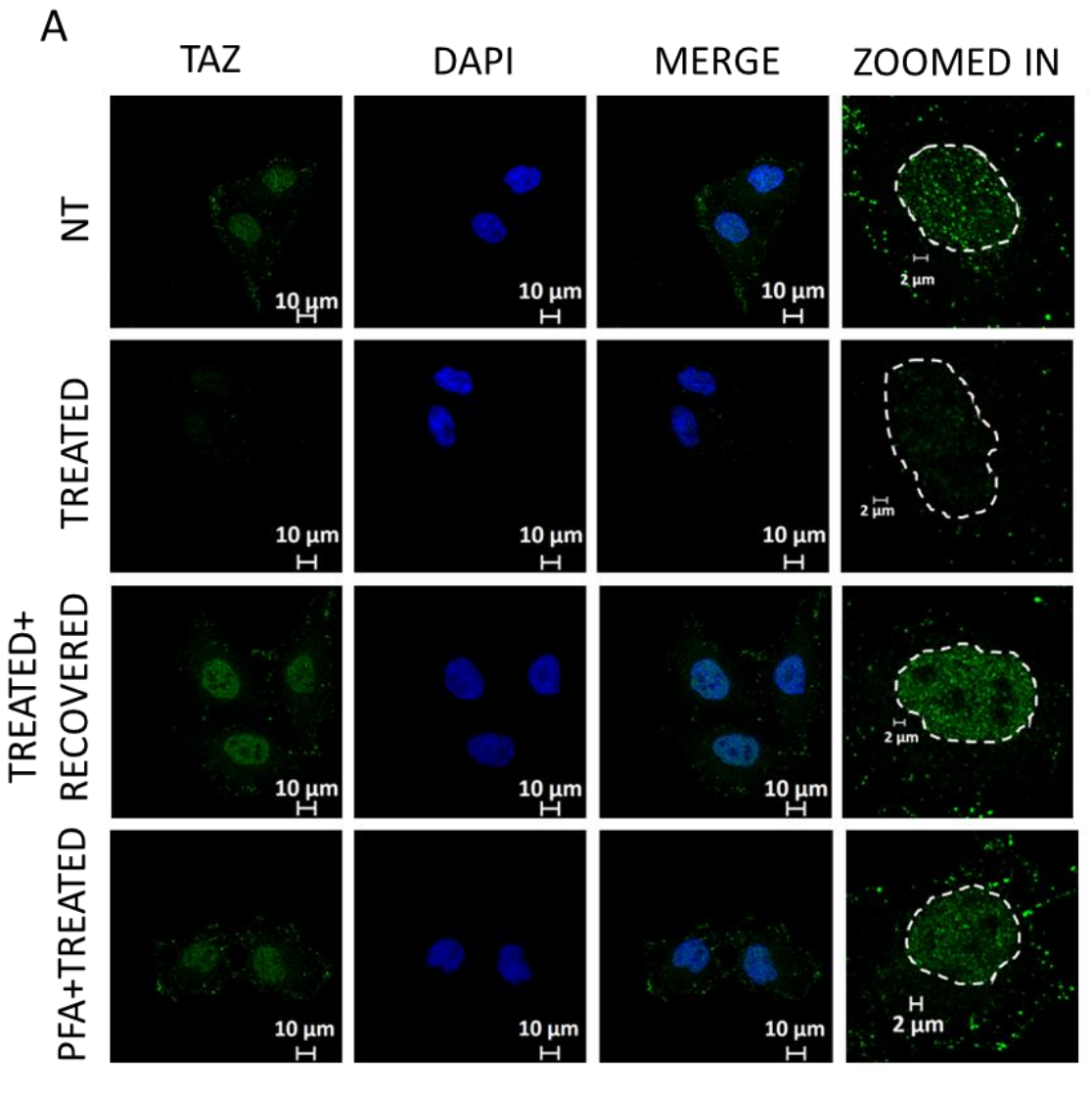

Figure 6.19 Disruption of liquid-liquid interactions prevents endogenous TAZ puncta formation. Immunofluorescence analysis of HeLa cells before either 6-Hexanediol treatment, treatment then 30 minutes recovery or PFA fixation and then treatment. Coverslips were stained for TAZ (green). Nuclei were visualised using DAPI. Scale bare 2 µm.

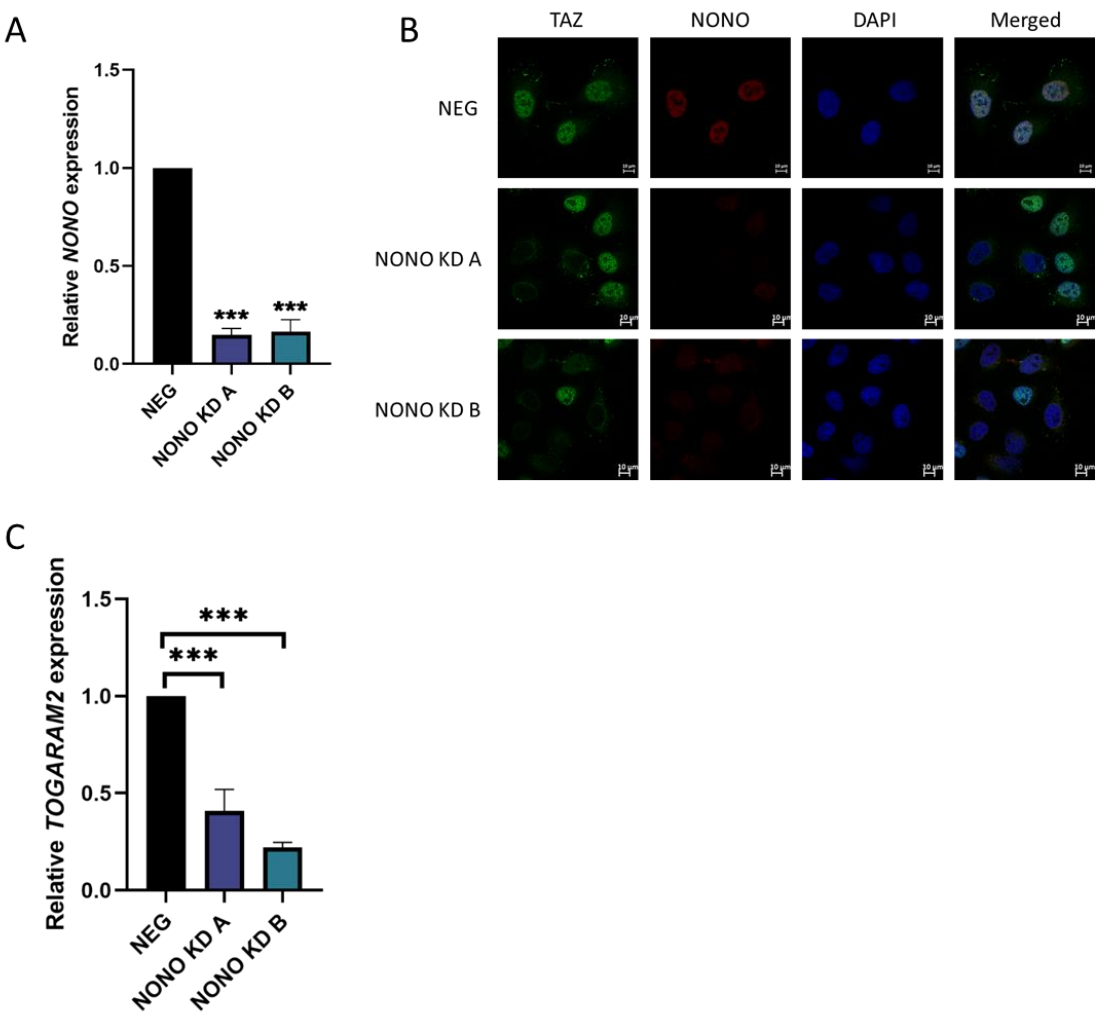

Figure 6.20 NONO knockdown inhibits TAZ nuclear localisation and TOGARAM2 expression A) qRT-PCR analysis of *NONO* mRNA expression in polyclonal shRNA-mediated NONO knockdown HeLa cells. U6 was used as a loading control. **B)** Immunofluorescence analysis of polyclonal shRNA-mediated NONO knockdown HeLa cells. Coverslips were stained for TAZ (green). Nuclei were visualised using DAPI. Scale bare 10 µm. **C)** qRT-PCR analysis of *TOGARAM2* mRNA expression in polyclonal shRNA-mediated NONO knockdown HeLa cells.

6.3 Discussion

This chapter aimed to elucidate novel TAZ-dependent genes and the role they play in cervical cancer. As qRT-PCR analysis of YAP-dependent genes showed TAZ did not promote their expression, this indicated TAZ promoted a transcriptome distinct to that of YAP. The differences in transcriptomes was unveiled using RNA-sequencing. Analysis revealed multiple TAZ-specific genes which were either promoted or repressed by TAZ. Interestingly, TAZ knockdown led to increased expression of a larger number of genes than were suppressed, indicating that in cervical cancer TAZ may play a larger role in repressing mRNA expression than promoting it. This could be due to TAZ forming inhibitory complexes with transcription factors such as TEAD. It is also possible that TAZ is promoting the expression of miRNAs that normally target these genes for degradation. This possibility could be easily investigated through use of miRNA-sequencing.

YAP and TAZ transcriptional repression is a poorly investigated area, however mechanistically, it is known that YAP and TAZ alongside TEAD bind to the Nucleosome Remodeling and Deacetylase (NuRD) complex to deacetylate histones and alters nucleosome occupancy leading to reduced recruitment of RNA Pol II (294). *SSTR5* and *IFIT2* were both repressed by TAZ, and so could be tested for repression by NuRD. However, intriguingly, the results show that IFIT2 repression was not TEAD-dependent, and the literature suggests that TEAD is required to recruit NuRD to TAZ-repressed promoters. Therefore, this offers the exciting possibility that TAZ may be repressing targets such as *IFIT2* through another mechanism. Additionally, lncSSTR5-AS1 is a major mechanism for SSTR5 repression observed in cancer and therefore, further investigations should be carried out first to decide if TAZ is repressing SSTR5 in a post-translational manner. To investigate if TAZ forms these repression complexes, more TAZ-specific upregulated genes that are TEAD dependent should be identified.

This chapter identifies *TOGARAM2* as not only a novel TAZ-dependent gene but also as a novel oncogene, specifically in HPV18+ cervical cancer. Interestingly,

TOGARAM2 inhibited proliferation in HPV16+ cervical cancer but the exact mechanism of its tumour suppressive activities remain elusive. TOGARAM2 is part of a family of proteins expressed in human cells including; TOGARAM1, chTOG and CLASP1 and further investigations could be undertaken to investigate if one of these relatives plays an important role in HPV16+ cells in place of TOGARAM2.

This chapter focuses specifically on cervical cancer but other cancers such as lung squamous cell carcinoma and breast cancer in particular have high TAZ expression. It is possible that *TOGARAM2* is a TAZ-dependent oncogene in other high-TAZ cancers and further studies should be undertaken to investigate this possibility. Furthermore, the results propose TOGARAM2 as a novel regulator of EMT, particularly a regulator of filopodia formation. Future studies should investigate the mechanism for how this occurs in more mechanistic detail. Other TOG domain containing proteins have microtubule binding abilities and it is hypothesised that this is essential for the control of filopodia by TOGARAM2. Mutating the TOG domains may help elucidate this. Interestingly, TOGARAM2 encodes fewer TOG domains than its related proteins, instead containing an extended disordered. Why TOGARAM2 requires fewer TOG domains and the function of this disordered region remains to be determined. One approach would be to undertake quantitative mass spectrometry approaches to determine the interactome of TOGARAM2 in cervical cancer cells.

This chapter briefly investigates the mechanism of TOGARAM2 regulation by TAZ and results show paraspeckle protein NONO and LLPS are involved. It is hypothesised that TAZ forms “puncta” in the nucleus of cells which contain NONO and transcription factors to promote transcription of TAZ-specific genes. This would explain how only TAZ promotes *TOGARAM2* expression and not YAP despite being TEAD-dependent. These puncta do not act as normal paraspeckles despite needing NONO, being small and too numerous in nature in cells, but likely hijack the protein for this function. It is hypothesised that TAZ uses NONO to interact with different transcription

factors or enhancers that TAZ cannot canonically interact with through direct interactions. This would lead to the transcription of TAZ-specific genes. To investigate this, proteomic analysis of TAZ-NONO interactors could be carried out.

SSTR5 was another gene determined to be a novel TAZ-dependent gene. Furthermore, results in this study demonstrate SSTR5 plays a novel tumour suppressive role in cervical cancer. Unlike TOGARAM2, SSTR5 functions similarly in both HPV16+ and HPV18+ cells, and therefore the function of SSTR5 should be investigated in other HPV16+ cancers such as oral and anal carcinoma. Although clearly regulated by TAZ in a TEAD-dependent manner in HPV18+ cervical cancer cells, SSTR5 is potentially regulated by YAP in HPV16+ cells. Although the role of SSTR5 in cancer is poorly elucidated, in normal physiology, SSTR5 agonists have been linked inhibition of phospholipase C activity, though the mechanism of how this occurs is unclear (295). The role of phospholipase C is controversial in cancer, but there is evidence that activity is oncogenic and therefore this may explain the tumour suppressive activity of SSTR5. Future studies should aim to explore this connection further to elucidate the function of SSTR5.

This chapter also demonstrates that *IFIT2* is a TAZ-dependent gene in HPV18+ cervical cancer. Similar to SSTR5, IFIT2 was found to be tumour suppressive in both HPV16+ and HPV18+ cervical cancer cells with preliminary evidence suggesting it to be YAP-dependent in HPV16+ cells. Therefore, the investigations into IFIT2 functions could be expanded to include other predominantly HPV16+ cancer such as oral carcinoma. Interestingly, IFIT2 was found to be TEAD-independent and therefore the question of how IFIT2 expression is repressed remains. Although not investigated in this present study, as IFIT2 plays roles in EMT, drug resistance and apoptosis, the effect of IFIT2 on these areas should be investigated in cervical cancer (296).

This chapter focuses on three TAZ-specific genes suggested by RNA-seq analysis but there were many other genes identified in the study. None of these analysed fully rescued the loss of proliferation seen with TAZ knockdown, supporting the hypothesis that TAZ acts through multiple genes. Gene ontology analysis of upregulated TAZ-specific genes reveals TAZ plays role in areas other than chemoresistance and apoptosis which are commonly reported. The group with the highest number of dysregulated genes is wound healing, agreeing with results from the previous chapter suggesting TAZ plays a key role in the regulation of it and EMT. Several other interesting areas appear in the gene ontology analysis including epithelia differentiation. As this function in particular is very important in HPV lifecycle and cancer, these TAZ-specific genes should be the focus of future studies.

Chapter 7- Final Discussion and Summary

The work presented in this thesis provides a mechanism for the decreased Hippo pathway activation observed in cervical cancer, via the down-regulation of the STK4 protein and represents the most detailed study of TAZ function in cervical cancer to date.

HPV requires the manipulation of host signalling pathways for its replication. In cancers, this leads to aberrant activation or targeting of such pathways including IL-6 - STAT3 and MAPK signal transduction, resulting in the promotion of cancerous phenotypes such as increased proliferation. Although past studies have highlighted YAP as an important oncogene in cervical cancer, it was not fully understood how the Hippo signalling pathway was targeted. This study characterises a mechanism for targeting of *STK4* by miR-18a, preventing activation of the Hippo pathway and therefore allowing YAP to remain nuclear. However, this study only touches on the possible function of miR-18a in cervical cancer, with our data hinting at a broader range of targets. Furthermore, although only the mature form of miR-18a was found to be increased, perhaps through changes in processing, the exact mechanism behind this increase remains unknown. This is of importance as it is possible other members of the miR17-92 cluster, which are also oncomiRs, are regulated in a similar manner. Identifying other targets of the cluster could unveil novel tumour suppressors and therefore novel therapeutic targets for the treatment of cervical cancer. To elucidate miR-18a regulation, firstly the role of DNMT1 activity should be confirmed. Previously identified miR-17-92 cluster regulatory factors such as SRSF3 should be priorities in follow-up investigations (297).

The majority of this study focuses on the role of the oncogene TAZ in cervical cancer (Summarised in Figure 7.1). Previous studies are contradictory and despite detailed characterisation of its paralog YAP, the role of TAZ remained elusive. For the first time, this study shows TAZ is an oncogene only in HPV18+ cervical cancer where its expression is increased at the mRNA level. We saw that TAZ was not stabilised a

protein level as has been previously reported with YAP in HPV+ cell lines. Two different mechanisms have been reported for the stabilisation of YAP; degradation of PTPN14 (a YAP inhibitor) induced by E7 and then binding of YAP by E6. It would be interesting to confirm why TAZ isn't stabilised by investigating if these interactions are YAP-specific. Using an orthogonal approach with target knockdown, use of small molecule inhibitors and overexpression of mutant forms of targets, we identify that the host EGFR/SP1 signalling pathway is responsible for increasing TAZ expression in cervical cancer and that this is controlled by the HPV18 E7 oncoprotein. Fascinatingly, this mechanism of regulation was restricted to TAZ, as YAP expression was unaffected by loss of the signalling pathway. This highlights that despite similarities in protein sequence, the YAP and TAZ promoters are likely under the control of different transcription factors. In this study we suggest that the TAZ promoter is under the control of SP1, with two binding sites predicted. Although the exact binding sites of SP1 in the TAZ promoter were confirmed with a mutation study of the promoter, they should be further validated with ChIP.

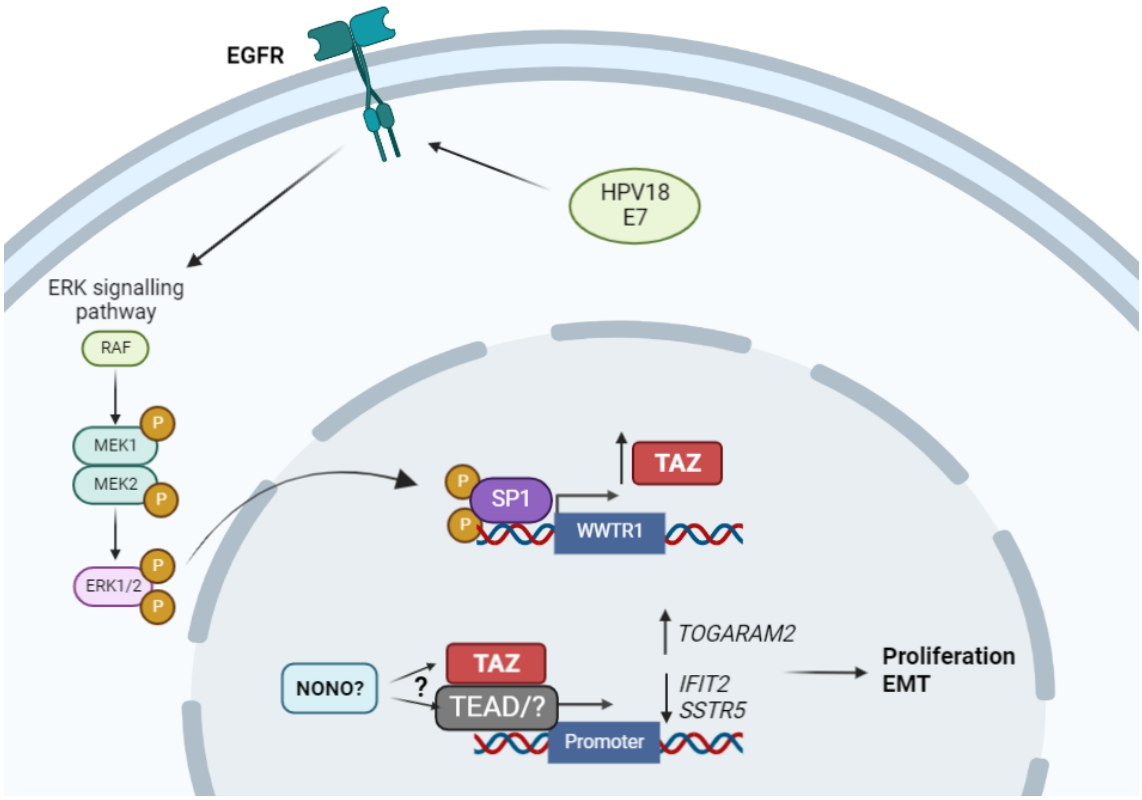

Figure 7.1- Summary of TAZ regulation and activity in HPV18+ cervical cancer. HPV18 E7 activates TAZ promoter activity through EGFR/ER/SP1 signalling. TAZ then upregulates *TOGARAM2* through NONO and TEAD and suppresses *IFIT2* and *SSTR5* expression (created in biorender).

Currently it is unclear why YAP and TAZ are seemingly regulated by two different mechanisms. One possibility is that TAZ is hard to stabilise on a protein level. Multiple studies report the dynamic nature of the protein, and therefore numerous cell factors control its stability whereas YAP appears more stable, in this instance dysregulating the upstream signalling pathway controlling its proteasomal degradation appears to have a major effect. Additionally, perhaps the difference in YAP and TAZ regulation stems from where their activity is necessary. As YAP seemingly plays a more essential role in HPV infection and the initiation of cervical cancer, TAZ may be critical for the development of cancer, particular in adenocarcinoma, a predominantly HPV18+ cancer. Clarifying the role of TAZ in squamous compared to adenocarcinoma is a priority as adenocarcinomas have a higher mortality rate and a poorer response to treatment.

Although we show in this study that HPV18 E7 controls TAZ expression through an EGFR/SP1 axis, it is unclear why HPV16 cannot perform the same role. HPV16 E7 promotes SP1 activity to increase expression of lncMALAT1 so it is unclear why this does not happen with *WWTR1* (298). Perhaps other factors play an unknown role in this. ChIP-sequencing could be used to get insight into the differences in SP1 activity between HPV16+ and HPV18+ cells.

Functionally, we demonstrated that TAZ has oncogenic activity only in HPV18+ cervical cancer, with the interesting observation that TAZ overexpression actually reduced proliferation in HPV16+ cervical cancer cells. The reasons for this are unclear. The simplest explanation, is that TAZ competes with YAP for transcription factors such as TEAD, as frequently we observed that shRNA-mediated knockdown of one paralogue led to increased expression of the other. Additionally, it could be due to TAZ-dependent genes playing tumour suppressive roles in HPV16+ but not in HPV18+ cells. We suggest

this is the case for *TOGARAM2*, which displayed tumour suppressive functions in SiHa cells. The reason for this is unclear but as other proteins such as TOGARAM1 could be expressed in SiHa cells and may play a similar role, perhaps TOGARAM2 prevents their correct functions? Further investigation could utilises RNA-seq to compare the YAP and TAZ-mediated transcription between SiHa and HeLa cells.

Perhaps the key finding of this study was identifying that TAZ had YAP-independent functions in cervical cancer, contradicting many historical studies which present TAZ as redundant. This was demonstrated by overexpressing YAP in TAZ knockdown cells and observing that this had minimal impact on cell proliferation. Importantly this emphasises that studies of YAP alone are unlikely to reveal the full extent of Hippo pathway function in cancer. However, the question arose, if TAZ was working independently of YAP, how was it functioning?

We attempted to address this question with RNA-seq analysis of TAZ- and YAP-driven transcriptomes. Although the sequencing identified several TAZ-specific genes, 3 were chosen for more intensive studies; *TOGARAM2*, *SSTR5* and *IFIT2*. Even though the full scope of functions of these genes was not elucidated here, we did identify all three genes were involved in TAZ-mediated proliferation, with TOGARAM2 upregulation playing a pro-proliferative role while conversely SSTR5 and IFIT2 needed repressing. In particular, it was revealed that *TOGARAM2* displays characteristics of a novel oncogene and is the crucial mediator of TAZ-induced EMT. There is the potential for exciting future studies on TOGARAM2 to fully explore its functions in normal healthy cells and in cancer. For example, TOGARAM1, the closest paralog of TOGARAM2, regulates cilia formation (284). Highly proliferative cells such as HeLa cells have a high number of cilia but their role in tumourigenesis is still controversial. Further studies of TOGARAM2 should not only include investigation into if TOGARAM2 is a regulator of ciliogenesis but if cilia are anti or pro-proliferative factors or potential biomarkers. With the novelty of TOGARAM2,

its function could also be explored in further cancer types, particularly those with high levels of TAZ expression.

The study into *SSTR5* was not as in-depth as *TOGARAM2* but has great potential. SSTR5 has been implicated in regulation of signalling such as the Notch and mTOR pathway (299, 300). Although not fully understood, SSTR5 activation leads to a decrease in Notch signalling through suppressing expression of Notch pathway receptors and ligands, leading to a decrease in NICD (299). Even though full function of Notch signalling in cervical cancer is controversial, negative regulators are often found to be repressed and this may be the case for SSTR5 (301). This should be an avenue of investigation when looking to elucidate the function of SSTR5 in cervical cancer. SSTR5 control of signalling pathways could be further investigated by utilising Qiagen RT² Profiler PCR Arrays, a tool to screen various signalling pathways relevant to cancer. With many current therapeutics targeting host kinases, exploring how SSTR5 modulates these pathways could be a potential target for future therapeutics. *IFIT2*, the third TAZ-dependent gene investigated in this study, is also known to modulate the PKC signalling pathway, so it should be investigated if this is needed for IFIT2 function in cervical cancer. Furthermore, as depletion of IFIT2 has also been linked to chemoresistance, a characteristic often associated with TAZ in cancer. It would be interesting to see if IFIT2 is responsible for TAZ-mediated chemoresistance.

The premise of TAZ negatively regulating target genes is not novel, other studies have also shown that TAZ represses more genes than it promotes (182). Interestingly, TAZ-dependent genes seem quite varied, perhaps depending on the cancer tissue. In glioblastoma and HEK293A cells, RNA-seq suggested *CYR61* was TAZ-dependent while our study suggests this to be a YAP-specific gene (182, 183). Meanwhile in breast cancer, a cancer where TAZ is known to play a prominent role, *CCND1* has been suggested as a major downstream effector of TAZ activity, another gene we show to be YAP-dependent. One reason for the differences observed could be that all these

sequencing studies were performed in different tissue types and perhaps TAZ-dependent genes are tissue specific, may be due to the role of YAP in each tissue. This could be investigated by using the same TAZ shRNAs in multiple different tissue types and performing sequencing. Interesting despite this, gene ontology analysis in the same breast cancer study still suggests TAZ plays a similar role to what we propose such as in cell adhesion and EMT (302). Bioinformatics analysis should be undertaken to investigate if therefore TAZ promotes the same cancerous hallmarks but through tissue specific genes.

Another interesting question that arose during the course of this study was, how does TAZ promote a different transcription profile to YAP in a TEAD-dependent manner? One potential answer is YAP and TAZ interact with different enhancers which influences YAP/TEAD or TAZ/TEAD transcription or, it has been proposed that YAP/TEAD may interact with other transcription factors to enhance binding to usually low-affinity promoters. To investigate if this is the case in cervical cancer, proteomics analysis of YAP and TAZ binding partners such be undertaken.

One aspect we focused on to attempt to answer this question was investigating the role of TAZ-NONO interactions. Unlike YAP, TAZ has the ability to interact with NONO and form puncta through LLPS. Our preliminary data shows NONO was essential for *TOGARAM2* transcription but further experiments should investigate if TAZ-mediated NONO transcription is NONO-dependent by investigating if a TAZ mutant unable to bind to NONO can rescue *TOGARAM2* expression in TAZ knock down cells. Furthermore, as the region of TAZ which is necessary for NONO interactions has been characterised, a YAP chimera should be generated (YAP with the region necessary for NONO interaction in TAZ replaced) and the ability of this mutant to induce *TOGARAM2* expression should be assessed.

It was observed in this study that TAZ forms puncta through LLPS in the nuclei of HeLa cells and NONO is crucial for TAZ nuclear localisation. Potentially, TAZ/TEAD could be recruited to specific puncta at the promoters of TAZ-dependent genes through this NONO interaction, perhaps using NONO to interact with other transcription factors, promoting the expression of these genes. This may explain why YAP does not promote the expression of these TAZ dependent genes as it lacks LLPS ability. However, a far more detailed study would be needed to investigate this hypothesis.

Although many of the changes throughout this study can be argued to be small, it is still demonstrated that the increase in TAZ expression by HPV18 E7 is biologically important. Additionally liquid cytology samples supports this as TAZ was seen to be significantly increase in CIN2 and CIN3 HPV18+ samples. However further studies are needed to fully explored the role of TAZ *in vivo*.

In conclusion, TAZ is controlled by HPV18 E7 and plays an essential oncogenic role in cervical cancer, independent to YAP. TAZ promotes a different transcription profile to YAP, controlling the expression of *TOGARAM2*, *SSTR5* and *IFIT2*, all of play roles in TAZ-mediated proliferation.

References

1. Bravo, I.G., de Sanjosé, S. and Gottschling, M. The clinical importance of understanding the evolution of papillomaviruses. *Trends Microbiol.* 2010, **18**(10), pp.432-438.
2. López-Bueno, A., Mavian, C., Labella, A.M., Castro, D., Borrego, J.J., Alcami, A. and Alejo, A. Concurrence of Iridovirus, Polyomavirus, and a Unique Member of a New Group of Fish Papillomaviruses in Lymphocystis Disease-Affected Gilthead Sea Bream. *J Virol.* 2016, **90**(19), pp.8768-8779.
3. Antonsson, A., Forslund, O., Ekberg, H., Sterner, G. and Hansson, B.G. The ubiquity and impressive genomic diversity of human skin papillomaviruses suggest a commensalic nature of these viruses. *J Virol.* 2000, **74**(24), pp.11636-11641.
4. de Villiers, E.M., Fauquet, C., Broker, T.R., Bernard, H.U. and zur Hausen, H. Classification of papillomaviruses. *Virology.* 2004, **324**(1), pp.17-27.
5. Pastrana, D.V., Peretti, A., Welch, N.L., Borgogna, C., Olivero, C., Badolato, R., Notarangelo, L.D., Gariglio, M., FitzGerald, P.C., McIntosh, C.E., Reeves, J., Starrett, G.J., Bliskovsky, V., Velez, D., Brownell, I., Yarchoan, R., Wyvill, K.M., Uldrick, T.S., Maldarelli, F., Lisco, A., Sereti, I., Gonzalez, C.M., Androphy, E.J., McBride, A.A., Van Doorslaer, K., Garcia, F., Dvoretzky, I., Liu, J.S., Han, J., Murphy, P.M., McDermott, D.H. and Buck, C.B. Metagenomic Discovery of 83 New Human Papillomavirus Types in Patients with Immunodeficiency. *mSphere.* 2018, **3**(6), pp.e00645-00618.
6. Ma, Y., Madupu, R., Karaoz, U., Nossa, C.W., Yang, L., Yooseph, S., Yachimski, P.S., Brodie, E.L., Nelson, K.E. and Pei, Z. Human papillomavirus community in healthy persons, defined by metagenomics analysis of human microbiome project shotgun sequencing data sets. *J Virol.* 2014, **88**(9), pp.4786-4797.
7. Van Doorslaer, K., Tan, Q., Xirasagar, S., Bandaru, S., Gopalan, V., Mohamoud, Y., Huyen, Y. and McBride, A.A. The Papillomavirus Episteme: a central resource for papillomavirus sequence data and analysis. *Nucleic acids research.* 2013, **41**(Database issue), pp.D571-D578.
8. Cubie, H.A. Diseases associated with human papillomavirus infection. *Virology.* 2013, **445**(1), pp.21-34.
9. Chen, X.S., Garcea, R.L., Goldberg, I., Casini, G. and Harrison, S.C. Structure of small virus-like particles assembled from the L1 protein of human papillomavirus 16. *Mol Cell.* 2000, **5**(3), pp.557-567.
10. Goetschius, D.J., Hartmann, S.R., Subramanian, S., Bator, C.M., Christensen, N.D. and Hafenstein, S.L. High resolution cryo EM analysis of HPV16 identifies minor structural protein L2 and describes capsid flexibility. *Scientific Reports.* 2021, **11**(1), p.3498.
11. Scarth, J.A., Patterson, M.R., Morgan, E.L. and Macdonald, A. The human papillomavirus oncoproteins: a review of the host pathways targeted on the road to transformation. 2021, **102**(3).
12. Van Doorslaer, K. Evolution of the papillomaviridae. *Virology.* 2013, **445**(1-2), pp.11-20.
13. Bernard, H.U. Gene expression of genital human papillomaviruses and considerations on potential antiviral approaches. *Antivir Ther.* 2002, **7**(4), pp.219-237.
14. Weng, S.L., Huang, K.Y., Weng, J.T., Hung, F.Y., Chang, T.H. and Lee, T.Y. Genome-wide discovery of viral microRNAs based on phylogenetic analysis and structural evolution of various human papillomavirus subtypes. *Brief Bioinform.* 2018, **19**(6), pp.1102-1114.

15. Grassmann, K., Rapp, B., Maschek, H., Petry, K.U. and Iftner, T. Identification of a differentiation-inducible promoter in the E7 open reading frame of human papillomavirus type 16 (HPV-16) in raft cultures of a new cell line containing high copy numbers of episomal HPV-16 DNA. *J Virol.* 1996, **70**(4), pp.2339-2349.
16. Smotkin, D. and Wettstein, F.O. Transcription of human papillomavirus type 16 early genes in a cervical cancer and a cancer-derived cell line and identification of the E7 protein. *Proc Natl Acad Sci U S A.* 1986, **83**(13), pp.4680-4684.
17. Schneider-Gädicke, A. and Schwarz, E. Different human cervical carcinoma cell lines show similar transcription patterns of human papillomavirus type 18 early genes. *Embo j.* 1986, **5**(9), pp.2285-2292.
18. Karlen, S., Offord, E.A. and Beard, P. Functional promoters in the genome of human papillomavirus type 6b. *J Gen Virol.* 1996, **77 (Pt 1)**, pp.11-16.
19. DiLorenzo, T.P. and Steinberg, B.M. Differential regulation of human papillomavirus type 6 and 11 early promoters in cultured cells derived from laryngeal papillomas. *J Virol.* 1995, **69**(11), pp.6865-6872.
20. Taniguchi, A., Kikuchi, K., Nagata, K. and Yasumoto, S. A cell-type-specific transcription enhancer of type 16 human papillomavirus (HPV 16)-P97 promoter is defined with HPV-associated cellular events in human epithelial cell lines. *Virology.* 1993, **195**(2), pp.500-510.
21. Moody, C.A. and Laimins, L.A. Human papillomavirus oncoproteins: pathways to transformation. *Nat Rev Cancer.* 2010, **10**(8), pp.550-560.
22. Giroglou, T., Florin, L., Schäfer, F., Streeck, R.E. and Sapp, M. Human papillomavirus infection requires cell surface heparan sulfate. *J Virol.* 2001, **75**(3), pp.1565-1570.
23. Selinka, H.-C., Giroglou, T., Nowak, T., Christensen, N.D. and Sapp, M. Further evidence that papillomavirus capsids exist in two distinct conformations. *J Virol.* 2003, **77**(24), pp.12961-12967.
24. Cerqueira, C., Samperio Ventayol, P., Vogeley, C. and Schelhaas, M. Kallikrein-8 Proteolytically Processes Human Papillomaviruses in the Extracellular Space To Facilitate Entry into Host Cells. *J Virol.* 2015, **89**(14), pp.7038-7052.
25. Huang, H.S. and Lambert, P.F. Use of an in vivo animal model for assessing the role of integrin α(6)β(4) and syndecan-1 in early steps in papillomavirus infection. *Virology.* 2012, **433**(2), pp.395-400.
26. Spoden, G., Freitag, K., Husmann, M., Boller, K., Sapp, M., Lambert, C. and Florin, L. Clathrin- and Caveolin-Independent Entry of Human Papillomavirus Type 16—Involvement of Tetraspanin-Enriched Microdomains (TEMs). *PLOS ONE.* 2008, **3**(10), p.e3313.
27. Scheffer, K.D., Gawlitza, A., Spoden, G.A., Zhang, X.A., Lambert, C., Berditchevski, F. and Florin, L. Tetraspanin CD151 mediates papillomavirus type 16 endocytosis. *J Virol.* 2013, **87**(6), pp.3435-3446.
28. Kines, R.C., Thompson, C.D., Lowy, D.R., Schiller, J.T. and Day, P.M. The initial steps leading to papillomavirus infection occur on the basement membrane prior to cell surface binding. *Proc Natl Acad Sci U S A.* 2009, **106**(48), pp.20458-20463.
29. Schelhaas, M., Shah, B., Holzer, M., Blattmann, P., Kühling, L., Day, P.M., Schiller, J.T. and Helenius, A. Entry of human papillomavirus type 16 by actin-dependent, clathrin- and lipid raft-independent endocytosis. *PLoS Pathog.* 2012, **8**(4), p.e1002657.
30. Abban, C.Y. and Meneses, P.I. Usage of heparan sulfate, integrins, and FAK in HPV16 infection. *Virology.* 2010, **403**(1), pp.1-16.
31. Smith, J.L., Campos, S.K., Wandinger-Ness, A. and Ozbun, M.A. Caveolin-1-dependent infectious entry of human papillomavirus type 31 in human

keratinocytes proceeds to the endosomal pathway for pH-dependent uncoating. *J Virol.* 2008, **82**(19), pp.9505-9512.
32. Bienkowska-Haba, M., Williams, C., Kim, S.M., Garcea, R.L. and Sapp, M. Cyclophilins facilitate dissociation of the human papillomavirus type 16 capsid protein L1 from the L2/DNA complex following virus entry. *J Virol.* 2012, **86**(18), pp.9875-9887.
33. Uhlorn, B.L., Jackson, R., Li, S., Bratton, S.M., Van Doorslaer, K. and Campos, S.K. Vesicular trafficking permits evasion of cGAS/STING surveillance during initial human papillomavirus infection. *PLoS Pathog.* 2020, **16**(11), p.e1009028.
34. Baek, J.H., Lee, G., Kim, S.N., Kim, J.M., Kim, M., Chung, S.C. and Min, B.M. Common genes responsible for differentiation and senescence of human mucosal and epidermal keratinocytes. *Int J Mol Med.* 2003, **12**(3), pp.319-325.
35. Cheng, S., Schmidt-Grimminger, D.C., Murant, T., Broker, T.R. and Chow, L.T. Differentiation-dependent up-regulation of the human papillomavirus E7 gene reactivates cellular DNA replication in suprabasal differentiated keratinocytes. *Genes Dev.* 1995, **9**(19), pp.2335-2349.
36. Pyeon, D., Pearce, S.M., Lank, S.M., Ahlquist, P. and Lambert, P.F. Establishment of Human Papillomavirus Infection Requires Cell Cycle Progression. *PLoS Pathog.* 2009, **5**(2), p.e1000318.
37. McBride, A.A. The papillomavirus E2 proteins. *Virology.* 2013, **445**(1-2), pp.57-79.
38. Baedyananda, F., Sasivimolrattana, T., Chaiwongkot, A., Varadarajan, S. and Bhattarakosol, P. Role of HPV16 E1 in cervical carcinogenesis. 2022, **12**.
39. Smith, J.A., Haberstroh, F.S., White, E.A., Livingston, D.M., DeCaprio, J.A. and Howley, P.M. SMCX and components of the TIP60 complex contribute to E2 regulation of the HPV E6/E7 promoter. *Virology.* 2014, **468-470**, pp.311-321.
40. Bergvall, M., Melendy, T. and Archambault, J. The E1 proteins. *Virology.* 2013, **445**(1-2), pp.35-56.
41. Dyson, N., Howley, P.M., Münger, K. and Harlow, E. The human papilloma virus-16 E7 oncoprotein is able to bind to the retinoblastoma gene product. *Science.* 1989, **243**(4893), pp.934-937.
42. Scheffner, M., Huibregtse, J.M., Vierstra, R.D. and Howley, P.M. The HPV-16 E6 and E6-AP complex functions as a ubiquitin-protein ligase in the ubiquitination of p53. *Cell.* 1993, **75**(3), pp.495-505.
43. Doorbar, J. The E4 protein; structure, function and patterns of expression. *Virology.* 2013, **445**(1-2), pp.80-98.
44. Akagi, K., Li, J., Broutian, T.R., Padilla-Nash, H., Xiao, W., Jiang, B., Rocco, J.W., Teknos, T.N., Kumar, B., Wangsa, D., He, D., Ried, T., Symer, D.E. and Gillison, M.L. Genome-wide analysis of HPV integration in human cancers reveals recurrent, focal genomic instability. *Genome Res.* 2014, **24**(2), pp.185-199.
45. Sabeena, S., Bhat, P., Kamath, V. and Arunkumar, G. Possible non-sexual modes of transmission of human papilloma virus. *J Obstet Gynaecol Res.* 2017, **43**(3), pp.429-435.
46. zur Hausen, H. Papillomaviruses and cancer: from basic studies to clinical application. *Nat Rev Cancer.* 2002, **2**(5), pp.342-350.
47. Tainio, K., Athanasiou, A., Tikkinen, K.A.O., Aaltonen, R., Cárdenas, J., Hernándes, Glazer-Livson, S., Jakobsson, M., Joronen, K., Kiviharju, M., Louvanto, K., Oksjoki, S., Tähtinen, R., Virtanen, S., Nieminen, P., Kyrgiou, M. and Kalliala, I. Clinical course of untreated cervical intraepithelial neoplasia grade 2 under active surveillance: systematic review and meta-analysis. 2018, **360**, p.k499.
48. Guan, P., Howell-Jones, R., Li, N., Bruni, L., de Sanjosé, S., Franceschi, S. and Clifford, G.M. Human papillomavirus types in 115,789 HPV-positive women: a

meta-analysis from cervical infection to cancer. *Int J Cancer.* 2012, **131**(10), pp.2349-2359.
49. Orth, G. Host defenses against human papillomaviruses: lessons from epidermodysplasia verruciformis. *Curr Top Microbiol Immunol.* 2008, **321**, pp.59-83.
50. Garbuglia, A.R., Lapa, D., Sias, C., Capobianchi, M.R. and Del Porto, P. The Use of Both Therapeutic and Prophylactic Vaccines in the Therapy of Papillomavirus Disease. *Frontiers in immunology.* 2020, **11**, pp.188-188.
51. Ferlay J, E.M., Lam F, Colombet M, Mery L, Piñeros M, Znaor A, Soerjomataram I, Bray F *Global Cancer Observatory: Cancer Today.* [Online]. [Accessed 22/09/2022].
52. Ferlay, J., Soerjomataram, I., Dikshit, R., Eser, S., Mathers, C., Rebelo, M., Parkin, D.M., Forman, D. and Bray, F. Cancer incidence and mortality worldwide: sources, methods and major patterns in GLOBOCAN 2012. *Int J Cancer.* 2015, **136**(5), pp.E359-386.
53. Bruni, L., Diaz, M., Castellsagué, X., Ferrer, E., Bosch, F.X. and de Sanjosé, S. Cervical human papillomavirus prevalence in 5 continents: meta-analysis of 1 million women with normal cytological findings. *J Infect Dis.* 2010, **202**(12), pp.1789-1799.
54. Hu, K., Wang, W., Liu, X., Meng, Q. and Zhang, F. Comparison of treatment outcomes between squamous cell carcinoma and adenocarcinoma of cervix after definitive radiotherapy or concurrent chemoradiotherapy. *Radiation Oncology.* 2018, **13**(1), p.249.
55. Parkin, D.M. and Bray, F. Chapter 2: The burden of HPV-related cancers. *Vaccine.* 2006, **24 Suppl 3**, pp.S3/11-25.
56. Kobayashi, K., Hisamatsu, K., Suzui, N., Hara, A., Tomita, H. and Miyazaki, T. A Review of HPV-Related Head and Neck Cancer. *J Clin Med.* 2018, **7**(9).
57. Pytynia, K.B., Dahlstrom, K.R. and Sturgis, E.M. Epidemiology of HPV-associated oropharyngeal cancer. *Oral oncology.* 2014, **50**(5), pp.380-386.
58. Bruni, L., Diaz, M., Barrionuevo-Rosas, L., Herrero, R., Bray, F., Bosch, F.X., de Sanjosé, S. and Castellsagué, X. Global estimates of human papillomavirus vaccination coverage by region and income level: a pooled analysis. *Lancet Glob Health.* 2016, **4**(7), pp.e453-463.
59. Bryant, E. The impact of policy and screening on cervical cancer in England. *Br J Nurs.* 2012, **21**(4), pp.S4, s6-10.
60. Santesso, N., Mustafa, R.A., Schünemann, H.J., Arbyn, M., Blumenthal, P.D., Cain, J., Chirenje, M., Denny, L., De Vuyst, H., Eckert, L.O., Forhan, S.E., Franco, E.L., Gage, J.C., Garcia, F., Herrero, R., Jeronimo, J., Lu, E.R., Luciani, S., Quek, S.C., Sankaranarayanan, R., Tsu, V. and Broutet, N. World Health Organization Guidelines for treatment of cervical intraepithelial neoplasia 2-3 and screen-and-treat strategies to prevent cervical cancer. *Int J Gynaecol Obstet.* 2016, **132**(3), pp.252-258.
61. Bobdey, S., Sathwara, J., Jain, A. and Balasubramaniam, G. Burden of cervical cancer and role of screening in India. *Indian J Med Paediatr Oncol.* 2016, **37**(4), pp.278-285.
62. Lind, H., Waldenström, A.C., Dunberger, G., al-Abany, M., Alevronta, E., Johansson, K.A., Olsson, C., Nyberg, T., Wilderäng, U., Steineck, G. and Åvall-Lundqvist, E. Late symptoms in long-term gynaecological cancer survivors after radiation therapy: a population-based cohort study. *British journal of cancer.* 2011, **105**(6), pp.737-745.
63. Šarenac, T. and Mikov, M. Cervical Cancer, Different Treatments and Importance of Bile Acids as Therapeutic Agents in This Disease. *Front Pharmacol.* 2019, **10**, p.484.

64. Yang, D.H., Wildeman, A.G. and Sharom, F.J. Overexpression, purification, and structural analysis of the hydrophobic E5 protein from human papillomavirus type 16. *Protein Expr Purif.* 2003, **30**(1), pp.1-10.
65. Um, S.J., Rhyu, J.W., Kim, E.J., Jeon, K.C., Hwang, E.S. and Park, J.S. Abrogation of IRF-1 response by high-risk HPV E7 protein in vivo. *Cancer Lett.* 2002, **179**(2), pp.205-212.
66. Leptak, C., Ramon y Cajal, S., Kulke, R., Horwitz, B.H., Riese, D.J., 2nd, Dotto, G.P. and DiMaio, D. Tumorigenic transformation of murine keratinocytes by the E5 genes of bovine papillomavirus type 1 and human papillomavirus type 16. *J Virol.* 1991, **65**(12), pp.7078-7083.
67. Pim, D., Collins, M. and Banks, L. Human papillomavirus type 16 E5 gene stimulates the transforming activity of the epidermal growth factor receptor. *Oncogene.* 1992, **7**(1), pp.27-32.
68. Wetherill, L.F., Holmes, K.K., Verow, M., Müller, M., Howell, G., Harris, M., Fishwick, C., Stonehouse, N., Foster, R., Blair, G.E., Griffin, S. and Macdonald, A. High-risk human papillomavirus E5 oncoprotein displays channel-forming activity sensitive to small-molecule inhibitors. *J Virol.* 2012, **86**(9), pp.5341-5351.
69. Genther Williams, S.M., Disbrow, G.L., Schlegel, R., Lee, D., Threadgill, D.W. and Lambert, P.F. Requirement of epidermal growth factor receptor for hyperplasia induced by E5, a high-risk human papillomavirus oncogene. *Cancer Res.* 2005, **65**(15), pp.6534-6542.
70. Kho, E.Y., Wang, H.K., Banerjee, N.S., Broker, T.R. and Chow, L.T. HPV-18 E6 mutants reveal p53 modulation of viral DNA amplification in organotypic cultures. *Proc Natl Acad Sci U S A.* 2013, **110**(19), pp.7542-7549.
71. Sanz, M.A., Madan, V., Carrasco, L. and Nieva, J.L. Interfacial domains in Sindbis virus 6K protein. Detection and functional characterization. *J Biol Chem.* 2003, **278**(3), pp.2051-2057.
72. Griffin, S.D. Plugging the holes in hepatitis C virus antiviral therapy. *Proc Natl Acad Sci U S A.* 2009, **106**(31), pp.12567-12568.
73. Leechanachai, P., Banks, L., Moreau, F. and Matlashewski, G. The E5 gene from human papillomavirus type 16 is an oncogene which enhances growth factor-mediated signal transduction to the nucleus. *Oncogene.* 1992, **7**(1), pp.19-25.
74. Wasson, C.W., Morgan, E.L., Müller, M., Ross, R.L., Hartley, M., Roberts, S. and Macdonald, A. Human papillomavirus type 18 E5 oncogene supports cell cycle progression and impairs epithelial differentiation by modulating growth factor receptor signalling during the virus life cycle. *Oncotarget.* 2017, **8**(61), pp.103581-103600.
75. Kolev, V., Mandinova, A., Guinea-Viniegra, J., Hu, B., Lefort, K., Lambertini, C., Neel, V., Dummer, R., Wagner, E.F. and Dotto, G.P. EGFR signalling as a negative regulator of Notch1 gene transcription and function in proliferating keratinocytes and cancer. *Nat Cell Biol.* 2008, **10**(8), pp.902-911.
76. Rodríguez, M.I., Finbow, M.E. and Alonso, A. Binding of human papillomavirus 16 E5 to the 16 kDa subunit c (proteolipid) of the vacuolar H+-ATPase can be dissociated from the E5-mediated epidermal growth factor receptor overactivation. *Oncogene.* 2000, **19**(33), pp.3727-3732.
77. Suprynowicz, F.A., Krawczyk, E., Hebert, J.D., Sudarshan, S.R., Simic, V., Kamonjoh, C.M. and Schlegel, R. The human papillomavirus type 16 E5 oncoprotein inhibits epidermal growth factor trafficking independently of endosome acidification. *J Virol.* 2010, **84**(20), pp.10619-10629.
78. Basto, D.L., Chaves, C.B.P., Felix, S.P., Amaro-Filho, S.M., Vieira, V.C., Martins, L.F.L., de Carvalho, N.A., Almeida, L.M. and Moreira MÂ, M. The papillomavirus E5 gene does not affect EGFR transcription and overall survival in cervical cancer. *J Med Virol.* 2020, **92**(8), pp.1283-1289.

79. Zhang, B., Srirangam, A., Potter, D.A. and Roman, A. HPV16 E5 protein disrupts the c-Cbl-EGFR interaction and EGFR ubiquitination in human foreskin keratinocytes. *Oncogene.* 2005, **24**(15), pp.2585-2588.
80. Purpura, V., Belleudi, F., Caputo, S. and Torrisi, M.R. HPV16 E5 and KGFR/FGFR2b interplay in differentiating epithelial cells. *Oncotarget.* 2013, **4**(2), pp.192-205.
81. Grose, R., Fantl, V., Werner, S., Chioni, A.-M., Jarosz, M., Rudling, R., Cross, B., Hart, I.R. and Dickson, C. The role of fibroblast growth factor receptor 2b in skin homeostasis and cancer development. *Embo j.* 2007, **26**(5), pp.1268-1278.
82. Oh, J.M., Kim, S.H., Cho, E.A., Song, Y.S., Kim, W.H. and Juhnn, Y.S. Human papillomavirus type 16 E5 protein inhibits hydrogen-peroxide-induced apoptosis by stimulating ubiquitin-proteasome-mediated degradation of Bax in human cervical cancer cells. *Carcinogenesis.* 2010, **31**(3), pp.402-410.
83. Kabsch, K. and Alonso, A. The human papillomavirus type 16 E5 protein impairs TRAIL- and FasL-mediated apoptosis in HaCaT cells by different mechanisms. *J Virol.* 2002, **76**(23), pp.12162-12172.
84. Miura, S., Kawana, K., Schust, D.J., Fujii, T., Yokoyama, T., Iwasawa, Y., Nagamatsu, T., Adachi, K., Tomio, A., Tomio, K., Kojima, S., Yasugi, T., Kozuma, S. and Taketani, Y. CD1d, a sentinel molecule bridging innate and adaptive immunity, is downregulated by the human papillomavirus (HPV) E5 protein: a possible mechanism for immune evasion by HPV. *J Virol.* 2010, **84**(22), pp.11614-11623.
85. Cortese, M.S., Ashrafi, G.H. and Campo, M.S. All 4 di-leucine motifs in the first hydrophobic domain of the E5 oncoprotein of human papillomavirus type 16 are essential for surface MHC class I downregulation activity and E5 endomembrane localization. *Int J Cancer.* 2010, **126**(7), pp.1675-1682.
86. Zhang, B., Li, P., Wang, E., Brahmi, Z., Dunn, K.W., Blum, J.S. and Roman, A. The E5 protein of human papillomavirus type 16 perturbs MHC class II antigen maturation in human foreskin keratinocytes treated with interferon-gamma. *Virology.* 2003, **310**(1), pp.100-108.
87. Scott, M.L., Woodby, B.L., Ulicny, J., Raikhy, G., Orr, A.W., Songock, W.K. and Bodily, J.M. Human Papillomavirus 16 E5 Inhibits Interferon Signaling and Supports Episomal Viral Maintenance. *J Virol.* 2020, **94**(2).
88. Horst, D., Geerdink, R.J., Gram, A.M., Stoppelenburg, A.J. and Ressing, M.E. Hiding lipid presentation: viral interference with CD1d-restricted invariant natural killer T (iNKT) cell activation. *Viruses.* 2012, **4**(10), pp.2379-2399.
89. Schwarz, E., Freese, U.K., Gissmann, L., Mayer, W., Roggenbuck, B., Stremlau, A. and zur Hausen, H. Structure and transcription of human papillomavirus sequences in cervical carcinoma cells. *Nature.* 1985, **314**(6006), pp.111-114.
90. Liu, Z., Ghai, J., Ostrow, R.S. and Faras, A.J. The expression levels of the human papillomavirus type 16 E7 correlate with its transforming potential. *Virology.* 1995, **207**(1), pp.260-270.
91. Band, V., De Caprio, J.A., Delmolino, L., Kulesa, V. and Sager, R. Loss of p53 protein in human papillomavirus type 16 E6-immortalized human mammary epithelial cells. *J Virol.* 1991, **65**(12), pp.6671-6676.
92. Hurlin, P.J., Kaur, P., Smith, P.P., Perez-Reyes, N., Blanton, R.A. and McDougall, J.K. Progression of human papillomavirus type 18-immortalized human keratinocytes to a malignant phenotype. *Proc Natl Acad Sci U S A.* 1991, **88**(2), pp.570-574.
93. Song, S., Liem, A., Miller, J.A. and Lambert, P.F. Human papillomavirus types 16 E6 and E7 contribute differently to carcinogenesis. *Virology.* 2000, **267**(2), pp.141-150.
94. Kiyono, T., Hiraiwa, A., Fujita, M., Hayashi, Y., Akiyama, T. and Ishibashi, M. Binding of high-risk human papillomavirus E6 oncoproteins to the human

homologue of the Drosophila discs large tumor suppressor protein. *Proc Natl Acad Sci U S A.* 1997, **94**(21), pp.11612-11616.
95. Zanier, K., ould M'hamed ould Sidi, A., Boulade-Ladame, C., Rybin, V., Chappelle, A., Atkinson, A., Kieffer, B. and Travé, G. Solution structure analysis of the HPV16 E6 oncoprotein reveals a self-association mechanism required for E6-mediated degradation of p53. *Structure.* 2012, **20**(4), pp.604-617.
96. Mantovani, F., Collavin, L. and Del Sal, G. Mutant p53 as a guardian of the cancer cell. *Cell Death & Differentiation.* 2019, **26**(2), pp.199-212.
97. Oliner, J.D., Pietenpol, J.A., Thiagalingam, S., Gyuris, J., Kinzler, K.W. and Vogelstein, B. Oncoprotein MDM2 conceals the activation domain of tumour suppressor p53. *Nature.* 1993, **362**, p.857.
98. Brady, C.A. and Attardi, L.D. p53 at a glance. *Journal of cell science.* 2010, **123**(Pt 15), pp.2527-2532.
99. Gajjar, M., Candeias, Marco M., Malbert-Colas, L., Mazars, A., Fujita, J., Olivares-Illana, V. and Fåhraeus, R. The p53 mRNA-Mdm2 Interaction Controls Mdm2 Nuclear Trafficking and Is Required for p53 Activation following DNA Damage. *Cancer Cell.* 2012, **21**(1), pp.25-35.
100. Menon, V. and Povirk, L. Involvement of p53 in the repair of DNA double strand breaks: multifaceted Roles of p53 in homologous recombination repair (HRR) and non-homologous end joining (NHEJ). *Sub-cellular biochemistry.* 2014, **85**, pp.321-336.
101. Westphal, D., Dewson, G., Czabotar, P.E. and Kluck, R.M. Molecular biology of Bax and Bak activation and action. *Biochimica et Biophysica Acta (BBA) - Molecular Cell Research.* 2011, **1813**(4), pp.521-531.
102. Elmore, S. Apoptosis: a review of programmed cell death. *Toxicologic pathology.* 2007, **35**(4), pp.495-516.
103. Krajewski, S., Krajewska, M. and Reed, J.C. Immunohistochemical analysis of in vivo patterns of Bak expression, a proapoptotic member of the Bcl-2 protein family. *Cancer Res.* 1996, **56**(12), pp.2849-2855.
104. Thomas, M. and Banks, L. Inhibition of Bak-induced apoptosis by HPV-18 E6. *Oncogene.* 1998, **17**(23), pp.2943-2954.
105. Shay, J.W. Are short telomeres predictive of advanced cancer? *Cancer discovery.* 2013, **3**(10), pp.1096-1098.
106. Yang, H.-J. Aberrant DNA methylation in cervical carcinogenesis. *Chinese journal of cancer.* 2013, **32**(1), pp.42-48.
107. Herman, J.G. and Baylin, S.B. Gene Silencing in Cancer in Association with Promoter Hypermethylation. *New England Journal of Medicine.* 2003, **349**(21), pp.2042-2054.
108. Ehrlich, M. DNA hypomethylation in cancer cells. *Epigenomics.* 2009, **1**(2), pp.239-259.
109. Zhang, W. and Xu, J. DNA methyltransferases and their roles in tumorigenesis. *Biomarker research.* 2017, **5**, pp.1-1.
110. Au Yeung, C.L., Pui Tsang, W., Yee Tsang, T., Na Co, N., Lun Yau, P. and Tak Kwok, T. *HPV-16 E6 upregulation of DNMT1 through repression of tumor suppressor p53.* 2010.
111. Leonard, S.M., Wei, W., Collins, S.I., Pereira, M., Diyaf, A., Constandinou-Williams, C., Young, L.S., Roberts, S. and Woodman, C.B. Oncogenic human papillomavirus imposes an instructive pattern of DNA methylation changes which parallel the natural history of cervical HPV infection in young women. *Carcinogenesis.* 2012, **33**(7), pp.1286-1293.
112. Chrun, E.S., Modolo, F. and Daniel, F.I. Histone modifications: A review about the presence of this epigenetic phenomenon in carcinogenesis. *Pathology - Research and Practice.* 2017, **213**(11), pp.1329-1339.

113. Maury, E. and Hashizume, R. Epigenetic modification in chromatin machinery and its deregulation in pediatric brain tumors: Insight into epigenetic therapies. *Epigenetics.* 2017, **12**(5), pp.353-369.
114. Patel, D., Huang, S.M., Baglia, L.A. and McCance, D.J. The E6 protein of human papillomavirus type 16 binds to and inhibits co-activation by CBP and p300. *Embo j.* 1999, **18**(18), pp.5061-5072.
115. Hsu, C.H., Peng, K.L., Jhang, H.C., Lin, C.H., Wu, S.Y., Chiang, C.M., Lee, S.C., Yu, W.C. and Juan, L.J. The HPV E6 oncoprotein targets histone methyltransferases for modulating specific gene transcription. *Oncogene.* 2012, **31**(18), pp.2335-2349.
116. Drews, C.M., Case, S. and Vande Pol, S.B. E6 proteins from high-risk HPV, low-risk HPV, and animal papillomaviruses activate the Wnt/β-catenin pathway through E6AP-dependent degradation of NHERF1. *PLoS Pathog.* 2019, **15**(4), p.e1007575.
117. Zhan, T., Rindtorff, N. and Boutros, M. Wnt signaling in cancer. *Oncogene.* 2017, **36**(11), pp.1461-1473.
118. Adey, N.B., Huang, L., Ormonde, P.A., Baumgard, M.L., Pero, R., Byreddy, D.V., Tavtigian, S.V. and Bartel, P.L. Threonine phosphorylation of the MMAC1/PTEN PDZ binding domain both inhibits and stimulates PDZ binding. *Cancer Res.* 2000, **60**(1), pp.35-37.
119. Spangle, J.M. and Münger, K. The human papillomavirus type 16 E6 oncoprotein activates mTORC1 signaling and increases protein synthesis. *J Virol.* 2010, **84**(18), pp.9398-9407.
120. Spangle, J.M. and Munger, K. The HPV16 E6 Oncoprotein Causes Prolonged Receptor Protein Tyrosine Kinase Signaling and Enhances Internalization of Phosphorylated Receptor Species. *PLoS Pathog.* 2013, **9**(3), p.e1003237.
121. Howie, H.L., Katzenellenbogen, R.A. and Galloway, D.A. Papillomavirus E6 proteins. *Virology.* 2009, **384**(2), pp.324-334.
122. Elbel, M., Carl, S., Spaderna, S. and Iftner, T. A Comparative Analysis of the Interactions of the E6 Proteins from Cutaneous and Genital Papillomaviruses with p53 and E6AP in Correlation to Their Transforming Potential. *Virology.* 1997, **239**(1), pp.132-149.
123. Thomas, M. and Banks, L. Human papillomavirus (HPV) E6 interactions with Bak are conserved amongst E6 proteins from high and low risk HPV types. *J Gen Virol.* 1999, **80 (Pt 6)**, pp.1513-1517.
124. Phelps, W.C., Yee, C.L., Münger, K. and Howley, P.M. The human papillomavirus type 16 E7 gene encodes transactivation and transformation functions similar to those of adenovirus E1A. *Cell.* 1988, **53**(4), pp.539-547.
125. Riley, R.R., Duensing, S., Brake, T., Münger, K., Lambert, P.F. and Arbeit, J.M. Dissection of human papillomavirus E6 and E7 function in transgenic mouse models of cervical carcinogenesis. *Cancer Res.* 2003, **63**(16), pp.4862-4871.
126. Liu, S., Tian, Y., Greenaway, F.T. and Sun, M.Z. A C-terminal hydrophobic, solvent-protected core and a flexible N-terminus are potentially required for human papillomavirus 18 E7 protein functionality. *Biochimie.* 2010, **92**(7), pp.901-908.
127. McIntyre, M.C., Frattini, M.G., Grossman, S.R. and Laimins, L.A. Human papillomavirus type 18 E7 protein requires intact Cys-X-X-Cys motifs for zinc binding, dimerization, and transformation but not for Rb binding. *J Virol.* 1993, **67**(6), pp.3142-3150.
128. Basukala, O., Mittal, S., Massimi, P., Bestagno, M. and Banks, L. The HPV-18 E7 CKII phospho acceptor site is required for maintaining the transformed phenotype of cervical tumour-derived cells. *PLoS Pathog.* 2019, **15**(5), p.e1007769.

129. Liang, Y.J., Chang, H.S., Wang, C.Y. and Yu, W.C. DYRK1A stabilizes HPV16E7 oncoprotein through phosphorylation of the threonine 5 and threonine 7 residues. *Int J Biochem Cell Biol.* 2008, **40**(11), pp.2431-2441.
130. Oh, K.J., Kalinina, A., Wang, J., Nakayama, K., Nakayama, K.I. and Bagchi, S. The papillomavirus E7 oncoprotein is ubiquitinated by UbcH7 and Cullin 1- and Skp2-containing E3 ligase. *J Virol.* 2004, **78**(10), pp.5338-5346.
131. Genovese, N.J., Broker, T.R. and Chow, L.T. Nonconserved lysine residues attenuate the biological function of the low-risk human papillomavirus E7 protein. *J Virol.* 2011, **85**(11), pp.5546-5554.
132. Fung, Y.K., Murphree, A.L., T'Ang, A., Qian, J., Hinrichs, S.H. and Benedict, W.F. Structural evidence for the authenticity of the human retinoblastoma gene. *Science.* 1987, **236**(4809), pp.1657-1661.
133. Sellers, W.R. and Kaelin, W.G., Jr. Role of the retinoblastoma protein in the pathogenesis of human cancer. *J Clin Oncol.* 1997, **15**(11), pp.3301-3312.
134. Thomas, D.M., Yang, H.S., Alexander, K. and Hinds, P.W. Role of the retinoblastoma protein in differentiation and senescence. *Cancer Biol Ther.* 2003, **2**(2), pp.124-130.
135. Manning, A.L. and Dyson, N.J. pRB, a tumor suppressor with a stabilizing presence. *Trends Cell Biol.* 2011, **21**(8), pp.433-441.
136. Xiao, B., Spencer, J., Clements, A., Ali-Khan, N., Mittnacht, S., Broceño, C., Burghammer, M., Perrakis, A., Marmorstein, R. and Gamblin, S.J. Crystal structure of the retinoblastoma tumor suppressor protein bound to E2F and the molecular basis of its regulation. *Proc Natl Acad Sci U S A.* 2003, **100**(5), pp.2363-2368.
137. Rubin, S.M., Gall, A.L., Zheng, N. and Pavletich, N.P. Structure of the Rb C-terminal domain bound to E2F1-DP1: a mechanism for phosphorylation-induced E2F release. *Cell.* 2005, **123**(6), pp.1093-1106.
138. Hiebert, S.W., Chellappan, S.P., Horowitz, J.M. and Nevins, J.R. The interaction of RB with E2F coincides with an inhibition of the transcriptional activity of E2F. *Genes Dev.* 1992, **6**(2), pp.177-185.
139. Brown, V.D., Phillips, R.A. and Gallie, B.L. Cumulative effect of phosphorylation of pRB on regulation of E2F activity. *Mol Cell Biol.* 1999, **19**(5), pp.3246-3256.
140. Dahlin, D.C. Pathology of osteosarcoma. *Clin Orthop Relat Res.* 1975, (111), pp.23-32.
141. White, E.A., Sowa, M.E., Tan, M.J., Jeudy, S., Hayes, S.D., Santha, S., Münger, K., Harper, J.W. and Howley, P.M. Systematic identification of interactions between host cell proteins and E7 oncoproteins from diverse human papillomaviruses. *Proc Natl Acad Sci U S A.* 2012, **109**(5), pp.E260-267.
142. Alvarado-Kristensson, M. γ-tubulin as a signal-transducing molecule and meshwork with therapeutic potential. *Signal Transduction and Targeted Therapy.* 2018, **3**(1), p.24.
143. Nguyen, C.L., Eichwald, C., Nibert, M.L. and Münger, K. Human papillomavirus type 16 E7 oncoprotein associates with the centrosomal component gamma-tubulin. *J Virol.* 2007, **81**(24), pp.13533-13543.
144. Kawasaki, T. and Kawai, T. Toll-like receptor signaling pathways. *Frontiers in immunology.* 2014, **5**, p.461.
145. Hasan, U.A., Zannetti, C., Parroche, P., Goutagny, N., Malfroy, M., Roblot, G., Carreira, C., Hussain, I., Müller, M., Taylor-Papadimitriou, J., Picard, D., Sylla, B.S., Trinchieri, G., Medzhitov, R. and Tommasino, M. The human papillomavirus type 16 E7 oncoprotein induces a transcriptional repressor complex on the Toll-like receptor 9 promoter. *J Exp Med.* 2013, **210**(7), pp.1369-1387.
146. Barnard, P. and McMillan, N.A. The human papillomavirus E7 oncoprotein abrogates signaling mediated by interferon-alpha. *Virology.* 1999, **259**(2), pp.305-313.

147. Zhou, F., Chen, J. and Zhao, K.N. Human papillomavirus 16-encoded E7 protein inhibits IFN-γ-mediated MHC class I antigen presentation and CTL-induced lysis by blocking IRF-1 expression in mouse keratinocytes. *J Gen Virol.* 2013, **94**(Pt 11), pp.2504-2514.
148. Burgers, W.A., Blanchon, L., Pradhan, S., de Launoit, Y., Kouzarides, T. and Fuks, F. Viral oncoproteins target the DNA methyltransferases. *Oncogene.* 2007, **26**(11), pp.1650-1655.
149. McCabe, M.T., Davis, J.N. and Day, M.L. Regulation of DNA Methyltransferase 1 by the pRb/E2F1 Pathway. *Cancer Res.* 2005, **65**(9), p.3624.
150. Justice, R.W., Zilian, O., Woods, D.F., Noll, M. and Bryant, P.J. The Drosophila tumor suppressor gene warts encodes a homolog of human myotonic dystrophy kinase and is required for the control of cell shape and proliferation. *Genes Dev.* 1995, **9**(5), pp.534-546.
151. Tapon, N., Harvey, K.F., Bell, D.W., Wahrer, D.C.R., Schiripo, T.A., Haber, D.A. and Hariharan, I.K. salvador Promotes Both Cell Cycle Exit and Apoptosis in Drosophila and Is Mutated in Human Cancer Cell Lines. *Cell.* 2002, **110**(4), pp.467-478.
152. Wu, S., Huang, J., Dong, J. and Pan, D. hippo encodes a Ste-20 family protein kinase that restricts cell proliferation and promotes apoptosis in conjunction with salvador and warts. *Cell.* 2003, **114**(4), pp.445-456.
153. Lai, Z.C., Wei, X., Shimizu, T., Ramos, E., Rohrbaugh, M., Nikolaidis, N., Ho, L.L. and Li, Y. Control of cell proliferation and apoptosis by mob as tumor suppressor, mats. *Cell.* 2005, **120**(5), pp.675-685.
154. Huang, J., Wu, S., Barrera, J., Matthews, K. and Pan, D. The Hippo Signaling Pathway Coordinately Regulates Cell Proliferation and Apoptosis by Inactivating Yorkie, the Drosophila Homolog of YAP. *Cell.* 2005, **122**(3), pp.421-434.
155. Dong, J., Feldmann, G., Huang, J., Wu, S., Zhang, N., Comerford, S.A., Gayyed, M.F., Anders, R.A., Maitra, A. and Pan, D. Elucidation of a universal size-control mechanism in Drosophila and mammals. *Cell.* 2007, **130**(6), pp.1120-1133.
156. Galan, J.A. and Avruch, J. MST1/MST2 Protein Kinases: Regulation and Physiologic Roles. *Biochemistry.* 2016, **55**(39), pp.5507-5519.
157. Boggiano, J.C., Vanderzalm, P.J. and Fehon, R.G. Tao-1 phosphorylates Hippo/MST kinases to regulate the Hippo-Salvador-Warts tumor suppressor pathway. *Developmental cell.* 2011, **21**(5), pp.888-895.
158. Plouffe, S.W., Meng, Z., Lin, K.C., Lin, B., Hong, A.W., Chun, J.V. and Guan, K.-L. Characterization of Hippo Pathway Components by Gene Inactivation. *Mol Cell.* 2016, **64**(5), pp.993-1008.
159. Fallahi, E., O'Driscoll, N.A. and Matallanas, D. The MST/Hippo Pathway and Cell Death: A Non-Canonical Affair. *Genes.* 2016, **7**(6), p.28.
160. Ardestani, A., Lupse, B. and Maedler, K. Hippo Signaling: Key Emerging Pathway in Cellular and Whole-Body Metabolism. *Trends in Endocrinology & Metabolism.* 2018, **29**(7), pp.492-509.
161. Dan, I., Watanabe, N.M. and Kusumi, A. The Ste20 group kinases as regulators of MAP kinase cascades. *Trends Cell Biol.* 2001, **11**(5), pp.220-230.
162. Rane, C.K. and Minden, A. P21 activated kinases: structure, regulation, and functions. *Small GTPases.* 2014, **5**.
163. Ling, P., Lu, T.J., Yuan, C.J. and Lai, M.D. Biosignaling of mammalian Ste20-related kinases. *Cell Signal.* 2008, **20**(7), pp.1237-1247.
164. Lim, S., Hermance, N., Mudianto, T., Mustaly, H.M., Mauricio, I.P.M., Vittoria, M.A., Quinton, R.J., Howell, B.W., Cornils, H., Manning, A.L. and Ganem, N.J. Identification of the kinase STK25 as an upstream activator of LATS signaling. *Nature Communications.* 2019, **10**(1), p.1547.

165. Ura, S., Masuyama, N., Graves, J.D. and Gotoh, Y. Caspase cleavage of MST1 promotes nuclear translocation and chromatin condensation. 2001, **98**(18), pp.10148-10153.
166. Lehtinen, M.K., Yuan, Z., Boag, P.R., Yang, Y., Villén, J., Becker, E.B.E., DiBacco, S., de la Iglesia, N., Gygi, S., Blackwell, T.K. and Bonni, A. A Conserved MST-FOXO Signaling Pathway Mediates Oxidative-Stress Responses and Extends Life Span. *Cell.* 2006, **125**(5), pp.987-1001.
167. Zhang, X., Tang, N., Hadden, T.J. and Rishi, A.K. Akt, FoxO and regulation of apoptosis. *Biochimica et Biophysica Acta (BBA) - Molecular Cell Research.* 2011, **1813**(11), pp.1978-1986.
168. Sudol, M. *Yes-Associated Protein (YAP65) is a proline-rich phosphoprotein that binds to the SH3 domain of the Yes proto-oncogene product.* 1994.
169. Kanai, F., Marignani, P.A., Sarbassova, D., Yagi, R., Hall, R.A., Donowitz, M., Hisaminato, A., Fujiwara, T., Ito, Y., Cantley, L.C. and Yaffe, M.B. TAZ: a novel transcriptional co-activator regulated by interactions with 14-3-3 and PDZ domain proteins. *Embo j.* 2000, **19**(24), pp.6778-6791.
170. Skibinski, A., Breindel, J.L., Prat, A., Galván, P., Smith, E., Rolfs, A., Gupta, P.B., LaBaer, J. and Kuperwasser, C. The Hippo transducer TAZ interacts with the SWI/SNF complex to regulate breast epithelial lineage commitment. *Cell Reports.* 2014, **6**(6), pp.1059-1072.
171. Xiao, J.H., Davidson, I., Matthes, H., Garnier, J.-M. and Chambon, P. Cloning, expression, and transcriptional properties of the human enhancer factor TEF-1. *Cell.* 1991, **65**(4), pp.551-568.
172. Chen, Z., Friedrich, G.A. and Soriano, P. Transcriptional enhancer factor 1 disruption by a retroviral gene trap leads to heart defects and embryonic lethality in mice. *Genes Dev.* 1994, **8**(19), pp.2293-2301.
173. He, C., Mao, D., Hua, G., Lv, X., Chen, X., Angeletti, P.C., Dong, J., Remmenga, S.W., Rodabaugh, K.J., Zhou, J., Lambert, P.F., Yang, P., Davis, J.S. and Wang, C. The Hippo/YAP pathway interacts with EGFR signaling and HPV oncoproteins to regulate cervical cancer progression. *EMBO molecular medicine.* 2015, **7**(11), pp.1426-1449.
174. Morgan, E.L., Patterson, M.R., Ryder, E.L., Lee, S.Y., Wasson, C.W., Harper, K.L., Li, Y., Griffin, S., Blair, G.E., Whitehouse, A. and Macdonald, A. MicroRNA-18a targeting of the STK4/MST1 tumour suppressor is necessary for transformation in HPV positive cervical cancer. *PLOS Pathogens.* 2020, **16**(6), p.e1008624.
175. Zhao, B., Ye, X., Yu, J., Li, L., Li, W., Li, S., Yu, J., Lin, J.D., Wang, C.Y., Chinnaiyan, A.M., Lai, Z.C. and Guan, K.L. TEAD mediates YAP-dependent gene induction and growth control. *Genes Dev.* 2008, **22**(14), pp.1962-1971.
176. Moya, I.M. and Halder, G. Hippo–YAP/TAZ signalling in organ regeneration and regenerative medicine. *Nature Reviews Molecular Cell Biology.* 2019, **20**(4), pp.211-226.
177. Santucci, M., Vignudelli, T., Ferrari, S., Mor, M., Scalvini, L., Bolognesi, M.L., Uliassi, E. and Costi, M.P. The Hippo Pathway and YAP/TAZ-TEAD Protein-Protein Interaction as Targets for Regenerative Medicine and Cancer Treatment. *J Med Chem.* 2015, **58**(12), pp.4857-4873.
178. Li, Z., Zhao, B., Wang, P., Chen, F., Dong, Z., Yang, H., Guan, K.-L. and Xu, Y. Structural insights into the YAP and TEAD complex. *Genes Dev.* 2010, **24**(3), pp.235-240.
179. Huang, W., Lv, X., Liu, C., Zha, Z., Zhang, H., Jiang, Y., Xiong, Y., Lei, Q.-Y. and Guan, K.-L. The N-terminal phosphodegron targets TAZ/WWTR1 protein for SCFβ-TrCP-dependent degradation in response to phosphatidylinositol 3-kinase inhibition. *J Biol Chem.* 2012, **287**(31), pp.26245-26253.

180. Lu, Y., Wu, T., Gutman, O., Lu, H., Zhou, Q., Henis, Y.I. and Luo, K. Phase separation of TAZ compartmentalizes the transcription machinery to promote gene expression. *Nature Cell Biology.* 2020, **22**(4), pp.453-464.
181. Huang, W., Lv, X., Liu, C., Zha, Z., Zhang, H., Jiang, Y., Xiong, Y., Lei, Q.Y. and Guan, K.L. The N-terminal phosphodegron targets TAZ/WWTR1 protein for SCFβ-TrCP-dependent degradation in response to phosphatidylinositol 3-kinase inhibition. *J Biol Chem.* 2012, **287**(31), pp.26245-26253.
182. Wei, Y., Luo, H., Yee, P.P., Zhang, L., Liu, Z., Zheng, H., Zhang, L., Anderson, B., Tang, M., Huang, S. and Li, W. Paraspeckle Protein NONO Promotes TAZ Phase Separation in the Nucleus to Drive the Oncogenic Transcriptional Program. *Adv Sci (Weinh).* 2021, **8**(24), p.e2102653.
183. Plouffe, S.W., Lin, K.C., Moore, J.L., 3rd, Tan, F.E., Ma, S., Ye, Z., Qiu, Y., Ren, B. and Guan, K.L. The Hippo pathway effector proteins YAP and TAZ have both distinct and overlapping functions in the cell. *J Biol Chem.* 2018, **293**(28), pp.11230-11240.
184. Jiang, Y., Xie, W.J., Chen, R.W., You, W.W., Ye, W.L., Chen, H., Chen, W.X. and Xu, J.P. The Hippo Signaling Core Components YAP and TAZ as New Prognostic Factors in Lung Cancer. *Front Surg.* 2022, **9**, p.813123.
185. Han, Y. Analysis of the role of the Hippo pathway in cancer. *Journal of Translational Medicine.* 2019, **17**(1), p.116.
186. Wu, Y., Zhang, J., Zhang, H. and Zhai, Y. Hepatitis B virus X protein mediates yes-associated protein 1 upregulation in hepatocellular carcinoma. *Oncology letters.* 2016, **12**(3), pp.1971-1974.
187. Lin, C.H., Hsu, T.I., Chiou, P.Y., Hsiao, M., Wang, W.C., Chen, Y.C., Lin, J.T., Wang, J.Y., Lin, P.C., Lin, F.C., Tseng, Y.K., Cheng, H.C., Chen, C.L. and Lu, P.J. Downregulation of STK4 promotes colon cancer invasion/migration through blocking β-catenin degradation. *Molecular oncology.* 2020, **14**(10), pp.2574-2588.
188. Camargo, F.D., Gokhale, S., Johnnidis, J.B., Fu, D., Bell, G.W., Jaenisch, R. and Brummelkamp, T.R. YAP1 Increases Organ Size and Expands Undifferentiated Progenitor Cells. *Current Biology.* 2007, **17**(23), pp.2054-2060.
189. Zanconato, F., Forcato, M., Battilana, G., Azzolin, L., Quaranta, E., Bodega, B., Rosato, A., Bicciato, S., Cordenonsi, M. and Piccolo, S. Genome-wide association between YAP/TAZ/TEAD and AP-1 at enhancers drives oncogenic growth. *Nature Cell Biology.* 2015, **17**, p.1218.
190. Cordenonsi, M., Zanconato, F., Azzolin, L., Forcato, M., Rosato, A., Frasson, C., Inui, M., Montagner, M., Parenti, Anna R., Poletti, A., Daidone, Maria G., Dupont, S., Basso, G., Bicciato, S. and Piccolo, S. The Hippo Transducer TAZ Confers Cancer Stem Cell-Related Traits on Breast Cancer Cells. *Cell.* 2011, **147**(4), pp.759-772.
191. Vahid, S., Thaper, D., Gibson, K.F., Bishop, J.L. and Zoubeidi, A. Molecular chaperone Hsp27 regulates the Hippo tumor suppressor pathway in cancer. *Scientific reports.* 2016, **6**, p.31842.
192. Korenchuk, S., Lehr, J.E., L, M.C., Lee, Y.G., Whitney, S., Vessella, R., Lin, D.L. and Pienta, K.J. VCaP, a cell-based model system of human prostate cancer. *In Vivo.* 2001, **15**(2), pp.163-168.
193. LaCanna, R., Liccardo, D., Zhang, P., Tragesser, L., Wang, Y., Cao, T., Chapman, H.A., Morrisey, E.E., Shen, H., Koch, W.J., Kosmider, B., Wolfson, M.R. and Tian, Y. Yap/Taz regulate alveolar regeneration and resolution of lung inflammation. *J Clin Invest.* 2019, **129**(5), pp.2107-2122.
194. Evans, D.G. Neurofibromatosis type 2 (NF2): a clinical and molecular review. *Orphanet J Rare Dis.* 2009, **4**, p.16.
195. He, C., Lv, X., Huang, C., Angeletti, P.C., Hua, G., Dong, J., Zhou, J., Wang, Z., Ma, B., Chen, X., Lambert, P.F., Rueda, B.R., Davis, J.S. and Wang, C. A Human Papillomavirus-Independent Cervical Cancer Animal Model Reveals

Unconventional Mechanisms of Cervical Carcinogenesis. *Cell Reports.* 2019, **26**(10), pp.2636-2650.e2635.
196. Hatterschide, J., Castagnino, P., Kim, H.W., Sperry, S.M., Montone, K.T., Basu, D. and White, E.A. YAP1 activation by human papillomavirus E7 promotes basal cell identity in squamous epithelia. *eLife.* 2022, **11**, p.e75466.
197. Liu, Y., Ren, M., Tan, X. and Hu, L. Distinct Changes in the Expression TAZ are Associated with Normal Cervix and Human Cervical Cancer. *J Cancer.* 2018, **9**(22), pp.4263-4270.
198. Han, Y., Liu, D. and Li, L. Increased expression of TAZ and associated upregulation of PD-L1 in cervical cancer. *Cancer Cell International.* 2021, **21**(1), p.592.
199. Cunningham, R. and Hansen, Carsten G. The Hippo pathway in cancer: YAP/TAZ and TEAD as therapeutic targets in cancer. *Clinical Science.* 2022, **136**(3), pp.197-222.
200. Wu, M., Huang, Q., Xie, Y., Wu, X., Ma, H., Zhang, Y. and Xia, Y. Improvement of the anticancer efficacy of PD-1/PD-L1 blockade via combination therapy and PD-L1 regulation. *Journal of Hematology & Oncology.* 2022, **15**(1), p.24.
201. Wang, X., Wang, H.-K., Li, Y., Hafner, M., Banerjee, N.S., Tang, S., Briskin, D., Meyers, C., Chow, L.T., Xie, X., Tuschl, T. and Zheng, Z.-M. microRNAs are biomarkers of oncogenic human papillomavirus infections. *Proc Natl Acad Sci U S A.* 2014, **111**(11), pp.4262-4267.
202. Wang, X., Wang, H.K., McCoy, J.P., Banerjee, N.S., Rader, J.S., Broker, T.R., Meyers, C., Chow, L.T. and Zheng, Z.M. Oncogenic HPV infection interrupts the expression of tumor-suppressive miR-34a through viral oncoprotein E6. *Rna.* 2009, **15**(4), pp.637-647.
203. O'Brien, J., Hayder, H., Zayed, Y. and Peng, C. Overview of MicroRNA Biogenesis, Mechanisms of Actions, and Circulation. *Frontiers in endocrinology.* 2018, **9**, pp.402-402.
204. Wang, X., Wang, H.K., Li, Y., Hafner, M., Banerjee, N.S., Tang, S., Briskin, D., Meyers, C., Chow, L.T., Xie, X., Tuschl, T. and Zheng, Z.M. microRNAs are biomarkers of oncogenic human papillomavirus infections. *Proc Natl Acad Sci U S A.* 2014, **111**(11), pp.4262-4267.
205. Lawrie, C.H., Gal, S., Dunlop, H.M., Pushkaran, B., Liggins, A.P., Pulford, K., Banham, A.H., Pezzella, F., Boultwood, J., Wainscoat, J.S., Hatton, C.S. and Harris, A.L. Detection of elevated levels of tumour-associated microRNAs in serum of patients with diffuse large B-cell lymphoma. *Br J Haematol.* 2008, **141**(5), pp.672-675.
206. Treiber, T., Treiber, N. and Meister, G. Regulation of microRNA biogenesis and its crosstalk with other cellular pathways. *Nature Reviews Molecular Cell Biology.* 2019, **20**(1), pp.5-20.
207. Wang, Y., Sheng, G., Juranek, S., Tuschl, T. and Patel, D.J. Structure of the guide-strand-containing argonaute silencing complex. *Nature.* 2008, **456**(7219), pp.209-213.
208. Diederichs, S. and Haber, D.A. Dual role for argonautes in microRNA processing and posttranscriptional regulation of microRNA expression. *Cell.* 2007, **131**(6), pp.1097-1108.
209. Agarwal, V., Bell, G.W., Nam, J.W. and Bartel, D.P. Predicting effective microRNA target sites in mammalian mRNAs. *eLife.* 2015, **4**.
210. Fukao, A., Mishima, Y., Takizawa, N., Oka, S., Imataka, H., Pelletier, J., Sonenberg, N., Thoma, C. and Fujiwara, T. MicroRNAs trigger dissociation of eIF4AI and eIF4AII from target mRNAs in humans. *Mol Cell.* 2014, **56**(1), pp.79-89.
211. Winter, J., Jung, S., Keller, S., Gregory, R.I. and Diederichs, S. Many roads to maturity: microRNA biogenesis pathways and their regulation. *Nature Cell Biology.* 2009, **11**(3), pp.228-234.

212. Chen, J., Zhong, Y. and Li, L. miR-124 and miR-203 synergistically inactivate EMT pathway via coregulation of ZEB2 in clear cell renal cell carcinoma (ccRCC). *Journal of Translational Medicine.* 2020, **18**(1), p.69.
213. Taube, J.H., Malouf, G.G., Lu, E., Sphyris, N., Vijay, V., Ramachandran, P.P., Ueno, K.R., Gaur, S., Nicoloso, M.S., Rossi, S., Herschkowitz, J.I., Rosen, J.M., Issa, J.P., Calin, G.A., Chang, J.T. and Mani, S.A. Epigenetic silencing of microRNA-203 is required for EMT and cancer stem cell properties. *Scientific reports.* 2013, **3**, p.2687.
214. Calin, G.A., Dumitru, C.D., Shimizu, M., Bichi, R., Zupo, S., Noch, E., Aldler, H., Rattan, S., Keating, M., Rai, K., Rassenti, L., Kipps, T., Negrini, M., Bullrich, F. and Croce, C.M. Frequent Deletions and Down-Regulation of Micro-RNA Genes miR15 and miR16 at 13q14 in Chronic Lymphocytic Leukemia. *Proc Natl Acad Sci U S A.* 2002, **99**(24), pp.15524-15529.
215. Garzon, R., Volinia, S., Liu, C.-G., Fernandez-Cymering, C., Palumbo, T., Pichiorri, F., Fabbri, M., Coombes, K., Alder, H., Nakamura, T., Flomenberg, N., Marcucci, G., Calin, G.A., Kornblau, S.M., Kantarjian, H., Bloomfield, C.D., Andreeff, M. and Croce, C.M. MicroRNA signatures associated with cytogenetics and prognosis in acute myeloid leukemia. *Blood.* 2008, **111**(6), pp.3183-3189.
216. Liu, C., Kelnar, K., Vlassov, A.V., Brown, D., Wang, J. and Tang, D.G. Distinct microRNA expression profiles in prostate cancer stem/progenitor cells and tumor-suppressive functions of let-7. *Cancer Res.* 2012, **72**(13), pp.3393-3404.
217. Png, K.J., Halberg, N., Yoshida, M. and Tavazoie, S.F. A microRNA regulon that mediates endothelial recruitment and metastasis by cancer cells. *Nature.* 2011, **481**, p.190.
218. Cameron, J.E., Yin, Q., Fewell, C., Lacey, M., McBride, J., Wang, X., Lin, Z., Schaefer, B.C. and Flemington, E.K. Epstein-Barr virus latent membrane protein 1 induces cellular MicroRNA miR-146a, a modulator of lymphocyte signaling pathways. *J Virol.* 2008, **82**(4), pp.1946-1958.
219. Pan, D., Li, G., Morris-Love, J., Qi, S., Feng, L., Mertens, M.E., Jurak, I., Knipe, D.M. and Coen, D.M. Herpes Simplex Virus 1 Lytic Infection Blocks MicroRNA (miRNA) Biogenesis at the Stage of Nuclear Export of Pre-miRNAs. *mBio.* 2019, **10**(1).
220. Hassani, A. and Khan, G. Epstein-Barr Virus and miRNAs: Partners in Crime in the Pathogenesis of Multiple Sclerosis? *Frontiers in immunology.* 2019, **10**, p.695.
221. Su, Y., Lin, T., Liu, C., Cheng, C., Han, X. and Jiang, X. microRNAs, the Link Between Dengue Virus and the Host Genome. *Front Microbiol.* 2021, **12**, p.714409.
222. Hong, S., Cheng, S., Songock, W., Bodily, J. and Laimins, L.A. Suppression of MicroRNA 424 Levels by Human Papillomaviruses Is Necessary for Differentiation-Dependent Genome Amplification. *J Virol.* 2017, **91**(24), pp.e01712-01717.
223. Melar-New, M. and Laimins, L.A. Human papillomaviruses modulate expression of microRNA 203 upon epithelial differentiation to control levels of p63 proteins. *J Virol.* 2010, **84**(10), pp.5212-5221.
224. Park, S., Eom, K., Kim, J., Bang, H., Wang, H.-Y., Ahn, S., Kim, G., Jang, H., Kim, S., Lee, D., Park, K.H. and Lee, H. MiR-9, miR-21, and miR-155 as potential biomarkers for HPV positive and negative cervical cancer. *BMC cancer.* 2017, **17**(1), pp.658-658.
225. Harden, M.E., Prasad, N., Griffiths, A. and Munger, K. Modulation of microRNA-mRNA Target Pairs by Human Papillomavirus 16 Oncoproteins. *mBio.* 2017, **8**(1), pp.e02170-02116.
226. Mogilyansky, E. and Rigoutsos, I. The miR-17/92 cluster: a comprehensive update on its genomics, genetics, functions and increasingly important and

numerous roles in health and disease. *Cell Death And Differentiation.* 2013, **20**(12), pp.1603-1614.
227. Ota, A., Tagawa, H., Karnan, S., Tsuzuki, S., Karpas, A., Kira, S., Yoshida, Y. and Seto, M. Identification and Characterization of a Novel Gene, C13orf25, as a Target for 13q31-q32 Amplification in Malignant Lymphoma. *Cancer Res.* 2004, **64**(9), p.3087.
228. Xu, X., Zhu, S., Tao, Z. and Ye, S. High circulating miR-18a, miR-20a, and miR-92a expression correlates with poor prognosis in patients with non-small cell lung cancer. *Cancer Med.* 2018, **7**(1), pp.21-31.
229. Trompeter, H.I., Abbad, H., Iwaniuk, K.M., Hafner, M., Renwick, N., Tuschl, T., Schira, J., Müller, H.W. and Wernet, P. MicroRNAs MiR-17, MiR-20a, and MiR-106b act in concert to modulate E2F activity on cell cycle arrest during neuronal lineage differentiation of USSC. *PLOS ONE.* 2011, **6**(1), p.e16138.
230. Brinkmann, K., Ng, A.P., de Graaf, C.A., Di Rago, L., Hyland, C.D., Morelli, E., Rautela, J., Huntington, N.D., Strasser, A., Alexander, W.S. and Herold, M.J. miR17~92 restrains pro-apoptotic BIM to ensure survival of haematopoietic stem and progenitor cells. *Cell death and differentiation.* 2020, **27**(5), pp.1475-1488.
231. Liu, S.Q., Jiang, S., Li, C., Zhang, B. and Li, Q.J. miR-17-92 cluster targets phosphatase and tensin homology and Ikaros Family Zinc Finger 4 to promote TH17-mediated inflammation. *J Biol Chem.* 2014, **289**(18), pp.12446-12456.
232. Ventura, A., Young, A.G., Winslow, M.M., Lintault, L., Meissner, A., Erkeland, S.J., Newman, J., Bronson, R.T., Crowley, D., Stone, J.R., Jaenisch, R., Sharp, P.A. and Jacks, T. Targeted deletion reveals essential and overlapping functions of the miR-17 through 92 family of miRNA clusters. *Cell.* 2008, **132**(5), pp.875-886.
233. Carraro, G., El-Hashash, A., Guidolin, D., Tiozzo, C., Turcatel, G., Young, B.M., De Langhe, S.P., Bellusci, S., Shi, W., Parnigotto, P.P. and Warburton, D. miR-17 family of microRNAs controls FGF10-mediated embryonic lung epithelial branching morphogenesis through MAPK14 and STAT3 regulation of E-Cadherin distribution. *Dev Biol.* 2009, **333**(2), pp.238-250.
234. Marcelis, C.L., Hol, F.A., Graham, G.E., Rieu, P.N., Kellermayer, R., Meijer, R.P., Lugtenberg, D., Scheffer, H., van Bokhoven, H., Brunner, H.G. and de Brouwer, A.P. Genotype-phenotype correlations in MYCN-related Feingold syndrome. *Hum Mutat.* 2008, **29**(9), pp.1125-1132.
235. Komatsu, S., Ichikawa, D., Takeshita, H., Morimura, R., Hirajima, S., Tsujiura, M., Kawaguchi, T., Miyamae, M., Nagata, H., Konishi, H., Shiozaki, A. and Otsuji, E. Circulating miR-18a: a sensitive cancer screening biomarker in human cancer. *In Vivo.* 2014, **28**(3), pp.293-297.
236. Liang, C., Zhang, X., Wang, H.-M., Liu, X.-M., Zhang, X.-j., Zheng, B., Qian, G.-R. and Ma, Z.-L. MicroRNA-18a-5p functions as an oncogene by directly targeting IRF2 in lung cancer. *Cell Death & Disease.* 2017, **8**(5), pp.e2764-e2764.
237. Hsu, T.I., Hsu, C.H., Lee, K.H., Lin, J.T., Chen, C.S., Chang, K.C., Su, C.Y., Hsiao, M. and Lu, P.J. MicroRNA-18a is elevated in prostate cancer and promotes tumorigenesis through suppressing STK4 in vitro and in vivo. *Oncogenesis.* 2014, **3**, p.e99.
238. Shuai, K. and Liu, B. Regulation of gene-activation pathways by PIAS proteins in the immune system. *Nat Rev Immunol.* 2005, **5**(8), pp.593-605.
239. He, T., McColl, K., Sakre, N., Chen, Y., Wildey, G. and Dowlati, A. Post-transcriptional regulation of PIAS3 expression by miR-18a in malignant mesothelioma. *Molecular oncology.* 2018, **12**(12), pp.2124-2135.
240. Dong, P., Xiong, Y., Yu, J., Chen, L., Tao, T., Yi, S., Hanley, S.J.B., Yue, J., Watari, H. and Sakuragi, N. Control of PD-L1 expression by miR-

140/142/340/383 and oncogenic activation of the OCT4-miR-18a pathway in cervical cancer. *Oncogene.* 2018, **37**(39), pp.5257-5268.
241. Thomas, M., Lange-Grünweller, K., Hartmann, D., Golde, L., Schlereth, J., Streng, D., Aigner, A., Grünweller, A. and Hartmann, R.K. Analysis of transcriptional regulation of the human miR-17-92 cluster; evidence for involvement of Pim-1. *Int J Mol Sci.* 2013, **14**(6), pp.12273-12296.
242. Northcott, P.A., Fernandez, L.A., Hagan, J.P., Ellison, D.W., Grajkowska, W., Gillespie, Y., Grundy, R., Van Meter, T., Rutka, J.T., Croce, C.M., Kenney, A.M. and Taylor, M.D. The miR-17/92 polycistron is up-regulated in sonic hedgehog-driven medulloblastomas and induced by N-myc in sonic hedgehog-treated cerebellar neural precursors. *Cancer Res.* 2009, **69**(8), pp.3249-3255.
243. Liu, H., Wu, Z., Zhou, H., Cai, W., Li, X., Hu, J., Gao, L., Feng, T., Wang, L., Peng, X., Qi, M., Liu, L. and Han, B. The SOX4/miR-17-92/RB1 Axis Promotes Prostate Cancer Progression. *Neoplasia.* 2019, **21**(8), pp.765-776.
244. Chaulk, S.G., Thede, G.L., Kent, O.A., Xu, Z., Gesner, E.M., Veldhoen, R.A., Khanna, S.K., Goping, I.S., MacMillan, A.M., Mendell, J.T., Young, H.S., Fahlman, R.P. and Glover, J.N. Role of pri-miRNA tertiary structure in miR-17~92 miRNA biogenesis. *RNA Biol.* 2011, **8**(6), pp.1105-1114.
245. Mayeda, A. and Krainer, A.R. Regulation of alternative pre-mRNA splicing by hnRNP A1 and splicing factor SF2. *Cell.* 1992, **68**(2), pp.365-375.
246. Hamilton, B.J., Burns, C.M., Nichols, R.C. and Rigby, W.F. Modulation of AUUUA response element binding by heterogeneous nuclear ribonucleoprotein A1 in human T lymphocytes. The roles of cytoplasmic location, transcription, and phosphorylation. *J Biol Chem.* 1997, **272**(45), pp.28732-28741.
247. Guil, S. and Cáceres, J.F. The multifunctional RNA-binding protein hnRNP A1 is required for processing of miR-18a. *Nat Struct Mol Biol.* 2007, **14**(7), pp.591-596.
248. Mandel, C.R., Kaneko, S., Zhang, H., Gebauer, D., Vethantham, V., Manley, J.L. and Tong, L. Polyadenylation factor CPSF-73 is the pre-mRNA 3'-end-processing endonuclease. *Nature.* 2006, **444**(7121), pp.953-956.
249. Dominski, Z., Yang, X.C. and Marzluff, W.F. The polyadenylation factor CPSF-73 is involved in histone-pre-mRNA processing. *Cell.* 2005, **123**(1), pp.37-48.
250. Heinrich, E.M., Wagner, J., Krüger, M., John, D., Uchida, S., Weigand, J.E., Suess, B. and Dimmeler, S. Regulation of miR-17-92a cluster processing by the microRNA binding protein SND1. *FEBS Lett.* 2013, **587**(15), pp.2405-2411.
251. Zhang, H., Wang, Y., Dou, J., Guo, Y., He, J., Li, L., Liu, X., Chen, R., Deng, R., Huang, J., Xie, R., Zhao, X. and Yu, J. Acetylation of AGO2 promotes cancer progression by increasing oncogenic miR-19b biogenesis. *Oncogene.* 2019, **38**(9), pp.1410-1431.
252. Wang, J., Qin, C., Zhong, C., Wen, Y., Ke, S. and Liao, B.O. Long non-coding RNA CASC2 targeting miR-18a suppresses glioblastoma cell growth, metastasis and EMT in vitro and in vivo. *J Biosci.* 2020, **45**.
253. Edgar, B.A. From cell structure to transcription: Hippo forges a new path. *Cell.* 2006, **124**(2), pp.267-273.
254. Muramatsu, T., Imoto, I., Matsui, T., Kozaki, K., Haruki, S., Sudol, M., Shimada, Y., Tsuda, H., Kawano, T. and Inazawa, J. YAP is a candidate oncogene for esophageal squamous cell carcinoma. *Carcinogenesis.* 2011, **32**(3), pp.389-398.
255. Baia, G.S., Caballero, O.L., Orr, B.A., Lal, A., Ho, J.S., Cowdrey, C., Tihan, T., Mawrin, C. and Riggins, G.J. Yes-associated protein 1 is activated and functions as an oncogene in meningiomas. *Mol Cancer Res.* 2012, **10**(7), pp.904-913.
256. Dacus, D., Cotton, C., McCallister, T.X. and Wallace, N.A. Beta Human Papillomavirus 8E6 Attenuates LATS Phosphorylation after Failed Cytokinesis. *J Virol.* 2020, **94**(12).

257. Guo, Z., Li, G., Bian, E., Ma, C.-C., Wan, J. and Zhao, B. TGF-β-mediated repression of MST1 by DNMT1 promotes glioma malignancy. *Biomedicine & Pharmacotherapy.* 2017, **94**, pp.774-780.
258. Liu, S., Pan, X., Yang, Q., Wen, L., Jiang, Y., Zhao, Y. and Li, G. MicroRNA-18a enhances the radiosensitivity of cervical cancer cells by promoting radiation-induced apoptosis. *Oncology reports.* 2015, **33**(6), pp.2853-2862.
259. Linsen, S.E.V., Tops, B.B.J. and Cuppen, E. miRNAs: small changes, widespread effects. *Cell Research.* 2008, **18**(12), pp.1157-1159.
260. Zhao, B., Li, L., Tumaneng, K., Wang, C.-Y. and Guan, K.-L. A coordinated phosphorylation by Lats and CK1 regulates YAP stability through SCF(beta-TRCP). *Genes Dev.* 2010, **24**(1), pp.72-85.
261. Wentzensen, N., Sherman, M.E., Schiffman, M. and Wang, S.S. Utility of methylation markers in cervical cancer early detection: appraisal of the state-of-the-science. *Gynecol Oncol.* 2009, **112**(2), pp.293-299.
262. Shen, J., Wang, S., Siegel, A.B., Remotti, H., Wang, Q., Sirosh, I. and Santella, R.M. Genome-Wide Expression of MicroRNAs Is Regulated by DNA Methylation in Hepatocarcinogenesis. *Gastroenterology Research and Practice.* 2015, **2015**, p.230642.
263. Liu, C.Y., Zha, Z.Y., Zhou, X., Zhang, H., Huang, W., Zhao, D., Li, T., Chan, S.W., Lim, C.J., Hong, W., Zhao, S., Xiong, Y., Lei, Q.Y. and Guan, K.L. The hippo tumor pathway promotes TAZ degradation by phosphorylating a phosphodegron and recruiting the SCF{beta}-TrCP E3 ligase. *J Biol Chem.* 2010, **285**(48), pp.37159-37169.
264. Miranda, M.Z., Bialik, J.F., Speight, P., Dan, Q., Yeung, T., Szászi, K., Pedersen, S.F. and Kapus, A. TGF-β1 regulates the expression and transcriptional activity of TAZ protein via a Smad3-independent, myocardin-related transcription factor-mediated mechanism. *J Biol Chem.* 2017, **292**(36), pp.14902-14920.
265. Deng, Y.R., Chen, X.J., Chen, W., Wu, L.F., Jiang, H.P., Lin, D., Wang, L.J., Wang, W. and Guo, S.Q. Sp1 contributes to radioresistance of cervical cancer through targeting G2/M cell cycle checkpoint CDK1. *Cancer Manag Res.* 2019, **11**, pp.5835-5844.
266. Sleiman, S.F., Langley, B.C., Basso, M., Berlin, J., Xia, L., Payappilly, J.B., Kharel, M.K., Guo, H., Marsh, J.L., Thompson, L.M., Mahishi, L., Ahuja, P., MacLellan, W.R., Geschwind, D.H., Coppola, G., Rohr, J. and Ratan, R.R. Mithramycin is a gene-selective Sp1 inhibitor that identifies a biological intersection between cancer and neurodegeneration. *J Neurosci.* 2011, **31**(18), pp.6858-6870.
267. Nagata, D., Suzuki, E., Nishimatsu, H., Satonaka, H., Goto, A., Omata, M. and Hirata, Y. Transcriptional activation of the cyclin D1 gene is mediated by multiple cis-elements, including SP1 sites and a cAMP-responsive element in vascular endothelial cells. *J Biol Chem.* 2001, **276**(1), pp.662-669.
268. Milanini-Mongiat, J., Pouysségur, J. and Pagès, G. Identification of Two Sp1 Phosphorylation Sites for p42/p44 Mitogen-activated Protein Kinases: THEIR IMPLICATION IN VASCULAR ENDOTHELIAL GROWTH FACTOR GENE TRANSCRIPTION*. *Journal of Biological Chemistry.* 2002, **277**(23), pp.20631-20639.
269. Han, R., Song, Y.-J., Sun, S.-Y., Zhou, Q., Chen, X.-Z., Zheng, Q.-L. and Cheng, H. Influence of Human Papillomavirus E7 Oncoprotein on Maturation and Function of Plasmacytoid Dendritic Cells In Vitro. *Virologica Sinica.* 2018, **33**(6), pp.493-501.
270. Morgan, E.L., Wasson, C.W., Hanson, L., Kealy, D., Pentland, I., McGuire, V., Scarpini, C., Coleman, N., Arthur, J.S.C., Parish, J.L., Roberts, S. and Macdonald, A. STAT3 activation by E6 is essential for the differentiation-dependent HPV18 life cycle. *PLoS Pathog.* 2018, **14**(4), p.e1006975.

271. Morgan, E.L., Scarth, J.A., Patterson, M.R., Wasson, C.W., Hemingway, G.C., Barba-Moreno, D. and Macdonald, A. E6-mediated activation of JNK drives EGFR signalling to promote proliferation and viral oncoprotein expression in cervical cancer. *Cell Death & Differentiation.* 2021, **28**(5), pp.1669-1687.
272. Carrillo-Beltrán, D., Muñoz, J.P., Guerrero-Vásquez, N., Blanco, R., León, O., de Souza Lino, V., Tapia, J.C., Maldonado, E., Dubois-Camacho, K., Hermoso, M.A., Corvalán, A.H., Calaf, G.M., Boccardo, E. and Aguayo, F. Human Papillomavirus 16 E7 Promotes EGFR/PI3K/AKT1/NRF2 Signaling Pathway Contributing to PIR/NF-κB Activation in Oral Cancer Cells. *Cancers (Basel).* 2020, **12**(7).
273. Gao, M., Fu, Y., Zhou, W., Gui, G., Lal, B., Li, Y., Xia, S., Ji, H., Eberhart, C.G., Laterra, J. and Ying, M. EGFR Activates a TAZ-Driven Oncogenic Program in Glioblastoma. *Cancer Res.* 2021, **81**(13), pp.3580-3592.
274. Koumangoye, R.B., Nangami, G.N., Thompson, P.D., Agboto, V.K., Ochieng, J. and Sakwe, A.M. Reduced annexin A6 expression promotes the degradation of activated epidermal growth factor receptor and sensitizes invasive breast cancer cells to EGFR-targeted tyrosine kinase inhibitors. *Mol Cancer.* 2013, **12**(1), p.167.
275. Roskoski, R., Jr. Small molecule inhibitors targeting the EGFR/ErbB family of protein-tyrosine kinases in human cancers. *Pharmacol Res.* 2019, **139**, pp.395-411.
276. Nagashima, S., Maruyama, J., Honda, K., Kondoh, Y., Osada, H., Nawa, M., Nakahama, K.I., Ishigami-Yuasa, M., Kagechika, H., Sugimura, H., Iwasa, H., Arimoto-Matsuzaki, K., Nishina, H. and Hata, Y. CSE1L promotes nuclear accumulation of transcriptional coactivator TAZ and enhances invasiveness of human cancer cells. *J Biol Chem.* 2021, **297**(1), p.100803.
277. Nishio, M., Sugimachi, K., Goto, H., Wang, J., Morikawa, T., Miyachi, Y., Takano, Y., Hikasa, H., Itoh, T., Suzuki, S.O., Kurihara, H., Aishima, S., Leask, A., Sasaki, T., Nakano, T., Nishina, H., Nishikawa, Y., Sekido, Y., Nakao, K., Shin-Ya, K., Mimori, K. and Suzuki, A. Dysregulated YAP1/TAZ and TGF-β signaling mediate hepatocarcinogenesis in Mob1a/1b-deficient mice. *Proc Natl Acad Sci U S A.* 2016, **113**(1), pp.E71-80.
278. Lin, M., Bu, C., He, Q., Gu, J., Wang, H., Feng, N. and Jiang, S.W. TAZ is overexpressed in prostate cancers and regulates the proliferation, migration and apoptosis of prostate cancer PC3 cells. *Oncology reports.* 2020, **44**(2), pp.747-756.
279. Chan, S.W., Lim, C.J., Guo, K., Ng, C.P., Lee, I., Hunziker, W., Zeng, Q. and Hong, W. A Role for TAZ in Migration, Invasion, and Tumorigenesis of Breast Cancer Cells. *Cancer Res.* 2008, **68**(8), pp.2592-2598.
280. Li, W., Dong, S., Wei, W., Wang, G., Zhang, A., Pu, P. and Jia, Z. The role of transcriptional coactivator TAZ in gliomas. *Oncotarget.* 2016, **7**(50), pp.82686-82699.
281. Wang, B., Zhao, L., Chi, W., Cao, H., Cui, W. and Meng, W. Aberrant methylation-mediated downregulation of lncRNA SSTR5-AS1 promotes progression and metastasis of laryngeal squamous cell carcinoma. *Epigenetics & Chromatin.* 2019, **12**(1), p.35.
282. Slep, K.C. and Vale, R.D. Structural basis of microtubule plus end tracking by XMAP215, CLIP-170, and EB1. *Mol Cell.* 2007, **27**(6), pp.976-991.
283. Leano, J.B., Rogers, S.L. and Slep, K.C. A cryptic TOG domain with a distinct architecture underlies CLASP-dependent bipolar spindle formation. *Structure.* 2013, **21**(6), pp.939-950.
284. Das, A., Dickinson, D.J., Wood, C.C., Goldstein, B. and Slep, K.C. Crescerin uses a TOG domain array to regulate microtubules in the primary cilium. *Mol Biol Cell.* 2015, **26**(23), pp.4248-4264.

285. Daugrois, C., Bessiere, C., Dejean, S., Anton-Leberre, V., Commes, T., Pyronnet, S., Brousset, P., Espinos, E., Brugiere, L., Meggetto, F. and Lamant, L. Gene Expression Signature Associated with Clinical Outcome in ALK-Positive Anaplastic Large Cell Lymphoma. *Cancers (Basel).* 2021, **13**(21).
286. Cui, S., Zhang, W., Xiong, L., Pan, F., Niu, Y., Chu, T., Wang, H., Zhao, Y. and Jiang, L. Use of capture-based next-generation sequencing to detect ALK fusion in plasma cell-free DNA of patients with non-small-cell lung cancer. *Oncotarget.* 2017, **8**(2), pp.2771-2780.
287. Yan, J., Zhou, X. and Pan, D. A case of one lung adenocarcinoma patient harboring a novel FAM179A-ALK (F1, A19) rearrangement responding to lorlatinib treatment. *Lung Cancer.* 2020, **147**, pp.26-29.
288. Yu, J.X., Chen, Q., Yu, Y.Q., Li, S.Q. and Song, J.F. Upregulation of colonic and hepatic tumor overexpressed gene is significantly associated with the unfavorable prognosis marker of human hepatocellular carcinoma. *Am J Cancer Res.* 2016, **6**(3), pp.690-700.
289. Petersenn, S., Rasch, A.C., Böhnke, C. and Schulte, H.M. Identification of an Upstream Pituitary-Active Promoter of Human Somatostatin Receptor Subtype 5. *Endocrinology.* 2002, **143**(7), pp.2626-2634.
290. Chen, L., Zhai, W., Zheng, X., Xie, Q., Zhou, Q., Tao, M., Zhu, Y., Wu, C. and Jiang, J. Decreased IFIT2 Expression Promotes Gastric Cancer Progression and Predicts Poor Prognosis of the Patients. *Cell Physiol Biochem.* 2018, **45**(1), pp.15-25.
291. Chen, L., Liu, S., Xu, F., Kong, Y., Wan, L., Zhang, Y. and Zhang, Z. Inhibition of Proteasome Activity Induces Aggregation of IFIT2 in the Centrosome and Enhances IFIT2-Induced Cell Apoptosis. *Int J Biol Sci.* 2017, **13**(3), pp.383-390.
292. Lai, K.C., Chang, K.W., Liu, C.J., Kao, S.Y. and Lee, T.C. IFN-induced protein with tetratricopeptide repeats 2 inhibits migration activity and increases survival of oral squamous cell carcinoma. *Mol Cancer Res.* 2008, **6**(9), pp.1431-1439.
293. Castro-Muñoz, L.J., Manzo-Merino, J., Muñoz-Bello, J.O., Olmedo-Nieva, L., Cedro-Tanda, A., Alfaro-Ruiz, L.A., Hidalgo-Miranda, A., Madrid-Marina, V. and Lizano, M. The Human Papillomavirus (HPV) E1 protein regulates the expression of cellular genes involved in immune response. *Scientific Reports.* 2019, **9**(1), p.13620.
294. Hillmer, R.E. and Link, B.A. The Roles of Hippo Signaling Transducers Yap and Taz in Chromatin Remodeling. *Cells.* 2019, **8**(5).
295. Buscail, L., Estève, J.P., Saint-Laurent, N., Bertrand, V., Reisine, T., O'Carroll, A.M., Bell, G.I., Schally, A.V., Vaysse, N. and Susini, C. Inhibition of cell proliferation by the somatostatin analogue RC-160 is mediated by somatostatin receptor subtypes SSTR2 and SSTR5 through different mechanisms. *Proc Natl Acad Sci U S A.* 1995, **92**(5), pp.1580-1584.
296. Pidugu, V.K., Pidugu, H.B., Wu, M.-M., Liu, C.-J. and Lee, T.-C. Emerging Functions of Human IFIT Proteins in Cancer. 2019, **6**.
297. Ratnadiwakara, M., Engel, R., Jarde, T., McMurrick, P.J., Abud, H.E. and Änkö, M.-L. SRSF3 confers selective processing of miR-17-92 cluster to promote tumorigenic properties in colorectal cancer. 2019, p.667295.
298. Wang, T., Zhang, W., Huang, W., Hua, Z. and Li, S. LncRNA MALAT1 was regulated by HPV16 E7 independently of pRB in cervical cancer cells. *J Cancer.* 2021, **12**(21), pp.6344-6355.
299. Song, S., Li, X., Geng, C., Li, Y. and Wang, C. Somatostatin stimulates colonic MUC2 expression through SSTR5-Notch-Hes1 signaling pathway. *Biochemical and Biophysical Research Communications.* 2020, **521**(4), pp.1070-1076.
300. Borga, C., Dal Pozzo, C.A., Trevellin, E., Bergamo, F., Murgioni, S., Milanetto, A.C., Pasquali, C., Cillo, U., Munari, G., Martini, C., De Carlo, E., Zagonel, V., Guzzardo, V., Pennelli, G., Dei Tos, A.P., Vettor, R. and Fassan, M. mTOR

pathway and somatostatin receptors expression intratumor-heterogeneity in ileal NETs %J Endocrine-Related Cancer. 2021, **28**(7), pp.449-456.
301. Rodrigues, C., Joy, L.R., Sachithanandan, S.P. and Krishna, S. Notch signalling in cervical cancer. *Experimental Cell Research.* 2019, **385**(2), p.111682.
302. Shen, H., Chen, Y., Wan, Y., Liu, T., Wang, J., Zhang, Y., Wei, L., Hu, Q., Xu, B., Chernov, M., Frangou, C. and Zhang, J. Identification of TAZ-Dependent Breast Cancer Vulnerabilities Using a Chemical Genomics Screening Approach. *Front Cell Dev Biol.* 2021, **9**, p.673374.

Appendix

Table A.1- Plasmids used in this study

Plasmid Name	Plasmid Backbone	Expression type	Source
pcDNA3	pcDNA3	Transient	Addgene
WWTR1 promoter luciferase reporter	pEZX-PL01	Transient	GeneCopoeia
WT STK4 3'UTR luciferase reporter	psiCheck2	Transient	Cloned by MRP
MT STK4 3'UTR luciferase reporter	psiCheck2	Transient	Cloned by Emma Ryder
WT p53	pcDNA3	Transient	Olivier Terrier
Empty vector	pMSCV-N-HA-IRES-Puro	Retroviral	Elizabeth White
HA-HPV18 E6	pMSCV-N-HA-IRES-Puro	Retroviral	Cloned by Yigen Li
HA-HPV18 E7	pMSCV-N-HA-IRES-Puro	Retroviral	Cloned by Yigen Li
HA-HPV16 E7	pMSCV-N-HA-IRES-Puro	Retroviral	GenScript
FLAG-WT SP1	pcDNA3.1(+)-N-DYK	Transient	GenScript
FLAG-Trunc SP1	pcDNA3.1(+)-N-DYK	Transient	GenScript
FLAG-SP1 2TD	pcDNA3.1(+)-N-DYK	Transient	GenScript
GFP-HPV18 E7	pEGFP--c1	Transient	Cloned by David Kealy
NEG	pLK0.1	Lentivirus	Katherine Harper
shRNA TAZ A KD	pLK0.1	Lentivirus	Henning Wackerhage
shRNA TAZ B KD	pLK0.1	Lentivirus	Henning Wackerhage
shRNA YAP A KD	pLK0.1	Lentivirus	Cloned by MRP
shRNA YAP B KD	pLK0.1	Lentivirus	Cloned by MRP

shRNA Y/T A KD	pLK0.1	Lentivirus	Cloned by MRP
shRNA Y/T B KD	pLK0.1	Lentivirus	Cloned by MRP
FLAG-TAZ	pcDNA3.1(+)-N-DYK	Transient	GenScript
FLAG-YAP	pcDNA3.1(+)-N-DYK	Transient	GenScript
FLAG-TAZ TEAD binding mutant	pcDNA3.1(+)-N-DYK	Transient	GenScript
FLAG-TAZ S89D	pcDNA3.1(+)-N-DYK	Transient	GenScript
shRNA TOGARAM2 A KD	pLK0.1	Lentivirus	MERCK
shRNA TOGARAM2 B KD	pLK0.1	Lentivirus	MERCK
shRNA SSTR5 A KD	pLK0.1	Lentivirus	MERCK
shRNA SSTR5 B KD	pLK0.1	Lentivirus	MERCK
shRNA IFIT2 A KD	pLK0.1	Lentivirus	MERCK
shRNA IFIT2 B KD	pLK0.1	Lentivirus	MERCK
FLAG-TOGARAM2	pcDNA3.1(+)-N-DYK	Transient	GenScript
FLAG-SSTR5	pcDNA3.1(+)-N-DYK	Transient	GenScript
FLAG-IFIT2	pcDNA3.1(+)-N-DYK	Transient	GenScript
shRNA NONO A KD	pLK0.1	Lentivirus	Katherine Harper
shRNA NONO B KD	pLK0.1	Lentivirus	Katherine Harper

Table A.2- Cloning primers submitted in this study

Name	Forward	Reverse
TAZ promoter SP1 site 1 site directed mutagenesis	GGACATTCCAATCCTCC CACAACCCTC	CAAAGGGAAAGTGGCCTG
TAZ promoter SP1 site 2 site directed mutagenesis	AAGTCCGTGGTAAAC TCAAAG	CCGGGGAGCCTGGAG CCG
STK4 3'UTR luciferase	AAAAAACTCGAGGCA AGGCCAGGCTGTGA	AAAAAAGCGGCCGCAC CTGACCAATGTACATAC

Table A.3- Antibodies used in this study

Antibody target	Manufacturer	Species	Use
HPV18 E6	SCBT (G-7: sc-365089),	Mouse	WB 1:500
HPV18 E7	Abcam (8E2: ab100953)	Mouse	WB 1:1000
HA	CST (3724)	Mouse	WB 1:1000
STK4	Abcam; ab51134	Mouse	WB 1:500
YAP	CST; D8H1X	Rabbit	WB 1:1000, IF 1:300
pYAP S127	CST; D9W2I	Rabbit	WB 1:1000
MOB1	CST; E1N9D	Rabbit	WB 1:1000
pMOB1	CST; D2F1O	Rabbit	WB 1:1000
Myc	9E10	Mouse	WB 1:1000
Cyclin D1	Abcam; ab13475	Rabbit	WB 1:1000
HPV16 E6	SCBT; sc-460	Mouse	WB 1:500
HPV16 E7	SCBT; sc-1587	Mouse	WB 1:1000
GAPDH	SCBT; sc365062	Mouse	WB 1:5000
TAZ	BD	Mouse	WB 1:500, IF 1:50
FLAG	F1804, Sigma-Aldrich	Mouse	WB 1:1000, IF 1:50
NONO	Proteintech 11058-1-AP	Rabbit	IF 1:50
GFP	B-2; sc-9996	Mouse	WB 1:2000
Slug	CST; 9585	Rabbit	WB 1:1000
Snail	CST; 3879	Rabbit	WB 1:1000
Vimentin	CST; 5741	Rabbit	WB 1:1000

Table A.4- qRT-PCR primers used in this study

Gene name	Forward	Reverse
HPV18 E6	TGGCGCGCTTTGAGGA	TGTTCAGTTCCGTGCACAGATC
HPV18 E7	GACCTAAGGCAACATTGCA	GCTCGTGACATAGAAGGTC
CCND1	CCGCTGGCCATGAACTACCT	ACGAAGGTCTGCGCGTGTT
STK4	GCTTCTGACTCAATGCTTAG	CCACATCCTCCTGCCAAG
AREG	GTGGTGCTGTCGCTCTTGATA	ACTCACAGGGGAAATCTCACT
Cyr61	AGCCTCGCATCCTATACAACC	TTCTTTCACAAGGCGGCACTC
PROM1	TGGATGCAGAACTTGACAACGT	ATACCTGCTACGACAGTCGTGGT
U6	CTCGCTTCGGCAGCACA	AACGCTTCACGAATTTGCGT
STK4 3'UTR region insert	AAAAAACTCGAGGCAA GGCCAGGCTGTGA	AAAAAAGCGGCCGCACC TGACCAATGTACATAC
Pre-miR18a	GGCTTTGTGCTAAGGTGCATCT AG	CAGAAGGAGCACTTAGGGCAGTAG
Pre-miR92a	ACACAGGTTGGGATCGGTTG	CAAACTCAACAGGCCGGGA
MMP2	TACAGGATCATTGGCTACACAC C	GGTCACATCGCTCCAGACT
SPARC	AGC ACC CCA TTG ACG GGT A	GGT CAC AGG TCT CGA AAA AGCF
IFIT2	GGGAAACTATGCCTGGGTC	CCTTCGCTCTTTCATTTTGGTTTC
SSTR5	CTTCTTCGTGGTCATCCTCTCC	TTGCGGAGGCACAGAACCTTCT
WWTR1	AGGGCCATATCATTCGAGGG	ATCAGGGAAACGGGTCTGTT
YAP1	CGCTCTTCAACGCCGTCA	AGTACTGGCCTGTCGGGAGT
VIM	GTTTCCCCTAAACCGCTAGG	AGCGAGAGTGGCAGAGGA
TJP1	CGGTCCTCTGAGCCTGTAAG	GGATCTACATGCGACGACAA
SNAI1	TCGGAAGCCTAACTACAGCGA	AGATGAGCATTGGCAGCGAG
SNAI2	TGTTGCAGTGAGGGCAAGAA	GACCCTGGTTGCTTCAAGGA
TWIST1	GGACAAGCTGAGCAAGATTCA GA	TCTGGAGGACCTGGTAGAGGAA

Table A.5- shRNA targeting sequences used in this study

shRNA	Targeting sequence
TAZ A KD	GCGTTCTTGTGACAGATTATA
TAZ B KD	TAAGCTTTATGGGTGTTAATT
YAP A KD	CCCAGTTAAATGTTCACCAAT
YAP B KD	CAGATTCCATTCAGGCAGAA
Y/T A KD	TGTGGATGAGATGGATACA
Y/T B KD	TGTGGATGAGATGGATACAGG
TOGARAM2 A KD	GCAGGTTACTTATCTTGGTTT

TOGARAM2 B KD	GATAATGATGAACTTCCCTCT
SSTR5 A KD	CGTCACCAACATCTACATTCT
SSTR5 B KD	CTTCACCGTCAACATCGTCAA
IFIT2 KD	GCAACCTACTGGCCTATCTAA
NONO A KD	AACGTCGCCGATACTAATAAG
NONO B KD	AAGTCAATTCTGTGTGGTATA

Table A.6- Small molecule inhibitors used in this study. All inhibitors were dissolved in DMSO

Drug name	Drug target	Manufacturer	Concentration
U0126	MEK1/2 inhibitor	Calbiochem	10 µM
PD153035	Inhibits EGFR activity	Calbiochem	2 µM
CHX	Inhibits translation	Calbiochem	10 µg/ml
MG132	Inhibits proteasomal degradation	Sigma	5 µM
Chloroquine	Inhibits lysosomal-mediated degradation	Thermo Fisher	100 µM
Ivermectin	Inhibits YAP/TAZ nuclear localisation	Sigma	10 µM
6079510	Prevents TAZ nuclear localisation	Chembridge	10 µM
JNK-IN-8	Irreversible JNK inhibitor	Calbiochem	3 µM
Mithramycin A	Inhibits SP1	Active motif	50 nM
Actinomycin D	Inhibits transcription	Sigma	50 nM
1,6-Hexanediol	Dissolve LLPS assemblies	Provided by the Whitehouse lab	5% in DMEM media